

**Rational Approaches to Regulating Polymer Properties
in Ring-Opening Metathesis Polymerization**

Thesis by
Alto D. Benedicto

In Partial Fulfillment of the Requirements
for the Degree of
Doctor of Philosophy

California Institute of Technology
Pasadena, California

1995
(Defended June 15, 1994)

To my family

The history of discovery is full of arrivals at unexpected destinations, and arrivals at the right destination by the wrong boat.

-- A. Koestler, *The Act of Creation*, 1964

Acknowledgments

I am fortunate to have spent my graduate life at Caltech-- the equipments and facilities are superb, the staff very helpful, the people friendly. "Red tape" is virtually non-existent and students are encouraged to explore and cross interdisciplinary line.

I'd like to thank my advisor "**Bob**" **Grubbs** for his immense patience. Though we rarely spoke, his few words were very highly informative. His enthusiasm towards chemistry has affected everyone. He always exudes cheerfulness and is one of the nicest and unassuming person I've met. Helen Grubbs, his wife, is remarkably caring as well.

I would also like to thank the members of my Ph.D. committee (Prof. Dennis Dougherty, Prof. Nathan Lewis, Prof. Z.G. Wang, and Prof. J.E.Bercaw) for their valuable time and task of browsing through this work. Their criticisms during both the Candidacy and Propositions Exam were very helpful.

I'm indebted to a lot of people. **Toshio Sasaki** got me started with polymers. **Christine Lepetit** helped me get acquainted with the lab facilities during my first year. **Dominic McGrath**, showed me how to take 2-D NMR spectra in the trouble-plagued 400 MHz NMR machine. **Jean-Pierre Schaller** taught me some valuable organic chemistry techniques.

Zhe Wu has been very helpful with various discussions, showed me how to take low-temperature 400 MHz NMR during my second year, and collaborated in ruthenium studies in Chapter 2.

Jerome Claverie is instrumental in Chapter 3 of this thesis, and I would like to thank him very much for a most wonderful collaboration. Strangely, the project started when I'm in a deep lull. He also proofread part of this thesis, and provided discussions not only about lab work but also on a wide variety of interesting topics.

Lin Pu, Javier de la Mata, Marcia France, and Eric Dias proofread part of this thesis, and provided discussions.

The tacticity studies in Chapter 1 was an extension of work done by then graduate student Bruce Novak. The isomerization studies was an extension of work done by Dominic McGrath. The evaluation of the chirality function in Chapter 4 was a collaboration between our group and that of Prof. Kurt Mislow of Princeton University.

Some of the most pleasant experiences in graduate life were spent with Prof. Kurt Mislow of Princeton University, and post-docs Andrzej Buda and Thomas Auf der Heyde. They have all been extremely nice and helpful during my two months work there. Prof. Mislow was always very enthusiastic, and paid close attention to students.

My thanks also goes to Eric Ginsburg, Elizabeth Burns, Christopher Gorman, Vijaya Subramanian, Marc Hillmyer, Sonbinh Nguyen, Michael Ru, Brenda Mar, and other members of the Grubbs group that I may forget to mention, who in one way or another, encouraged me, provided a few mg. of catalyst, shared their wisdom, and assisted me. I would also like to thank the rest of Grubbs group post-docs and/or research fellows Philip D. Hampton, T. Randall Lee, Gregory Fu, Detlef Kraatz, Osamu Fujiwara, Shokyoku Kanaoka, and Vincent Conticello, for their advice. Prof. Fred Anson's group allowed me to use their cyclic voltammetry instrument, Prof. Sunney Chan's group the use of low-temperature ESR instrument, Prof. Daniel Weitekamp's group introduced me to multinuclear NMR spectroscopy and supervised my initiation into ^{99}Ru NMR.

ABSTRACT

The molecular weight distribution of a living polymerization when chain-transfer agents are intentionally added were computed numerically. Results showed that traditional expressions for number-average degree of polymerization (\bar{X}_n) and polydispersity index (PDI) of chain-growth polymerization cannot be used. The well-known Mayo equation fails even when the system has achieved steady-state polymerization. Although the behavior of the system is complex, an analytical expression for \bar{X}_n was derived. Plots based on the analytical expression showed excellent agreement with that from numerical solutions. The implications of the calculations were discussed. The kinetics of living ring-opening metathesis polymerization (ROMP) of norbornene in the presence of neohexene catalyzed by Mo was investigated.

The living ROMP of norbornene (n) and bicyclo[3.2.0]hept-2-ene (c) by $\text{Cl}_2(\text{PPh}_3)_2\text{Ru}(=\text{CHCHCPh}_2)$ was demonstrated. The molecular weight varied linearly with conversion. Discrete propagating species showed that PPh_3 ligand dissociated during polymerization of c, and that CuCl (abstracts PPh_3) enhanced the rate of polymerization of n. The specific propagation rate constants (k_{nn} and k_{cc} , respectively) of homopolymerization of n and c were measured, respectively. Block copolymers were easily prepared. From reactivity ratio studies, the ordering of the specific propagation rate constants are $k_{nc} \gg k_{nn} > k_{cc} > k_{cn}$. The effect of styrene as chain-transfer agent on the molecular weight was examined.

The hitherto unassigned (and unknown) microstructure of polymers prepared from 7-oxabicyclo[2.2.1]hept-2-ene derivatives have finally been unambiguously assigned. Polymers catalyzed by $\text{W}(\text{CH-}i\text{-Bu})(\text{NAr})(\text{OCMe}(\text{CF}_3)_2)_2$ have all cis double bonds and highly syndiotactic, while those from $\text{RuCl}_3 \cdot 3\text{H}_2\text{O}$ and $[\text{RuCl}(\mu\text{-Cl})(\eta^3\text{:}\eta^3\text{-C}_{10}\text{H}_{16})]_2$ { $\text{C}_{10}\text{H}_{16}$ = 2,7-dimethyloctadienediyl} have high trans double bond content and highly isotactic.

Studies on the olefin isomerization catalyzed by $\text{Ru}(\text{H}_2\text{O})_6\text{tos}_2$ revealed that the presence of hydroxyl functionality on the terminal olefin resulted in formation of 1 : 1 ratio of cis : trans double bonds on the isomerized internal olefin product, in contrast with near exclusive isomerization of double bond to trans when no hydroxyl group was present.

A numerical algorithm was developed for the evaluation of a chirality function for triangles on a plane, showing that such algorithm may be easily extended into the case of tetrahedron in 3-dimensional space.

TABLE OF CONTENTS

ACKNOWLEDGMENTS	iv
ABSTRACT	vi
Chapter 1. Selected Reactions of $\text{Ru}(\text{H}_2\text{O})_6\text{tos}_2$	1
I. Microstructural Studies of Poly(7-Oxabicyclo[2.2.1]hept-2-ene) Derivatives ..	2
Introduction	2
Results and Discussion	5
Conclusion	23
II. The Influence of Hydroxyl Group on the Cis:Trans Ratio of Internal Olefins ..	25
Introduction	25
Results and Discussion	27
Conclusion	34
Experimental Section	34
References and Notes	39
Appendix A: ^{13}C spectrum of cyclopentene-norbornene copolymer, etc.	45
Appendix B: Further figures on isomerization of olefins	47
Chapter 2. Living Ring-Opening Metathesis Polymerization of Bicyclo[2.2.1]hept-2-ene and Bicyclo[3.2.0]hept-2-ene Catalyzed by $\text{Cl}_2(\text{PPh}_3)_2\text{Ru}(=\text{CHCHCPh}_2)$	50
Introduction	51
Results and Discussion	51
Reaction of bicyclo[2.2.1]hept-2-ene	51
Reaction of bicyclo[3.2.0]hept-2-ene	56
Speculations on the role of phosphines	60
Determination of reactivity ratios	60
Reactions with chain-transfer agents, and other reactions	66

Conclusion	67
Experimental Section	68
References	71
Chapter 3. On the Molecular Weight Distribution of Living Polymerization Involving Chain-Transfer Agents: Computational Results, Analytical Solutions, and Experimental Investigations using Ring-Opening Metathesis Polymerization	74
Introduction	75
Prior Works	82
Formulation of the Problem	85
Computational Methods	86
Computational Results and Discussion	87
Cases where $k_{tr} = 0$ or $k_{tr} \ll k_p$	87
Cases where $k_{tr} \gg k_p$	90
Cases where k_{tr} is within an order of magnitude from k_p	93
Mayo Plot and k_{tr}/k_p	98
Analytical Results and Discussion	106
Steady-State Approximation and Closed-Form Solution	106
Experimental Section	109
Experimental Results and Discussion	117
Conclusions	124
References and Notes	125
Appendix A: More Figures	131
Appendix B: More Polymerization Scheme	137
I. Multiple Initiators	137
II. Reactivation of Dead Chains	139

Chapter 4. A Chirality Measure for Triangular Polygons (An Algorithm for Evaluating the Chirality Function)	142
Introduction	143
Computational Details	145
Definition of the domain	145
Calculation of the area of overlap (two methods)	147
Determination of maximum area of overlap (normalized)	148
Results and Discussion	148
Conclusion	151
Acknowledgment	151
References	151
Appendix A	154
Nomenclature for Exact Area Calculation	154
Some cases (and positions) encountered during optimization	154
Appendix B: Source Listing of Computer Program "triang"	156
Appendix C: Monte Carlo Algorithm	173

Chapter 1

Selected Reactions of $\text{Ru}(\text{H}_2\text{O})_6(\text{tosylate})_2$

I. Microstructural Studies of Poly(7-Oxabicyclo[2.2.1]hept-2-ene) Derivatives

II. The Influence of Hydroxyl Group on the Cis:Trans Ratio of Internal Olefins during the Isomerization of Terminal Olefins to Internal Olefins by $\text{Ru}(\text{H}_2\text{O})_6\text{tos}_2$

I. Microstructural Studies of Poly(7-Oxabicyclo[2.2.1]hept-2-ene) Derivatives

Introduction

Ring-opening metathesis polymerization (**ROMP**) has been the subject of numerous studies since its discovery in the 1960s.¹ The process involves the [2 + 2] cycloaddition of metal-alkylidene species with a cyclic olefin to form a metallacyclobutane intermediate which subsequently undergoes ring-opening to regenerate the metal-alkylidene species (Figure 1).^{2a} The reaction is driven forward by the release of ring strain in the cyclic olefin. The recent emphasis has been on the synthesis of more versatile catalysts and the use of these catalysts to prepare polymers with interesting properties.³

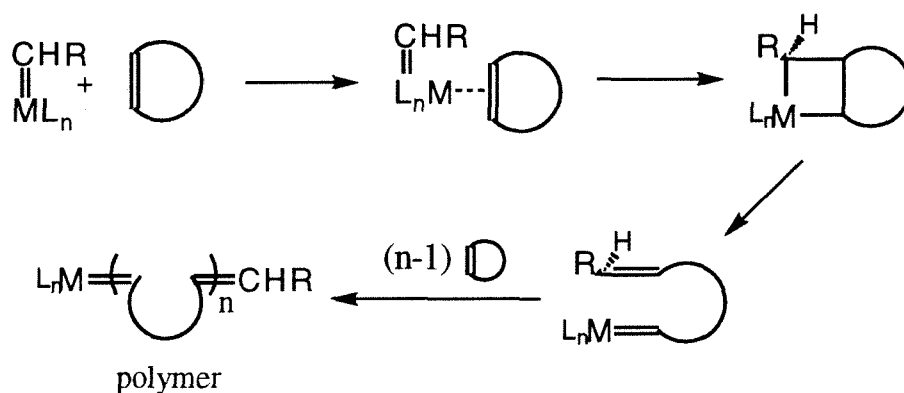


Figure 1. Ring-opening metathesis polymerization (ROMP) of cyclic olefins.

Polymer properties depend on chemical composition (as determined by the monomers used), molecular weight, and microstructure.⁴ Recently, some insights have been gained in controlling polymer properties through studies on the mechanism and kinetics of polymerization.^{1b,5} New metal-alkylidene catalysts have been developed that are tolerant to certain functional groups in the monomer.⁶ This enables the incorporation of non-carbon atoms into polymer chain. Knowledge of reactivity ratios of various monomers is also being used to design block copolymers.⁷ The role of Lewis bases (such as phosphines, amines) in changing the kinetics of initiation versus chain propagation has

been clarified, and thus allows precise control of molecular weight and its distribution.⁸ However, inspite of all these developments, limited progress has been made in elucidating the conditions that control polymer microstructure.⁹

For example, the propensity of *trans* stereoselectivity in **ROMP** polymers has been postulated to be caused primarily by steric interaction of the substituents in the (1,2)-position of a puckered metallacyclobutane intermediate (Figure 2).¹⁰ Metallacyclobutane having (1,2)-(equatorial,equatorial) interaction exhibits less steric crowding and was presumed to be the favored intermediate, thus resulting in *trans* stereoselectivity. The role of (1,3)-substituent and the ligand substituent interactions on the stereoselectivity is unknown.

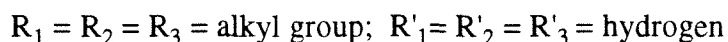
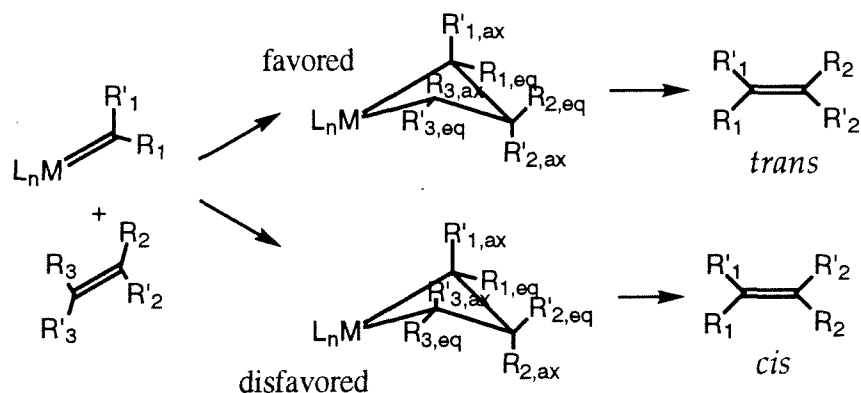
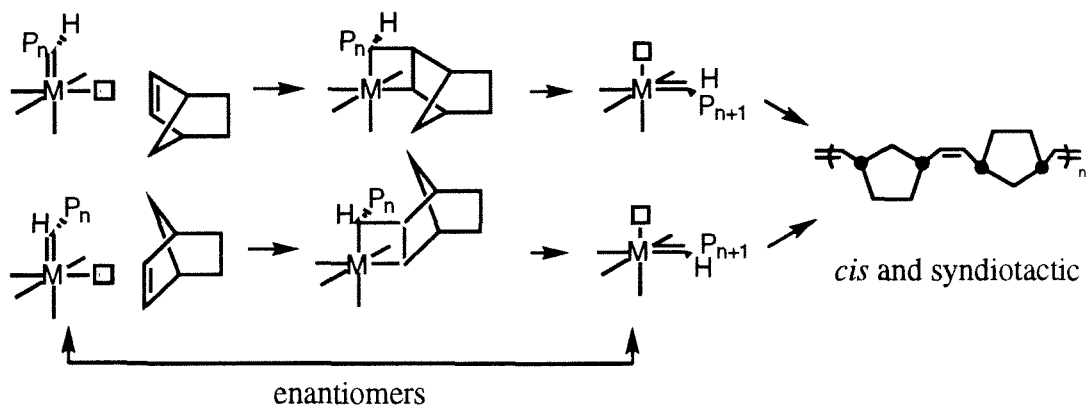
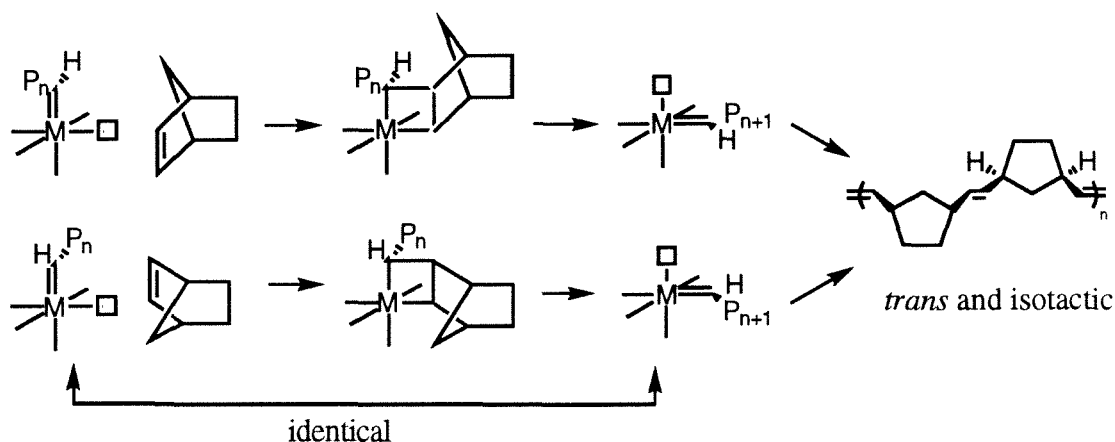


Figure 2. 1,2-Interaction determining the stereochemistry of the product.

A different mechanism was proposed to account for the observed relation of *cis-trans* isomerism with tacticity in ring-opened poly(norbornene).² The lability of the ligands on the metal is a key feature of the postulate. In each propagation step, a pseudooctahedral metal-carbene complex with nonlabile ligands can only produce one vacant site for olefin coordination. As seen from figure 3, if the ligands around the metal are nonlabile and the rotation about the metal-carbene bond is slow, isotactic segments are produced whenever *trans* double bonds are produced. The same mechanism accounts for the relation of syndiotactic segments with *cis* double bonds.



Rac dyads are formed whenever *cis* double bonds are formed.



Similarly, *meso* dyads are formed whenever *trans* double bonds are formed.

Figure 3. Proposed propagation mechanism for observed *cis* double bond association with syndiotacticity and *trans* double bond association with isotacticity in norbornene-type polymers prepared from classical ROMP catalyst.^{2a} P_n = polymer chain, M = metal, \square = vacant site.

In order to test these models, the precise identification of microstructures in a polymer is essential. NMR spectroscopy is currently the most powerful tool in microstructural assignments of polymers and has been used to determine the microstructure on poly(norbornene) derivatives.¹¹ In order to further test these models, a careful study of the microstructure of poly(7-oxanorbornene) derivatives prepared with a variety of catalysts has been carried out. The results of such study can be compared with

those of poly(norbornene). The study with 7-oxanorbornene allows a comparison of the late transition metal catalyst in aqueous media to more defined early catalysts. Norbornenes due to their insolubility in water can only be studied with early transition metal catalysts. The robustness of $[\text{Ru}(\text{H}_2\text{O})_6](\text{tosylate})_2$ in aqueous media, its tolerance of functional groups,¹² the symmetrical geometry around the metal center, and the facile substitution of aqua ligands with other ligands,^{13,14} make $[\text{Ru}(\text{H}_2\text{O})_6](\text{tosylate})_2$ an ideal system to study the effect of ligand lability on the stereochemistry of the polymer.

Results and Discussion.

The microstructure of a norbornene-type polymer depends on the relationship between adjacent chain units. The simplest isomeric relationships between two units (dyads) in a polymer are usually divided into the following types:¹⁵

1. *cis(c)* - *trans(t)* isomerism for the double bond in the dyad
2. *meso(m)* (i.e., isotactic) - *racemic(r)* (i.e., syndiotactic) relationship of the two tetrahydrofuran rings of the dyad (Figure 4)

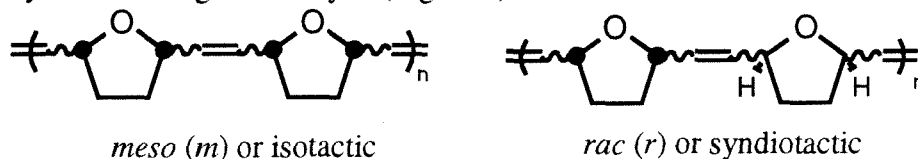


Figure 4. Meso-rac isomerism. The labels are non-interchangeable ($mr \neq rm$).

3. Head(H) - Tail (T) isomerism for the substituent in one ring of the dyad relative to the second ring (Figure 5). This isomerism exists only if the norbornene-type monomer possesses C_1 symmetry. The dyad is labelled as (HH), (HT), (TH), or (TT) depending on whether the substituent in one ring of the dyad is near (Head) or far (Tail) from the second ring of the dyad, and vice-versa.

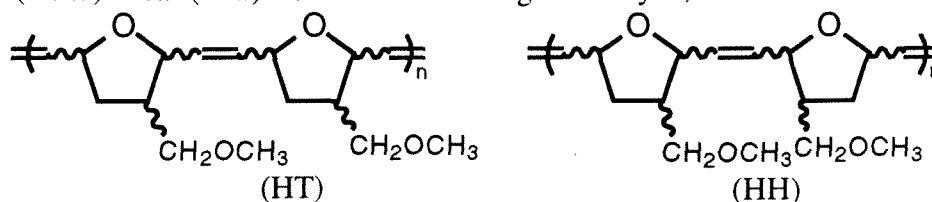


Figure 5. Head-tail isomerism. Labels are non-interchangeable ($HT \neq TH$).

Similar types of isomerism exist for triads and higher order n -ads. In each n -ad, the total number of possible isomers increases geometrically with n .¹⁵

When monomers **1**, **2**, and **3** were polymerized (Figure 6), the number and position of ^1H and ^{13}C NMR peaks for each polymer were found to be dependent on the **ROMP** catalyst used (Figure 7). These differences are correlated to the microstructure variation in the polymers (*vide infra*).

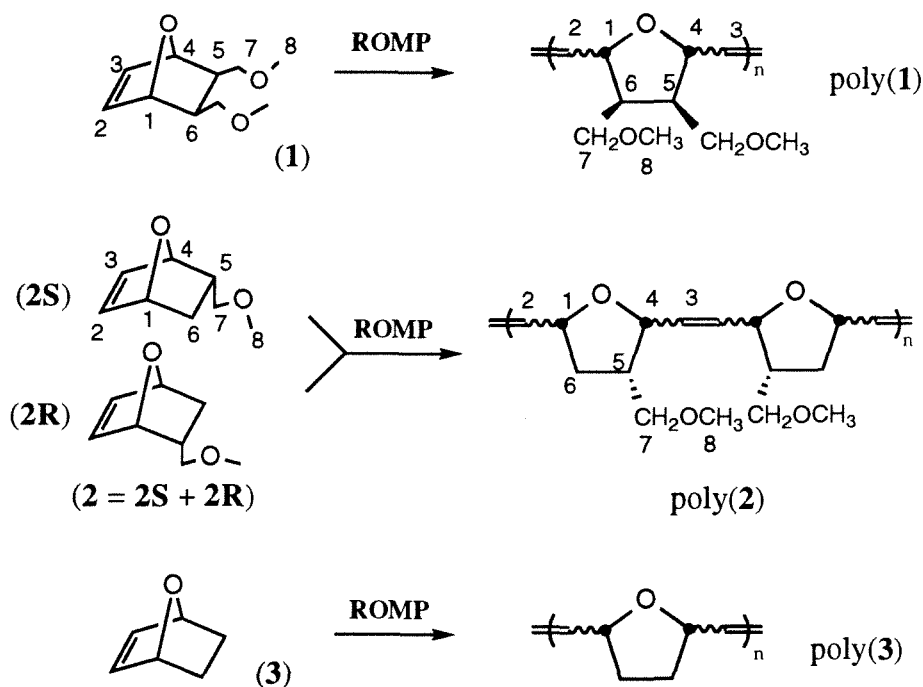


Figure 6. ROMP of 7-oxanorbornene monomers **1**, **2** ($= \mathbf{2R} + \mathbf{2S}$), and **3**.

Olefin and bridgehead proton and carbon NMR resonances give *cis* to *trans* content of the polymer. Aside from IR spectroscopy, the *cis* to *trans* double bond content in the polymer can be determined by integration of the ^1H NMR peaks of olefin and allyl protons. The ^1H NMR peak of a *trans* olefin proton in a disubstituted alkene is always downfield from that of a *cis* olefin proton, while that of a bridgehead proton one carbon removed from a *trans* double bond was upfield from that of a *cis* (Table I).^{16,17} Some of these resonances have further splittings not arising from spin-spin couplings. Unfortunately, these splittings within the (*cis*,*trans*) isomerism resonances, that

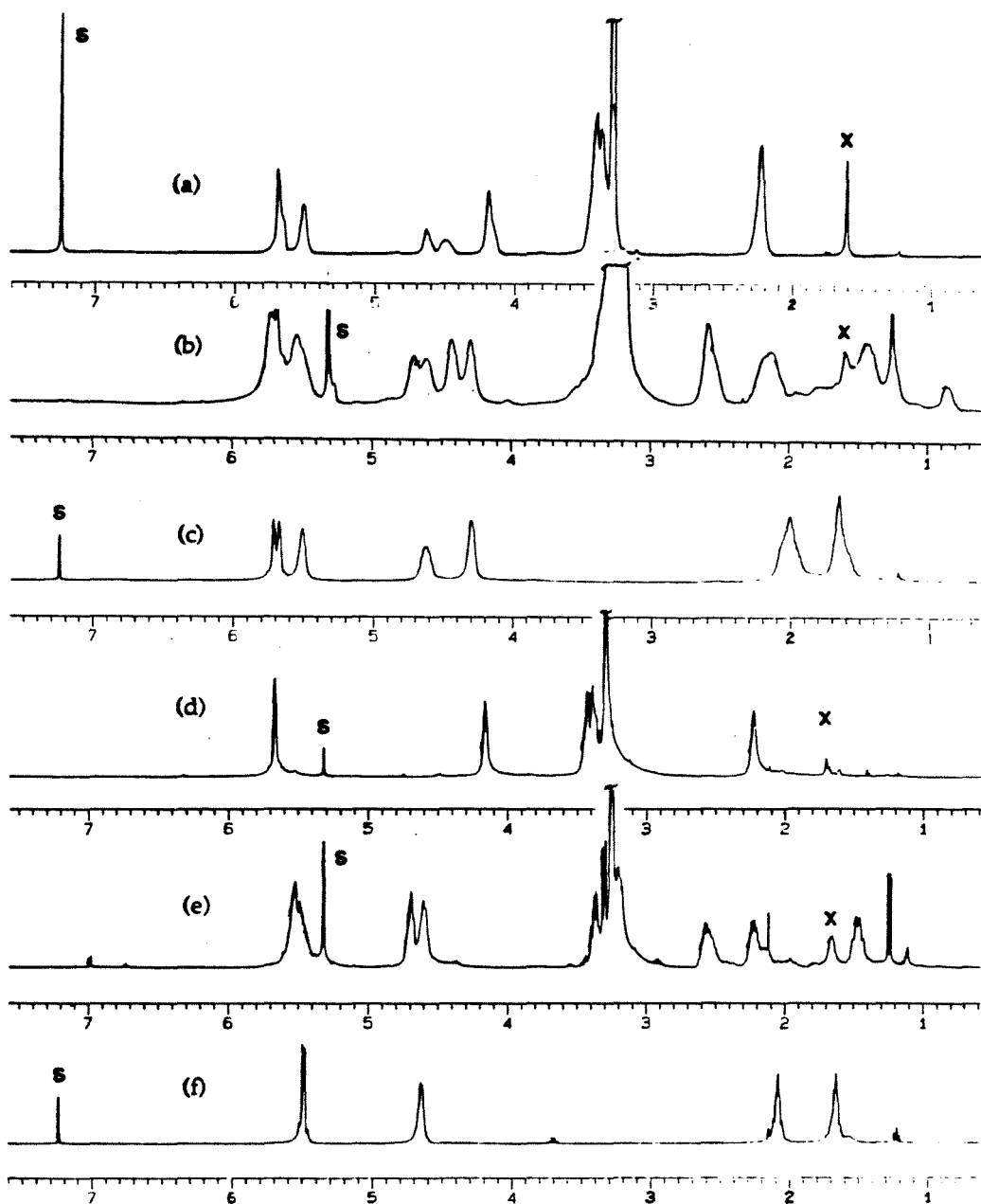


Figure 7. ^1H NMR spectra of (a): poly(1), (b): poly(2), (c): poly(3) prepared from $[\text{Ru}(\text{H}_2\text{O})_6](\text{tosylate})_2$. ^1H NMR spectra of these polymers using catalysts **6**, **8**, **9** are similar to those above except they are much simpler in appearance due to the absence of particular microstructures. (e.g., (d): poly(1) using **9**; (e): poly(2) using **6**; (f): poly(3) using **6**). Peak assignments in poly(2) are deduced from ^1H - ^1H COSY. See Table I for peak assignments. x = water. s = solvent

Table I
 ^1H NMR Assignments for Poly(1), Poly(2), Poly(3)
in CDCl_3 or CD_2Cl_2

polymer	chemical shift (ppm)	H# (type)	peak assignment
poly(1)	5.69-5.65	2,3 (olefin)	<i>trans</i>
	5.52-5.50	2,3 (olefin)	<i>cis</i>
	4.63-4.50	1,4 (bridgehead)	<i>cis</i>
	4.19-4.16	1,4 (bridgehead)	<i>trans</i>
	3.42 and 3.37	7 (methylene)	insensitive
	3.29	8 (methyl)	insensitive
	2.23	5,6 (ring)	insensitive
poly(2)	5.73	2 (olefin)	<i>trans</i> , Tail
	5.69	3 (olefin)	<i>trans</i> , Head
	5.52	2 (olefin)	<i>cis</i> , Tail
	5.49	3 (olefin)	<i>cis</i> , Head
	4.69	4 (bridgehead)	<i>cis</i> , Head
	4.60	1 (bridgehead)	<i>cis</i> , Tail
	4.43	4 (bridgehead)	<i>trans</i> , Head
	4.30	1 (bridgehead)	<i>trans</i> , Tail
	3.39-3.30	7 (methylene)	insensitive
	3.26	8 (methyl)	insensitive
	2.56	5 (ring)	insensitive
	2.22	6 (<i>exo</i> , ring)	<i>exo</i>
poly(3)	1.48	6 (<i>endo</i> , ring)	<i>endo</i>
	5.71-5.67	2,3 (olefin)	<i>trans</i>
	5.51-5.48	2,3 (olefin)	<i>cis</i>
	4.62	1,4 (bridgehead)	<i>cis</i>
	4.30	1,4 (bridgehead)	<i>trans</i>
	2.04	5,6 (<i>exo</i> , ring)	<i>exo</i>
	1.66	5,6 (<i>endo</i> , ring)	<i>endo</i>

may be due to (*meso,rac*) isomerism, are too poorly resolved to make definite assignments. On the basis of ^1H NMR, the double bonds in poly(**1**) prepared with the tungsten catalyst **6** were *cis*, those from ruthenium catalysts **8** and **9** were highly *trans* (85% and 96% of double bond are *trans*, respectively), and those from ruthenium catalyst **7** were roughly equal amounts of *cis* and *trans* (Table II). Similar trends are observed for poly(**2**) and poly(**3**) prepared using these catalysts (Figure 7).

^{13}C NMR spectra of the polymers provide another method for determining the (*cis,trans*) ratio of the double bonds. Chemical shifts of carbons alpha to a *trans* double bond generally occur 4-5 ppm downfield from those of *cis* double bonds.¹⁷ This observation also holds for poly(**1**), poly(**2**), and poly(**3**). The bridgehead carbons of poly(**1**) exhibit two major clusters around $\delta = 81.8$ and $\delta = 77.3$, arising from *trans* and *cis* dyads, respectively (Figure 8). Evaluation of the areas under these peaks yielded the same *cis/trans* double bond ratio, as obtained from ^1H NMR spectra (Table II). For poly(**3**), the bridgehead carbon allylic to a *trans* double bond resonated at $\delta = 79.5$, while that to a *cis* appeared at $\delta = 75.3$. For poly(**2**), the chemical shift of the bridgehead carbon was further resolved into four peaks instead of two due to (Head,Tail) isomerism caused by the methoxymethyl substituent. The bridgehead carbons C4 and C1 of the *trans* dyad occurred at 80.7 and 79.4 ppm, about 4.0 and 4.5 ppm downfield from C4 and C1 of the *cis* dyad (76.7 and 74.9 ppm, respectively).

The ring (or bridge) carbon and methylene carbon NMR peaks allowed determination of *cis* and *trans* blockiness (degree of clustering of *cis* or *trans* double bonds) of the ring-opened polymer. In contrast with some of the carbons in poly(**1**) wherein only two peaks corresponding to (*cis,trans*) isomerism of the double bond in the dyad were observed, the remaining ring carbon C5 in poly(**1**) had four identifiable chemical shifts ($\delta = 48.3$, $\delta = 47.9$, $\delta = 47.5$, $\delta = 47.2$) (Figure 8). The same held for methylene carbon C7 ($\delta = 71.1$, $\delta = 70.8$, $\delta = 70.5$, $\delta = 70.2$). Since poly(**1**) cannot exhibit (Head-Tail) isomerism because of the symmetric nature of the monomer,

Table II
Percent of Double Bonds in Poly(1) that are *trans*^a

catalyst	H _{2,3}	H _{1,4}	C _{1,4}	C _{5,6}	C ₇
	(olefin)	(bridgehead)	(bridgehead)	(ring)	(methylene)
6	3	3	not integ. ^b	not integ. ^b	not integ. ^b
7	59	58	58	57	not integ. ^b
8	84	85	84	83	85
9	96	96	not integ. ^b	not integ. ^b	not integ. ^b

^aValue as determined by integration of NMR peak areas of particular proton and carbon nuclei. ^bsignal to noise ratio in the spectra not acceptable (see Figure 8).

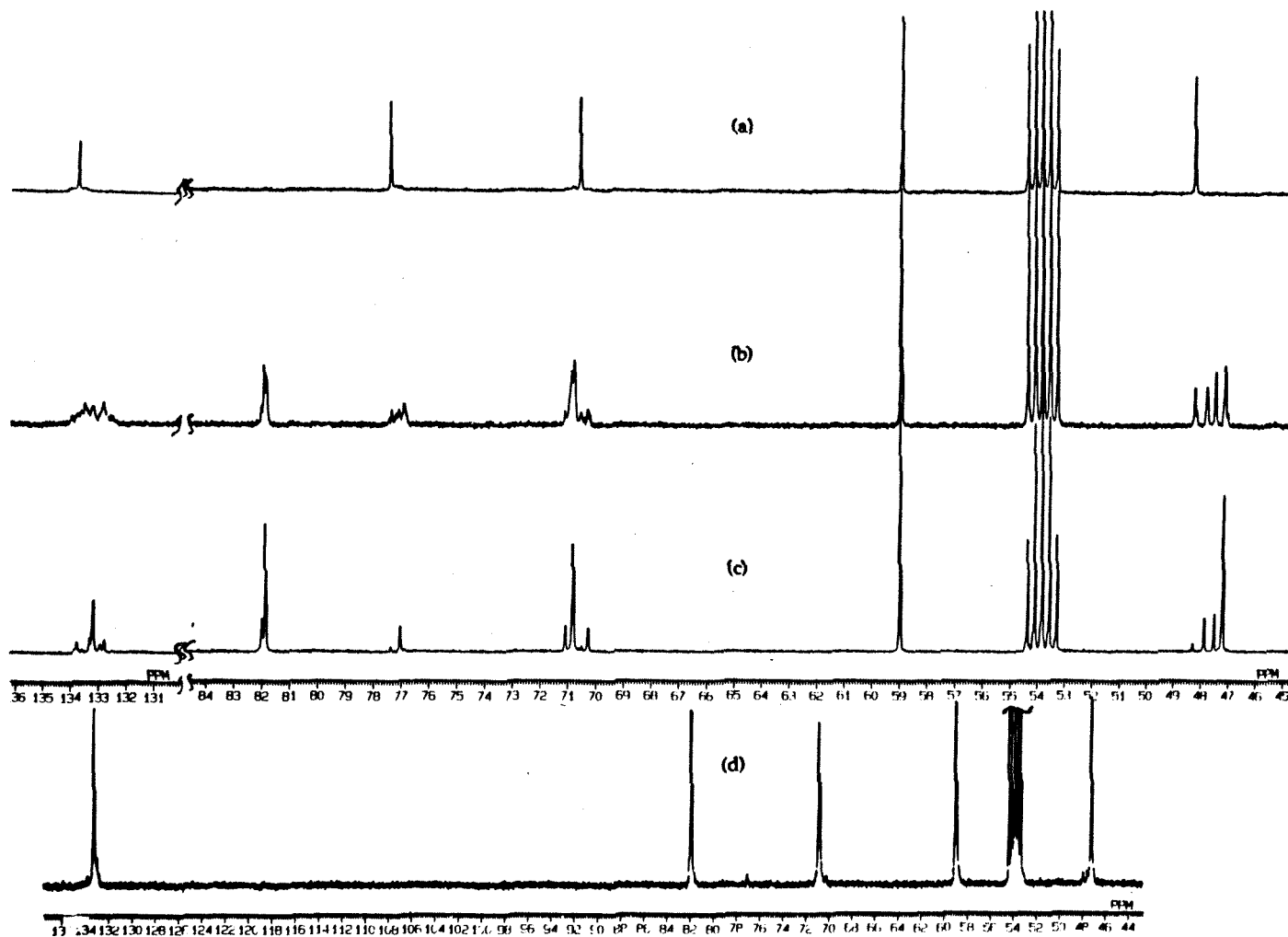


Figure 8. ^{13}C NMR spectra of poly(1). Spectra (a), (b), (c), and (d) correspond to poly(1) prepared using catalysts **6**, **7**, **8**, and **9**, respectively. (d) does not have the same scale as the others. See Table III for peak assignments.

these peaks are either due to dyads sensitive to both (*cis,trans*) and (*meso,rac*) isomerisms, or due to triads that are sensitive to only one type of isomerism. The former case would give rise to quadruple peaks corresponding to (*cr*), (*cm*), (*tr*), (*tm*). The latter case also gives rise to quadruple peaks-- [(*cc*), (*ct*), (*tc*), (*tt*)] or [(*rr*), (*rm*), (*mr*), (*mm*)] depending on which type of isomerism the said carbon was sensitive to. This ambiguity as to whether the resonances observed are the result of general sensitivity to all types of dyad configurations or just to a selective sensitivity to certain triad configurations was resolved by hydrogenating poly(**1**), which removes (*cis,trans*) isomerism. The *meso/rac* ratio in the polymer remains unaffected since (*meso,rac*) isomerism was determined by the stereochemistry of the bridgehead carbons. Regardless of which catalyst was used to synthesize poly(**1**), upon hydrogenation, hydrogenated poly(**1**) exhibits double peaks for carbons C2(former olefin), C1(bridgehead), and C5(ring) (Figure 9). These double resonances must be due to *meso* and *rac* dyads. Thus, none of the original poly(**1**) synthesized using different catalysts were completely tactic. This result, combined with the previous observation (Figure 8) that both pure *cis* poly(**1**) made from tungsten catalyst **6** and high *trans* poly(**1**) made from ruthenium catalyst **9** show a *single* ring carbon C5 NMR peak, imply that quadruple resonances cannot result from (*meso,rac*) isomerism. In other words, the quadruple resonances arise from (*cc*, *ct*, *tc*, *tt*) triads, and not from (*cr*, *cm*, *tr*, *tm*) dyads nor (*rr*, *rm*, *mr*, *mm*) triads. This conclusion was not totally surprising. Related studies using poly(norbornene) also show that the remaining ring carbon C5 of poly(norbornene) was sensitive to (*cis,trans*) isomerism of triads only-- the chemical shift difference arising from (*meso,rac*) isomerism being too small to be observed.¹⁸

Thus, the lone peak at $\delta = 48.3$ (Figure 8) of poly(**1**) using tungsten catalyst **6** was (*cc*) (Table III). The predominant peak with $\delta = 47.2$ for poly(**1**) by ruthenium catalysts **8** and **9** was (*tt*). The remaining two peaks of equal intensity at $\delta = 47.9$ and $\delta = 47.5$ that are also present in poly(**1**) using ruthenium catalyst **7** are (*ct*) and (*tc*). The resonances of methylene carbon are assigned similarly. Internal consistency of the assignments was also

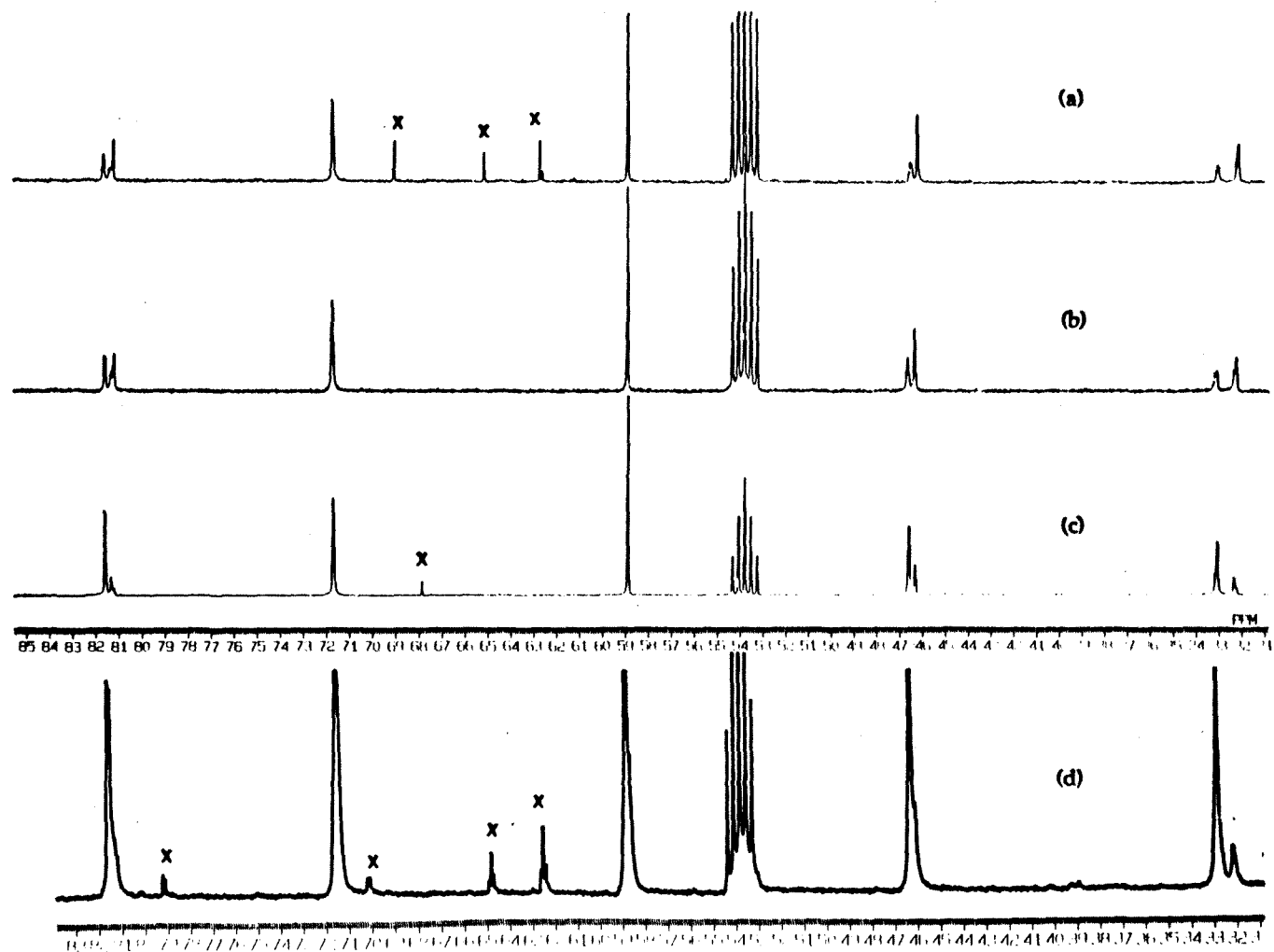


Figure 9. ^{13}C NMR spectra of hydrogenated poly(1). Spectra (a), (b), (c), and (d) correspond to hydrogenated poly(1) prepared using catalysts 6, 7, 8, and 9, respectively. p-Toluenesulfonylhydrazide is used to hydrogenate poly(1). x = impurities. See Table V for peak assignments.

Table III
 ^{13}C NMR Assignments for Poly(1) in CD_2Cl_2

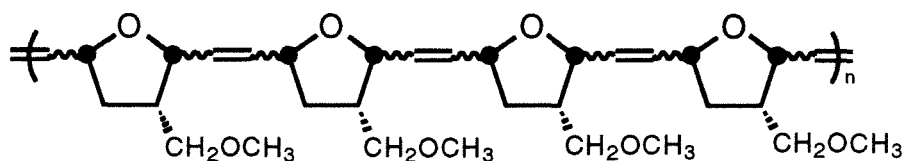
chemical shift (ppm)	C# (type)	peak assignment
133.8	2,3 (olefin)	" <i>cis</i> "
133.7	2,3 (olefin)	<i>ccc</i>
133.5	2,3 (olefin)	" <i>cis</i> "
133.3	2,3 (olefin)	" <i>cis</i> "
133.1	2,3 (olefin)	<i>ttt</i>
132.9	2,3 (olefin)	" <i>trans</i> "
132.7	2,3 (olefin)	" <i>trans</i> "
82.0	1,4 (bridgehead)	<i>tc</i>
81.8	1,4 (bridgehead)	<i>tt</i>
77.3	1,4 (bridgehead)	<i>cc</i>
77.0-76.9	1,4 (bridgehead)	<i>ct</i>
71.1	7 (methylene)	<i>tc</i>
70.8	7 (methylene)	<i>tt</i>
70.5	7 (methylene)	<i>ct</i>
70.2	7 (methylene)	<i>cc</i>
48.3	5,6 (ring)	<i>cc</i>
47.9	5,6 (ring)	<i>ct</i>
47.5	5,6 (ring)	<i>tc</i>
47.2	5,6 (ring)	<i>tt</i>
59.0	8 (methyl)	insensitive

found when the necessary interdependent relationships of higher n -ads to lower n -ads are used. The $(cc + ct)/(tc + tt)$ ratio calculated by integrating the remaining ring carbon C5 or methylene carbon was equal to the $cis/trans$ ratio calculated by integrating ^{13}C or ^1H bridgehead peaks (Table II).¹⁹

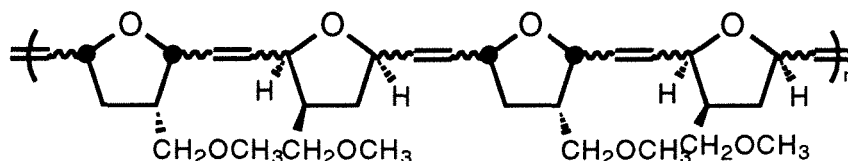
Stereochemistry of higher n -ads ($n > 2$) can be observed by carbon NMR but can only be partially assigned. The presence of at least six resolvable resonances coming from olefin carbons in poly(**1**) and poly(**3**) implies that the carbon was sensitive either to tetrads of ($cis,trans$) isomerism or to the combined effects of {triads of ($cis,trans$) and dyads of ($meso,rac$) isomerism}, both of which give rise to eight possible resonances. Occasionally, the former was invoked even though the olefinic carbons in adjacent double bonds are at least four or five bonds away.¹⁵ Without any other experimental data available, these resonances cannot be assigned unambiguously. It can only be noted that ($cis,trans$) n -ads occurred in two distinct regions. For poly(**1**), cis olefin carbons resonate in the region $\delta = 133.8$ to 133.3 while $trans$ olefin carbons resonate from $\delta = 133.1$ to 132.7 (Table III). Similarly, for poly(**3**), cis olefin carbons resonate from $\delta = 133.1$ to $\delta = 132.7$, while $trans$ olefin carbons resonate from $\delta = 132.5$ to $\delta = 132.1$.

Hydrogenated ROMP polymer provides a way to determine $meso$ to rac content of the original ROMP polymer. Definitive peak assignments of hydrogenated poly(1**) are achieved by using enantiomerically pure monomer **2S**.** Assignment of the two ^{13}C NMR peaks arising for each type of carbons of the hydrogenated poly(**1**) to $meso$ or rac is achieved by knowing that the tacticity of poly(**1**) can be deduced using an enantiomerically pure monomer **2S**. When an enantiomerically pure monomer of C_1 symmetry was polymerized with a **ROMP** catalyst, (HT) and (TH) dyads can only give rise to $meso$ dyad, while (HH) and (TT) dyads to rac dyad (Figure 10).²⁰ Provided that differences in ^{13}C NMR chemical shifts for (Head,Tail) dyads are large enough to be resolved, ($meso,rac$) isomerism can thus be determined indirectly by examining (Head,Tail) isomerism in the polymer. The pendant methoxymethyl group

attached to the ring carbon C5 of **2S** was too far from the double bond to favor the existence of one dyad isomer over the other.²¹



(HT) and (TH) can only correspond to *meso*



(HH) and (TT) can only correspond to *rac*

Figure 10. For an enantiomerically pure monomer such as **2S**, the only possible relationship between Head-Tail isomerism and *meso-rac* isomerism is illustrated above.

Since (*meso*,*rac*) isomerism for (7-oxanorbornene)-type polymer cannot be determined directly by ¹³C NMR due to the absence of resolvable peak splittings, the theoretical number of olefin resonances arising from the combination of (*cis*,*trans*) and (Head,Tail) isomerism in poly(**2**) is 8 for dyads and 32 for triads; poly(**2S**) theoretically also gives 8 dyads and 32 triads. Any further reduction in the number of peaks observed implies either an absence of certain microstructure or that the resonances are again not well separated enough to show unique chemical shifts. An example of the former case is pure *cis* or *trans* poly(**2**) which theoretically gives 4 (dyad isomer) and 8 (triad isomer) olefin resonances, and pure *cis* or *trans* poly(**2S**) which gives 4 (dyad) and 8 (triad) resonances (Table IV). A *cis* and at the same time tactic poly(**2**) gives 4 (dyad) and 8 (triad) while *cis* tactic poly(**2S**) gives 2 (dyad) and 2 (triad). Note that only if the polymer has a high degree of microstructural order is the number of olefin resonances arising from polymer

Table IV
Theoretical Number of ^{13}C NMR Resonances
for Olefinic Carbon of Polymer^f

<i>n</i> -ads	polymer	A ^a	B ^b	C ^c	D ^d	E ^e
dyads	poly(2)	16	8	4	8	4
	poly(2S)	8	8	4	2	2
triads	poly(2)	128	32	8	32	8
	poly(2S)	32	32	8	4	2

^a**A** = all types of microstructures arising from the three different types of isomerisms can be resolved by ^{13}C NMR. ^b**B** = *cis/trans* and Head/Tail isomerisms resolvable but not *meso/rac* isomerism. ^c**C** = same as B with the added condition that the double bonds in the polymer are either all *cis* or all *trans*. ^d**D** = same as B with the added condition that the polymer is tactic. ^e**E** = both conditions in C and D are fulfilled simultaneously.

^ffor dyads ((*c,t*), (*m,r*), (HH, HT, TH, TT)), and for triads ((*cc*, *ct*, *tc*, *tt*), (*mm*, *mr*, *rm*, *rr*), (HHH, HHT, HTH, THH, HTT, THT, TTH, TTT)). Note that HHT ≠ THH.

prepared from **ROMP** of (*R,S*)-monomer different from (*S*)-monomer, as was possible in the case of poly(**2**) and poly(**2S**).

Since tungsten catalyst **6** gives *cis* while ruthenium catalyst **9** gives *trans* polymer, the spectra are simplified by reducing the theoretical allowable number of resonances. Using catalyst **6**, the olefinic carbons of poly(**2**) show four predominant peaks at $\delta = 134.0$, $\delta = 133.8$, $\delta = 130.2$, $\delta = 129.7$ while those from poly(**2S**) only give rise to two peaks at $\delta = 133.8$ and $\delta = 130.2$ (Figure 11). This difference in number of peaks observed must only be from (Head,Tail) isomerism. The exact assignment of the two peaks with $\delta = 133.8$ and $\delta = 130.2$ to *cis*TT and *cis*HH in poly(**2S**), and to the additional two at $\delta = 134.0$ and $\delta = 129.7$ to *cis*TH and *cis*HT in poly(**2**) was by analogy with poly(norbornene) that has pendant substituent at ring carbon C5 --which always show the same ordering of chemical shifts for the isomeric olefin carbons.²² Therefore, poly**2S** was a predominant (TT) and (HH) polymer, implying that the larger peak in the double peak splittings in the ^{13}C spectrum of hydrogenated poly(**1**) using **6** is *rac* (Table V, Figure 11). Consequently, the original poly(**1**) synthesized using catalyst **6** is a *cis*, highly syndiotactic polymer.

For poly(**2**) prepared using catalyst **9**, four peaks are discernible at $\delta = 133.5$, $\delta = 133.3$, $\delta = 130.2$, $\delta = 129.7$, while that from poly(**2S**) has only two peaks at $\delta = 133.5$, $\delta = 129.8$. By similar reasoning, the four peaks from poly(**2**) are assigned as *trans*TH, *trans*TT, *trans*HH, and *trans*HT, respectively. Hence, polymers from **9** were high *trans*, highly isotactic. The high *trans* nature of polymers obtained from **ROMP** of cyclic monomers was a general feature observed for late-transition metal with chloro ligands in non-aqueous solvents.²³ However, the *meso* content of these norbornene-derivative polymers ranges from 50% (atactic) to 66%, as opposed to at least 75% *meso* for 7-oxanorbornene derivatives.^{22b,22c}

Table V
 ^{13}C NMR Assignments for Hydrogenated Poly(1) in CD_2Cl_2

chemical shift (ppm)	C# (type)	peak assignment
81.63-81.58	1,4 (bridgehead)	<i>meso</i>
81.37-81.19	1,4 (bridgehead)	<i>rac</i>
71.74	7 (methylene)	insensitive
58.92	8 (methyl)	insensitive
46.74-46.63	5,6 (ring)	<i>meso</i>
46.44-46.35	5,6 (ring)	<i>rac</i>
33.22-33.16	2,3 (post-olefin)	<i>meso</i>
32.39-32.29	2,3 (post-olefin)	<i>rac</i>

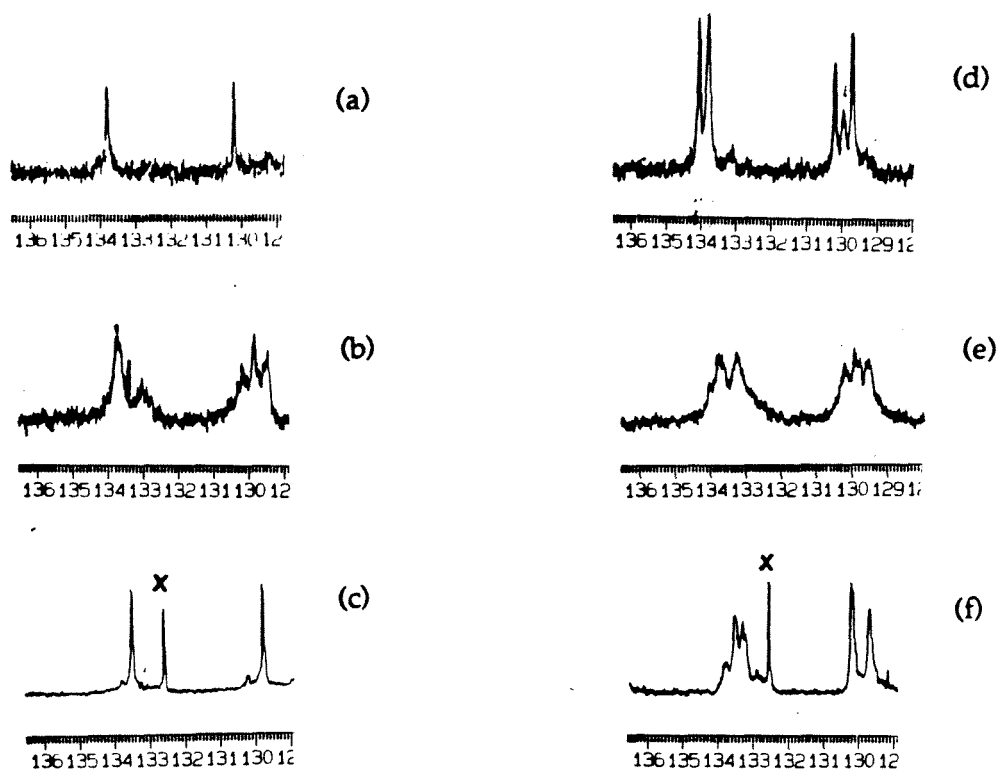


Figure 11. ^{13}C NMR spectra of olefin region of poly(2) and poly(2S). Spectra (a), (b), (c) correspond to poly(2S) prepared using catalysts 6, 7, 9, respectively. Spectra (d), (e), (f) correspond to poly(2) prepared using catalysts 6, 7, 9, respectively. x = starting monomer.

Using the above assignments, polymers prepared using **7** as catalyst showed no *cis* or *trans* preference and were also atactic. The *cis* and *trans* double bonds along the backbone of poly(**1**) are also randomly distributed as the area under ^{13}C NMR triads ($cc \times tt$)/($ct \times tc$) gives a value of 1.2.²⁴ Consequently, labile symmetrical ligand spheres result in total scrambling of all stereochemistry in the polymer.

In this limited survey of catalysts, there exists a correlation between tacticity and double bond isomerism in poly(7-oxanorbornene) derivatives. *Meso* dyads are associated with *trans* dyads, and *rac* dyads with *cis* dyads. Whether this correlation is the result of the proposed propagation mechanism for classical catalysts (Figure 3) or other factors is not understood at this point. Certainly, the chloro ligands in catalyst **8** and the allyl ligands in catalyst **9** are essentially inert whereas the aqua ligands of catalyst **7** are relatively labile.^{13,25} Based on the model, the observation that catalyst **7** gave the most atactic polymer among the ruthenium catalysts studied implies that the aqua ligand dissociation rate is comparable to the polymer propagation rates. The kinetics of dissociation of various ligands and olefins on the metal center are currently being investigated.

The *cis* and highly syndiotactic poly(**1**) prepared using the well-defined tungsten catalyst **6** could be the result of chain-end control (Figure 12). The incoming monomer **1** adds alternately from the frontside and backside due to steric hindrance imposed by the 5,6 position of the carbon atoms in **1**. The syn-anti rotation of the carbene double bond must be slower than monomer addition. Moreover, the addition of related norbornene monomer to anti configuration of the catalyst are generally much faster than addition to its syn form (Figure 13).[Oskam, J.H.; Schrock, R.R. J. Am. Chem. Soc. 1993, 115, 11831] The diisopropyl groups on the catalyst could be preventing the addition of monomer **1** with O-7 on the same side as the arylamido group (Figure 14). It is also probable that the addition of the monomer with O-7 on the opposite side of the arylamido ligand to be caused by prior coordination of the O-7 to the W center since tetrahydrofuran is known to coordinate to the tungsten center.

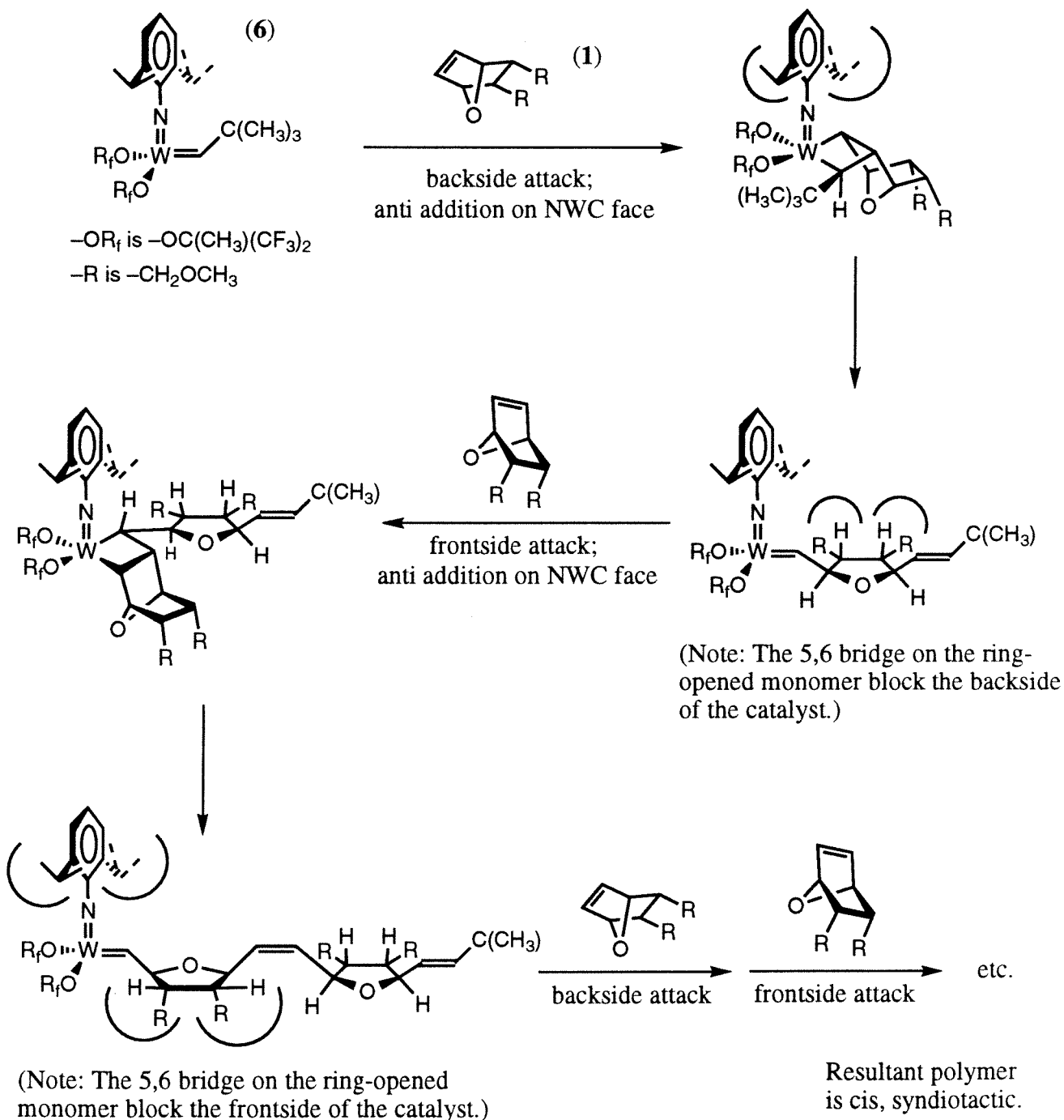


Figure 12. Proposed mechanism for observed cis-syndiotactic polymer when **1** is polymerized by **6**. This chain-end control mechanism is probably induced by the 5,6 bridge of **1**, and the diisopropyl substituents on the aromatic ring of the catalyst, and possible prior coordination of O-7 of **1** to the W center.

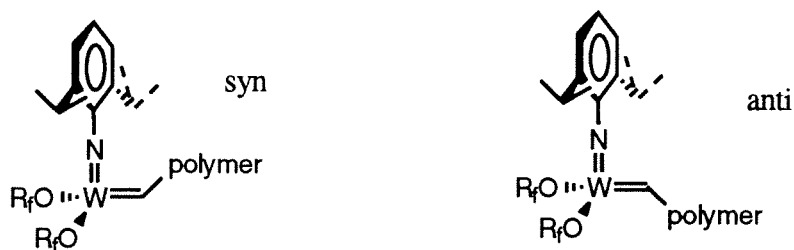


Figure 13. syn and anti forms of the well-defined tungsten catalyst **6**.

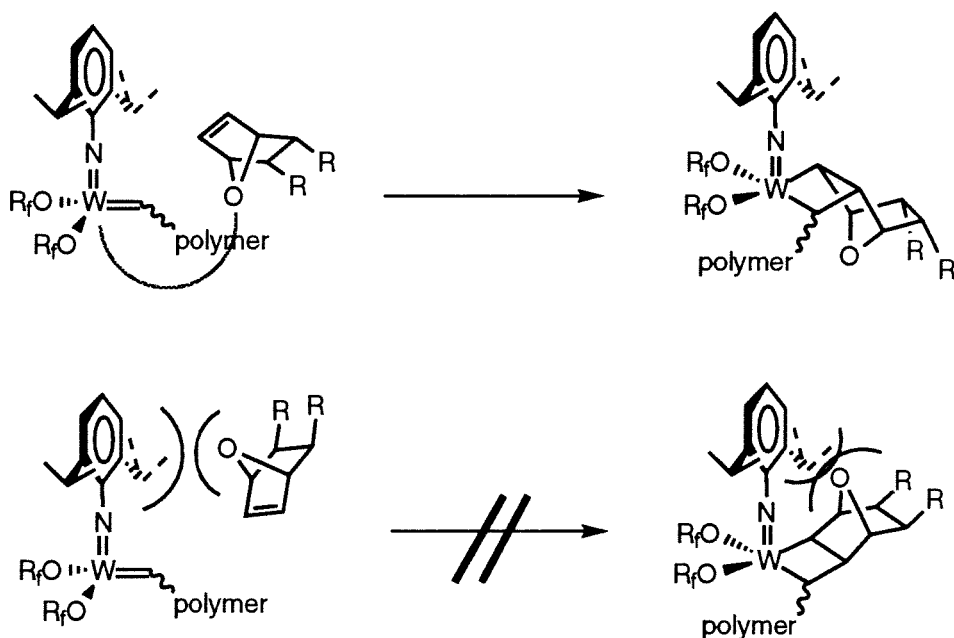


Figure 14. Proposed method of addition of monomer to the propagating tungsten species. It is possible that O-7 of the monomer coordinates to the W center prior to metathesis of the double bond.

Conclusion

By employing a wide variety of methods, the microstructure of poly(**1**) was assigned. In particular, tacticities were determined by hydrogenation of the polymers (which removed double bond isomerism), and also by ROMP of (*S*)-endo-5-methoxymethyl-7-oxanorbornene (**2S**) (which related head-tail isomerism with tacticity). Polymers prepared from $W(CH-t-Bu)(NAr)(OCMe(CF_3)_2)_2$ {Ar = 2,6-diisopropylphenyl} (**6**) have all *cis* double bonds and are highly syndiotactic, while those

from $\text{RuCl}_3 \cdot 3\text{H}_2\text{O}$ (**8**) and $[\text{RuCl}(\mu\text{-Cl})(\eta^3\text{:}\eta^3\text{-C}_{10}\text{H}_{16})]_2$ { $\text{C}_{10}\text{H}_{16}$ = 2,7-dimethyloctadienediyl} (**9**) have a high *trans* double bond content and are highly isotactic. Polymers prepared from $[\text{Ru}(\text{H}_2\text{O})_6](\text{tosylate})_2$ (**7**) exhibit roughly equal amounts of *cis* and *trans* double bonds that are randomly distributed in the polymer chain, and are atactic. The apparent correlation between double bond isomerism and tacticity for classical hexacoordinated metal center is consistent with the model proposed by Ivin and coworkers.

II. The Influence of Hydroxyl Group on the Cis:Trans Ratio of Internal Olefins during the Isomerization of Terminal Olefins to Internal Olefins by $\text{Ru}(\text{H}_2\text{O})_6\text{tos}_2$

Introduction

The ability to control the synthesis of substances with a specified stereochemistry is undoubtedly one of the most important issues in organic synthesis. Towards this end, recognition of functional groups that can direct the production of a stereospecific product are important. Hydroxyl groups are well known to direct the stereochemistry of several reactions. The hydrogenation of several alkenols by Crabtree's catalyst is a classic example of hydroxy-mediated stereoselective reaction.²⁶⁻³⁰ In general, the knowledge of the reaction mechanism is essential for a rational approach to synthesis. Olefin isomerization by classical catalysts generally proceed by either the addition and subsequent elimination of a metal-hydride across the unsaturation, or through the formation of a π -allyl metal hydride by abstraction of a hydrogen from the olefin (Figures 1 & 2).³¹⁻³⁴

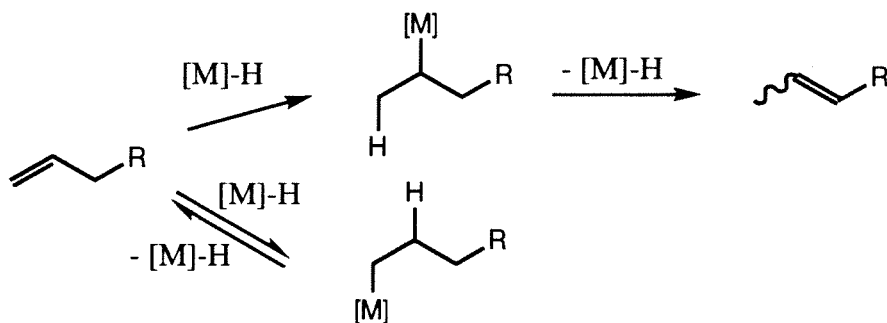


Figure 1. Metal hydride addition-elimination pathway

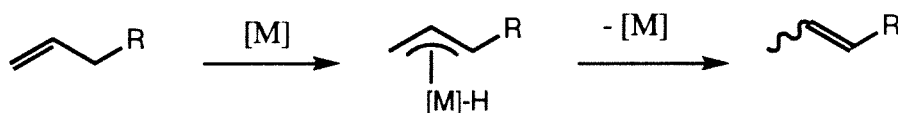


Figure 2. π -allyl metal hydride pathway

Our group has recently been interested in the mechanism of olefin isomerization reaction by $\text{Ru}(\text{H}_2\text{O})_6\text{tos}_2$ (**7**). **7** is a well-known catalyst for the ring-opening metathesis reaction of

cyclic olefins.¹² The reduction of the molecular weight of the polymer by the addition of acyclic olefins have been investigated.³⁵

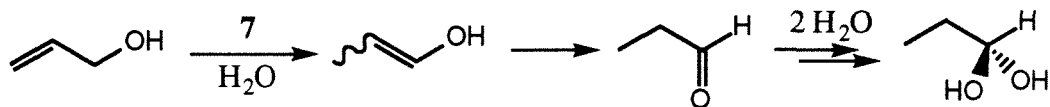


Figure 3. The isomerization of 2-propen-1-ol (allyl alcohol).

Recently, McGrath showed that 2-propen-1-ol cleanly isomerize to propanal in the presence of **7** (Figure 3).³⁶ From the products observed from labeling and crossover studies (Figure 4), the mechanism is most consistent with a selective ruthenium hydride addition-elimination pathway (Figure 1).³⁶ The ruthenium hydride presumably adds exclusively in a

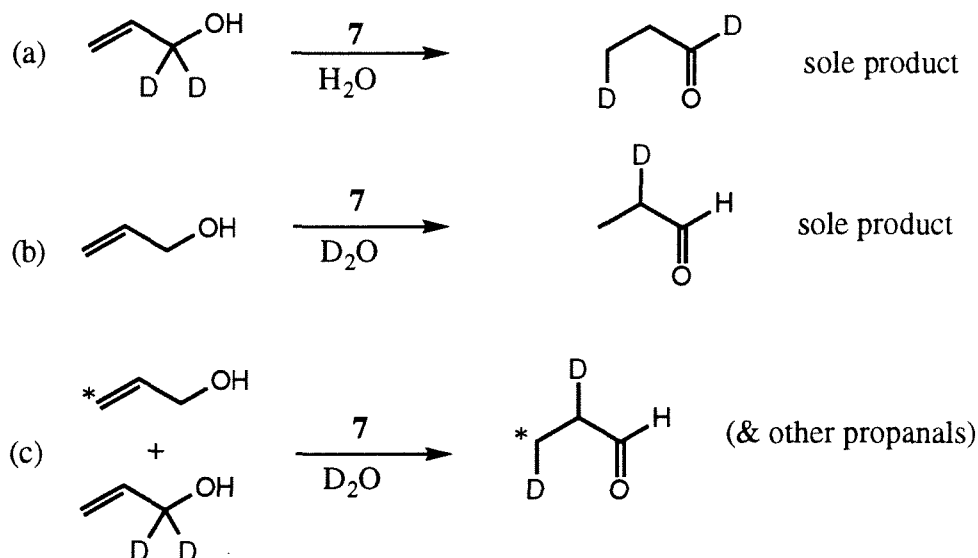


Figure 4. (a) Isomerization of allyl alcohol into 1-propanol, and subsequent hydrolysis. (b) The deuteration of C2 of propanal occurred during the hydrolysis of 1-propanol. (c) Crossover product demonstrating the intermolecularity of the reaction. * = ¹³C-labeled

Markovnikov fashion to the double bond of the allyl alcohol, then undergo β -elimination with the deuterium to regenerate the ruthenium-deuteride species to start the catalytic cycle again.³⁶ This curious exclusive Markovnikov addition is postulated to be directed by the

hydroxyl functionality in the allyl alcohol.³⁷ Indeed, though 4-pentenol was isomerized to 3-pentenol by **7**, there was no reaction observed with 3-butenol by **7**.³⁶ A $[(\text{H}_2\text{O})_4\text{Ru}(\eta(\text{O}):\eta(\text{C},\text{C}')\text{-HOCH}_2\text{CH}_2\text{CH}=\text{CH}_2)](\text{tosylate})_2$ species has also been isolated. Moreover, a crystal structure of the product $\text{Ru}(\text{H}_2\text{O})_2(\text{C}_5\text{H}_7\text{O}_2)_2$ from reaction of 3-pentenoic acid with **7** also revealed the coordination of both the oxygen and double bond to the Ru center.³⁸ These results show that double bond migrate only up to a certain specified distance from the oxygen functionality (i.e., 3 bonds away) because this presumably gives the ideal "bite" for coordination of double bond and oxygen group to the Ru center.

In this chapter, we report the effect of oxygen group on the cis/trans ratio of the internal olefin during the isomerization of oxygen-containing terminal olefins to internal olefins by **7**.

Results and Discussion

$\text{Ru}(\text{H}_2\text{O})_6\text{tos}_2$ (**7**) catalyzes the isomerization of several terminal olefins to internal olefins. In general, it was observed that further isomerization of the internal olefins is difficult. Unless specified otherwise, the isomerization is generally very clean, with no formation of side products. In general, about 25 eq. of the olefin was mixed with **7** in a 15% solution of $\text{CD}_3\text{OD}/\text{C}_6\text{D}_6$. The homogeneous solution was freeze-pump-thawed degassed thrice and refilled with Ar. The reaction was monitored at 50°C by variable temperature ^1H NMR to near completion. Figures 5, 6 & 7 summarized the reactions with various olefins.

As can be seen from Figures 5 & 6, the ratio of cis : trans product formed is strongly dependent on whether there is a hydroxyl functionality at correct distance from the olefinic double bond or not. To take a specific example, when 2-allylphenol was reacted, the cis : trans ratio of the product 2-(1-propenyl)phenol observed at various percent

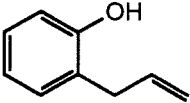
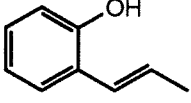
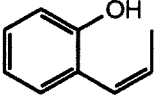
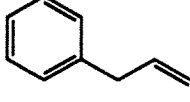
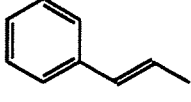
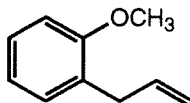
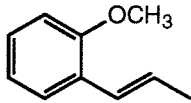
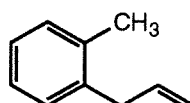
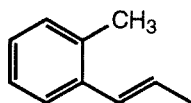
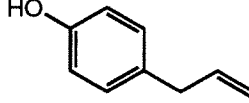
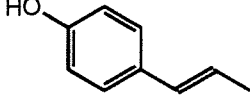
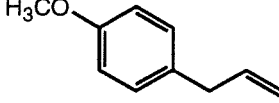
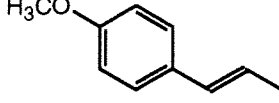
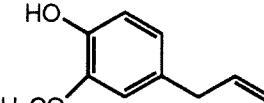
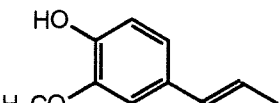
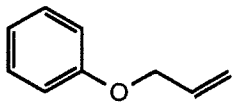
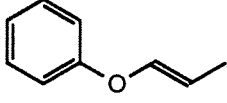
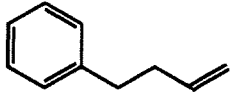
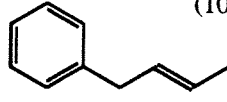
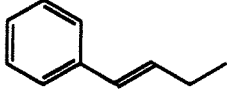
Reactant	Products	
 2-allylphenol	 trans-2-(1-propenyl)phenol	(1:1)  cis-2-(1-propenyl)phenol
 allylbenzene	 trans-1-propenylbenzene	
 2-allylanisole	 trans-2-(1-propenyl)anisole	
 2-allyltoluene	 trans-2-(1-propenyl)toluene	
 4-allylphenol	 4-(1-propenyl)phenol	
 4-allylanisole	 4-(1-propenyl)anisole	
 4-allyl-2-methoxyphenol	 trans-2-methoxy-4-(1-propenyl)phenol	
 allylphenylether	 phenyl(1-propenyl)ether	
 3-butenylbenzene	 trans-2-butenylbenzene	(10:1)  trans-1-butenylbenzene

Figure 5. Isomerization of terminal olefins to internal olefins catalyzed by 7. The right hand column shows the only products observed. Values in parenthesis are ratios of products observed.






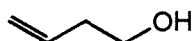
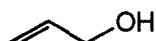
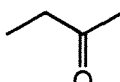
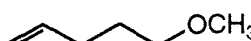
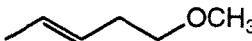



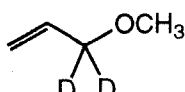
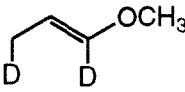
Reactant	Kinetic Products
	
	 :  (1 : 1)
	no isomerization; chelation observed (McGrath)
	
	
	no isomerization; chelation observed (McGrath)
	
	 (McGrath)

Figure 6. Effect of distance of hydroxyl group to olefin bond in determining the product ratio observed. Except for 3-buten-1-ol, the ether group does not participate. Value in parenthesis is the ratio of products observed. Some substrates were first studied by D.V.McGrath (thesis), as indicated above.

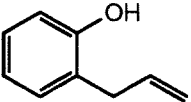
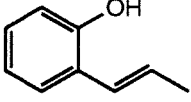
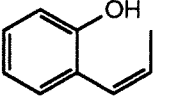
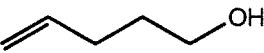
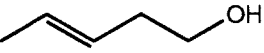
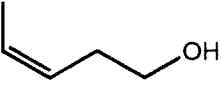

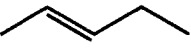
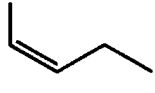
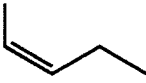
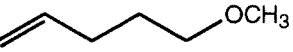
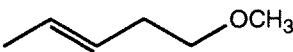
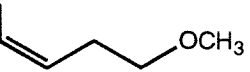
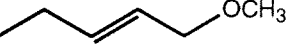
Reactant	Products
 2-allylphenol	<div>  :  </div> <div> trans-2-(1-propenyl)phenol cis-2-(1-propenyl)phenol </div> <div> 51.7% : 48.3% at 37% conversion 50.5% : 49.5% at 66% conversion 54.3% : 45.7% at 81% conversion 56.6% : 43.4% at 94% conversion </div>
	<div>  :  </div> <div> 50 % : 50 % at 43% conversion 81.7% : 18.3% at 84% conversion </div>
	<div>  :  </div> <div> all : none at 91.3% conversion 84% : 16% at 97 % conversion </div>
	only 12% isomerized to trans even after 12 hrs; about 1.5% isomerized back to terminal olefin
	<div>  :  :  </div> <div> practically all : 0 : 0 even at 57.5% conversion </div>

Figure 7. Product ratios at different conversion, showing that hydroxyl group (that are at a correct distance from the olefin bond) plays a role in determining product ratios whereas the ether group does not.

conversion are given in Figure 7. Hence the ratio is approximately 1 : 1 even when more than half of the terminal olefin has isomerized. In contrast, when allylbenzene is isomerized to 1-propenylbenzene, only trans product is detected by ^1H NMR throughout the reaction. To ensure that the cis-1-propenylbenzene is never formed in the above reaction, when cis-1-propenylbenzene was reacted with **7**, after a day, only 2.3% of cis-1-propenylbenzene had isomerized to trans-1-propenylbenzene. To further rule out the possibility that the active species catalyzing the isomerization reaction can only be formed through the presence of terminal olefins, when a 37% : 63% mixture of allylbenzene and cis-1-propenylbenzene was allowed to react with **7**, only the allylbenzene was isomerized to trans-1-propenylbenzene. Figure 7 shows the kinetic products early in the reaction gradually transforming into the thermodynamic product at long reaction time.

The oxygen functionality in the terminal olefin should be a hydroxyl group in order for this 1:1 ratio of cis/trans product to be observed. When 2-allylanisole is used, even at 93% conversion, only trans-2-(1-propenyl)anisole is detected. Similarly, only trans-2-(1-propenyl)toluene is observed when allyltoluene is isomerized.

The distance between the hydroxyl functional to the olefinic double bond is important. When 4-allylphenol is used, only trans-4-(1-propenyl)phenol is observed, since the distance between the olefinic double bond to the hydroxyl group is too great for any chelation with **7**.

Based on the above observations, and absence of further data, a possible mechanism of selective Ru-hydride addition-elimination mechanism that can account for such cis/trans ratio is given in Figure 8 (Another possible mechanism is presented in the Appendix). The conformation of the cyclic intermediate (**10**) determines the stereochemical outcome of the product (Figure 8). In the absence of the hydroxyl group, **10** becomes **11**. The rotation about the C2-C3 bond of intermediate **11** may "make possible" the assumption of the thermodynamically more stable configuration where the methyl and ethyl substituents in **12** will not be eclipsed during the 4-centered transition state β -hydrogen abstraction by

the Ru center (Figure 9). This results in the near exclusive formation of trans olefin. In contrast, the presence of the hydroxyl group in **10** constrains the rotation about the C2-C3 axis by the formation of the stable six-member ring intermediate (cf **12** vs **13**). **13** can only β -eliminate with $H_{\text{pro-cis}}$ to give the cis olefin, while **14** can only β -eliminate with $H_{\text{pro-trans}}$ to give the trans olefin (Figure 9).

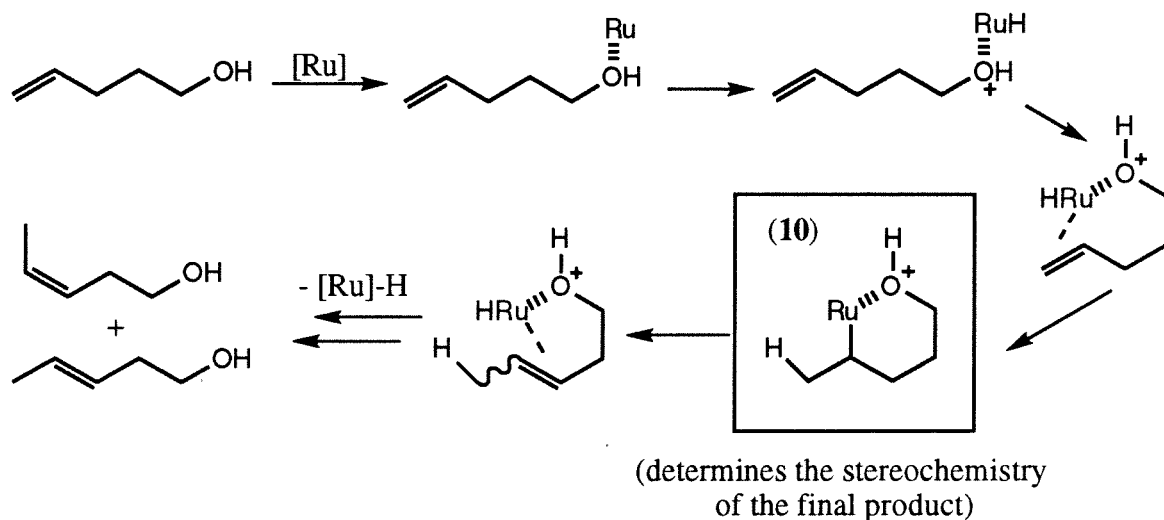
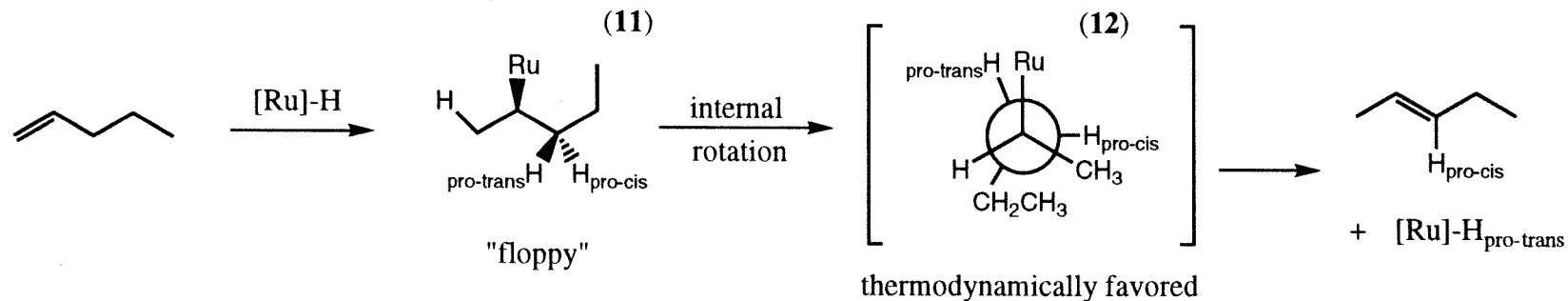


Figure 8. A proposed mechanism for the isomerization of hydroxyl-containing olefin.

This mechanism presumes that the dissociation of the Ru-O "bond" is slower than the insertion of the Ru-H across the olefinic bond. Since the dissociation (or exchange rate) of H_2O ligand of **7** is $1.8 \times 10^{-2} \text{ s}^{-1}$ and therefore one to three orders of magnitude less than the typical rate of addition of metal-hydride addition across the olefin bond, this mechanism might be plausible.^{13,39,40}

The above proposed mechanism accounted for all the observed product ratios observed with non-aromatic olefins (Figures 6 & 7). The only exception is the case of 3-butenol and 3-butenyl methyl ether. McGrath had observed the formation of a bidentate olefin complex of both compounds with **7**.³⁶ We may only speculate that such formation hampers the addition of Ru-H across the olefin bond. Halpern and Okamoto have shown that for $RhH_2Cl(PPh_3)_3$, the greater the stability of the Rh π -bonded adduct, the slower is

- In the absence of hydroxyl group



- In the presence of hydroxyl group

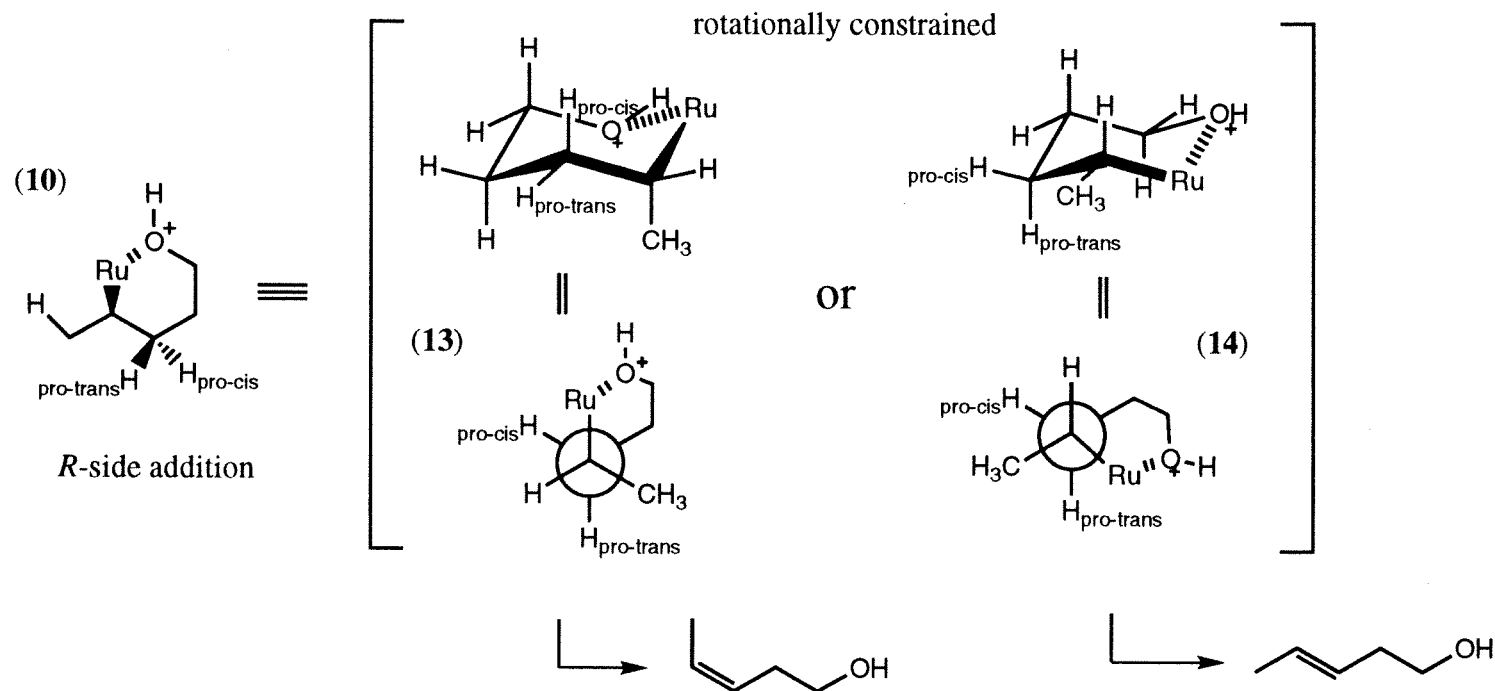


Figure 9. Proposed selective Ru-H addition-elimination mechanism for olefin isomerization.

the rate of insertion of the hydride.⁴¹ 3-butenyl methyl ether is thus the only ether studied thus far that not only won't isomerize to the trans 2-butenyl methyl ether, but also shuts down the isomerization as well. In fact, no isomerization of 1-pentene is observed when 3-butenyl methyl ether is present in the solution.

(Note: About half a year after these studies were conducted, Karlen and Ludi published a similar study involving mostly non-hydroxyl containing terminal olefins. Although only one hydroxyl-containing olefin was used in their published results, they were able to measure the kinetic parameters associated with the isomerization of this 4-allyl-2-methoxyphenol. A very negative $\Delta S^\ddagger = -180 \text{ J K}^{-1} \text{ mol}^{-1}$ strongly suggested an associative pathway.)⁴²

Conclusion

The cis/trans ratio of the internal olefins formed from the isomerization of terminal olefins by $\text{Ru}(\text{H}_2\text{O})_6(\text{tosylate})_2$ is strongly influenced by whether there is a hydroxyl group present in the terminal olefins. The presence of the hydroxyl group at the correct distance from the olefinic double bond results in an initial formation of equal amount of cis and trans double bond in the internal olefins. This is different from the near exclusive formation of the trans double bond when the hydroxyl group is not present. These results are consistent with the selective Ru-hydride addition-elimination mechanism where the hydroxyl group directs the addition of the Ru-hydride across the olefin double bond.

Experimental Section

Instrumentation. ^1H and ^{13}C NMR spectra were acquired on Jeol GX-400 (399.65 MHz ^1H), optical rotation measured on Jasco DIP-181 Digital Polarimeter, IR spectra on Perkin-Elmer 1600 Series FTIR, polymer molecular weight on gel permeation

chromatography (GPC) column (American Polymer Standard, Porosity: Linear 10mm, methylene chloride) on Knauer Differential Refractometer relative to polystyrene standard.

Materials and Methods. All manipulations of air- and/or moisture sensitive compounds were carried out under argon using standard Schlenk and vacuum line techniques. Argon was purified by passing through columns of activated BASF RS-11 (ChemalogTM) oxygen scavenger and Linde 4A molecular sieves. Solids were weighed in dry box equipped with a MO-40-1 purification train. Solvents were purified as follows: benzene, tetrahydrofuran, and toluene were distilled from sodium benzophenone ketyl into solvent flasks equipped with Teflon screw-type valves; chlorobenzene, chloroform, and dichloromethane were distilled from calcium hydride under vacuum into small Schlenk flasks and subsequently freeze-pump-thaw degassed. Absolute ethanol was used directly from a new bottle without further drying.

$\text{RuCl}_3 \cdot 3\text{H}_2\text{O}$ (**8**) (Johnson-Matthey), $\text{RhCl}(\text{PPh}_3)_3$ (Aldrich), *p*-toluenesulfonylhydrazide (Aldrich), were obtained commercially and used directly without further purification. Catalysts **6**, **7**, and **9** were prepared by previously reported procedures.⁴³⁻⁴⁵ Monomers **1** and **3** were prepared by previously reported procedures.^{12b,46} (*R,S*)-*endo*-7-oxanorbornene-5-carboxylic acid, (*R*)-(+)- and (*S*)-(-)-*endo*-7-oxanorbornene-5-carboxylic acid were prepared from previously reported procedures with the following modification.⁴⁷

(*R,S*)-*endo*-7-oxanorbornene-5-carboxylic acid. Acrylic acid (21.6 g, 0.3 mol), furan (40.8 g, 0.6 mol), and hydroquinone (0.1 g) were stirred under Ar for 90 days. From 32 g of the mixture (ca. 50% conversion), (*R,S*)-*endo*-7-oxanorbornene-5-carboxylic acid, (*R,S*)-*exo*-7-oxanorbornene-5-carboxylic acid, and unreacted acrylic acid were separated by silica gel flash chromatography using 1:2 hexane-diethylether (done in 4 g increments).

Endo-isomer : ^1H NMR δ (CDCl_3): 6.45 (d), 6.44 (d), 5.18 (d), 5.03 (d), 3.15 (qn), 2.11 (ddd), 1.55 (dd). ^{13}C NMR δ (CDCl_3): 177.97 (C_7), 137.18 (C_3), 132.62 (C_2), 79.05 (C_4), 78.62 (C_1), 42.76 (C_5), 28.38 (C_6).

Exo-isomer: ^1H NMR δ (CDCl_3): 6.41 (d), 6.35 (d), 5.21 (s), 5.10 (d), 2.47 (dd), 2.15 (dt), 1.60 (dd). ^{13}C NMR δ (CDCl_3): 179.50 (C_7), 137.16 (C_3), 134.49 (C_2), 80.92 (C_4), 78.02 (C_1), 42.63 (C_5), 29.21 (C_6).

(*R*)-(+)-*endo*-7-oxanorbornene-5-carboxylic acid.⁴⁷ 1.7 g of white solid (*R,S*)-*endo*-7-oxanorbornene-5-carboxylic acid (12.3 mmol) was dissolved in minimum amount of absolute ethanol. (*S*)-(-)- α -methylbenzylamine (1.49 g, 12.3 mmol) was added. Resultant salt was recrystallized four times in hot ethanol, redissolved in water and finally passed through cation ion-exchange resin (Dowex 50X2-400 previously treated with HCl and rinsed until Cl^- free). Product was obtained by pumping off the solvent under vacuum. $[\alpha]_{\text{D}}^{22} = 98.7$ in EtOH. Optical purity = 89%. Analogous procedure was followed for (*S*)-(-)-*endo*-7-oxanorbornene-5-carboxylic acid using (*R*)-(+)- α -methylbenzylamine.

(*S*)-*endo*-5-methoxymethyl-7-oxanorbornene (**2S**). LiAlH_4 (0.25 g, 6.69 mmol) in THF (5 mL) was added to stirred solution of (*R*)-(+)-*endo*-7-oxanorbornene-5-carboxylic acid (1 g, 7.14 mmol) in THF. After the mixture has been heated to 60°C for 10 hours, water was added and the salts were filtered off. The filtrate was dried with MgSO_4 , and the solvent rotovapped off. The product 7-oxanorbornene-5-carbinol was redissolved in THF, and NaH (0.2 g) added. Iodomethane (0.5 mL) was syringed into the solution and the mixture stirred for three hours. Water was added, followed by copious amount of ether. After the salts were filtered off and filtrate dried with MgSO_4 , the solvent was rotovapped off. The crude product was purified via Kugelrohr at 50°C , 0.01 mm Hg. After redrying with NaH, the product was vacuum distilled into a Schlenk tube. Total yield: 40-61%. **2R** is prepared in similar manner.

^1H NMR δ (CDCl_3): 6.35 (dd), 6.23 (dd), 4.97 (d), 4.91 (d), 3.29 (m), 3.27 (s), 2.48 (qn), 2.1.97 (ddd), 0.66 (dd). ^{13}C NMR δ (CDCl_3): 136.27 (C_3), 132.32 (C_2), 79.54 (C_4), 78.23 (C_1), 75.32 (C_7), 37.75 (C_5), 27.95 (C_6).

For comparison, the (*R,S*)-*exo*-isomer, synthesized in similar manner, has the following δ . ^1H NMR δ (CDCl_3): 6.28 (s), 6.28 (s), 4.91 (d), 4.81 (s), 3.35 (m), 3.34 (s), 1.80 (m), 1.35 (dd), 1.21 (m). ^{13}C NMR δ (CDCl_3): 135.72 (C_3), 134.93 (C_2), 79.45 (C_4), 77.74 (C_1), 75.66 (C_7), 58.78 (C_8), 37.94 (C_5), 28.45 (C_6).

General Procedure for Polymerization using $\text{W}(\text{CH-}i\text{-Bu})(\text{NAr})(\text{OCMe}(\text{CF}_3)_2)_2$ {Ar = 2,6- C_6H_3 -*i*-Pr $_2$ } (**6**). Monomer (1.26 mmol, degassed and NaH-dried) was added to -40°C solution of **6** (20 mg, 0.0252 mmol) in toluene (2 mL). Solution was gradually warmed to room temperature. After 1.5 hours, wet acetone (2 mL) was added into the reaction mixture. Polymer was obtained by pumping off the solvent or by adding the reaction mixture to pentane. Yield: 40-75%.

General Procedure for Polymerization using $[\text{Ru}(\text{H}_2\text{O})_6](\text{tosylate})_2$ (**7**). Monomer (0.3 mmol, degassed) was added to a stirred solution of **7** (3.5 mg, 0.0063 mmol) in previously degassed water (0.5 mL) under Ar. These immiscible liquids were stirred vigorously and heated to 50°C. White solid polymer can be detected within a minute. After an hour, the polymer was dissolved in 50 mL ethanol, reprecipitated in 200 mL 0.02 M Na_2EDTA /water, and dried overnight under vacuum. Yield: quantitative.

General Procedure for Polymerization using $\text{RuCl}_3 \cdot 3\text{H}_2\text{O}$ (**8**). In a typical experiment, a stirred solution of **8** (33 mg, 0.126 mmol) in chlorobenzene (1.5 mL) and absolute ethanol (1 mL) was degassed. Monomer (5.79 mmol, degassed) was added to this solution which was then heated to 50°C for 30 hours. The resultant viscous solution was poured into ethanol, centrifuged, and liquid portion precipitated into water. Typical yield: 48%.

General Procedure for Polymerization using $[\text{RuCl}(\mu\text{-Cl})(\eta^3\text{:}\eta^3\text{-C}_{10}\text{H}_{16})]_2$ $\{\text{C}_{10}\text{H}_{16} = 2,7\text{-dimethyloctadienediyl}\}$ (**9**). Monomer (0.3 mmol, degassed) was added to stirred solution of **9** (3.8 mg, 0.00617 mmol) in CH_2Cl_2 (0.15 mL) and then heated to 50°C for 12-24 hours. Viscous solution was then filtered through silica gel. Polymer was obtained by pumping off the solvent. Yield: ca 70%.

General Procedure for Hydrogenation of Polymer using *p*-toluenesulfonylhydrazide. Polymer (0.8 g, 4.34 mmol in double bond) was dissolved in hot xylene (30 mL, 60°C). TsNHNH_2 (4.63 g, 24.9 mmol) was added, and the solution gradually heated to 110°C and maintained for 3 hours. The hot solution was decanted and cooled. Xylene was distilled off under vacuum. Polymer was isolated using silica gel flash chromatography in THF/ligroin.

Hydrogenation of poly(*exo,exo*-5,6-bis(methoxymethyl)-7-oxanorbornene) with $\text{RhCl}(\text{PPh}_3)_3/\text{H}_2$. In the dry box, $\text{RhCl}(\text{PPh}_3)_3$ was added to a solution of polymer in toluene in a Fisher-Porter bottle. Nitrogen gas was pumped off from the bottle, and the bottle was repressurized with hydrogen gas (40 psi). The solution was heated to 50°C for 8 hours and then filtered through silica gel. Product was isolated by pumping off solvent.

Typical procedure for isomerization of terminal olefins to internal olefins. In a J-Young (sealable) NMR tube, about 50 μL of the olefin (passed through alumina) was mixed with 0.5 mL C_6D_6 and 0.1 mL CD_3OD . About 10 mg of **7** was added. The tube was immediately freeze-pump-thaw degassed three times, and refilled with Ar. By variable-temperature ^1H NMR, the solution was heated to 50°C . The reaction was monitored every few minutes for an hour (typical time when about 50% conversion of terminal olefin is isomerized to the internal olefin). Typically, the reaction was monitored until it was at least 90% complete. ^{13}C NMR was also taken to ensure the correct identification of all products. If necessary, APT, ^1H - ^1H COSY, and ^1H - ^{13}C HETCOR were also taken.

References and Notes

- (1) (a) For a survey of catalysts and monomers used in ring-opening metathesis polymerization up to 1985, see Dragutan, V.; Balaban, A.T.; Dimonie, M. *Olefin Metathesis and Ring Opening Polymerization of Cycloolefins* Wiley, New York, **1985**. (b) Schrock, R.R. *Acc. Chem. Res.* **1990**, *23*, 158. (c) Grubbs, R.H.; Tumas, W. *Science* **1989**, *243*, 907.
- (2) (a) Ivin, K.J. *Olefin Metathesis*, Academic Press, London, **1983**, p. 216. Further refinements and variations to the mechanism are found in (b) Greene, R.M.E.; Ivin, K.J.; McCann, G.M.; Rooney, J.J. *Makromol. Chem.* **1987**, *188*, 1933. (c) Greene, R.M.E.; Hamilton, J.G.; Ivin, K.J.; Rooney, J.J. *Makromol. Chem.* **1986**, *187*, 619. (d) Hamilton, J.G.; Ivin, K.J.; McCann, G.M.; Rooney, J.J. *Makromol. Chem.* **1985**, *186*, 1477. (e) Hamilton, J.G.; Ivin, K.J.; McCann, G.M.; Rooney, J.J. *J. Chem. Soc. Chem. Commun.* **1984**, 1379.
- (3) (a) Sailor, M.J.; Ginburg, E.J.; Gorman, C.B.; Kumar, A.; Grubbs, R.H.; Lewis, N.L. *Science*, **1990**, *249*, 1146. (b) Bazan, G.C.; Schrock, R.R. *Macromolecules* **1991**, *24*, 817. (c) Klavetter, F.L.; Grubbs, R.H. *J. Am. Chem. Soc.* **1988**, *110*, 7807. (d) Schlund, R.; Schrock, R.R.; Crowe, W.E. *J. Am. Chem. Soc.* **1989**, *111*, 8004.
- (4) Seymour, R.B.; Carraher, C.E. *Structure-Property Relations in Polymers* Plenum Press, New York, **1984**.
- (5) Gilliom, L.R.; Grubbs, R.H. *J. Am. Chem. Soc.* **1986**, *108*, 733.
- (6) (a) Bazan, G.C.; Oskam, J.H.; Cho, H.N.; Park, L.Y.; Schrock, R.R. *J. Am. Chem. Soc.* **1991**, *113*, 6899. (b) Bazan, G.C.; Schrock, R.R.; Cho, H.N.; Gibson, V.C. *Macromolecules* **1991**, *24*, 4495. (c) Bazan, G.C.; Khosravi, E.; Schrock, R.R.; Feast, W.J. *J. Am. Chem. Soc.* **1990**, *112*, 8378.

- (7) (a) Stelzer, F.; Grubbs, R.H.; Leising, G. *Polymer* **1991**, 32, 1851. (b) Risse, W.; Grubbs, R.H. *J. Mol. Catal.* **1991**, 65, 211. (c) Park, L.Y.; Schrock, R.R.; Stielitz, S.G.; Crowe, W.E. *Macromolecules* **1991**, 24, 3489. (d) Cannizzo, L.F.; Grubbs, R.H. *Macromolecules* **1988**, 21, 1961. (e) Risse, W.; Grubbs, R.H. *Macromolecules* **1989**, 22, 1558.
- (8) (a) Wu, Z.; Wheeler, D.R.; Grubbs, R.H. *J. Am. Chem. Soc.* **1992**, 114, 146. (b) Schlund, R.; Schrock, R.R.; Crowe, W.E. *J. Am. Chem. Soc.* 1989, 111, 8004. (c) Klavetter, F.; Grubbs, R.H. *J. Am. Chem. Soc.* **1988**, 110, 7807.
- (9) Polymer microstructure can be affected by such mundane effect as stirring the solution. Katz, T.J.; Acton, N. *Tetrahedron Lett.* **1976**, 4251.
- (10) (a) Leconte, M.; Bilhou, J.L.; Reimann, W.; Basset, J.M. *J. Chem. Soc. Chem. Commun.* **1978**, 341. (b) Leconte, M.; Basset, J.M. *J. Am. Chem. Soc.* **1979**, 101, 7296. (c) Calderon, N.; Lawrence, J.P.; Ofstead, E.A. *Adv. Organomet. Chem.*, **1979**, 17, 449. (d) Casey, C.P. Albin, L.D.; Burkhardt, T.J. *J. Am. Chem. Soc.* **1977**, 99, 2533. (e) Katz, T.J.; McGinnis, J. *J. Am. Chem. Soc.* **1975**, 97, 1592.
- (11) For samples of poly(norbornene)-derivatives microstructure characterization, see Ho, H.T.; Ivin, K.J.; Reddy, B.S.; Rooney, J.J. *Eur. Polym. J.* **1989**, 25, 805. and references 5 to 13 cited therein
- (12) (a) Novak, B.M.; Grubbs, R.H.; *J. Am. Chem. Soc.* **1988**, 110, 960. (b) Novak, B.M.; Grubbs, R.H. *J. Am. Chem. Soc.* **1988**, 110, 7542.
- (13) Rapaport, I.; Helm, L.; Merbach, A.E.; Bernhard, P.; Ludi, A. *Inorg. Chem.* **1988**, 27, 873. The ligand-exchange rate constant for hexaaquaruthenium(II) tosylate at 298°K is $1.8 \times 10^{-2} \text{ s}^{-1}$. Although small compared to that of other transition metals, the rate constant is the largest among homoleptic hexacoordinated ruthenium (II) complexes.

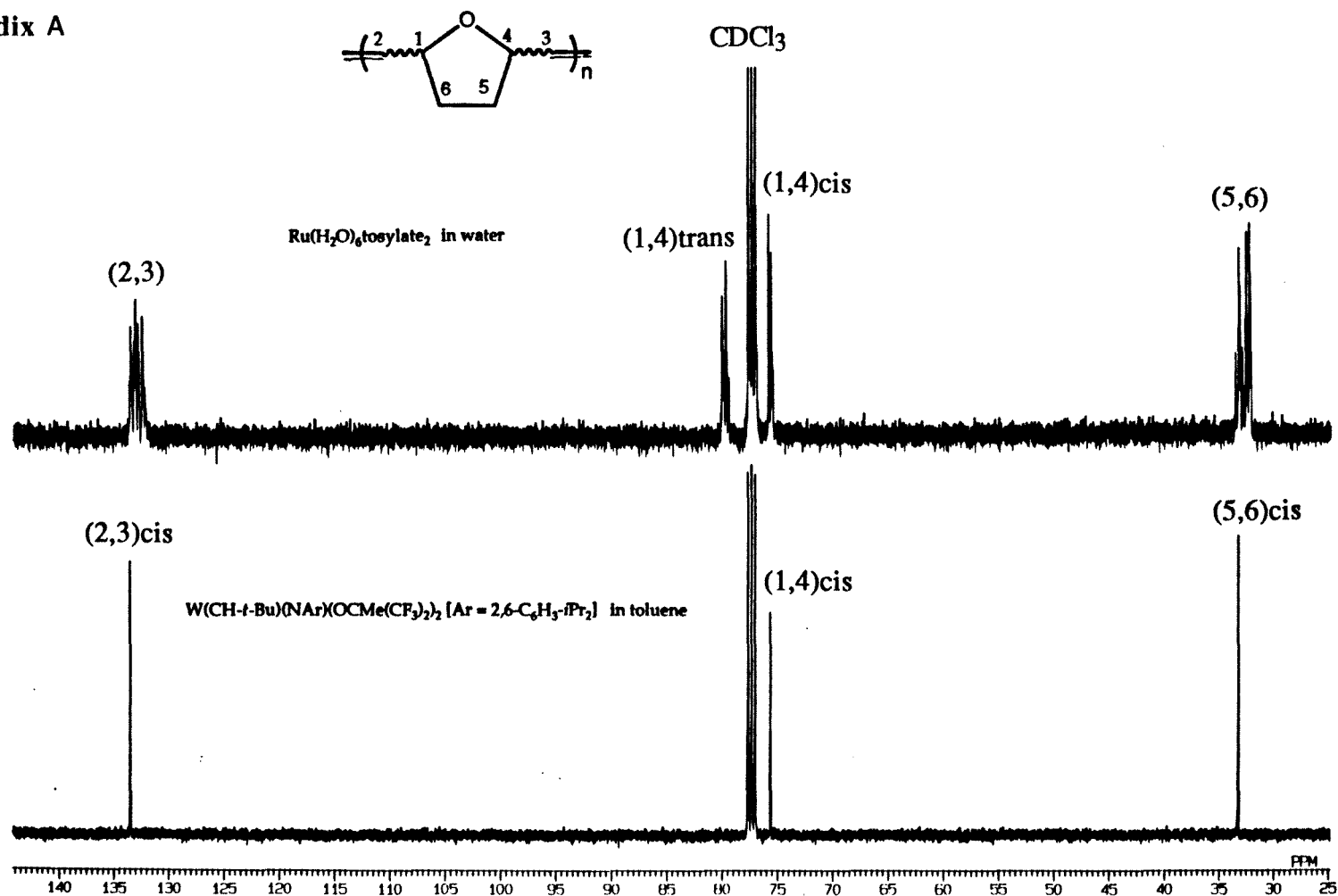
- (14) (a) Bailey, O.; Ludi, A. *Inorg. Chem.* **1985**, *24*, 2582. Bernhard, P.; Lehmann, H.; Ludi, A. *J. Chem. Soc. Chem. Commun.* **1981**, 1216. (b) Stebler-Rothlisberger, M.; Hummel, W.; Pittet, P.A.; Burgi, H.B.; Ludi, A.; Merbach, A.E. *Inorg. Chem.* **1988**, *27*, 1358.
- (15) For general discussions of these concepts, see (a) Ivin, K.J. *Olefin Metathesis* Academic Press, London, **1983**. (b) Bovey, F.A. *Chain Structure and Conformation of Macromolecules* Academic Press, New York, **1982**. (c) Tonelli, A. *NMR Spectroscopy and Polymer Microstructure : the Conformation Connection* VCH Publishers, New York, **1989**.
- (16) Feast, W.J.; Harrison, D.B. *Polymer*, **1991**, *32*, 558.
- (17) (a) Dorman, D.E.; Jautelat, M.; Roberts, J.D. *J. Org. Chem.* **1971**, *36*, 2757. (Erratum: See *J. Org. Chem.* **1971**, *38*, 4217.) (b) Chen, H.Y. *Appl. Polym. Spectroscopy* **1978**, *7*, 688. Gatti, G.; Carbonaro, A. *Makromol. Chem.* **1974**, *175*, 1627. (c) Woelfenden, W.R.; Grant, D.M. *J. Am. Chem. Soc.* **1966**, *88*, 1496. (d) Grant, D.M.; Cheney, B.V. *J. Am. Chem. Soc.* **1967**, *89*, 5315.
- (18) Ivin, K.J.; Lavery, D.T.; Rooney, J.J. *Makromol. Chem.* **1977**, *178*, 1545.
- (19) T_1 (relaxation time) difference between $C(tc)$, $C(tt)$ is negligible for the same C type being compared. Ivin and Rooney have measured T_1 's (relaxation time) of same types of carbon in poly(norbornene) using the standard inversion recovery sequence and found them essentially constant (0.56 ± 0.08 s). Ivin, K.J.; Lavery, D.T.; O'Donnell, J.H.; Rooney, J.J.; Stewart, C.D. *Makromol. Chem.* **1979**, *180*, 1989.
- (20) Ivin, K.J.; Lavery, D.T.; Rooney, J.J.; Watt, P. *Recl. Trav. Chim. Pays-Bas* **1977**, *96*, 54. For a revised interpretation of the NMR of hydrogenated polymer cited above, see Hamilton, J.G.; Ivin, K.J.; Rooney, J.J. *Br. Polym. J.* **1984**, *16*, 21.

- (21) In general, only large pendant groups attached to the bridgehead carbon of norbornene influences the microstructure of the polymer. Certain bulky substituents on the bridgehead carbon of 7-oxanorbornene derivative shut down the polymerization completely. Novak, B.M., Grubbs, R.H. unpublished results.
- (22) Extensive microstructural studies on poly(norbornene) derivatives to date has been carried out by the groups of Ivin and Rooney. The olefin region of polymers from 5,5-dimethylnorbornene, *endo*-5-methylnorbornene, *exo*-5-methylnorbornene, *endo*-5-(COOCH₃)-norbornene, *exo*-5-(COOCH₃)-norbornene and *all* that of 5-substituted norbornene that has been studied to date always shows TH, TT, HH, to HT olefin carbons in increasing upfield chemical shifts. Papers with the monomers cited above are: (a) Devine, G.I.; Ho, H.T.; Ivin, K.J.; Mohamed, M.A.; Rooney, J.J. *J. Chem. Soc. Chem. Commun.* **1982**, 1229. (b) Ho, H.T. Ivin, K.J.; Rooney, J.J. *J. Mol. Catal.* **1982**, 15, 245. (c) Ivin, K.J.; Rooney, J.J.; Bencze, L.; Hamilton, J.G.; Lam, L.M.; Lapienis, G.; Reddy, B.; Thoi, H.H. *Pure Appl.Chem.* **1982**, 54, 447. (d) Ivin, K.J.; Lapienis, G.; Rooney, J.J. *Polymer* **1980**, 21, 436.
- (23) The solvent is usually chlorobenzene mixed with a small amount of ethanol.
- (24) A value greater than unity implies blockiness in the polymer *cis-trans* microstructure, while a value less than unity implies the alternation of *cis* and *trans* along the polymer backbone. A random occurrence of *cis* and *trans* bonds gives a value of unity. Value as high as 8.8 have been reported using norbornene with WCl₆/cocatalyst.
- (25) Head, R.A.; Nixon, J.F.; Swain, J. R.; Woodard, C.M. *J. Organomet. Chem.* **1974**, 76, 393.
- (26) Evans, D.A.; Morrissey, M.M. *Tetrahedron Lett.* **1984**, 25, 4637.
- (27) Brown, J.M.; Hall, S.A. *Tetrahedron Lett.* **1984**, 25, 1393.
- (28) Crabtree, R.H.; Davis, M.W. *Organometallics* **1983**, 2, 681.

- (29) Brown, J.M.; Naik, R.G. *J. Chem. Soc. Chem. Commun.* **1982**, 348.
- (30) Thompson, J.W.; McPherson, E. *J. Am. Chem. Soc.* **1974**, 96, 6232.
- (31) Collman, J.P.; Hegedus, L.S.; Norton, J.R.; Finke, R.G. *Principles and Applications of Organotransition Metal Chemistry*; University Science Books: Mill Valley, 1987.
- (32) Cramer, R. *J. Am. Chem. Soc.* **1966**, 88, 2272.
- (33) Tolman, C.A. *J. Am. Chem. Soc.* **1972**, 94, 2994.
- (34) Hendrix, W.T.; von Rosenberg, J.L. *J. Am. Chem. Soc.* **1976**, 98, 4850.
- (35) France, M.B.; Grubbs, R.H.; McGrath, D.V.; Paceillo, R.A. *Macromolecules* **1993**, 26, 4742.
- (36) McGrath, D.V.; Grubbs, R.H. *Organometallics* **1994**, 13, 224.
- (37) Curiously, on the time scale of the reaction, no hydrogen exchange occurred between the ruthenium-hydride and the protic solvent in the course of isomerization.
- (38) McGrath, D.V.; Grubbs, R.H.; Ziller, J.W. *J. Am. Chem. Soc.* **1991**, 113, 3611.
- (39) For kinetics of metal-hydride insertion, see (a) Doherty, N.M.; Bercaw, J.E. *J. Am. Chem. Soc.* **1985**, 107, 2670. and references therein. (b) Pearson, R.G. *Chem. Rev.* **1985**, 85, 41. (c) Halpern, J. *Inorganica Chim. Acta* **1985**, 100, 41.
- (40) For additional information on the kinetics and reactions of **7**, see (a) Bernhard, P. Helm L.; Ludi, A.; Merbach, A.E. *J. Am. Chem. Soc.* **1985**, 107, 312. (b) Bernhard, P.; Helm, L.; Rapaport, I.; Ludi, A.; Merbach, A.E. *J. Chem. Soc., Chem. Commun.* **1984**, 302. (c) Aebischer, N.; Laurency, G.; Ludi, A.; Merbach, A.E. *Inorg. Chem.* **1993**, 32, 2810. (d) Laurency, G.; Helm, L.; Ludi, A.; Merbach, A.E. *Helv. Chim. Acta* **1991**, 74, 1236.
- (41) Halpern, J.; Okamoto, T.; *Inorg. Chim. Acta* **1984**, 89, L53.
- (42) Karlen, T.; Ludi, A. *Helv. Chim. Acta* **1992**, 75, 1604.
- (43) Schrock, R.R.; Depue, R.T.; Feldman, J.; Schaverien, C.J.; Dewan, J.C.; Liu, A.H. *J. Am. Chem. Soc.* **1988**, 110, 1423.

- (44) Bernhard, P.; Biner, M.; Ludi, A. *Polyhedron* **1990**, *9*, 1095.
- (45) (a) Cox, D.; Roulet, R. *Inorg. Chem.* **1990**, *29*, 1360. (b) Porri, L.; Gallazzi, M.; Colombo, A.; Allegra, G. *Tetrahedron Lett.* **1965**, 4187.
- (46) (a) Mirsadeghi, S.; Rickborn, B. *J. Org. Chem.* **1985**, *50*, 4340. (b) De Lucchi, O.; Lucchini, V.; Pasquato, L.; Modena, G. *J. Org. Chem.* **1984**, *49*, 597.
- (47) (a) Suami, T.; Ogawa, S.; Nakamoto, K.; Kasahara, I. *Carbohydrate Res.* **1977**, *58*, 240. (b) Ogawa, S.; Kasahara, I.; Suami, T. *Bull. Chem. Soc. Jpn.* **1979**, *52*, 118.

Appendix A



45

Figure A1. ^{13}C NMR spectrum of poly(7-oxabicyclo[2.2.1]hept-2-ene) catalyzed by $\text{Ru}(\text{H}_2\text{O})_6\text{tos}_2$ in water (top spectrum) and $\text{W}(\text{=CH-}t\text{-Bu})(\text{NAr})(\text{OCMe}(\text{CF}_3)_2)_2$ [Ar = 2,6- $\text{C}_6\text{H}_3\text{-}i\text{Pr}_2$] in toluene (bottom spectrum). The bottom spectrum showed a pure cis polymer. NMR solvent is CDCl_3 .

M_1 = cyclopentene

M_2 = norbornene

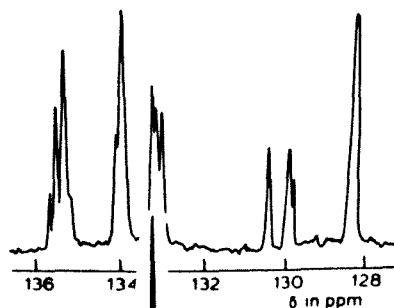
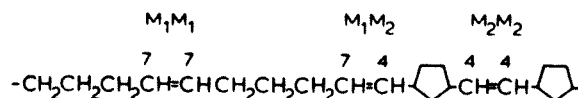
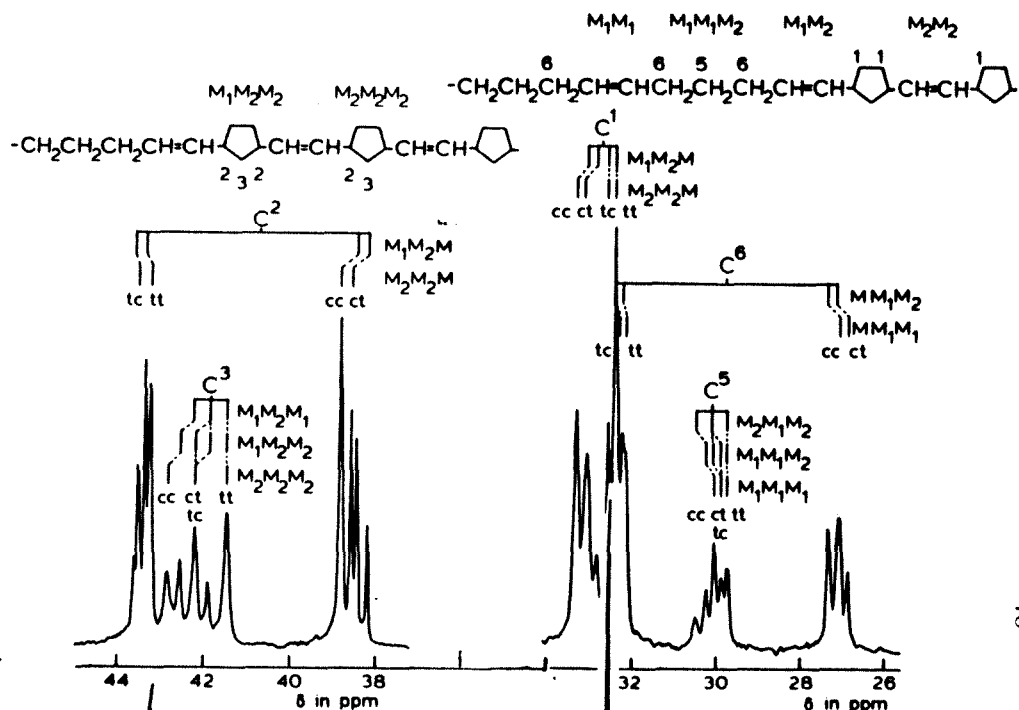
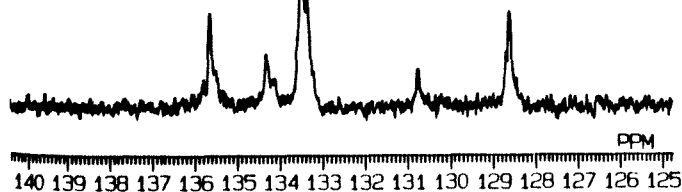


Fig. 2. Expansion of the olefinic region of Fig. 1. Peak positions are given in Tab. 1.



b) Expansion of the C^1 and C^2 regions of Fig. 1. Peak positions for C^1 are given in Tab. 3 and for C^2 in Tab. 4. M denotes the more reactive component of the triad, and may be M_1 or M_2 .

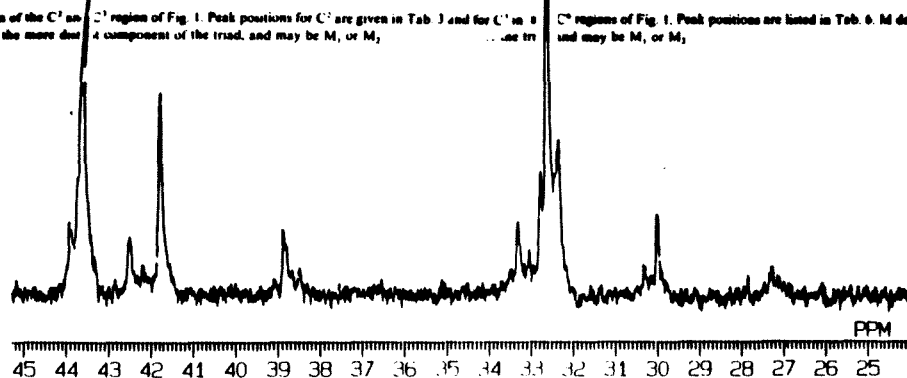


Figure A2. ^{13}C NMR spectrum of the copolymer of norbornene and cyclopentene when $Ru(H_2O)_6tos_2$ (in methanol) was used as catalyst (bottom spectrum). Ratio of reactants used is norbornene : cyclopentene : $Ru(H_2O)_6tos_2$ = 12.5 : 122.8 : 1. The cyclopentene-norbornene junction can clearly be seen. The top spectrum is copied from literature (Ivin, et al. Pure Appl. Chem. 1982, 54, 447.) where $WCl_6/(C_6H_5)_4Sn$ in chlorobenzene was used. Note that not all cyclopentene reacted.

Appendix B (Isomerization of Olefins by $\text{Ru}(\text{H}_2\text{O})_6\text{tos}_2$)

Figure B1 gives an alternative mechanism to that of Figure 8 in Chapter 1 Section II. Figure B2 rationalizes possible unreactivity of 3-buten-1-ol. Figure B3 shows the observed experimental ratio of products observed by D.V.McGrath (thesis, California Institute of Technology 1993). A careful examination of the two mechanisms show that neither fully account for the observed ratio.

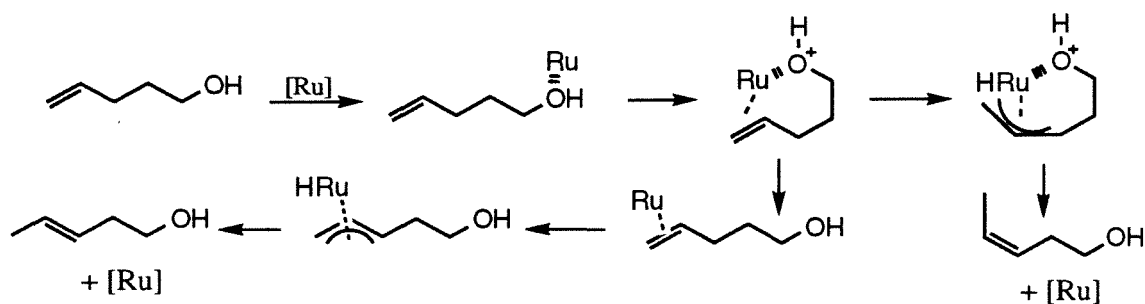
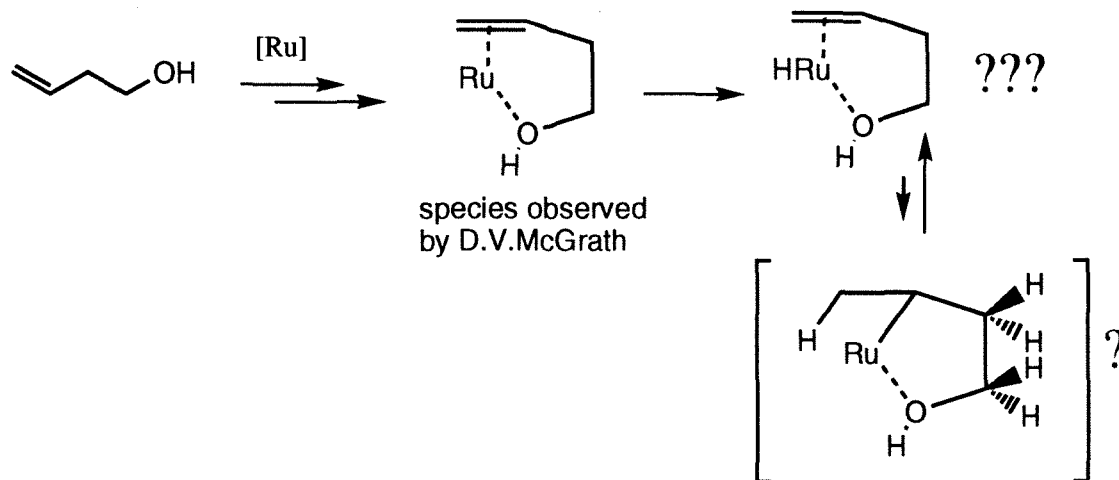


Figure B1. Modified Allyl-H Mechanism.

- selective Ru-H addition-elimination mechanism



- modified allyl-H mechanism

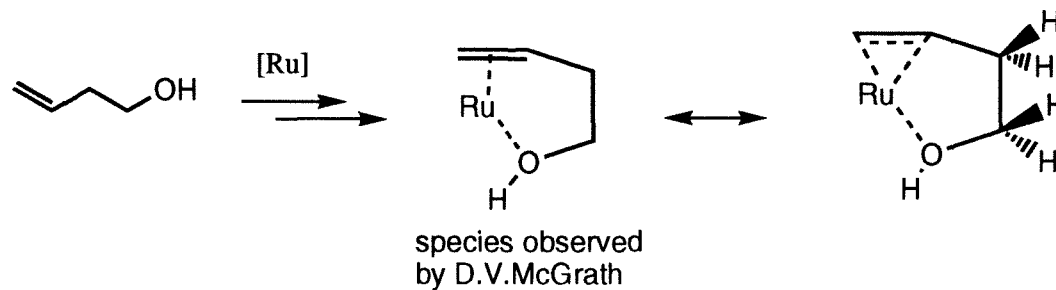
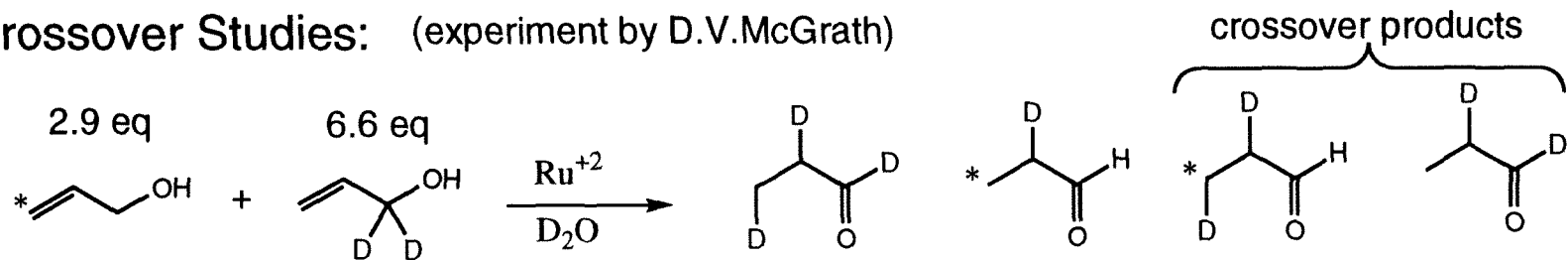


Figure B2. Proposed mechanism for unreactivity of 3-buten-1-ol.

Crossover Studies: (experiment by D.V.McGrath)



modified allyl hydride mech. (theoretical)	69.5%	30.5%	0%	0%
modified metal-H add.-elim. (theoretical)	48.3%	9.3%	21.2%	21.2%

modified allyl hydride mech. (theoretical)	100 %	0%
modified metal-H add.-elim. (theoretical)	30.5%	69.5%
observed	66%	34%

6

Another mechanism?

1. If dinuclear allyl-hydride mechanism, ratio of crossover products should change as the solution is diluted. Rate of exchange could be calculated by varying the concentration of ^{13}C vs deuterium labeled reactants.
2. If isotope effect involved in rate-determining step in modified metal-H add.-elim., then rate of reaction of deuterium-labeled should be different from non-labeled.

Figure B3. Isomerization of Allyl Alcohol Revisited.

Chapter 2

**Living Ring-Opening Metathesis Polymerization of
Bicyclo[2.2.1]hept-2-ene and Bicyclo[3.2.0]hept-2-ene
Catalyzed by $\text{Cl}_2(\text{PPh}_3)_2\text{Ru}(=\text{CHCHCPh}_2)$**

Introduction

Our group recently demonstrated a group VIII metal-carbene complex as possible intermediate in the ring-opening metathesis polymerization (ROMP) of bicyclo[2.2.1]hept-2-ene (norbornene) (**1**) in a solution of $\text{CH}_2\text{Cl}_2/\text{C}_6\text{H}_6$.¹ Specifically, a ^1H NMR signal ($\delta = 17.79$ ppm) attributed to the α -proton of the propagating vinylcarbene species was shown to appear, disappear, and reappear again when $\text{Cl}_2(\text{PPh}_3)_2\text{Ru}(=\text{CHCHCPh}_2)$ (**4**) was reacted sequentially with norbornene, 2,3-dideutero-norbornene, and norbornene, respectively. Because of the unusual stability of **4** in protic media, and the scarcity of data on this particular system, we were motivated to explore the details of the polymerization. In particular, the kinetics of the reactions of **4** with **1**, and with bicyclo[3.2.0]hept-2-ene ("substituted cyclobutene") (**2**) will be studied in order better understand how to prepare block copolymers.^{2,3} The molecular weight of the polymers formed will be regulated with and without the presence of chain-transfer agents. Some characterization of the polymers will also be presented.

Results and Discussion

Reaction of bicyclo[2.2.1]hept-2-ene (**1**) with $\text{Cl}_2(\text{PPh}_3)_2\text{Ru}(=\text{CHCHCPh}_2)$ (**4**).

One of the criteria for living polymerization is the linear variation of the molecular weight of the polymer with the extent of reaction.⁴ When **4** was reacted with successively increasing concentration of **1** in dichloromethane at 40°C , a linear increase in the molecular weight of the polymer was observed (Figure 1). The polydispersity index (**PDI**) ranges from 1.31 to 1.15, consistent with values normally observed for a living polymerization. The double bonds in poly(**1**) is about 88% trans, a value higher than that observed when $\text{Ru}(\text{H}_2\text{O})_6\text{tosylate}_2$ was used (see chapter 1). Poly(**1**) was hydrogenated with p-toluenesulfonylhydrazide in xylene, but tacticity information cannot be obtained by ^{13}C NMR.⁵

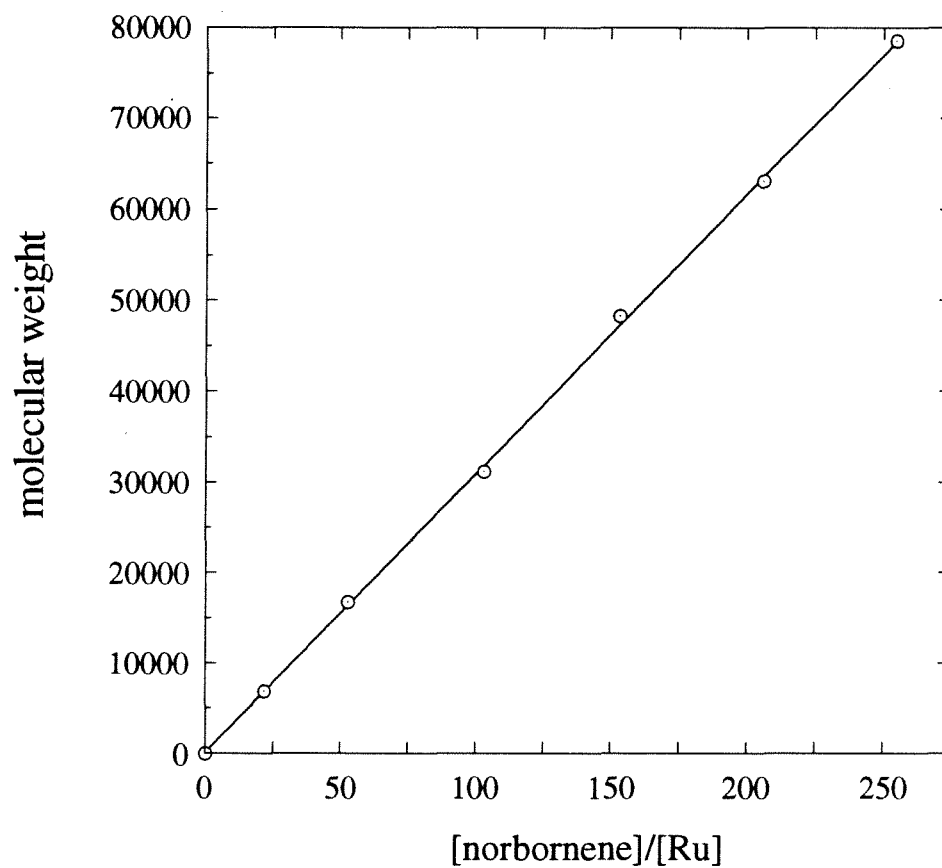


Figure 1. Molecular weight of polymer versus [monomer]/[catalyst] in the polymerization of 1 by 4 in dichloromethane at 40°C. Mol. wt. is relative to polystyrene standard. Correlation coefficient = 0.999

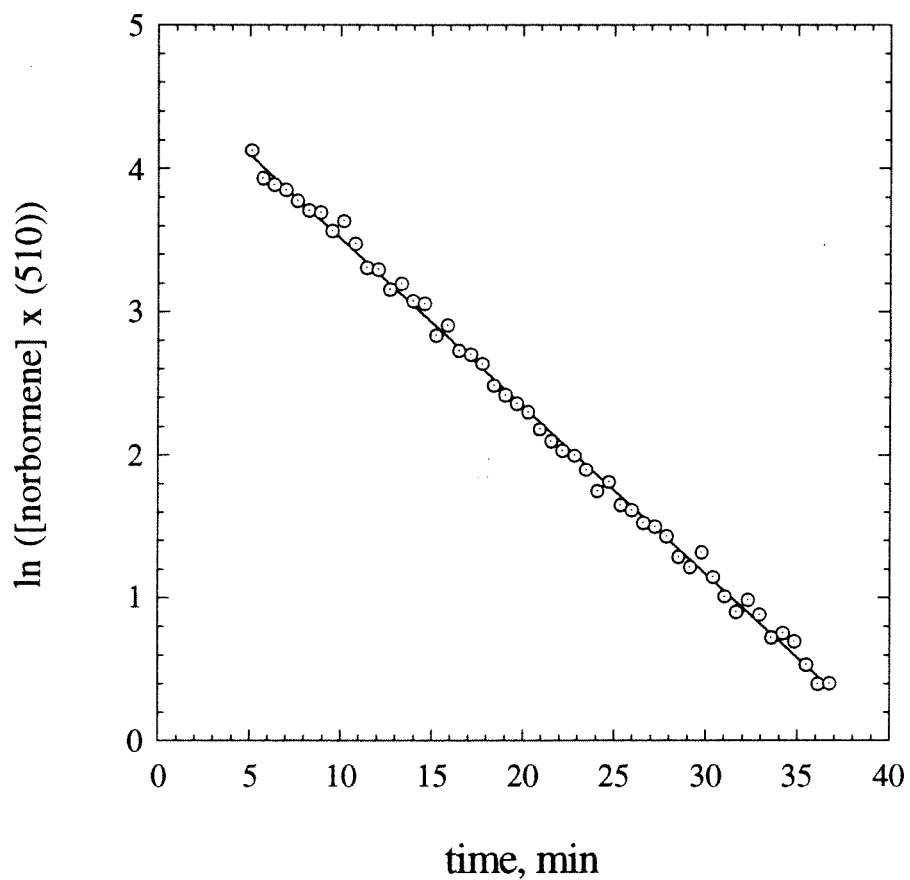


Figure 2. Determination of specific rate constant of propagation during polymerization of bicyclo[2.2.1]hept-2-ene (norbornene) catalyzed by **3** (Ru) in dichloromethane at 40°C. Correlation coefficient = 0.999

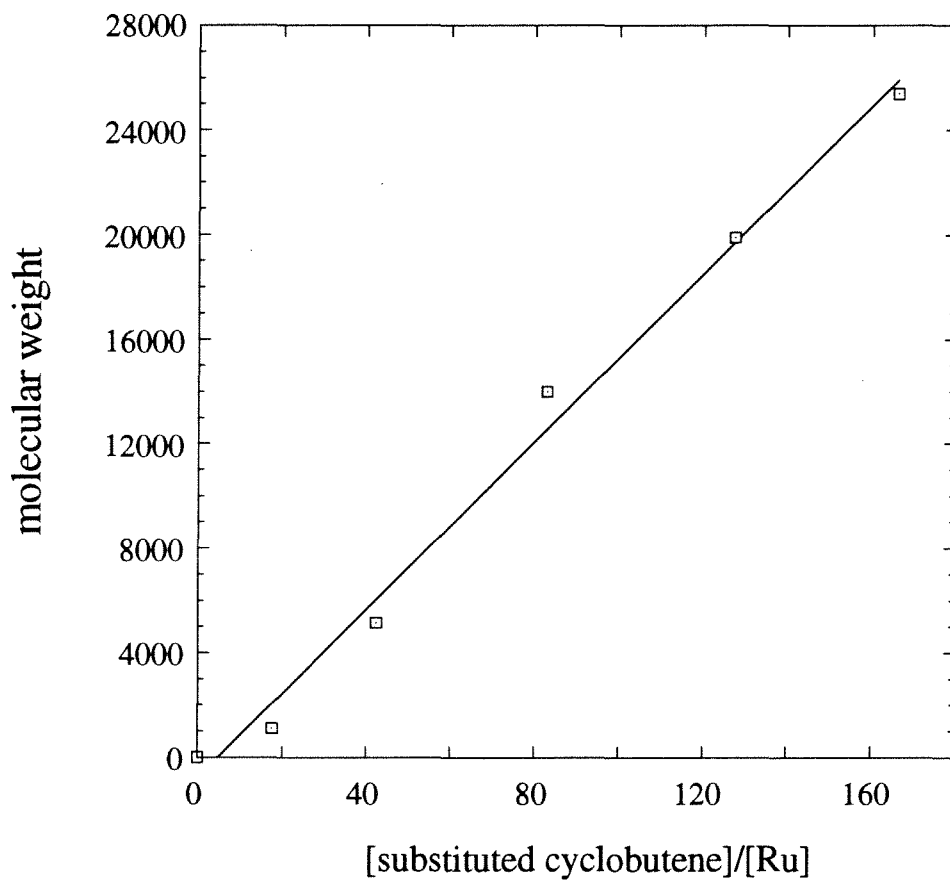


Figure 3. Molecular weight of polymer versus [monomer]/[catalyst] in the polymerization of 2 by 4 in dichloromethane at 40°C. Mol. wt. is relative to polystyrene standard. Correlation coefficient = 0.996

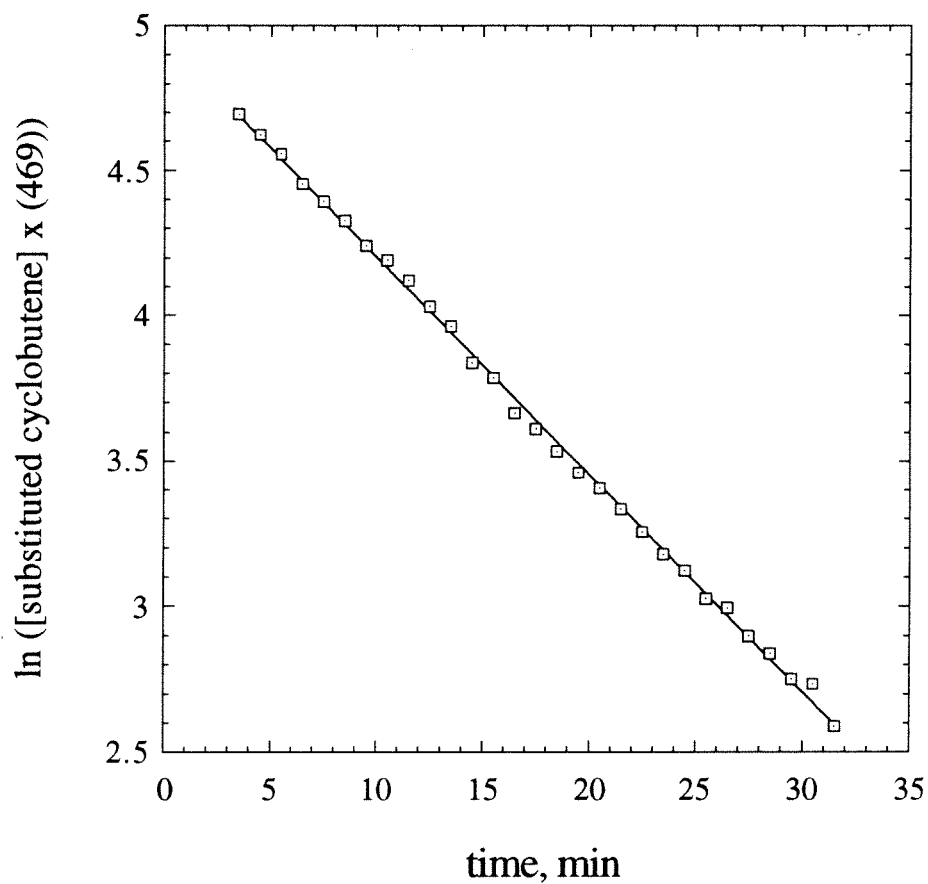


Figure 4. Determination of specific rate constant of propagation during polymerization of bicyclo[3.2.0]hept-2-ene (subst. cyclobutene) catalyzed by 3 (Ru) in dichloromethane at 40°C. Correlation coefficient = 0.999

The specific propagation rate constant k_p (or k_{nn}) of the reaction of **1** catalyzed by **4** in dichloromethane was $0.23 \text{ M}^{-1} \text{ s}^{-1}$ at 40°C (Figure 2). k_p/k_i (where k_i is specific rate of initiation) was determined to be $55 (\pm 15)$ at 40°C .⁶ By ^1H NMR, a single propagating species **5** was observed ($\alpha\text{-H}$ of propagating vinylcarbene **5** in CD_2Cl_2 is $\delta = 17.65$ ppm (pseudoquartet; $^3J_{\text{HP}} = 10 \text{ Hz}$ and $^3J_{\text{H}\alpha\text{H}\beta} = 10 \text{ Hz}$) of). By ^{31}P NMR (reference H_3PO_4), only the propagating species **5** at 30.06 ppm was observed.

Reaction of bicyclo[3.2.0]hept-2-ene (**2**) with $\text{Cl}_2(\text{PPh}_3)_2\text{Ru}(=\text{CHCHCPh}_2)$ (**4**).

Similarly, when **4** was reacted with successively increasing concentration of **2** in dichloromethane at 40°C , a linear increase in the molecular weight of the polymer was observed (Figure 3). The polydispersity index ranges from 1.48 to 1.22. In contrast to poly(**1**), the double bonds in poly(**2**) is about 43% trans.⁷ Upon hydrogenation with *p*-toluenesulfonylhydrazide, hydrogenated poly(**2**) exhibits no tacticity (as indicated by the presence of equal amounts of meso and racemo dyads in Figure 5).⁸

The specific propagation rate constant k_p (or k_{cc}) of the reaction of **2** catalyzed by **4** in dichloromethane was $0.183 \text{ M}^{-1} \text{ s}^{-1}$ at 40°C (Figure 4). k_p/k_i (where k_i is specific rate of initiation) was equal to 7 at 40°C ; hence, the catalyst **4** initiates better with **2** rather than with **1**. In contrast with the reaction of **4** with **1**, three discrete propagating species **6**, **7**, and **8** were observed at $\delta = 18.07$ (multiplet), $\delta = 17.36$ (doublet), $\delta = 16.96$ (doublet) (Figure 6). From the coupling patterns observed at low-temperature ^1H NMR, **6**, **7**, and **8** were most consistent with being a diphosphine adduct, monophosphine adduct, and monophosphine adduct, respectively (Figure 6).⁹ At -40°C , the ratio of **6** : **7** : **8** were 7.96 : 1.6 : 1.0 but gradually raising the temperature to 40°C results in a ratio of 2.01 : 1.88 : 1.00. Hence, higher temperature leads to greater dissociation of a PPh_3 ligand from diphosphine adduct **6** to form monophosphines **7** and **8**. By ^{31}P NMR, immediately after **2** was added to **4**, free phosphine ($\delta = -4.9$ ppm) was observed together with propagating species at $\delta = 41.70$ (broad) and $\delta = 29.17$ ppm (Figure 7). The ratio of intensity of the peaks at $\delta = 41.70$ and $\delta = 29.17$ in the ^{31}P NMR at 40°C (which is consistent with the

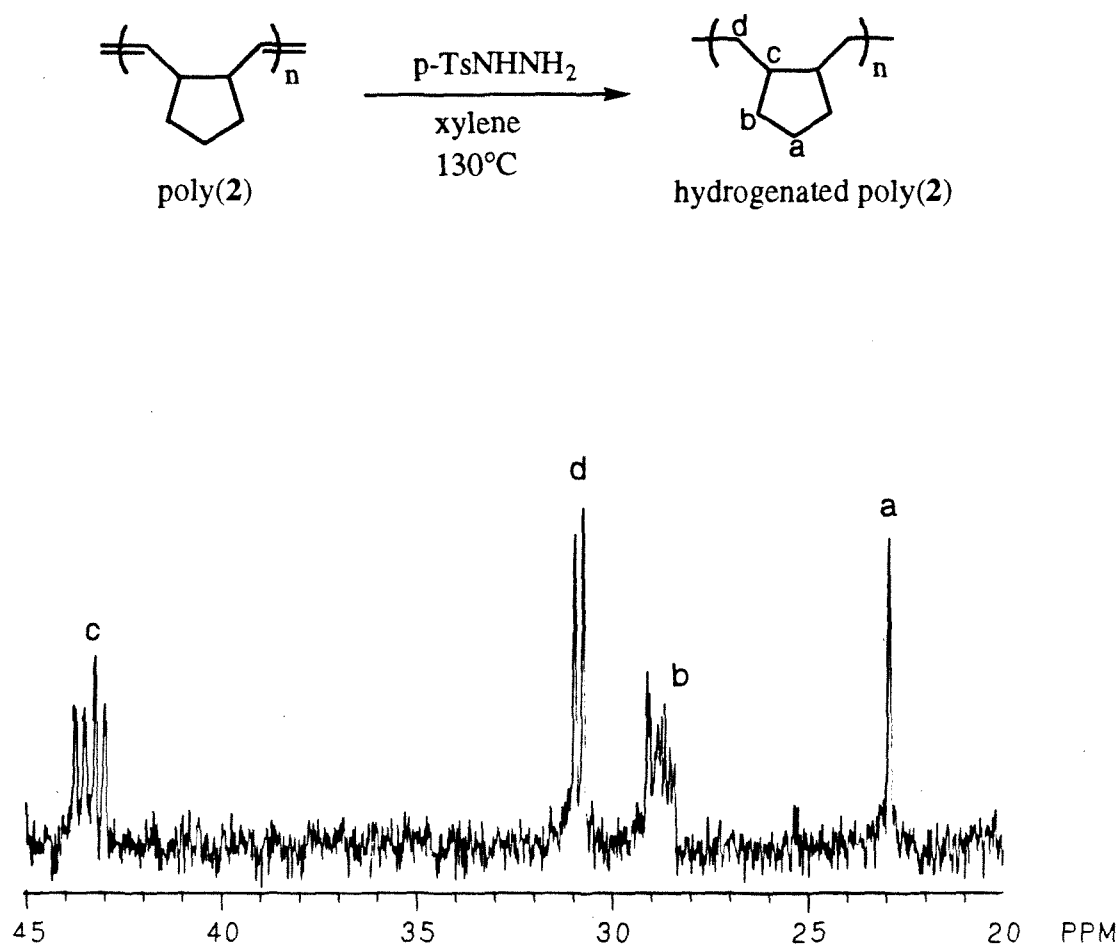


Figure 5. ^{13}C NMR spectrum of hydrogenated poly(2) in CD_2Cl_2 .

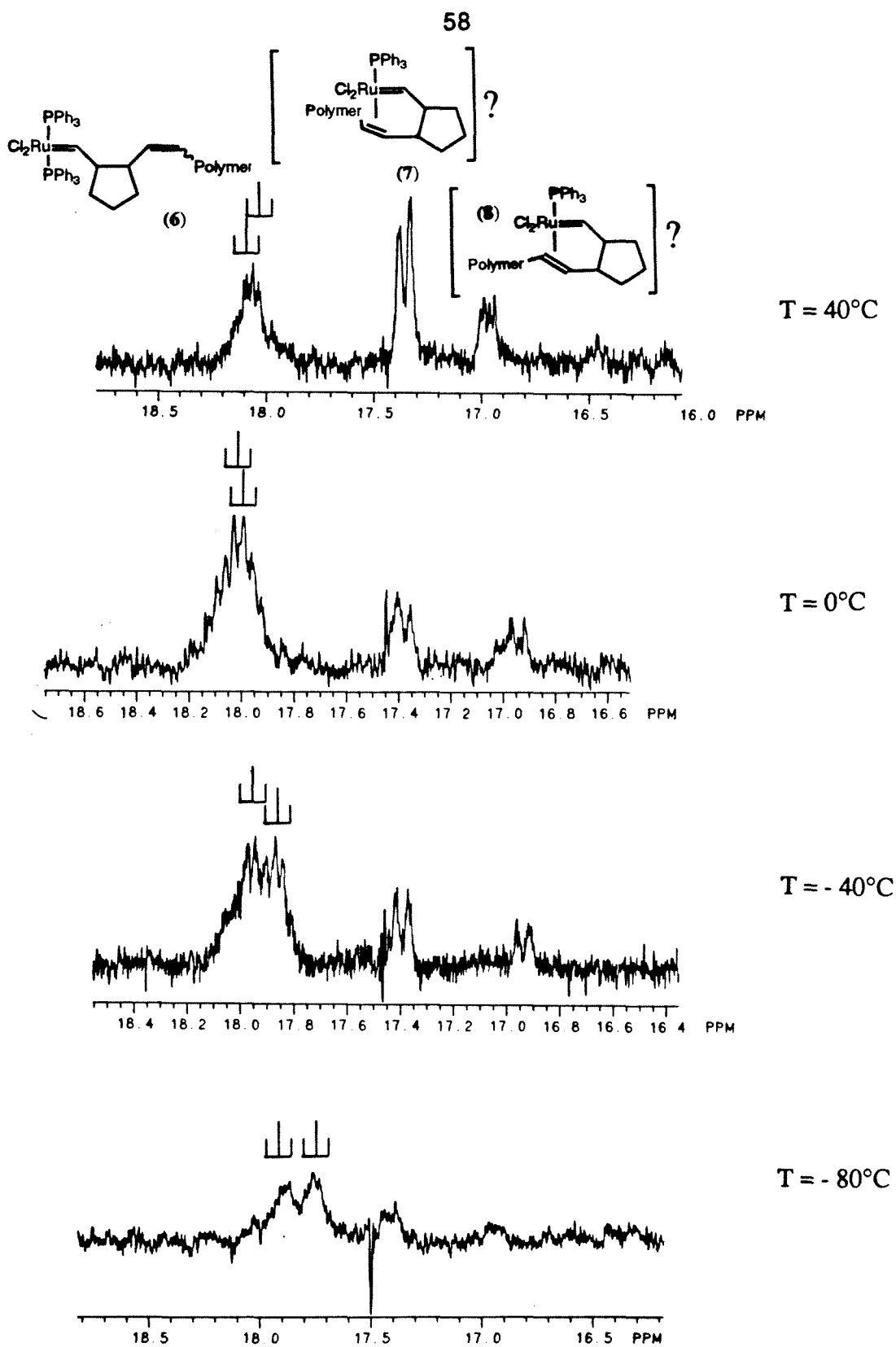


Figure . Variable temperature ^1H NMR spectra of $\alpha\text{-H}$ of propagating carbenes 6, 7, 8 when 4 is reacted with bicyclo[3.2.0]hept-2-ene (2).

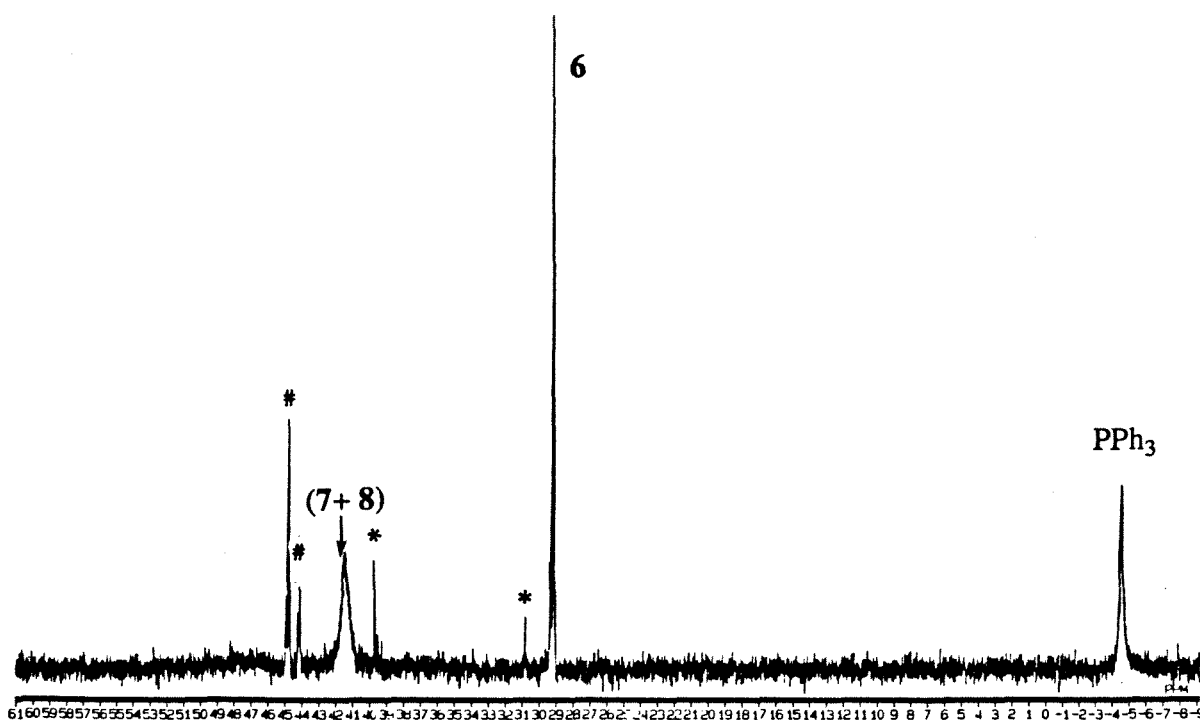
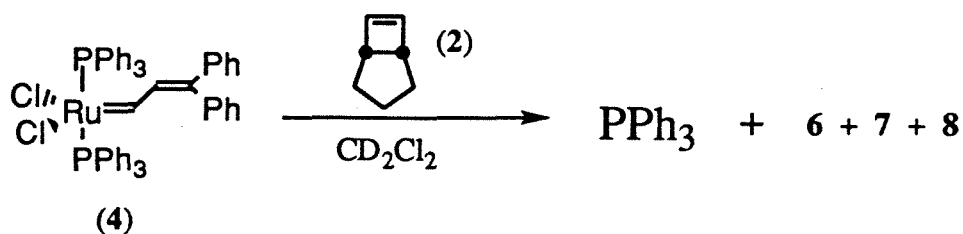


Figure 7. ^{31}P NMR spectrum during the polymerization of **2** by **4** in CD_2Cl_2 . Note the emergence of free phosphine during polymerization. δ (H_3PO_4) ppm: 41.63 (7 + 8), 29.14 (6), -4.93 (PPh_3). * = impurities present initially in **4**; # = possible reaction product of **2** with impurities present initially.

ratio observed earlier in ^1H NMR) suggest that they correspond to monophosphine adduct (**7+8**) and diphosphine adduct **6**, respectively. By ^1H NMR, addition of 0.792 eq. of PPh_3 to the solution results in the peak area of **6** increasing substantially, while **7** and **8** decreases. No tris- PPh_3 adduct is observed even by the addition of 3.39 eq. PPh_3 relative to an equivalent of **6+7+8**. The rate of polymerization of **2** is also slowed down considerably in the presence of PPh_3 .

Speculations on the role of diphosphine adduct and monophosphine adduct on ROMP.

From the above data, due to the steric crowding about the Ru-alkylidene bond in **6**, it might be conceivable that the dissociation of a phosphine to form a monophosphine adduct (**7 + 8**) is necessary for polymerization.¹⁰ The reversibly-binding phosphine could moderate the reactivity of **7** and **8**, similar to the reversible binding of PMe_3 to the propagating species during the polymerization of cyclobutene (**3**) by $\text{W(=CH-CMe}_3\text{)(NAr)(OCMe}_3\text{)}_2$ {Ar = 2,6-diisopropylphenyl}.¹¹ Since excess phosphines slowed down the polymerization of either **1** or **2**, the abstraction of the PPh_3 ligand by CuCl might increase the rate of polymerization. Indeed, the addition of CuCl to a solution of **4** results in much more rapid polymerization of **1**.¹² The formation of a monophosphine adduct (**9**) upon addition of CuCl to **4** was observed by ^1H NMR at $\delta_{\text{H}\alpha} = 17.95$ ppm (pseudotriplet; $^3J_{\text{H}\alpha-\text{P}} = 12.4$ Hz, $^3J_{\text{H}\alpha\text{H}\beta} = 12.4$ Hz). This monophosphine adduct **9** gradually decomposes within a day. However, this **4**- CuCl mixture did not react with cyclopentene nor cyclooctene. Addition of **1** to the CuCl solution containing cyclopentene resulted only in the homopolymerization of **1**. This result is in contrast to the random copolymerization of **1** and cyclopentene when $\text{Ru(H}_2\text{O)}_6\text{tos}_2$ is used (see Chapter 1).

Block copolymers from bicyclo[2.2.1]hept-2-ene (**1**) and bicyclo[3.2.0]hept-2-ene (**2**) catalyzed by $\text{Cl}_2(\text{PPh}_3)_2\text{Ru(=CHCHCPh}_2\text{)}$ (**4**): the determination of reactivity ratios.

The living nature of the polymerization of **1** and **2** was further demonstrated by the formation of block copolymers. Sequential addition of 50 eq of **1** followed by 54 eq of **2**

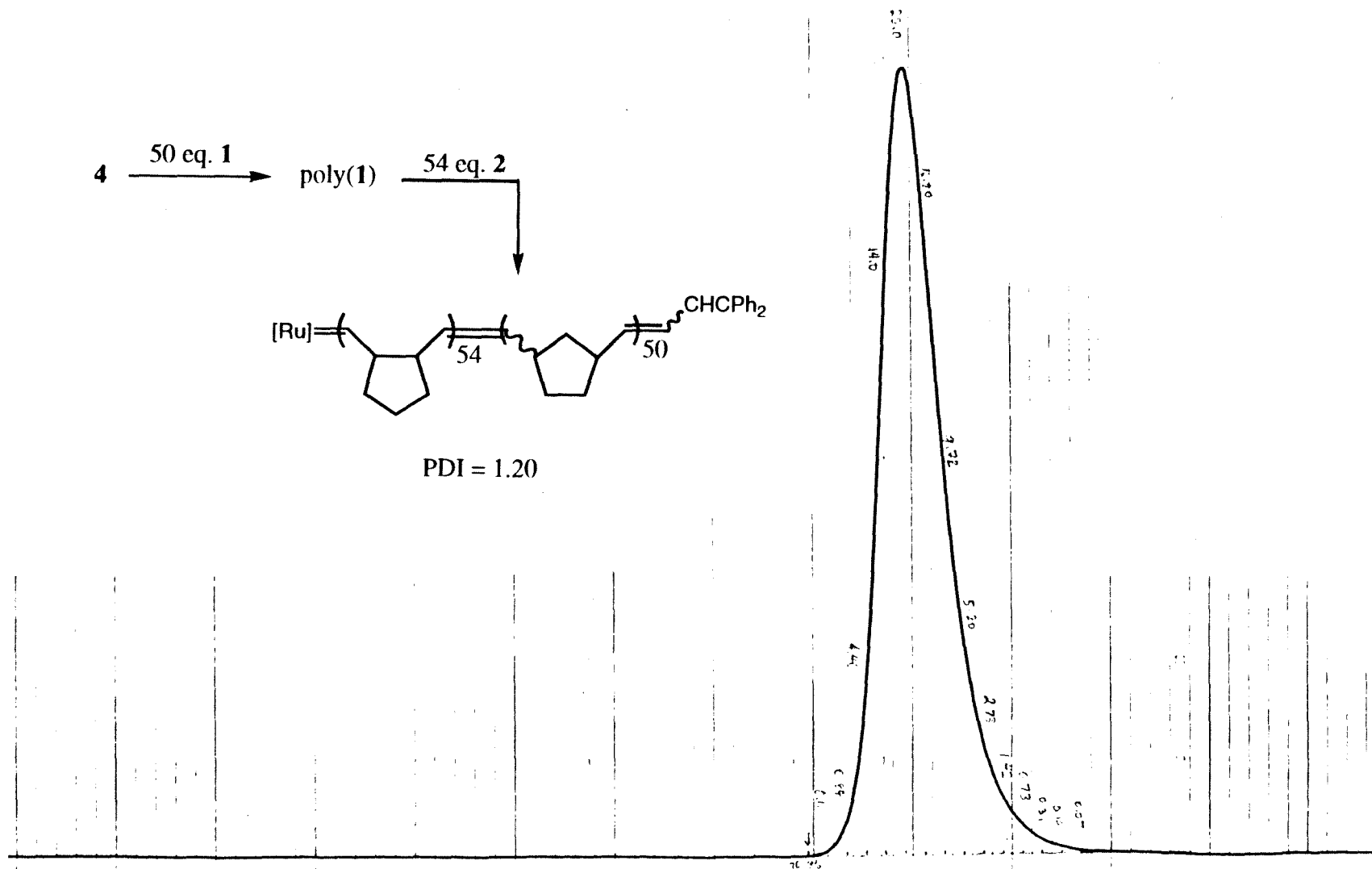


Figure 8. GPC trace of diblock copolymer from sequential addition of **1** and **2** to catalyst **4** in dichloromethane at 40°C.

to an initial solution of 1 eq of **4** resulted in the formation of a diblock copolymer with a polydispersity index of 1.20 (Figure 8). By ^1H NMR, the propagating carbene **5** formed upon addition of **1** was replaced by propagating carbenes **6**, **7**, and **8**. These two results suggest that the specific rate constant of reaction (k_{nc}) of **5** towards **2** is greater than the specific rate constant of propagation (k_{cc}) of **6+7+8** with **2** (Figure 9). Similarly, triblock copolymer poly(**2-1-2**) may be formed by sequential addition of **2**, then **1** (added in two steps), then **2** again, respectively. Typically in this triblock experiment, after the consumption of 27 eq of **2** in 1.5 hours, the propagating carbenes **6+7+8** ($\delta = 18.07$, $\delta = 17.36$, $\delta = 16.96$) were not completely replaced by propagating carbene **5** ($\delta = 17.65$ ppm) when 21.3 eq of **1** was added. Only after an additional addition of 18.6 eq of **1** did **5** completely replaced **6+7+8** as seen by ^1H NMR. This result strongly suggest that the specific rate constant of reaction (k_{cn}) of **6+7+8** towards **1** is less than the specific rate constant of propagation (k_{nn}) of **5** with **1** (Figure 9). Finally, after 1 hour at 40°C in CD_2Cl_2 , 27 eq. of **2** was added again to generate the propagating species **6+7+8** from **5**. A polydispersity index of 1.21 was obtained.¹³

Since $k_{nc} > k_{cc}$, and $k_{nn} > k_{cn}$, and $k_{nn} \approx k_{cc}$ (Note: Actually k_{nn} is slightly greater than k_{cc} ; see Figures 2 & 4), therefore $k_{nc} > k_{nn} > k_{cc} > k_{cn}$. *This ordering predicts that it might be possible to form diblock copolymers by directly adding **4** to a solution of **1** and **2**.* Indeed, when **4** was added to a mixture of 21.8 eq of **1** and 22.1 eq. of **2**, we observed the consumption of **2** first before any **1** was consumed, inspite the fact that the specific rate of propagation k_{nn} of **1** is faster than the specific rate of propagation k_{cc} of **2** (Figure 10). This implies that either the reactivity ratio $\gamma_n (= k_{nn}/k_{nc}) \ll 1$, and/or the reactivity ratio $\gamma_c (= k_{cc}/k_{cn}) \gg 1$. Therefore, a more realistic ordering of specific propagation rate constant is $k_{nc} \gg k_{nn} > k_{cc} > k_{cn}$. This system thus nicely illustrates the fact that even when the *homopolymerization* of **1** is faster than that of **2**, it does not mean that the *copolymerization* of **1** and **2** necessarily results in the consumption of **1** first. The polydispersity index of this reaction is 1.2.¹⁴ Since the thermal gravimetric analysis and

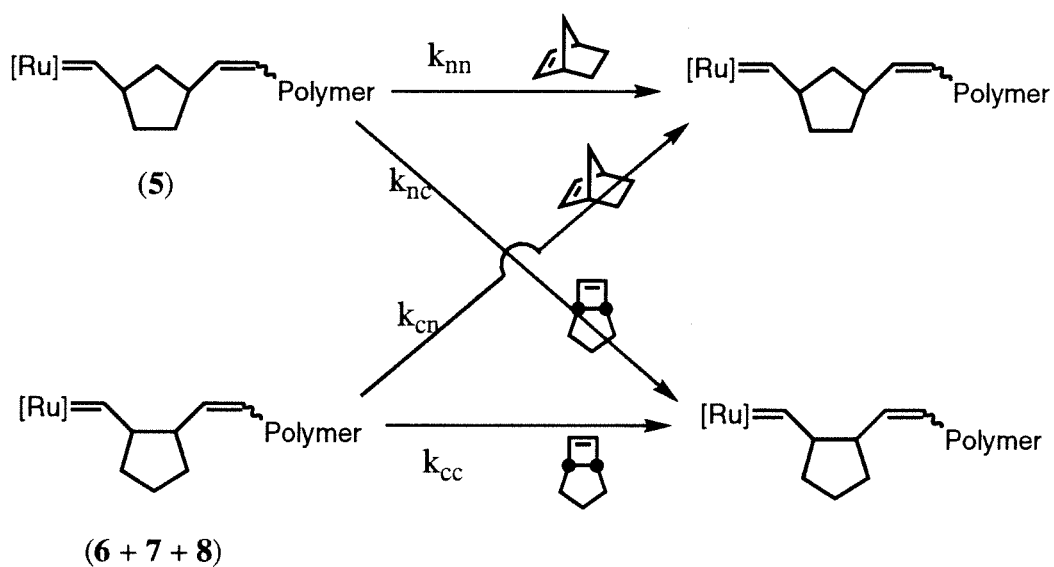


Figure 9. The reaction of propagating species with monomers **1** (norbornene) and **2** ("substituted cyclobutene"). The most likely ordering of the specific rate constant is $k_{nc} \gg k_{nn} > k_{cc} > k_{cn}$.

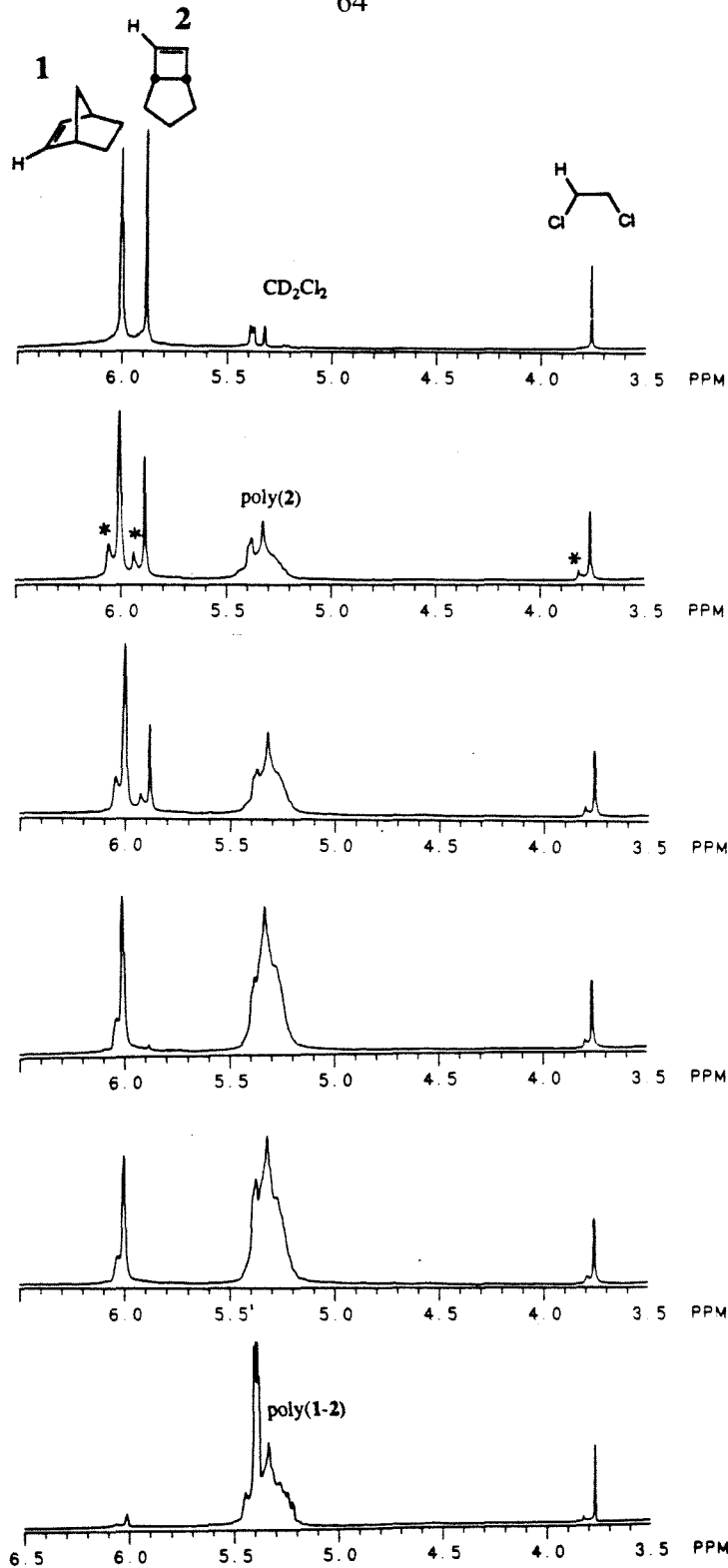


Figure 10. Competition experiment for copolymerization of **1** and **2** in dichloromethane at 40°C.

Internal standard is 1,2-dichloroethane. * = spinning sideband.

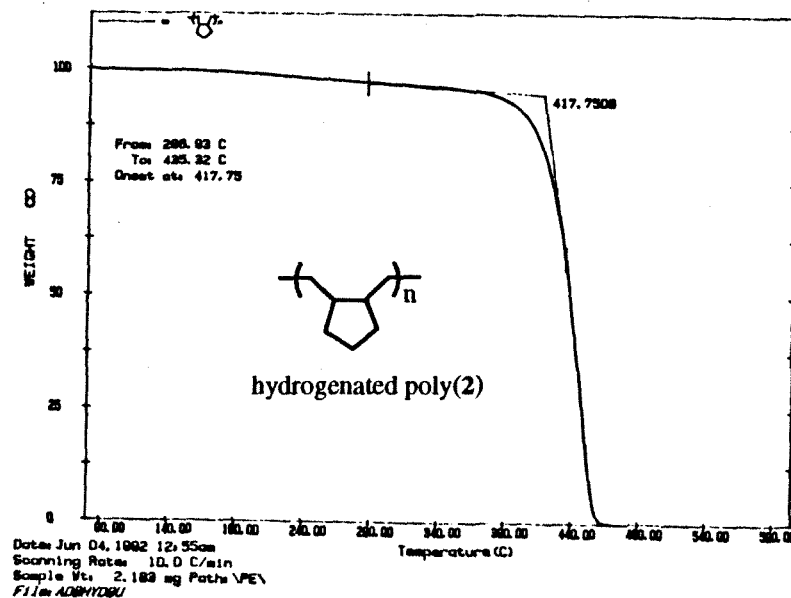
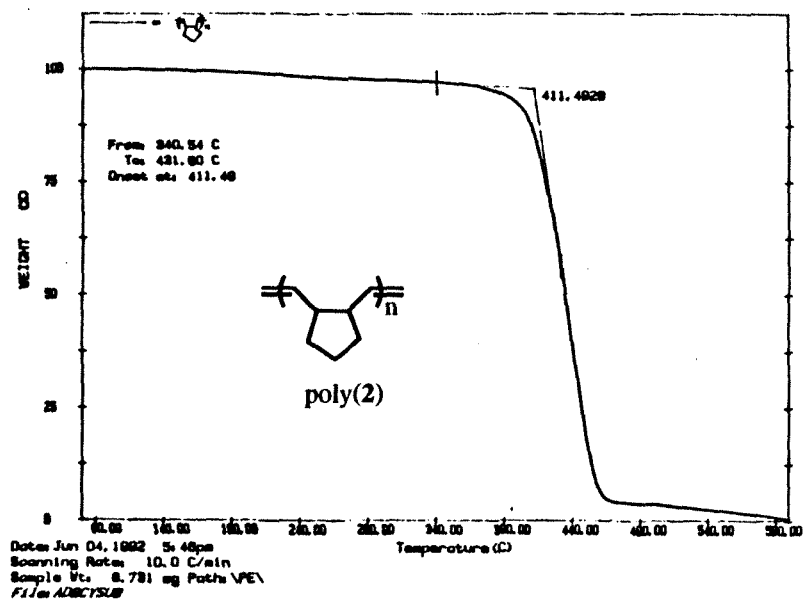
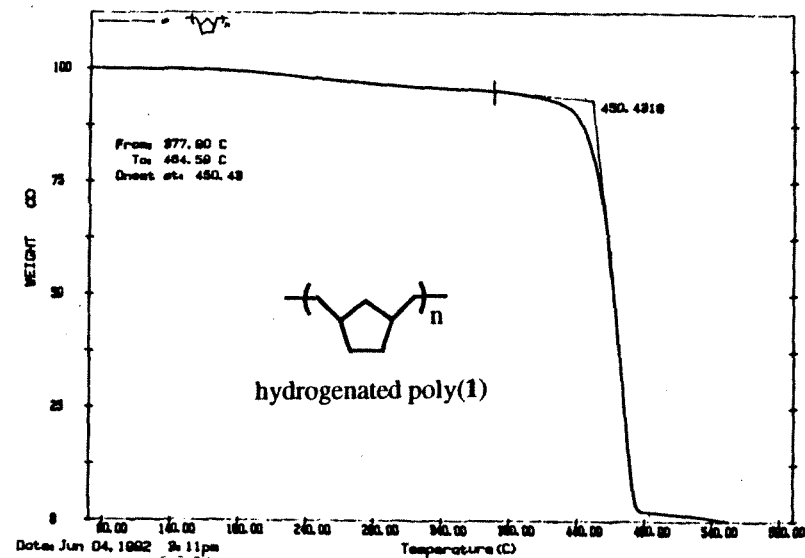
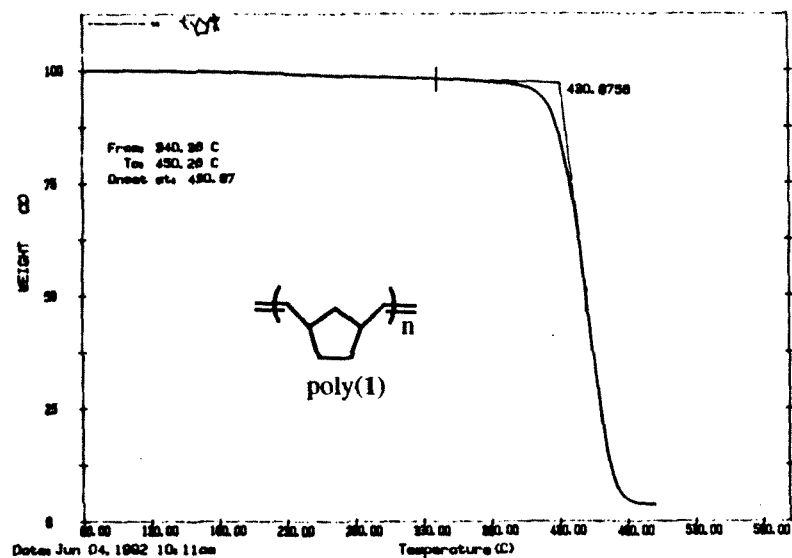


Figure 11. Thermal gravimetric analysis curve of : (a) poly(1); (b) poly(2);
(c) hydrogenated poly(1); (d) hydrogenated poly(2).

differential scanning calorimetry studies revealed similar behavior between poly(**1**) and poly(**2**), no such studies were attempted on the block copolymers obtained (Figure 11).

Reactions of $\text{Cl}_2(\text{PPh}_3)_2\text{Ru}(=\text{CHCHCPh}_2)$ (**4**) with bicyclo[2.2.1]hept-2-ene (**1**) in the presence of chain transfer agents, and other miscellaneous reactions.

Cyclobutene (**3**) slowly reacts with **4**, just as the former also reacts with $\text{Ru}(\text{H}_2\text{O})_6\text{tos}_2$.¹⁵ Even at 50°C, the reaction of about 20 equivalents of **3** with **4** in CD_2Cl_2 (in an NMR tube equipped with J-Young valve; no boiling of CD_2Cl_2 seen) took about 45 minutes. No propagating carbenes are observed. Moreover, not all of **4** is consumed. These two results suggest that the rate of propagation is much faster than the rate of initiation. The polymerization is clearly not living. In fact, $\text{Cl}_2(\text{PPh}_3)_2\text{Ru}(=\text{CHCH}_2\text{CH}_2\text{CH}_2\text{CH}_3)$ (**10**) (formed separately by the reaction of **4** with 1-hexene; ^1H NMR (CD_2Cl_2) $\delta = 18.27$ (multiplet)) gradually decomposes in a matter of hours. Thus the propagating species derived from the ROMP of **3** must also be unstable, since both have the same structure.

Surprisingly, **4** decomposes when reacted with an excess of exo,exo-5,6-bis-methoxymethyl-7-oxabicyclo[2.2.1]hept-2-ene (**11**), and no polymer formed (*cf.* chapter 1). When 0.8 equiv of **11** was used, five unidentified sets of doublet of doublets in the olefinic region of the ^1H NMR spectra were observed. Not surprisingly, **4** remained stable when one equiv of 7-oxabicyclo[2.2.1]heptane was used alone.

Styrene act as chain-transfer agent for the polymerization of **1** by **4**. The molecular weight reduction of the polymer is about an order of magnitude greater compared with that when $\text{Mo}(=\text{CH-CMe}_3)(\text{NAr})(\text{OCMe}_3)_2$ {Ar = 2,6-diisopropylphenyl} is used. This result is consistent with the poor reactivity of this Mo catalyst with other acyclic olefins.¹⁶

Table I. Reduction of molecular weight as chain-transfer agent styrene is added. $[4] = 0.0015$ M. $[1] = 0.59$ M. (PS = polystyrene standard; PDI = polydispersity index). A correction factor of 3.8 is applied to obtain the true \overline{M}_n .

$[\text{styrene}]/[1]$	\overline{M}_n (relative to PS)	\overline{M}_n	PDI
0	140900	37080	1.21
0.2045	27480	7230	2.81
0.4090	15530	4090	3.62
0.8179	6800	1790	3.43
1.6358	4470	1180	3.29
2.4542	2668	700	4.50

Table II. Reduction of molecular weight as chain-transfer agent styrene is added. $[\text{Mo}] = 0.0020$ M. $[1] = 0.60$ M. (PS = polystyrene standard; PDI = polydispersity index). A correction factor of 2.5 is applied to obtain the true \overline{M}_n .

$[\text{styrene}]/[1]$	\overline{M}_n (relative to PS)	\overline{M}_n	PDI
0	70370	28150	1.12
0.2383	23160	9260	2.83
0.4767	23770	9510	3.00
0.9534	18660	7460	3.37
1.4300	12880	5150	3.81
1.907	11380	4550	4.10

Conclusion

The living ring-opening metathesis polymerization of bicyclo[2.2.1]hept-2-ene (**1**) and bicyclo[3.2.0]hept-2-ene (**2**) catalyzed by $\text{Cl}_2(\text{PPh}_3)_2\text{Ru}(\text{=CHCHCPh}_2)$ has been demonstrated. The molecular weight varies linearly with conversion. Discrete propagating species showed that PPh_3 ligand dissociated during polymerization of **2**, and that CuCl

(abstracts PPh₃) enhanced the rate of polymerization of **1**. The specific propagation rate constants (k_{nn} and k_{cc} , respectively) of homopolymerization of **1** and **2** were measured, respectively. Block copolymers are easily prepared. From the reactivity ratio study, the ordering of the specific propagation rate constants are $k_{nc} \gg k_{nn} > k_{cc} > k_{cn}$. The effect of styrene as chain-transfer agent on the molecular weight was studied.

Experimental Section

Instrumentation. ¹H, ¹³C, and ³¹P NMR spectra were acquired on Jeol GX-400 (399.65 MHz ¹H), or on GE NMR instrument QE-Plus-300 (300.19 MHz ¹H). The molecular weights of the polymers were measured either on Waters 150-C ALC/GPC [gel permeation chromatography column (Waters Ultrastyrigel 10⁵, 10⁴, 10³, 500Å; toluene), relative to polystyrene standard], or on gel permeation chromatography (GPC) column (American Polymer Standard, Porosity: Linear 10mm, methylene chloride) on Knauer Differential Refractometer relative to polystyrene standard. Hewlett Packard 5890 Series II Gas Chromatograph (0.25u Alltech- OV101 column). Thermal analysis were performed on Perkin Elmer DSC-7, TGS-2 thermogravimetric analyzer at 10°C scan rate.

General Methods. All manipulations of air- and/or moisture sensitive compounds were carried out under argon using standard Schlenk and vacuum line techniques. Argon was purified by passing through columns of activated BASF RS-11 (ChemalogTM) oxygen scavenger and Linde 4A molecular sieves. Solids were weighed in dry box equipped with a MO-40-1 purification train. Solvents were purified as follows: benzene, tetrahydrofuran, toluene and mesitylene were distilled from sodium benzophenone ketyl into solvent flasks equipped with Teflon screw-type valves; chlorobenzene, chloroform, and dichloromethane were distilled from calcium hydride under vacuum into small Schlenk flasks and subsequently freeze-pump-thaw degassed. Absolute ethanol was used directly from a new bottle without further drying. **1** (Aldrich) was stirred with sodium at 60°C and distilled

into a small Schlenk flask and degassed; **2** and **4** were provided by Zhe Wu and Sonbinh Nguyen, respectively, and which they synthesized according to published procedures.^{1,17} **3** was synthesized according to published method.¹⁸ 1,2-dichloroethane (Aldrich) and styrene (Aldrich) were dried with 4A molecular sieves and then distilled under vacuum into medium Schlenk flask and subsequently freeze-pump-thaw degassed. Prior to use, all olefins (except **1**, which was distilled) were passed through a small column of alumina (activated) inside the dry box. $\text{Mo}(=\text{CH-CMe}_2\text{Ph})(\text{NAr})(\text{OCMe}_3)_2$ {Ar = 2,6-diisopropylphenyl} (Strem Chemicals), CuCl (Aldrich), PPh₃ (Aldrich) *p*-toluenesulfonylhydrazide (Aldrich) were used directly without further purification. Procedure for hydrogenation of the polymers is same as that in Chapter 1 (*vide supra*).

Construction of Figure 1 (molecular weight of poly(1**) versus [1]/[**4**]).** In dry box, 2.0 ml CH₂Cl₂ was added to a 26.8 mg of **4** to make a stock solution of **4**. Six separate aliquots of the stock solution (200 ul each) was transferred into six sealable vial (equipped with screw top filled with gas-impermeable plug). To each sealable vial was added 1.8 ml CH₂Cl₂ and a spin bar. The vials were sealed, brought out of dry box, and heated to 40°C. Back in the dry box, 375 mg of **1** is dissolved in 3 ml CH₂Cl₂ to make approximately 3.4 ml monomer stock solution. With an airtight syringe, 83, 200, 390, 580, 780, 964 ul was withdrawn from this monomer stock solution and injected into the previous six vials, respectively. After 2 hours, P(CH₃)₃ was added to the vials. 50 ul from each vial was withdrawn, passed through alumina, diluted appropriately, and the polymer's molecular weight taken.

Construction of Figure 3 (molecular weight of poly(2**) versus [2]/[**4**]).** In dry box, 1.2 ml CH₂Cl₂ was added to a 27.8 mg of **4** to make a stock solution of **4**. Six separate aliquots of the stock solution (200 ul each) was transferred into six sealable vial (equipped with screw top filled with gas-impermeable plug). To each sealable vial was added 1.8 ml CH₂Cl₂ and a spin bar. The vials were sealed, brought out of dry box, and heated to 40°C for three minutes. 10, 24, 47, 70, 94, and 116 ul of **2** were

injected (via airtight syringes) into the six vials, respectively. After 1.5 hours, $\text{P}(\text{CH}_3)_3$ was added to the vials, and the polymer was precipitated out with methanol. The polymers were centrifuged, and then vacuum-dried overnight.

Typical procedure for determination of propagation rate constant (k_{nn}) for homopolymerization of **1.** In dry box, 400 μl CD_2Cl_2 was added to a 4.5 mg (0.005 mmol) **4** in an NMR tube. 0.5 μl 1,2-dichloroethane was injected as an internal standard. In another vial, 29.2 mg (0.31 mmol) of **1** was dissolved in 250 μl CD_2Cl_2 to make a 280 μl solution. After cooling the NMR tube in an dry ice/acetone bath, 100 μl of a solution of **1** was injected, and shaken. The NMR tube was put into the NMR probe set at 40°C . The disappearance of the olefin protons of **1** was monitored every minute for 40 minutes (> 90% of monomer consumed).

Typical procedure for determination of propagation rate constant (k_{cc}) for homopolymerization of **2.** Procedure is same as that for **1**, except that 500 μl CD_2Cl_2 is used (instead of 400 μl), and 15 μl of liquid **2** was injected from an air-tight syringe into the NMR tube. Reaction is also monitored for 40 minutes (> 90% of monomer consumed).

Qualitative determination of reactivity ratio γ_n and γ_c . In the drybox, 9.0 μl (0.0923 mmol) of **2** was added to 8.8 mg (0.0936 mmol) of **1**, in an NMR tube. 400 μl CD_2Cl_2 and 0.5 μl 1,2-dichloroethane (internal standard) was added as well. After a ^1H NMR spectrum at 40°C of the above solution was taken, a 100 μl CD_2Cl_2 solution of 3.8 mg (0.00423 mmol) of **4** was injected to the NMR tube. The consumption of **1** and **2** (as evidenced by disappearance of olefin protons) was monitored for an hour.

Typical procedure for formation of block copolymers of **1 and **2** (Sequential Addition Method).** In the drybox, 3.1 mg of **4** was dissolved in 0.5 ml CD_2Cl_2 in an NMR tube. 10 μl (8.68 mg, 0.9234 mmol, 26.5 eq) of **2** was added, and the NMR spectrum at 40°C showed complete conversion of the initiating carbene to the propagating carbenes. After 1.5 hours, 7 mg (21.3 eq) of **1** was added, and solution

heated to 40°C. After an hour, an additional 6.1 mg (18.6 eq) of **1** was added. All the propagating species **6+7+8** were converted into **5**. Finally, after 1.5 hours at 40°C, another 10 ul of **2** was injected, to convert all of **5** into **6+7+8**.

Qualitative determination of ratio k_p/k_i for homopolymerization of **1.**

In dry box, 17.5 mg **3** was dissolved in 400 ul CD_2Cl_2 . 100 ul of a solution of **1** (prepared by dissolving 109.2 mg **1** in 200 ul to make a total volume of 295 ul) was injected into the NMR tube, and the temperature raised to 40°C. After one hour, the ratio of area of overlapping α -H's of (**4+5**) to the area of β -H of **5** was obtained. This ratio, together with the ratio of initial concentration of **1** to initial concentration of **4**, allowed the determination of k_p/k_i .⁶ An approximate k_p/k_i value of 55 ± 15 is obtained (see Chapter 3 for discussion of error bars associated with this magnitude of k_p/k_i ; in particular, see curve a of Figure 39 in Chapter 3).

References

- (1) Nguyen, S.T.; Johnson, L.K.; Grubbs, R.H. *J. Am. Chem. Soc.* **1992**, *114*, 3974.
- (2) Bicyclo[2.2.1]hept-2-ene (**1**) has a strain energy of 27.2 kcal/mol. Schleyer, P.v.R.; Williams, J.E.; Blanchard, K.R. *J. Am. Chem. Soc.* **1970**, *92*, 2377.
- (3) Bicyclo[3.2.0]hept-2-ene (**2**) has a strain energy of 36.9 kcal/mol by AM1 method. Computation was done in Prof. D.A.Dougherty's machine.
- (4) Quirk, R.P.; Lee, B. *Polym. Int.* **1992**, *27*, 359.
- (5) Previous studies by Ivin and co-workers showed that tacticity of **1** cannot be obtained through hydrogenation. Ivin, K.J.; Lavery D.T.; Rooney, J.J.; Watt, P. *Recl. Trav. Chim. Pays-Bas* **1977**, *96*, 54.
- (6) In general, the error increases *exponentially* with the magnitude of the ratio k_p/k_i , see: (a) Figure 39 and eqn 46 of Chapter 3 for discussion, and (b) Gold, L. *J. Chem. Phys.* **1958**, *28*, 91.

- (7) The trans/cis ratio of near unity could be indicative of scrambling of the ligands about the Ru center; see discussion on PPh₃ dissociation later on in the chapter; cf. Chapter 1
- (8) By ¹³C NMR, the former olefinic carbon of now hydrogenated poly(**2**) exhibits two peaks (corresponding to meso and racemo dyads) of equal height at $\delta = 31.18$ and 30.97 ppm. Similarly, the trisubstituted carbon of hydrogenated poly(**2**) exhibits four triads (mm, mr, rm, rr) of equal height at $\delta = 43.96, 43.74, 43.45, 43.22$ (not respectively). see Chapter 1 for definition of tacticity.
- (9) We speculate that **7** and **8** are isomers and have the structure shown in Figure 6. Doherty, M; Siove, A.; Parlier, A.; Rudler, H.; Fontanille, M. *Makromol. Chem., Macromol. Symp.* **1986**, 6, 33.
- (10) (a) A space filling molecular model based on the crystal structure of **4** indicates that access to Ru atom is difficult due to bulky nature of the two phosphine ligands. (b) Fontanille has shown that intramolecular coordination of polymer's double bond on the metallacarbene is the kinetically limiting step in polymerization of norbornene. see Ref. 9.
- (11) Wu, Z.; Wheeler, D.R.; Grubbs, R.H. *J. Am. Chem. Soc.* **1992**, 114, 146.
- (12) We are unable to measure to the rate of propagation by NMR due to extreme rapidness of reaction. Typically, to an NMR tube solution of 7.5 mg **4** in 500 ul CD₂Cl₂ in the dry box, was added 2.15 eq CuCl (to form a heterogeneous mixture). About 0.5 ul 1,2-dichloroethane was added as an internal standard. After about 15 min at room temperature, the ratio of **4** : **9** is 10: 26. In another vial, 100 ul was withdrawn via syringe from a solution of 29 mg **1** in 250 ul CD₂Cl₂ . The contents of the syringe was injected into the NMR tube. The solution polymerized completely before several NMR spectra could be taken to determine k_p .
- (13) Not more than 14% of the polymer is "diblock." This value is obtained by cutting out and weighing the area under the GPC trace of this reaction. Since the retention

volume (x-axis of the GPC trace) is logarithmic function of the molecular weight, the value of 14% is a gross overestimation of the actual amount of "diblock" relative to triblock copolymer. The "diblock" could be poly(**2-2**), due to incomplete reaction of **6+7+8** with **1**. The propagating carbenes **6+7+8** must be present in extremely small amount relative to **5** when **1** was added (second step of the reaction) since it was not detected by ^1H NMR.

- (14) No more than 20% of the polymer is monoblock, i.e., poly(**2**). Method used is similar to Ref. 13.
- (15) To effect a polymerization of cyclobutene without a catalyst, it is necessary to heat the solution to greater than 150°C (literature).
- (16) (a) Schrock, R.R.; DePue, R.T.; Feldman, J.; Schaverien, C.J.; Dewan, J.C.; Liu, A.H. *J. Am. Chem. Soc.* **1988**, *110*, 1423. (b) Crowe, W.E.; Michell, J.P.; Gibson, V.C.; Schrock, R.R. *Macromolecules* **1990**, *23*, 3534.
- (17) For synthesis of **2**, see (a) Chapman, O.L.; Pasto, D.J.; Borden, G.W.; Griswold, A.A. *J. Am. Chem. Soc.* **1962**, *84*, 1220. (b) Liu, R.S.H. *J. Am. Chem. Soc.* **1966**, *88*, 112.
- (18) Salaun, J.; Fadel, A. *Organic Synthesis* **1986**, *64*, 50.

Chapter 3

On the Molecular Weight Distribution of Living Polymerization Involving Chain-Transfer Agents: Computational Results, Analytical Solutions, and Experimental Investigations using Ring-Opening Metathesis Polymerization

Introduction

Several factors affect the properties of a given polymer. Two of the most important parameters are number-average degree of polymerization \bar{X}_n of the polymer, and the distribution of the individual chain-lengths relative to each other.¹ The degree of polymerization X_n of a polymer is simply the number of monomer units incorporated into the polymer chain. The number-average degree of polymerization \bar{X}_n is the arithmetic mean of degree of polymerization X_n of all the polymer chains.^{1b} Since the number-average molecular weight \bar{M}_n is simply the number-average degree of polymerization multiplied by the molecular weight of the constituent monomer, knowing \bar{M}_n is tantamount to knowing \bar{X}_n . From the colligative properties imparted by the polymer chains to the solution, \bar{M}_n can be measured experimentally by methods such as membrane osmometry or vapor pressure osmometry.^{1b} By definition, \bar{X}_n is also the ratio of the first moment of distribution to the zeroth moment. Among the polymer properties affected by \bar{X}_n include mechanical and tensile strength, viscosity, glass transition temperature, elasticity, and processability.¹

As equally important as \bar{X}_n is the distribution of individual X_n , since the ensemble of polymer chains is rarely monodisperse (or contain the same number of units). Instead of using the variance σ^2 (or second moment) of the distribution to characterize the polydispersity of the sample, it is customary to use the quantity called polydispersity index (PDI). PDI is readily read off from the experimental data (e.g., size-exclusion chromatography or gel-permeation chromatography). PDI is the ratio of the weight-average degree of polymerization \bar{X}_w to the number-average degree of polymerization \bar{X}_n . \bar{X}_w is simply the ratio of second moment of distribution to the first moment. The corresponding weight-average molecular weight of the polymer is readily measured by light-scattering. It may be shown that PDI is related to the variance σ^2 by the equation

$$\sigma^2 = \bar{M}_n^2 (PDI - 1) . \quad (1)$$

The PDI of a polymer sample where all the polymer chains have the same number of units is unity (since $\sigma^2 = 0$). Theoretically, the best PDI value achievable in a chain polymerization where the primary mode of chain termination is the disproportionation of the propagating species is two (*vide infra*). The polydispersity index of a polymer determines such polymer properties as tackiness (generally characterized by a high PDI), crystallinity (generally low PDI value), etc.¹

Because of the great importance of \bar{X}_n and PDI in influencing polymer properties, it is therefore of great interest to be able to predict the molecular weight distribution as a function of various reagent concentrations and rate parameters characterizing a particular polymerization system.

Generally, there are two types of polymerization based on the mechanism of polymerization, namely, the step polymerization and the chain polymerization.¹ A typical chain polymerization consists of number of different steps in the reactions such as initiation, propagation, chain-transfer, termination (by disproportionation and/or by combination). The \bar{X}_n for both the step polymerization and that for a chain polymerization consisting of initiation, propagation and termination by disproportionation of propagating species have the same form and are both given by

$$\bar{X}_n = 1/(1 - p), \quad (2)$$

where p is the degree of conversion (of the monomer) in the case of a step polymerization, while p is the fraction of the propagation steps among the total propagation and termination steps for the case of chain polymerization.^{1c} Representative plots of the \bar{X}_n versus the degree of conversion are illustrated below. As can be seen in both plots, achieving the desired \bar{X}_n by controlling the degree of conversion is difficult.

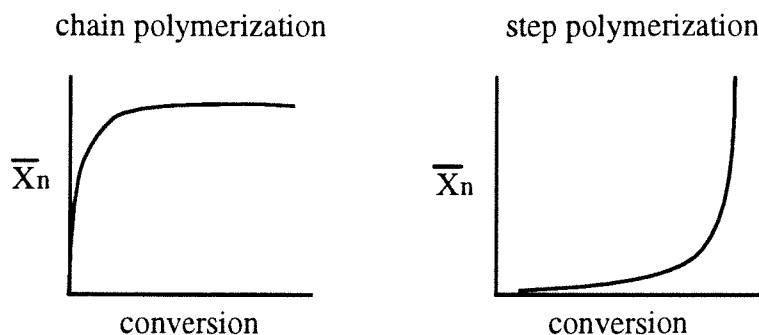


Figure 1. number-average degree of polymerization \bar{X}_n versus conversion (or extent of reaction) for two types of polymerization.

The PDI of both the step polymerization and a typical chain polymerization is given by

$$\text{PDI} = 1 + p, \quad (3)$$

where p is defined as above. Ideally, the PDI of both cases increases monotonically to two as the reaction proceeds to completion (*vide infra*) (Figure 4).

If only initiation and propagation steps are present in a chain polymerization, the process is called a "living" polymerization. Living polymerization differs from typical chain polymerization because the former allows precise control of the molecular weight of the polymer.² Ideally, the number-average degree of polymerization \bar{X}_n is simply the ratio of monomer to catalyst, while the molecular weight distribution is Poisson in character.³ (Figures 2-4) Flory derived the relations of \bar{X}_n and PDI to the degree of conversion for the case where specific rate of initiation k_i is equal to the specific rate of propagation k_p .⁴

$$\bar{X}_n = v + 1 \quad (4)$$

$$\text{PDI} = \frac{\bar{X}_w}{\bar{X}_n} = 1 + \frac{v}{(v+1)^2} \quad (5)$$

$$\text{where } v = \frac{\text{MON} - M}{\text{CAT}} = \text{kinetic chain-length}, \quad (6)$$

MON and CAT are initial concentrations of monomer and catalyst, and M is concentration of monomer at time t .

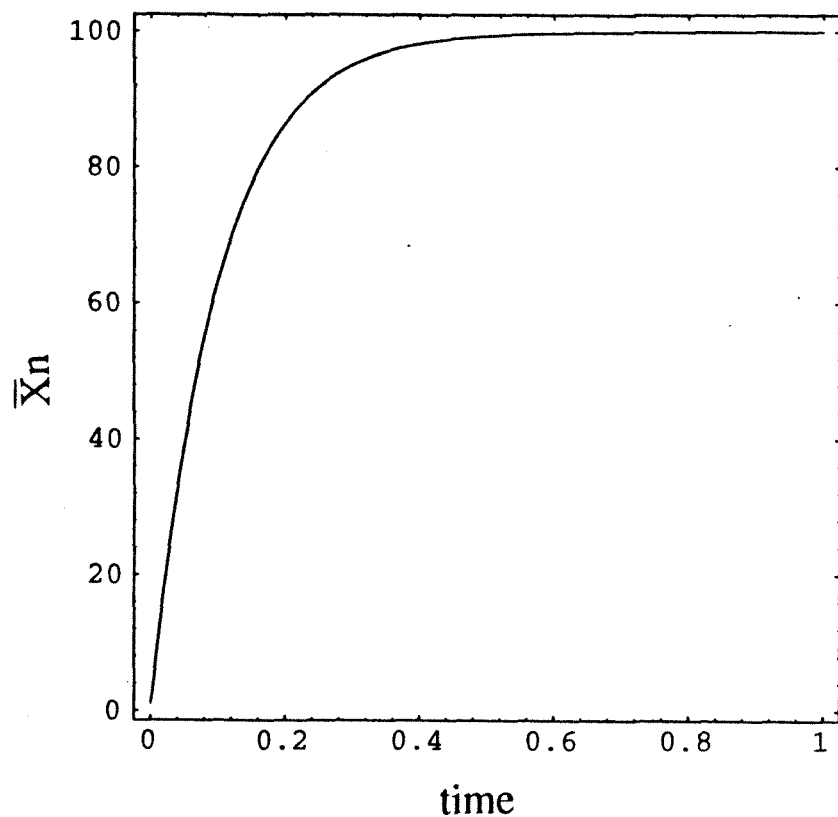


Figure 2. Variation of the number-average degree of polymerization with time in a living polymerization. $k_i : k_p = 1 : 1$. Concentration of catalyst : monomer = 1 : 100.

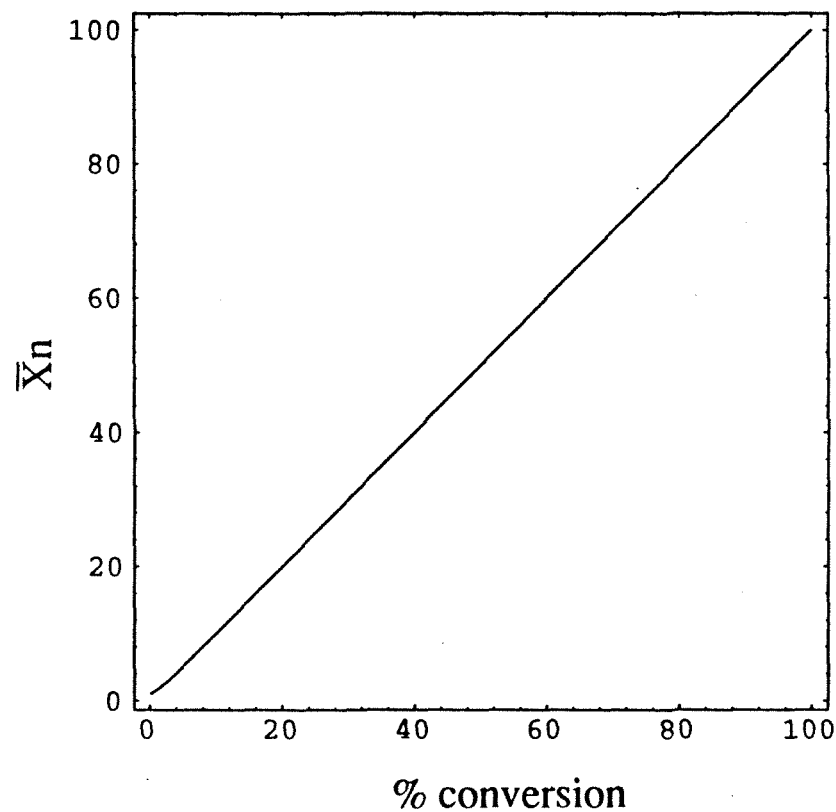


Figure 3. Variation of the number-average degree of polymerization with conversion in a living polymerization. $k_i : k_p = 1 : 1$. Concentration of catalyst : monomer = 1 : 100.

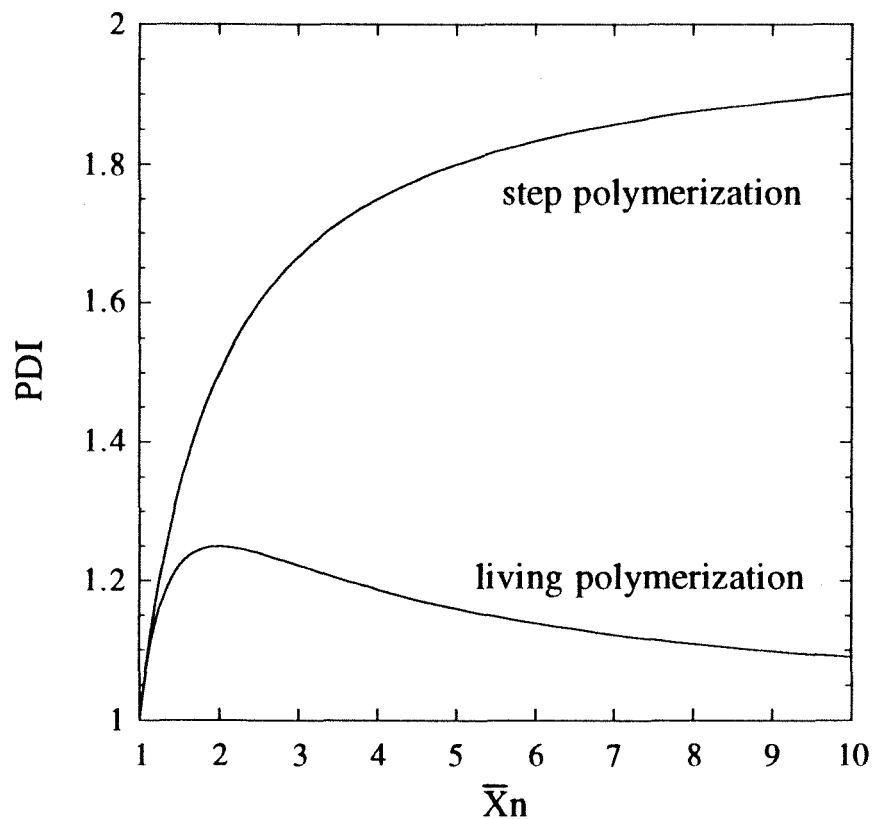


Figure 4. Variation of polydispersity index versus number-average degree of polymerization for two different mechanisms of polymerization.

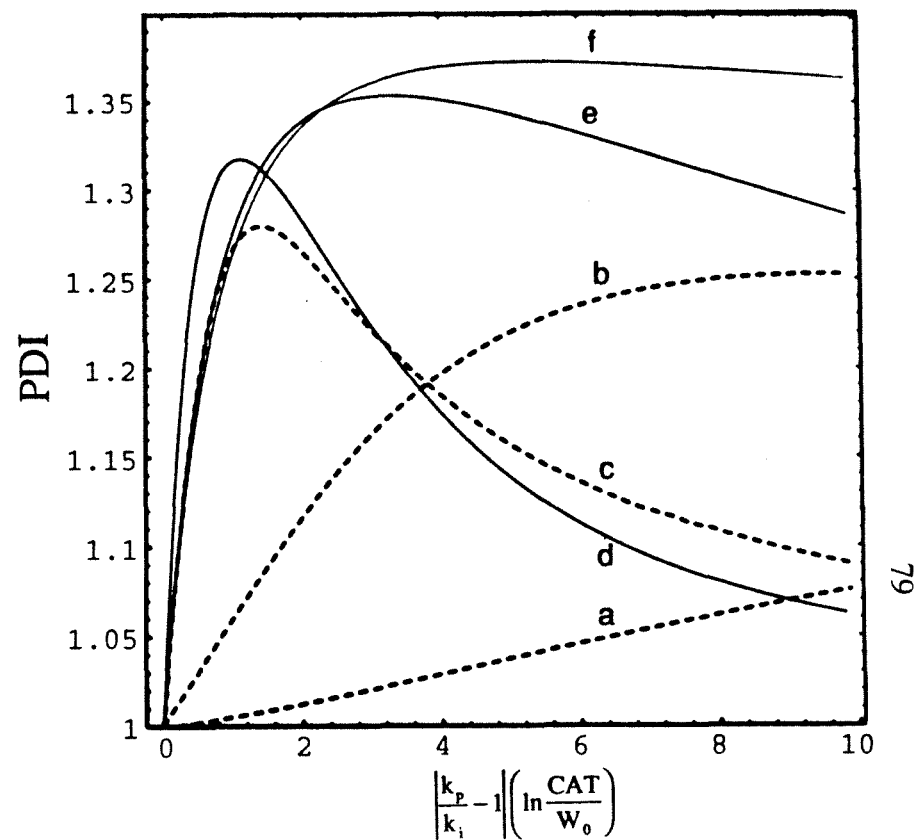


Figure 5. Polydispersity indices as reaction progresses for a true living system when k_p/k_i is (a) 10^{-2} , (b) 10^{-1} , (c) 0.5, (d) 2, (e) 10, (f) 10^2 . CAT is initial concentration of catalyst (or initiator). W_0 is concentration of unconsumed catalyst in the reaction at time t .²⁰

As expected, \bar{X}_n varies linearly with conversion (Figure 3). This is a consequence of the absence of termination steps. The behavior of the PDI is remarkable since it rapidly increases to a maximum and then drops back down towards unity as the reaction proceeds to completion (Figure 4).

Another process of controlling \bar{X}_n involves using chain-transfer agents in non-living polymerization systems (i.e., a typical chain polymerization). The molecular weight of the polymer can be controlled by varying the amount of added chain-transfer agent because $1/\bar{X}_n$ is a linear function of the ratio [chain-transfer agent]/[monomer].⁴

$$\left(\frac{1}{\bar{X}_n}\right)_{\text{with chain-transfer agent}} = \left(\frac{1}{\bar{X}_n}\right)_{\text{without chain-transfer agent}} + \frac{k_{tr}}{k_p} \left(\frac{\text{CTA}}{\text{MON}}\right) \quad (7)$$

Such a plot (Mayo plot) gives a slope equal to k_{tr}/k_p , where k_{tr} and k_p are the specific rate constants for chain transfer and propagation, respectively. The intercept is simply the reciprocal of \bar{X}_n when no chain-transfer agents are present.

In this chapter, we direct our attention to the prediction of \bar{X}_n and PDI of a living polymerization when chain transfer agents are added.⁵ To a polymer chemist, it is clear that \bar{X}_n will not be equal to MON/CAT (as obtained by rewriting eqn 4, for a pure living polymerization) nor to MON/CTA (as given in eqn 7 for a non-living polymerization). Nor will \bar{X}_n be equal to MON/(CTA + CAT) since not all chain-transfer agents are necessarily consumed at the end of the reaction. An understanding of the behavior of \bar{X}_n and PDI for a living polymerization when chain transfer agents are added is essential because in a living polymerization (i.e., without chain transfer), to obtain low molecular weight polymers, a fixed (and usually substantial) amount of catalyst (i.e., initiator) has to be used because of the absence of any termination step or chain transfer step. The addition of chain-transfer agents to this system stops the growing polymer chain by transferring the active center from the polymer to the chain-transfer agent, thus starting another chain-growth cycle. A molecule of initiator (or catalyst) thus gives rise to several shorter chain polymers, as if several initiator molecules were used in the first place.

The intentional addition of chain-transfer agents instead of using more catalysts to lower the molecular weight of the polymer is desirable for several reasons. First, catalysts used in certain living polymerization (e.g., ring-opening metathesis polymerization **ROMP**) are usually more expensive, more difficult to synthesize, and generate more undesirable by-products than chain-transfer agents.⁶ The cheaper and easier to synthesize chain-transfer agents offer alternatives for making low-molecular weight oligomers. Secondly, chain-transfer agents added in proper amounts to a living system afford regulation of molecular weight distribution—ranging from the narrow Poisson to broad Flory-Schulz distributions (*vide infra*). Thirdly, polymers with functionalized chain ends could be synthesized readily by allowing the transfer of the desired functional group from the chain-transfer agents bearing such group to the growing polymer chain.⁷ These type of polymers (telechelic polymers) cannot be made in a mixed one-batch process through conventional living polymerization because the growing end of the polymer will not contain the desired functional group, unless the chain was end-capped by such group *at the end of the reaction*.

To our knowledge, the prediction of the chain length and the polydispersity index of living systems with chain-transfer agents has not been dealt with adequately before. Most schemes in literature involve the presence of termination steps (disproportionation or combination) in addition to the usual initiation, propagation, and chain-transfer steps.⁸ Such schemes have already been studied intensively, and chain-length dependence of the termination rate constant still remains an area of active investigation.⁸

In this chapter, we report the computational results of molecular weight and its distribution for a living system when chain-transfer agents are added deliberately. We examine the validity of the steady-state approximation (constancy of the propagating species) to obtain the distribution of *low-molecular weight* oligomers in *living* systems. The significance of the slope of the Mayo plot for a *living* polymerization is re-evaluated because the slope has been taken for granted to be equal to k_{tr}/k_p .^{7d,7e} Pre-steady state

and post-steady state behaviors of the reaction are examined as well. Furthermore, the kinetic parameters for a living system are measured experimentally, and the molecular weights obtained experimentally are compared with those obtained by computation.

Prior Works

Here we briefly examine selected analytical and numerical approaches on molecular weight distributions.

When dealing with *non-living* systems, the theoretical molecular weight distribution characterizing a particular polymerization scheme is usually obtained through a "kinetic" approach. "Kinetic" approach involves solving a set of differential equations having rate constants as parameters.⁹

One common approach expresses the rate of change of concentration of each propagating species as functions of the concentration of the propagating species of equal or shorter lengths. These equations may be solved successively for increasingly longer chains by a number of methods (e.g., Laplace transform).¹⁰ Moreover, since the equation governing the consumption of active species of particular chain length depends on the concentration of the active species with length one unit less than the former, a difference equation is obtained. Through recursion, the distribution function is obtained as functions of the initial reactant concentrations.

An alternative method rewrites the above steps in terms of various moments of the distribution. Knowledge of all the moments is equivalent to knowing the concentration of each species.¹¹ Tompa elegantly illustrates this concept and that of generating functions to obtain the solution *in the case of high molecular weight polymer* in a variety of polymerization schemes by expressing the distribution as an expansion into Laguerre polynomials.¹²

For certain chain-growth polymerization scheme, it is more advantageous to rewrite the former equations into partial differential equations where the concentrations

of the various active species are expressed as functions of the extent of reaction. This approach was used by Saito *et al.* to calculate the number of branch points in chains of specified length in the case of branched polymers.¹³

With regards to *living* polymerization, the case where the monomer itself acts as a chain-transfer agent has been the scope of several investigations.^{14,15} Kyner, Radok, and Wales solved this problem by using a modified time variable (introduced by Ginell and Simha) to linearize the systems of differential equations.¹⁴ Their expressions for the number-average and weight-average degree of polymerization are:

$$\bar{X}_n = \frac{\lambda\mu(1+\sigma)(1-\mu)\tau + (1+\sigma-2\mu)(\mu-\lambda)(1-e^{-\mu\tau}) + \mu^2(1-e^{-\tau})}{\lambda\mu\sigma(1-\mu)\tau + (\sigma-\mu)(\mu-\lambda)(1-e^{-\mu\tau}) + \lambda\mu^2\sigma(1-e^{-\tau})} \quad (8)$$

$$\bar{X}_w = 1 + \frac{2\lambda(a_1 + a_2 + a_3 + \sigma)\tau + 2\left(1 - \frac{\lambda a_1}{\mu} - \frac{\lambda\sigma}{\mu(1-\mu)}\right)(1-e^{-\mu\tau}) - \left(\frac{2\lambda a_2}{\sigma}\right)(1-e^{-\sigma\tau})}{\lambda(1+\sigma)\tau + \left(\frac{(1+\sigma-2\mu)(\mu-\lambda)}{\mu(1-\mu)}\right)(1-e^{-\mu\tau}) + \left(\frac{\lambda^2\mu\sigma}{1-\mu}\right)(1-e^{-\tau})} \quad (9)$$

$$\text{where } \mu = \frac{k_i}{k_p + k_{tr}}, \quad \sigma = \frac{k_r}{k_p + k_{tr}}, \quad \lambda = 1 - \sigma, \quad \tau = \int_0^t (k_p + k_{tr})M ds,$$

$$a_1 = \frac{2\mu - [\lambda\sigma / (1-\mu)] - \lambda}{\mu - \sigma}, \quad a_3 = \frac{\sigma^2}{1-\mu}, \quad a_1 + a_2 + a_3 = \frac{\lambda^2 + 2\lambda\sigma}{\sigma}, \quad (10)$$

M is the concentration of monomer at time t.

The molecular weight distribution has the character of a damped wave. As expected, the distribution reduced to the Gold distribution (i.e., modified Poisson distribution) when the monomer cannot act as a chain-transfer agent.¹⁶

$$\bar{X}_n = \frac{(1-r)(1-e^{-(u/R)}) + (r/R)u}{(1-e^{-(u/R)})} \quad (11)$$

$$\bar{X}_w = \frac{\frac{r}{R}u(1 + \frac{r}{R}u) \pm 2ru + (2r-1)(r-1)(1-e^{-(u/R)})}{(1-r)(1-e^{-(u/R)}) + (r/R)u} \quad (12)$$

$$\text{where } R = \begin{cases} r-1, & \text{for } r > 1 \\ 1-r, & \text{for } r < 1 \end{cases}, \quad r = k_p / k_i, \quad u = -R \ln\left(\frac{W_0}{CAT}\right), \quad (13)$$

W_0 and CAT are concentrations of catalyst at time t and 0 , respectively.

The latter set of equations (Eqns 11 & 12) are extensions of Flory's eqns 4 & 5 where $k_i \neq k_p$. Naturally, when $k_i = k_p$, the Gold distribution is simplified further into the Poisson distribution first derived by Flory (eqns 4 & 5).^{3b}

Largo-Cabrerizo and Guzman dealt with the nature of the molecular weight distribution for living polymerization when chain-transfer agents are added deliberately.¹⁷ Because of the additional degree of freedom introduced by using a chain-transfer agent that is not the monomer itself, their solution imposes additional constraints on the system (e.g., the constancy of the monomer concentration and/or chain-transfer agent throughout the reaction; fast initiation; $k_p > k_{tr}$). If the concentration of the chain-transfer agent *remains constant with time* and the initiation is infinitely fast, the expressions obtained are

$$\bar{X}_n = \frac{1 + Y\beta}{1 - \alpha\beta \ln\left(1 - \frac{Y}{1 + \alpha}\right)} \quad (14)$$

$$\begin{aligned} \bar{X}_w = 1 + \frac{1}{(\alpha + Y\beta)(\alpha\beta - 1)} & \left\{ Y\beta^2(1 + \alpha)\left(2 - \frac{Y}{1 + \alpha}\right) - 2Y\alpha\beta^2 \right. \\ & \left. + 2(1 + \beta)\left[1 - \left(1 - \frac{Y}{1 + \alpha}\right)^{\alpha\beta}\right] - \frac{2\beta(1 + \beta)(1 + \alpha)}{1 + \alpha\beta}\left[1 - \left(1 - \frac{Y}{1 + \alpha}\right)^{1 + \alpha\beta}\right] \right\} \quad (15) \end{aligned}$$

$$\text{where } \alpha = \frac{k_{tr} \text{ CTA}}{k_p \text{ MON}} \quad , \quad \beta = \frac{\text{MON}}{\text{CAT}} \quad , \quad Y = \frac{\text{MON} - M}{\text{MON}} \quad , \quad (16)$$

MON, CAT, CTA are initial concentrations of monomer, catalyst, chain-transfer agent, respectively, and M is concentration of monomer at time t .

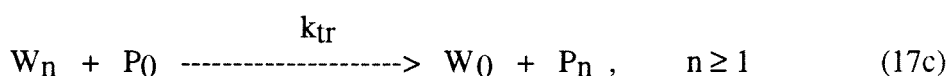
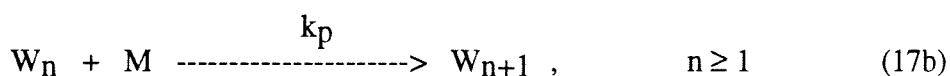
We are interested in a general solution since that can be applied to any given values of rate constants or reactant concentrations. It may be seen from all the above equations that the general analytical solution will involve several parameters (*vide infra*). Such a solution will also be more complicated than any of the above forms, and might be impossible to solve explicitly for \bar{X}_n .

Cases where the systems have instantaneous initiation or complete initiation have been investigated (especially in the case where the monomer is capable of acting as a chain-transfer agent itself) but the expression for the number-average degree of polymerization is not suitable when the degree of conversion is high.¹⁸

Formulation of the Problem

Let CAT, MON, and CTA be the concentration of catalyst, monomer, and chain-transfer agent, respectively at time 0; while W_0 , M , P_0 are the concentration of catalyst, monomer, and chain-transfer agent at time t . W_n and P_n are the concentration of active and dead polymer chains containing n units of monomer, respectively, at time t . k_i , k_p , and k_{tr} are specific rate constants for initiation, propagation, and chain transfer.^{19a}

The polymerization scheme is as follows:



In this scheme, the initiating species W_0 produced by the reaction of the chain-transfer agent P_0 with the active chain W_n has the same reactivity as the original catalyst W_0 . This is intentionally done to illustrate the important feature of the system.^{19b}

The following kinetic equations describe the above process:

$$dM/dt = -k_i M W_0 - k_p M \sum_{n=1}^{\infty} W_n \quad (18)$$

$$dW_0/dt = -k_i M W_0 + k_{tr} P_0 \sum_{n=1}^{\infty} W_n \quad (19)$$

$$dW_1/dt = k_i M W_0 - k_p M W_1 - k_{tr} P_0 W_1 \quad (20)$$

$$dW_n/dt = -k_p M W_n + k_p M W_{n-1} - k_{tr} P_0 W_n \quad n \geq 2 \quad (21)$$

$$dP_0/dt = -k_{tr} P_0 \sum_{n=1}^{\infty} W_n \quad (22)$$

$$dP_n/dt = k_{tr} P_0 W_n, \quad n \geq 1 \quad (23)$$

Using the conservation laws,

$$MON = M + \sum_{n=0}^{\infty} (n W_n) + \sum_{n=0}^{\infty} (n P_n) \quad (24)$$

$$CAT = \sum_{n=0}^{\infty} W_n \quad (25)$$

$$CTA = \sum_{n=0}^{\infty} P_n \quad (26)$$

the above equations can be transformed into

$$dM/dt = (k_p - k_i) M W_0 - (k_p CAT) M \quad (27)$$

$$dW_0/dt = (k_{tr} CAT) P_0 - k_i M W_0 - k_{tr} P_0 W_0 \quad (28)$$

$$dP_0/dt = k_{tr} W_0 P_0 - (k_{tr} CAT) P_0 \quad (29)$$

$$dA/dt = -k_{tr} P_0 A + (k_p CAT) M + (k_i - k_p) M W_0 \quad (30)$$

$$dD/dt = k_{tr} P_0 A \quad (31)$$

$$dB/dt = -k_{tr} P_0 B + k_p M (CAT + 2A - W_0) + k_i M W_0 \quad (32)$$

$$dF/dt = k_{tr} P_0 B \quad (33)$$

$$\text{where } A = \sum_{n=1}^{\infty} (n W_n), \quad B = \sum_{n=1}^{\infty} (n^2 W_n), \quad D = \sum_{n=1}^{\infty} (n P_n), \quad F = \sum_{n=1}^{\infty} (n^2 P_n) \quad (34)$$

The number-average degree of polymerization (\bar{X}_n) of the dead and active chains are thus given by

$$\bar{X}_{n, \text{dead}} = D/(CTA - P_0) \quad \bar{X}_{n, \text{active}} = A/(CAT - W_0) \quad (35)$$

while the polydispersity index (**PDI**) of the dead and active chains are

$$PDI_{\text{dead}} = [F (CTA - P_0)]/D^2 \quad PDI_{\text{active}} = [B (CAT - W_0)]/A^2 \quad (36)$$

Computational Methods

The calculations of the differential equations have been performed on Sun SPARCserver 670MPs, using software Mathematica v2.0(Wolfram Research Inc.). The temporal evolution of the quantities M , W_0 , P_0 , \bar{X}_n , and PDI has been followed. Unless noted otherwise, the resultant values \bar{X}_n and PDI are those for which the percent conversion of monomer is practically complete (unreacted monomer $< 10^{-5} \%$).

A wide range of magnitudes of rates of initiation, propagation, and chain transfer has been examined. In particular, the specific rates of initiation and propagation range from 100 to 0.01 while those for chain transfer range from 5 to 0.0005. Generally, the concentration of monomer used is from 100 to 1000 times that of the catalyst. The ratio of chain-transfer agent to catalyst has been varied from 2 to 500. Only the relative concentrations of catalyst : monomer : chain-transfer agent and relative values $k_i : k_p : k_{tr}$ are needed in the calculations (i.e., every quantity can be scaled).

Computational Results and Discussion

We first examine the general features of the polymerization for various rate parameters with the intent of gaining insight to how the molecular weight of the polymer can be controlled by varying the chain-transfer agent to monomer ratio. Note that \bar{X}_n is not simply $[\text{monomer}]/([\text{chain-transfer agent}] + [\text{catalyst}])$.

Cases where $k_{tr} = 0$ or $k_{tr} \ll k_p$. In order to check the validity of the numerical approach, we begin by reproducing the results obtained previously from exact mathematical solutions in cases when no chain transfer can occur.^{3c,16} When $k_i = k_p$, and in the absence of any chain transfer, \bar{X}_n varies linearly with conversion of the monomer (i.e., extent of reaction) (Figure 3). Similarly, the distribution of the molecular weight is Poisson. As expected, when $k_i \neq k_p$, the \bar{X}_n and PDI follow exactly that obtained by Gold.^{16a,20} (Figure 5). Note that when $k_i \neq k_p$, the PDI also retains the same behavior as that for $k_i = k_p$, where the value of the PDI reaches a maximum before decreasing asymptotically to unity (Figure 5).

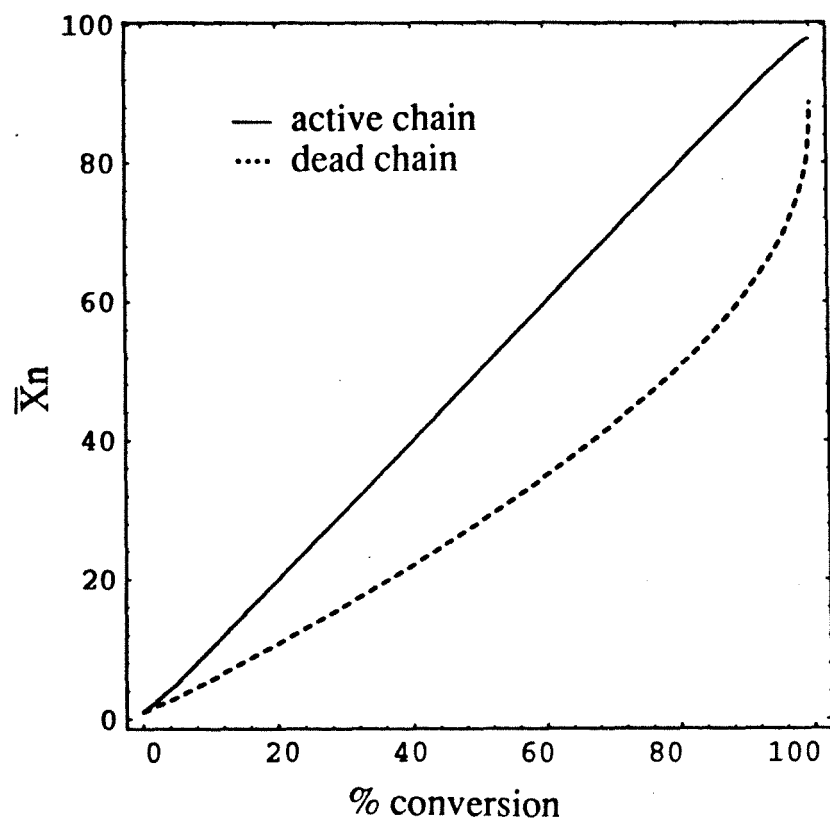


Figure 6. Variation of the number-average degree of polymerization with conversion— poor chain-transfer agent case. $k_i : k_p : k_{tr} = 125 : 100 : 0.05$. Concentration of catalyst : monomer : chain-transfer agent = 1 : 100 : 10.

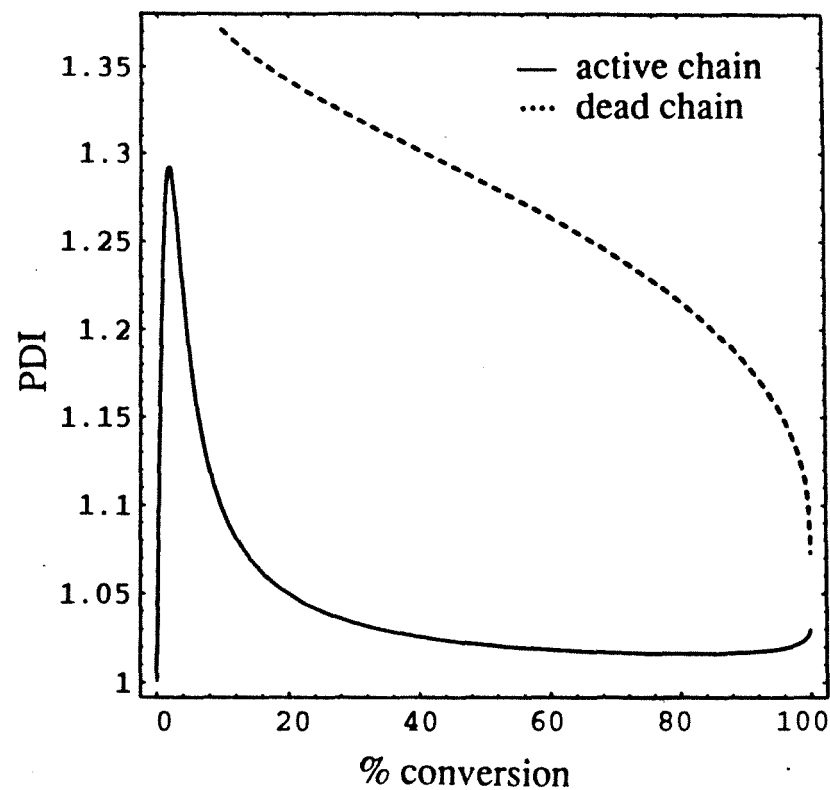


Figure 7. Variation of the polydispersity index with conversion— poor chain-transfer agent case. $k_i : k_p : k_{tr} = 125 : 100 : 0.05$. Concentration of catalyst : monomer : chain-transfer agent = 1 : 100 : 10.

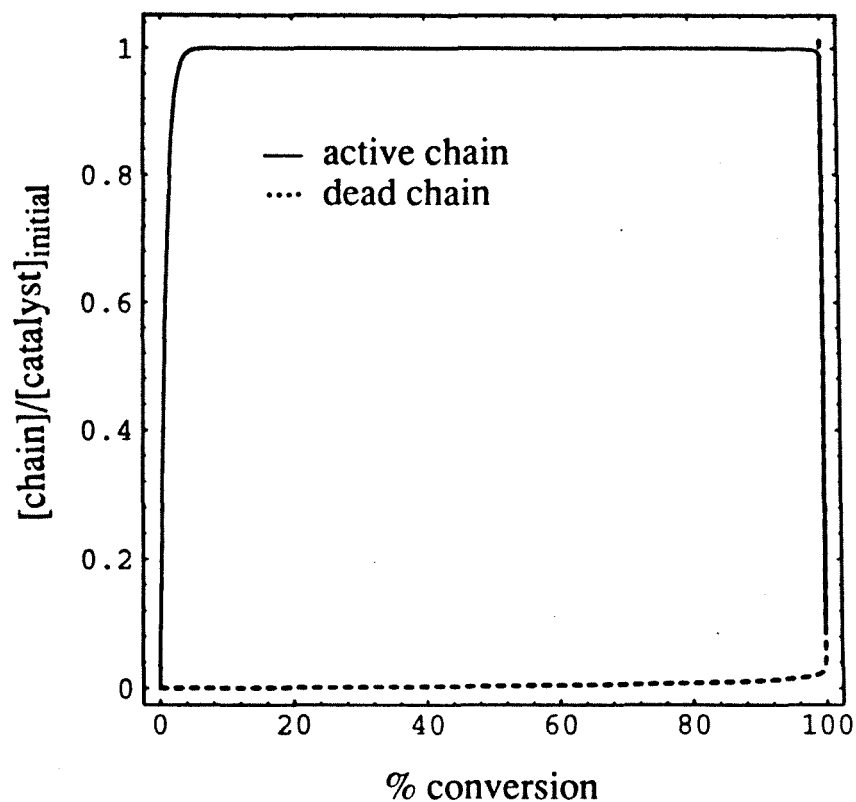


Figure 8. Variation of the number of active and dead chains with conversion— poor chain-transfer agent case. $k_i : k_p : k_{tr} = 125 : 100 : 0.05$. Concentration of catalyst : monomer : chain-transfer agent = 1 : 100 : 10.

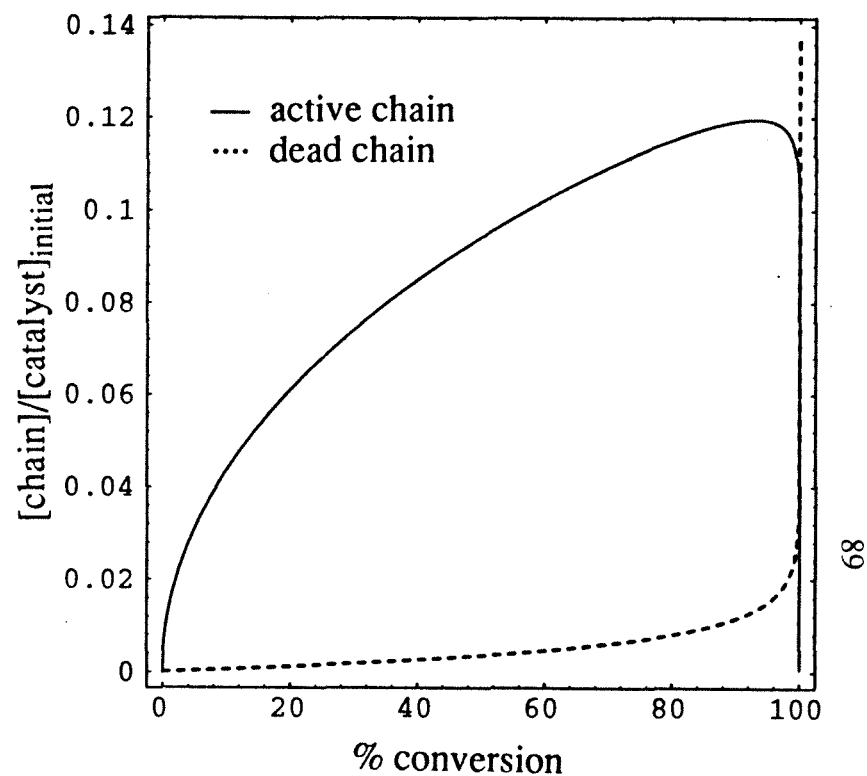


Figure 9. Variation of the number of active and dead chains with conversion— poor chain-transfer agent case. $k_i : k_p : k_{tr} = 0.01 : 100 : 0.05$. Concentration of catalyst : monomer : chain-transfer agent = 1 : 100 : 10.

When the system is perturbed by the addition of a poor chain-transfer agent ($k_{tr} \ll k_p$), the amount of dead chains in the first 98% of the reaction is an extremely small fraction of the total number of chains (active + dead) (Figure 8). Moreover, the \bar{X}_n of the dead chains ($\bar{X}_{n,dead}$) is not a linear function of the extent of reaction (Figure 6). Similarly, the PDI of the active chains (PDI_{active}) follows closely that of a true living polymerization, while that for the dead chains (PDI_{dead}) is much greater than PDI_{active} but slowly decreases monotonically and converges to PDI_{active} as the reaction progresses towards completion (Figure 7). These behaviors are observed because a dead chain is produced only when a *poor* chain-transfer agent reacts occasionally with the active growing chain. Thus, the average molecular weight of the dead chains lags behind that of the active chains, and the distribution of the former is broader. For this reaction, the constancy of the number of propagating species over most of the course of the reaction implies that steady-state approximation can be applied to simplify the eqns 27 to 33 (*vide infra*) (Figure 8). [Note: The concentration of the propagating species does not always reaches a steady-state, e.g., Figure 9 shows the case when k_i is small.]

Cases where $k_{tr} \gg k_p$. Now consider the case where the chain-transfer agent is very efficient ($k_{tr} \gg k_p$). A large percentage of the chain-transfer agent is consumed early in the reaction (Figure 10). This leads initially to dead-chain polymers with short chain lengths (usually between one to ten units long, depending on the concentration of chain-transfer agent). However, once sufficient amount of chain-transfer agent is depleted, the active chains can only react with the remaining large amount of monomers. The polymerization starts to behave like a true living polymerization (i.e., no chain transfer), and results in active chains with huge chain lengths (Figure 12). This behavior is also apparent in the PDI of the system (Figure 13). Initially, the distribution of the active chains starts to broaden immediately due to rapid chain transfer. At 40% conversion, when most of the chain-transfer agent have been consumed (less than 15% of chain-transfer agent left), the PDI_{active} starts to decrease towards that of a living system

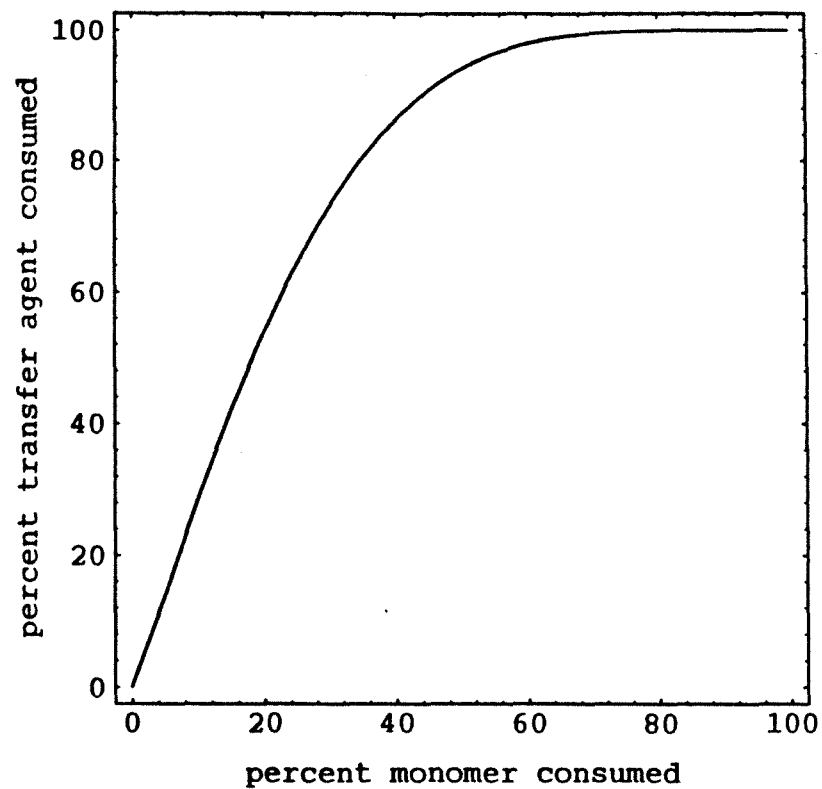


Figure 10. Percent chain-transfer agent consumed versus percent monomer consumed. $k_i : k_p : k_{tr} = 1.25 : 1 : 5$. Concentration of catalyst : monomer : chain-transfer agent = 1 : 100 : 10.

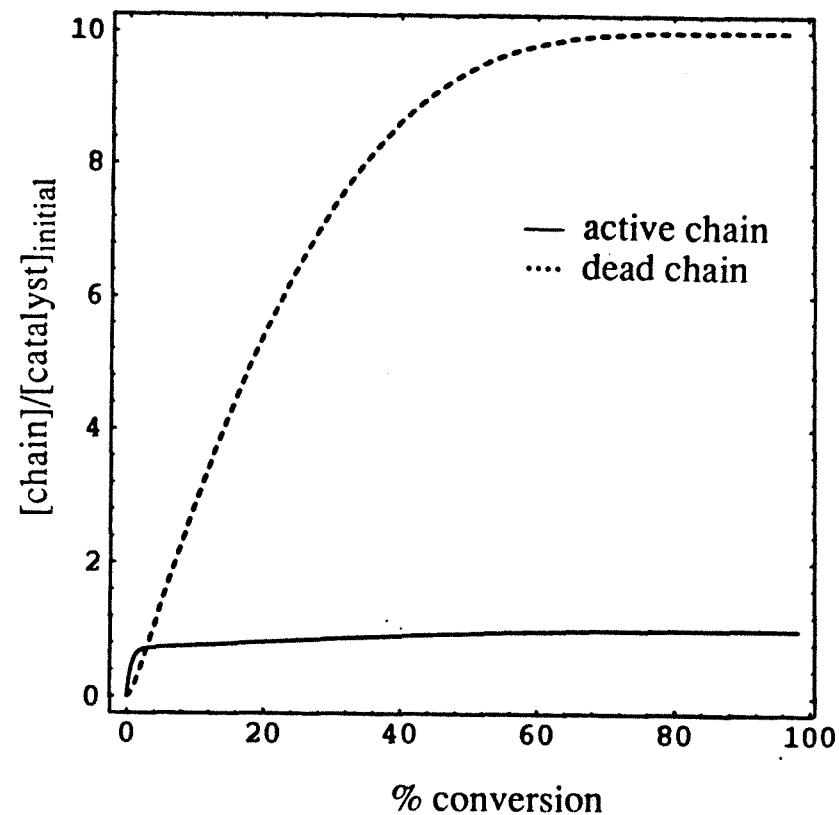


Figure 11. Variation of the number of active and dead chains with conversion— poor chain-transfer agent case. $k_i : k_p : k_{tr} = 1.25 : 1 : 5$. Concentration of catalyst : monomer : chain-transfer agent = 1 : 100 : 10.

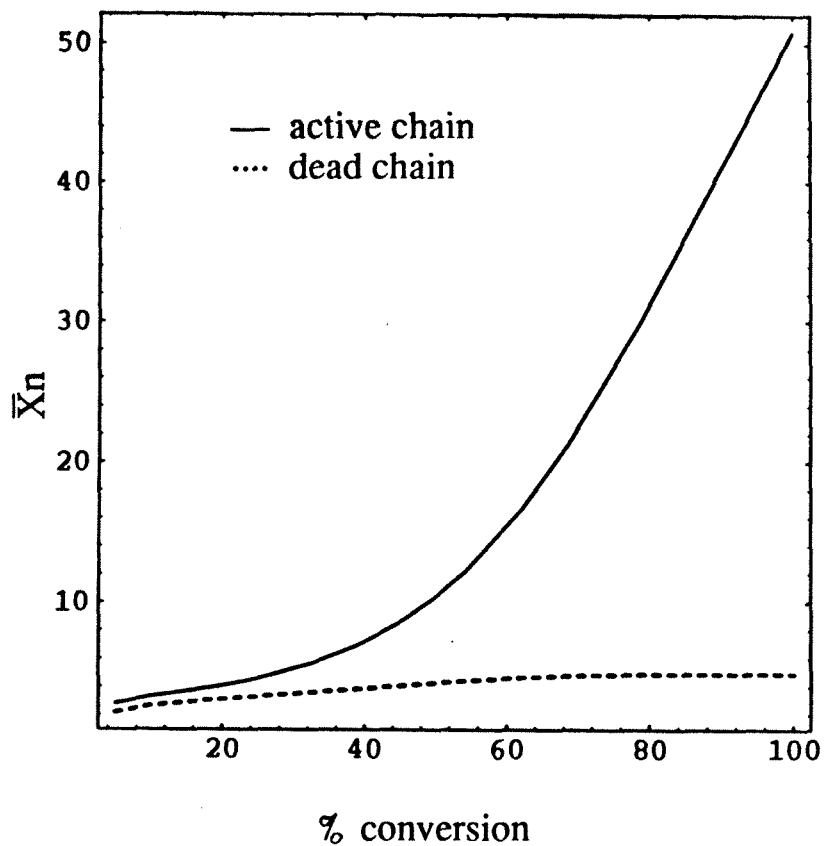


Figure 12. Variation of the number-average degree of polymerization with conversion— efficient chain-transfer agent case. $k_i : k_p : k_{tr} = 1.25 : 1 : 5$. Concentration of catalyst : monomer : chain-transfer agent = 1 : 100 : 10.

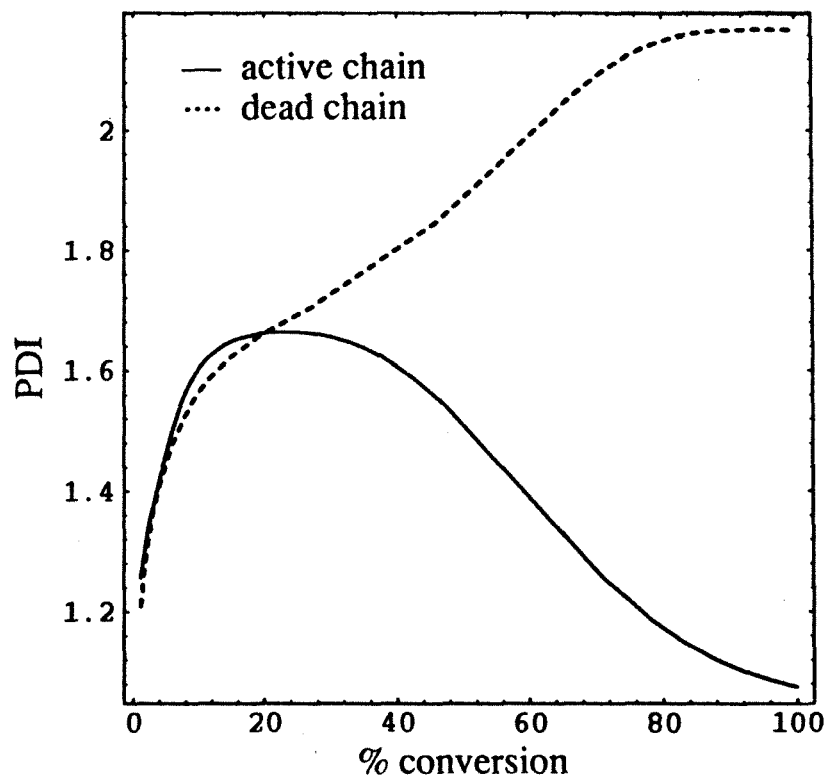


Figure 13. Variation of the polydispersity index with conversion— efficient chain-transfer agent case. $k_i : k_p : k_{tr} = 1.25 : 1 : 5$. Concentration of catalyst : monomer : chain-transfer agent = 1 : 100 : 10.

(i.e., unity) (Figures 10 & 13). The polymerization system thus contains large numbers of short oligomers (5 units long) with broad molecular weight dispersion ($PDI_{\text{dead}} = 2.17$) together with a small number of polymers with long chain lengths (50 units long) with narrow dispersion ($PDI_{\text{active}} = 1.07$) (Figures 11 & 12). Since a significant fraction of the monomers end up as part of the active chains, *a large k_{tr} ($\gg k_p$) does not lead to an efficient yield of short-chain polymers (oligomers).*²¹

Cases where k_{tr} is within an order of magnitude from k_p . Thus, it is only when k_{tr} is *nearly* of the same order of magnitude as k_p (i.e., within one order of magnitude) does the possibility exist for one to control the molecular weight of the polymer. As an example, when k_{tr} is exactly equal to k_p , the \bar{X}_n 's (and also the PDI's) of the active and dead chains are virtually identical at the reaction (Figures 14 & 15).

Figures 16-18 shows how \bar{X}_n varies with the ratio [monomer]/[chain-transfer agent], when k_{tr} is within one order of magnitude from k_p and the reaction is complete. We define the ability to control molecular weight to be as follows: First, the desired chain length is easily achieved by varying the initial monomer concentration to chain-transfer agent ratio. Second, the molecular weight distribution (or polydispersity) should be monomodal. Third, the yield of the reaction should be high. For telechelic polymer synthesis, the last condition implies that most of the monomers should end up as part of the dead chains, formed from active chains end-capped during the reaction by chain-transfer agent bearing functional groups.²²

When $k_{tr} = k_p$, a linear relationship exists between the amount of chain-transfer agent consumed with that of monomer (Figure 19). In spite of this, if insufficient chain-transfer agents are added, the polydispersity remains bimodal (e.g., $MON/CTA = 100$, a non-negligible portion of the chains are 63 monomer units in length while a certain portion is 38 monomer units in length) (Figure 17). *Thus, a necessary condition that the molecular weight be controllable is that there should be enough chain-transfer agents in the system.*

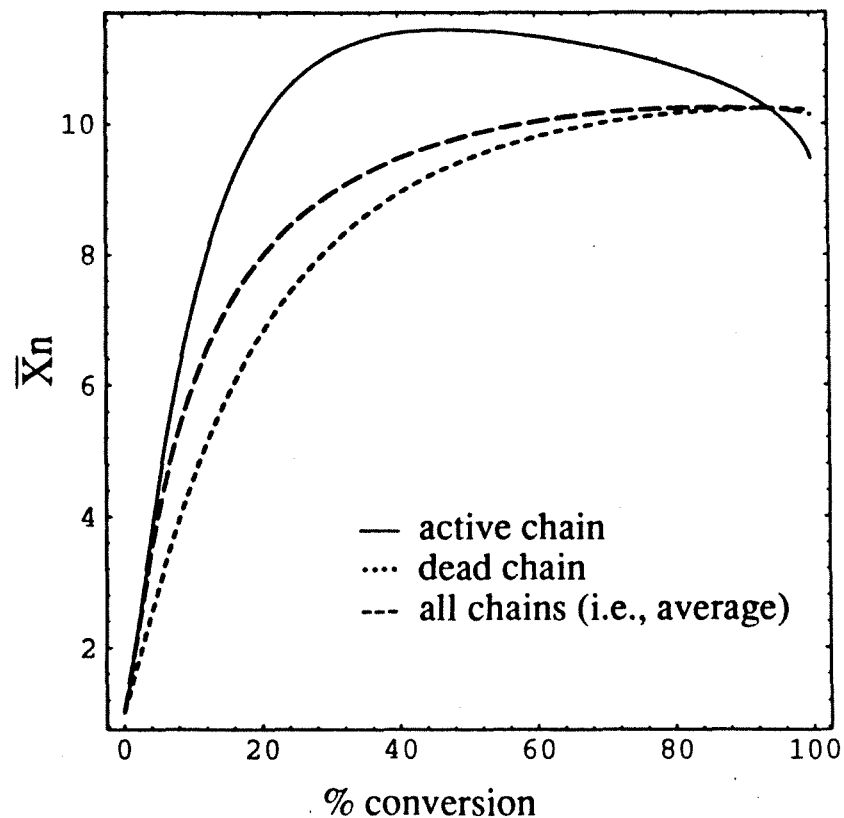


Figure 14. Variation of the number-average degree of polymerization with conversion— case where $k_{tr} \sim k_p$. $k_i : k_p : k_{tr} = 1 : 1 : 1$. Concentration of catalyst : monomer : chain-transfer agent = 1 : 100 : 9.

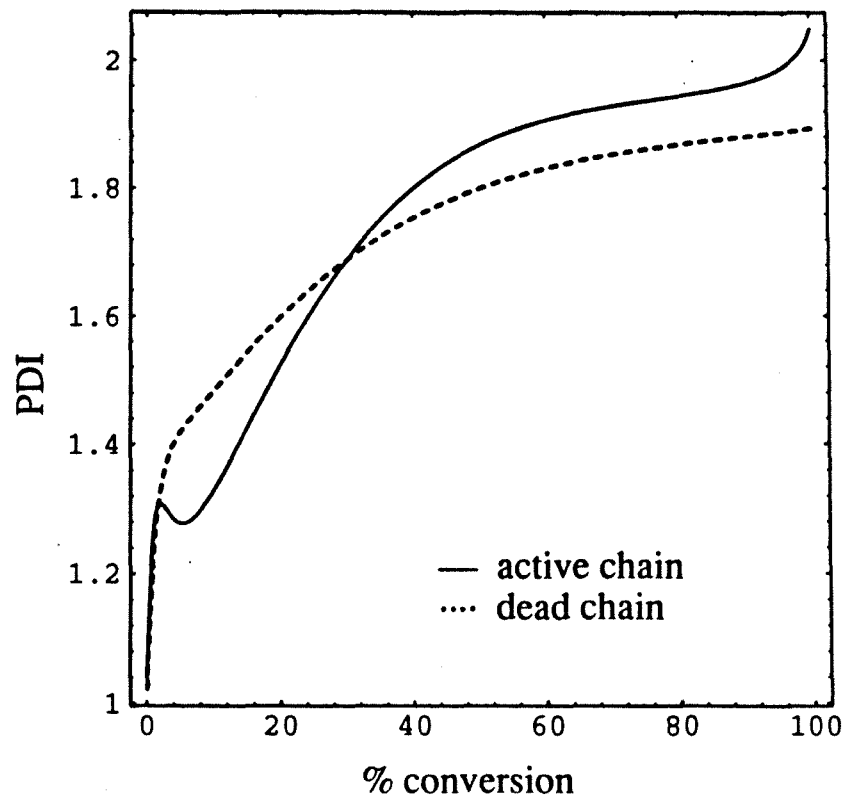


Figure 15. Variation of the polydispersity index with conversion— case where $k_{tr} \sim k_p$. $k_i : k_p : k_{tr} = 1 : 1 : 1$. Concentration of catalyst : monomer : chain-transfer agent = 1 : 100 : 9.

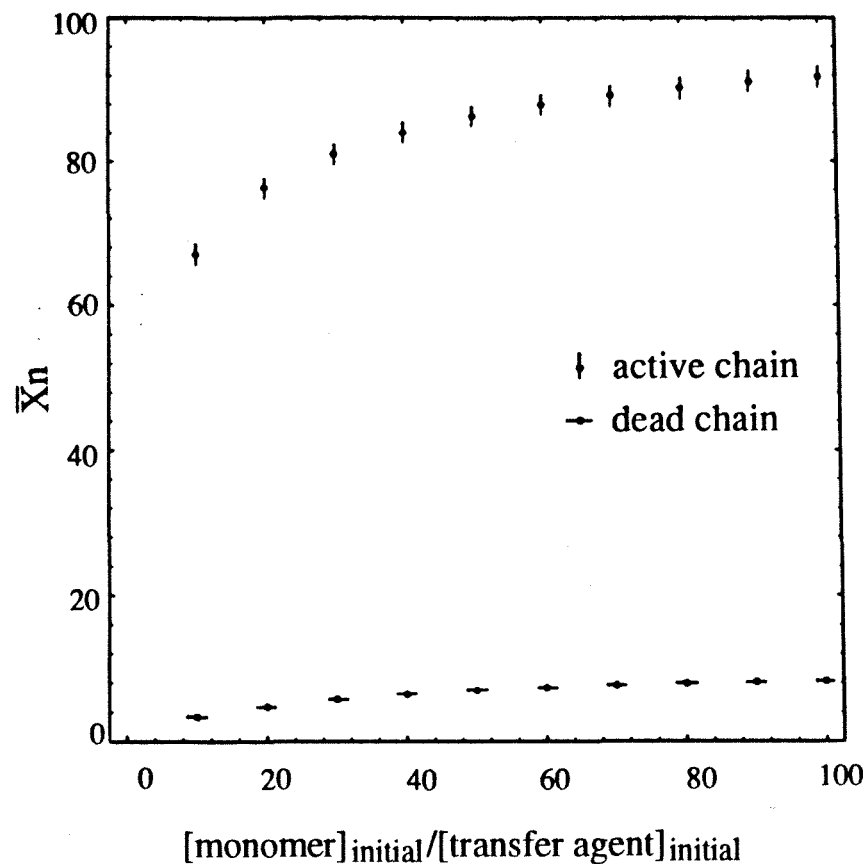


Figure 16. Effect of initial ratio of monomer to chain-transfer agent on the final number-average degree of polymerization. Concentration of catalyst : monomer = 1 : 100. The concentration of the chain-transfer agent is varied with respect to the monomer accordingly. $k_i : k_p : k_{tr}$ is 1 : 1 : 10.

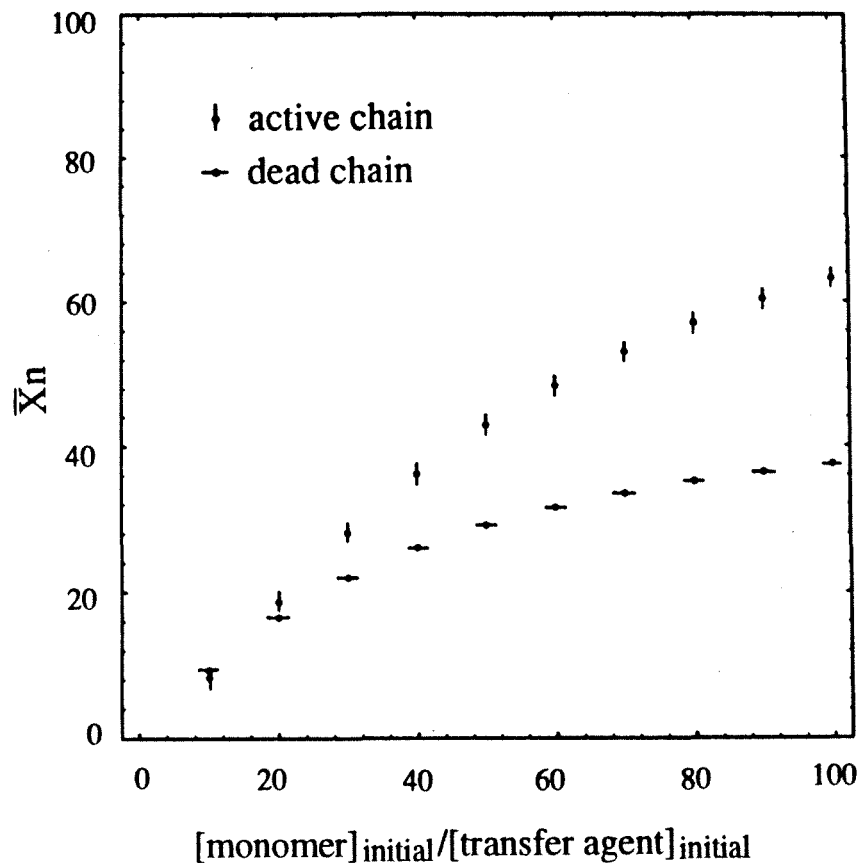


Figure 17. Effect of initial ratio of monomer to chain-transfer agent on the final number-average degree of polymerization. Concentration of catalyst : monomer = 1 : 100. The concentration of the chain-transfer agent is varied with respect to the monomer accordingly. $k_i : k_p : k_{tr}$ is 1 : 1 : 1.

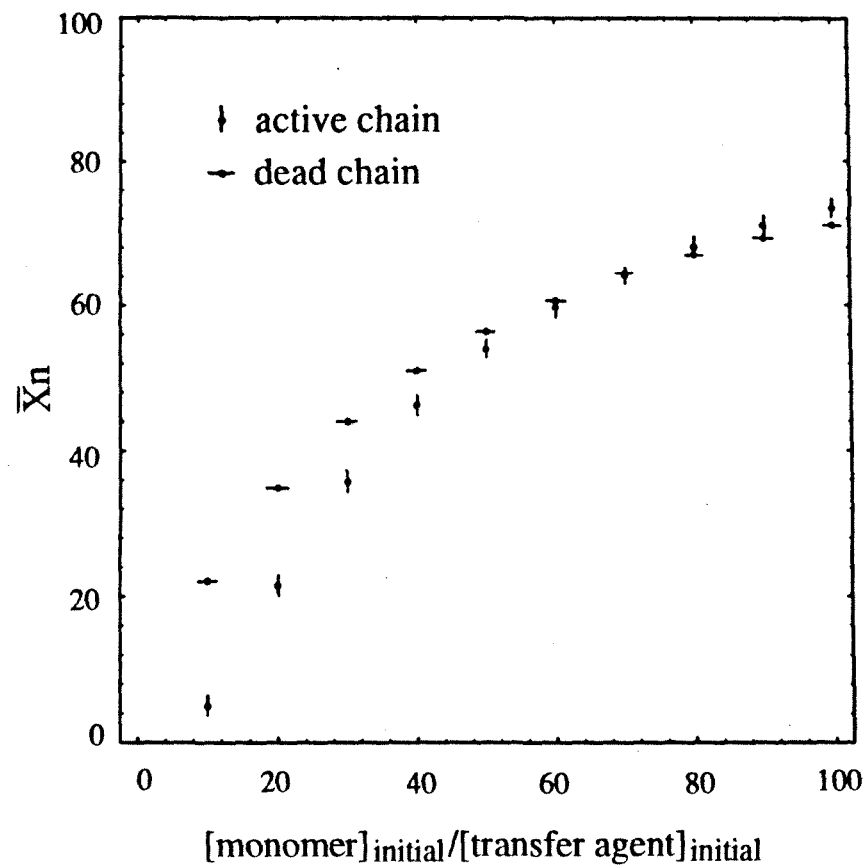


Figure 18. Effect of initial ratio of monomer to chain-transfer agent on the final number-average degree of polymerization. Concentration of catalyst : monomer = 1 : 100. The concentration of the chain-transfer agent is varied with respect to the monomer accordingly. $k_i : k_p : k_{tr}$ is 1 : 1 : 0.1.

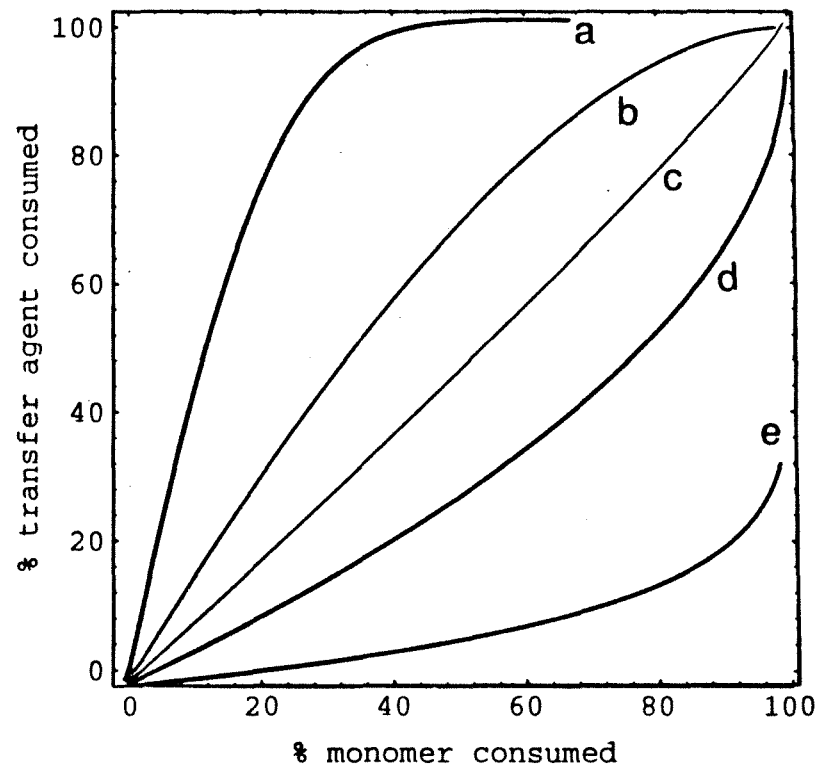


Figure 19. Percent chain-transfer agent consumed versus percent monomer consumed when $k_i = k_p = 1$, and k_{tr} is (a) 10, (b) 2, (c) 1, (d) 0.5, (e) 0.1. Concentration of catalyst : monomer : chain-transfer agent = 1 : 100 : 10.

When $k_{tr} = 0.1 k_p$, two regions arise depending on whether there is an excess of chain-transfer agent or not (Figure 18). When $[\text{monomer}]/[\text{chain-transfer agent}] < 70$, not all chain-transfer agents are consumed at the end of the reaction. Though the distribution seems bimodal, the actual amount of active chains at high conversion is extremely small and negligible. Thus at the end of the reaction, the number-average degree of polymerization of all chains $\bar{X}_{n,\text{all}}$ (i.e., regardless of whether the chain is active or dead) is weighted toward $\bar{X}_{n,\text{dead}}$ (Figure 20). The PDI_{dead} for the first 90% of the reaction is about 1.5, and rises steeply to 2.2 only in the last 4% of the reaction (Figure 21). For this particular set of rate constants, the molecular weight can therefore be controlled in this region.

When $[\text{monomer}]/[\text{chain-transfer agent}] > 70$, the plot of percent chain-transfer agent consumed versus percent monomer consumed still has the same form as curve *e* in Figure 19. Although only about 20% of the chain-transfer agent has reacted at 90% conversion of the monomer, both are used up eventually.²² Under this condition, 29% of the monomer ends up as part of the active chains. Unlike the preceding case, $\bar{X}_{n,\text{all}}$ is weighted towards $\bar{X}_{n,\text{active}}$ throughout most of the reaction (Figure 22). Nevertheless, the active and dead chains each have a \bar{X}_n that ultimately *converge to the same value* while their PDI's remain below 1.4 (Figure 23). Therefore, *complete consumption of both chain-transfer agent and monomer plus a monomodal molecular weight distribution do not guarantee the total absence of active chains*. Hence, if both chain-transfer agent and monomer are totally consumed, a *necessary but not sufficient* condition for the controlled synthesis of *telechelic* polymer is the presence of enough chain-transfer agents to endcap the remaining active chains near the end of the reaction. [Note that for $k_{tr} = 0.1 k_p$, the concentration of the propagating species reaches a steady-state (Figures 24 & 25)].

Mayo Plot and k_{tr}/k_p . We now examine the features of the Mayo plot to determine whether its slope has the same significance for a living system (with deliberately addition of chain-transfer agent) as compared with that of a non-living

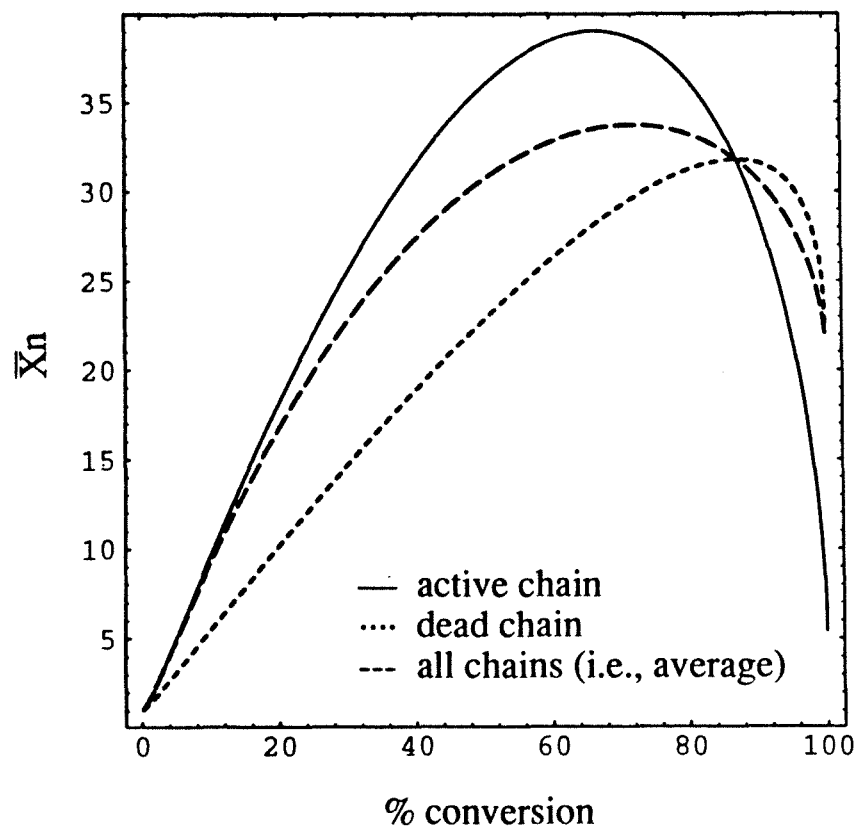


Figure 20. Variation of the number-average degree of polymerization with conversion. $k_i : k_p : k_{tr} = 1 : 1 : 0.1$. Concentration of catalyst : monomer : chain-transfer agent = 1 : 100 : 10.

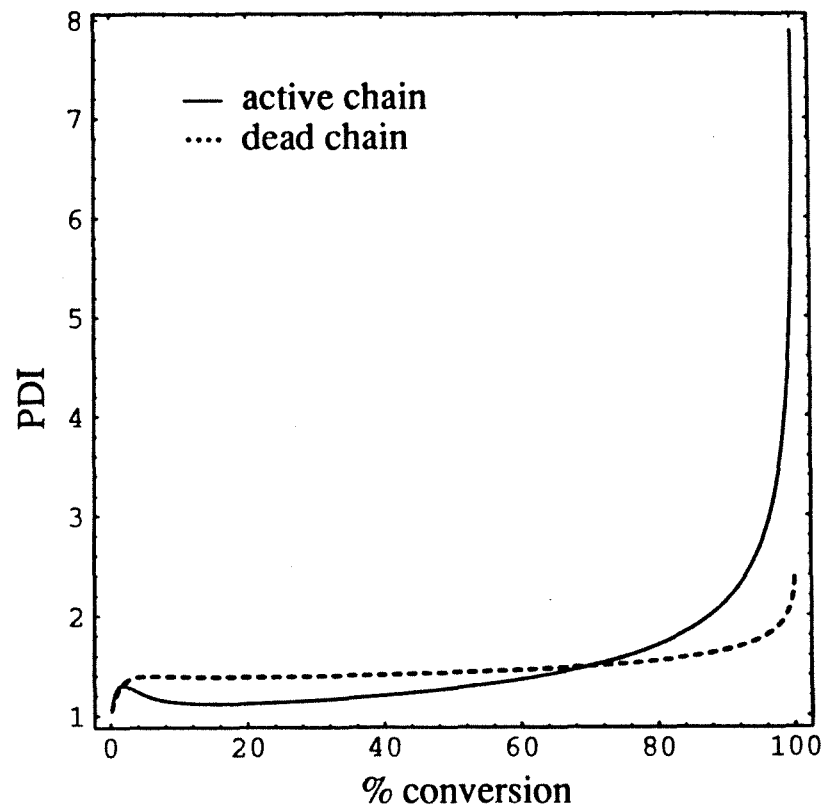


Figure 21. Variation of the polydispersity index with conversion. $k_i : k_p : k_{tr} = 1 : 1 : 0.1$. Concentration of catalyst : monomer : chain-transfer agent = 1 : 100 : 10.

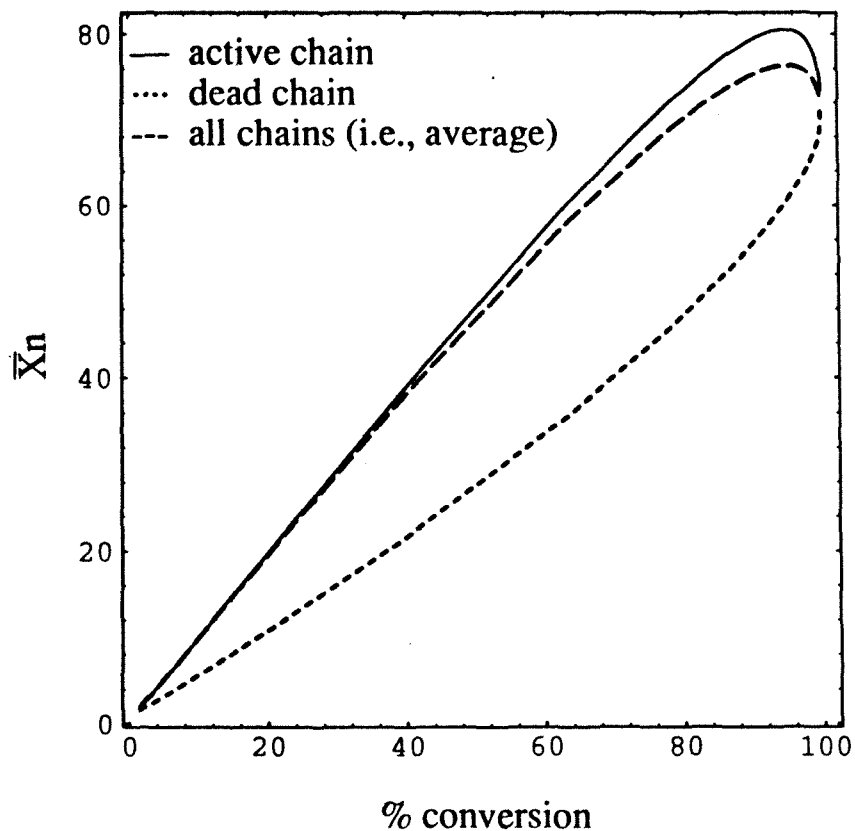


Figure 22. Variation of the number-average degree of polymerization with conversion. $k_i : k_p : k_{tr} = 1 : 1 : 0.1$. Concentration of catalyst : monomer : chain-transfer agent = 1 : 100 : 1.

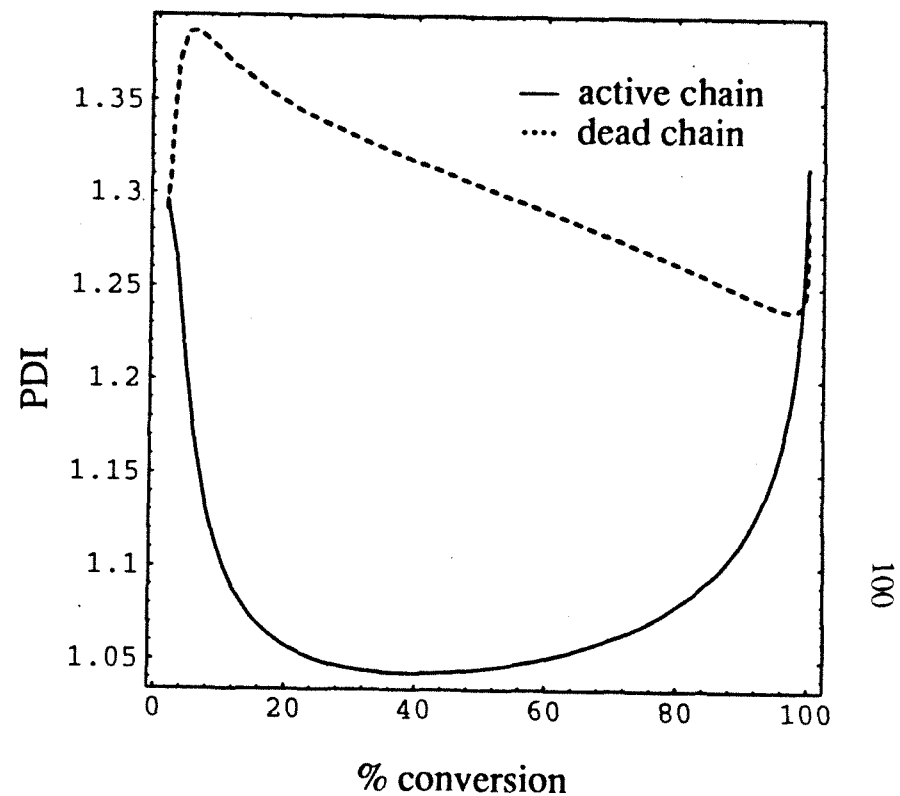


Figure 23. Variation of the polydispersity index with conversion. $k_i : k_p : k_{tr} = 1 : 1 : 0.1$. Concentration of catalyst : monomer : chain-transfer agent = 1 : 100 : 1.

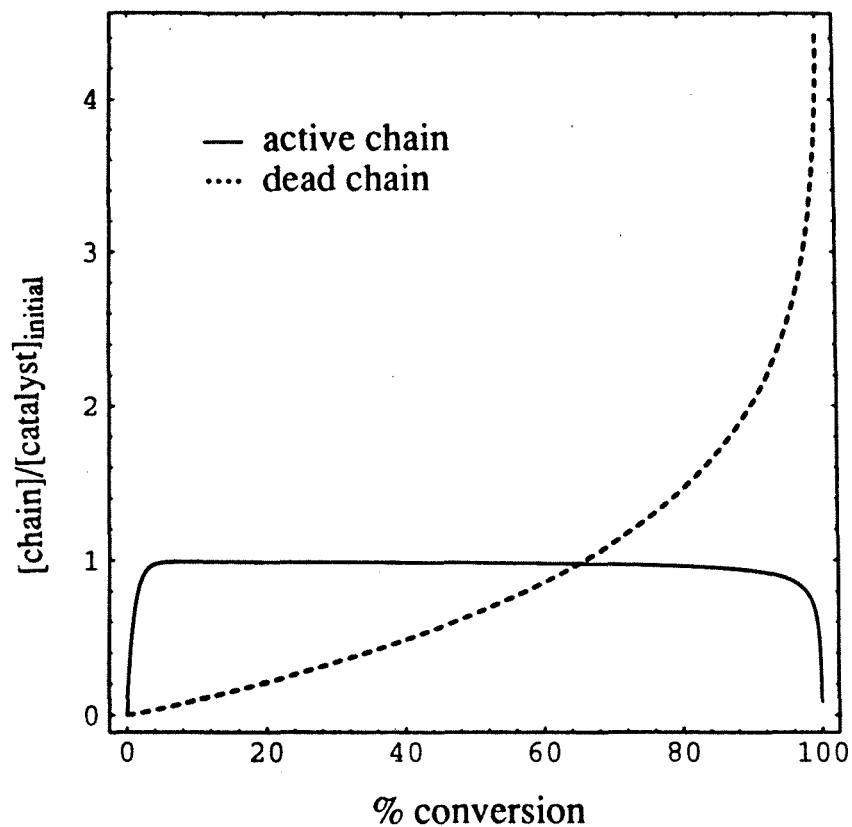


Figure 24. Variation of the number of active and dead chains with conversion. $k_i : k_p : k_{tr} = 1 : 1 : 0.1$. Concentration of catalyst : monomer : chain-transfer agent = 1 : 100 : 10. At 100% conversion, only an extremely small fraction of the chains are active.

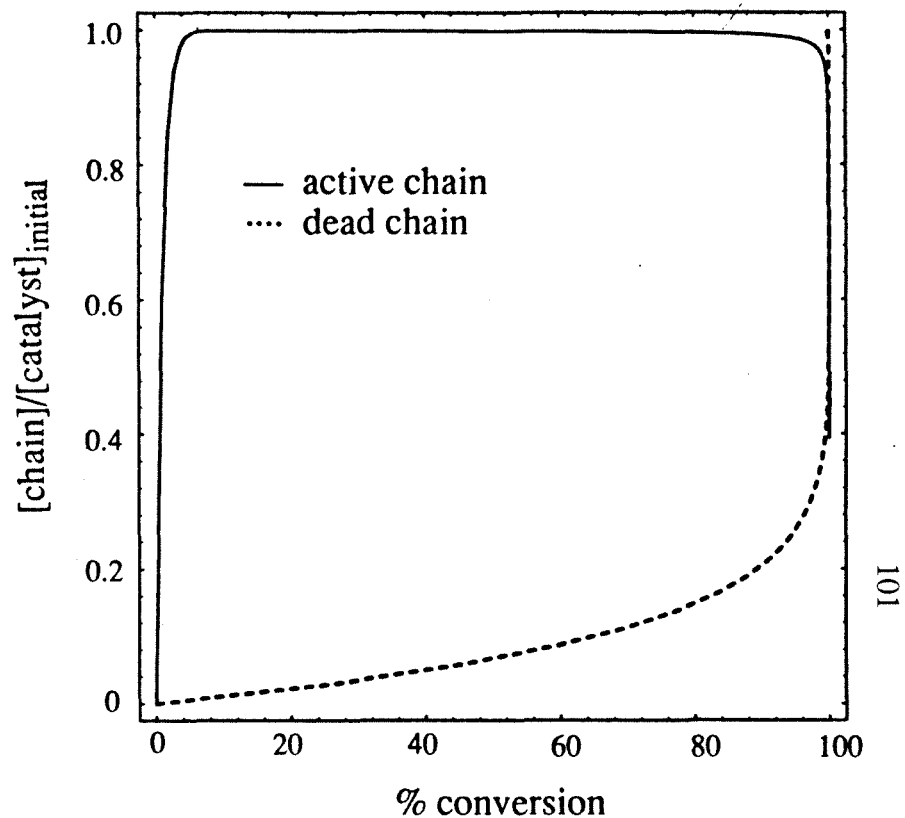


Figure 25. Variation of the number of active and dead chains with conversion. $k_i : k_p : k_{tr} = 1 : 1 : 0.1$. Concentration of catalyst : monomer : chain-transfer agent = 1 : 100 : 1.

system, as certain literatures have employed its slope as a measure of k_{tr}/k_p regardless of whether the polymerization is living or not.^{4,23} A correlation of greater than 0.98 is always obtained in this polymerization scheme when $1/\bar{X}_n$ is plotted against $[\text{chain-transfer agent}]_{\text{initial}}/[\text{monomer}]_{\text{initial}}$ (see explanation in Analytical Results and Discussion).²⁴ However, in contrast to *non-living* polymerization (i.e., presence of termination not arising from chain transfer), *the slope Ss of the Mayo plot for a living polymerization may differ from k_{tr}/k_p by orders of magnitude.*^{4,23} (Figures 26-28). The slope Ss also changes with k_i and is not related to the ratio k_{tr}/k_p in a simple manner (Figures 26-28). As expected, as the specific rate of initiation increases relative to propagation, \bar{X}_n decreases and therefore the slope Ss increases.

Before deriving a graphical relationship between k_{tr}/k_p to the slope (*vide infra*), it should be noted that even when the ratio $[\text{chain-transfer agent}]_{\text{initial}}/[\text{monomer}]_{\text{initial}}$ remains a constant, the degree of polymerization $\bar{X}_{n,\text{dead}}$ at the end of the reaction is dependent on the amount of catalyst used in the polymerization. (Figure 29). This result implies that for a living polymerization, the slope Ss depends on which reagent (chain-transfer agent or monomer) is varied when constructing the Mayo plot. To further illustrate, the Mayo plot that is obtained by varying the concentration of chain-transfer agent while keeping the ratio $[\text{monomer}]_{\text{initial}}/[\text{catalyst}]_{\text{initial}}$ constant, is dramatically different from that obtained when it is the concentration of monomer that is varied but ratio $[\text{chain-transfer agent}]_{\text{initial}}/[\text{catalyst}]_{\text{initial}}$ is kept constant (Figure 30). Note that in both cases the value of \bar{X}_n is different for the same values of $[\text{chain-transfer agent}]_{\text{initial}}/[\text{monomer}]_{\text{initial}}$ by virtue of how the experiment is conducted.

For a given k_p/k_i , we next constructed a graphical relationship between Ss and k_{tr}/k_p as a way to obtain k_{tr}/k_p by using slope from the Mayo plot. The values k_p/k_i can easily be measured experimentally by an independent method.^{16a}

When $[\text{chain-transfer agent}]_{\text{initial}}/[\text{catalyst}]_{\text{initial}}$ is fixed while $[\text{monomer}]_{\text{initial}}$ is allowed to vary, the graph shows three well-defined region (Figure 31). In the rightmost

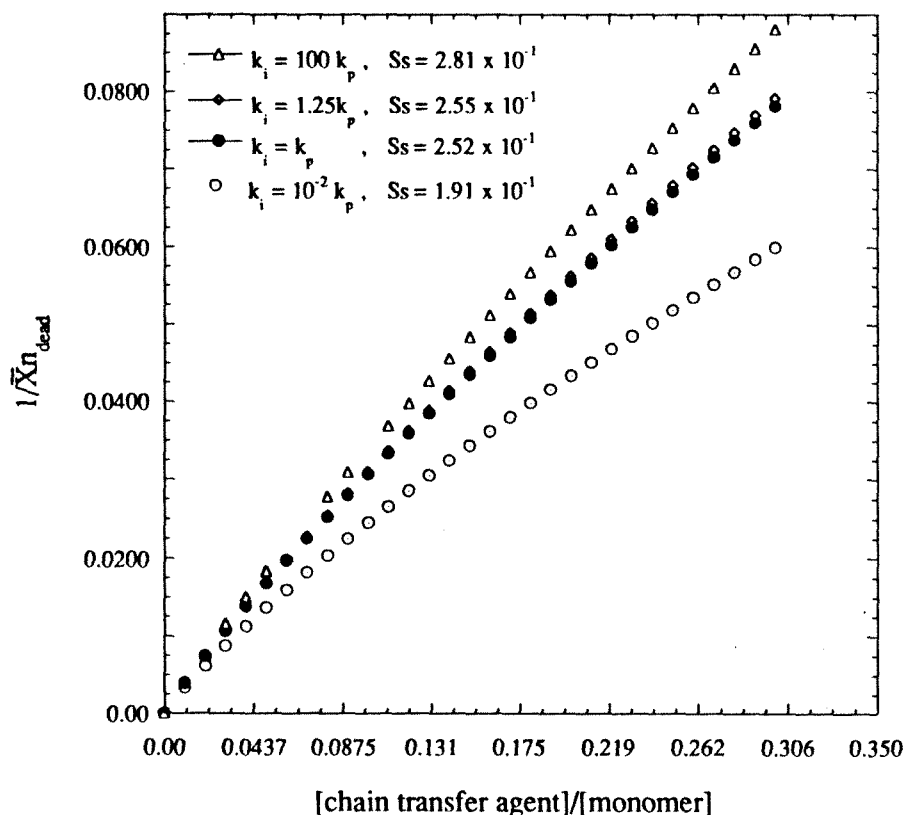


Figure 26. Mayo plot. k_{tr}/k_p is set at 5.0×10^{-2} . Concentration of catalyst : chain-transfer agent = 1 : 10. Concentration of monomer is varied accordingly. The slope S_s varies with initiation rates and is not equal to k_{tr}/k_p . The slope S_s is derived from a least-square fit of $1/X_{nall}$ with $[chain-transfer agent]_{initial} / [monomer]_{initial}$.

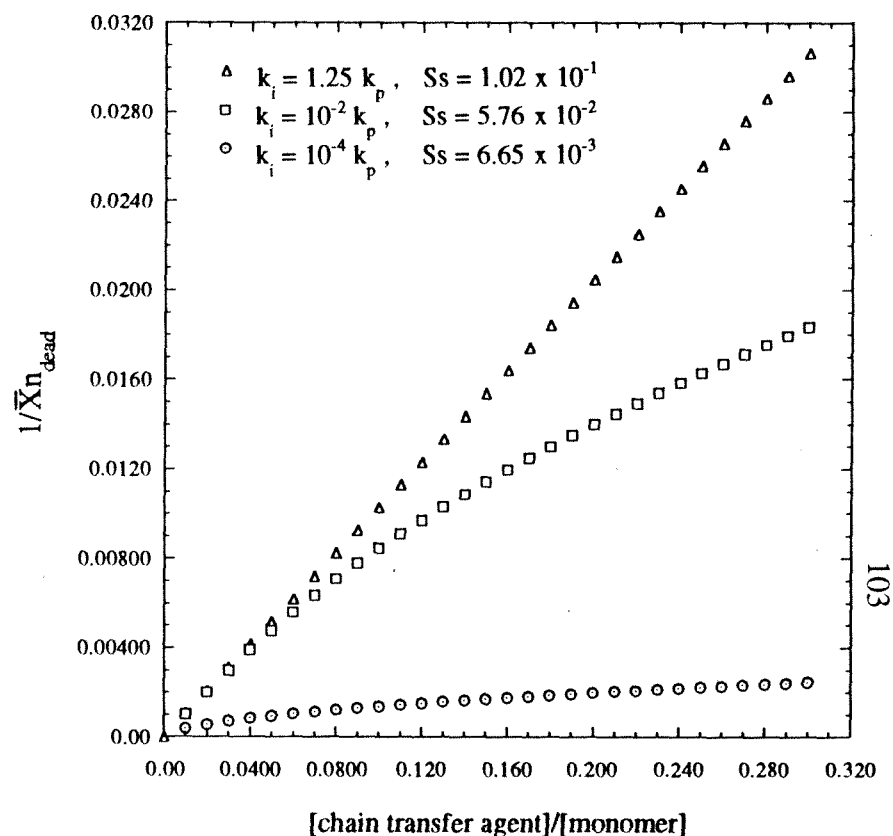


Figure 27. Mayo plot. k_{tr}/k_p is set at 5.0×10^{-4} . Concentration of catalyst : chain-transfer agent = 1 : 10. Concentration of monomer is varied accordingly. The slope S_s varies with initiation rate and is not equal to k_{tr}/k_p . The slope S_s is derived from a least-square fit of $1/X_{nall}$ with $[chain-transfer agent]_{initial} / [monomer]_{initial}$.

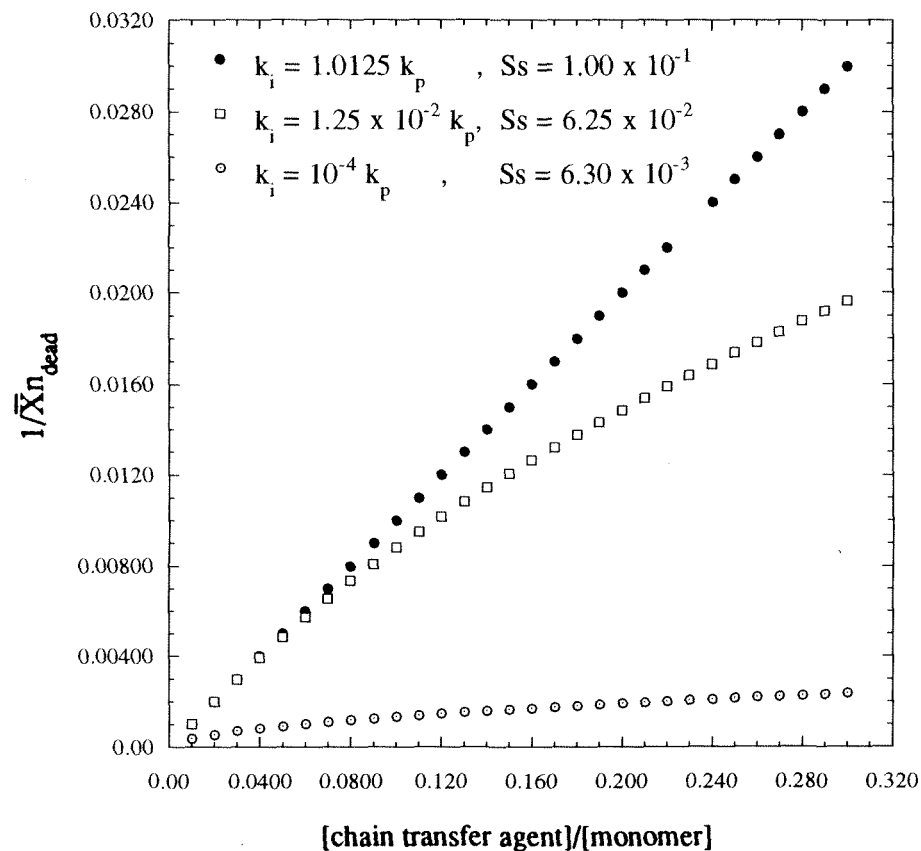


Figure 28. Mayo plot. k_{tr}/k_p is set at 5.0×10^{-6} .
 Concentration of catalyst : chain-transfer agent = 1 : 10.
 Concentration of monomer is varied accordingly. The
 slope S_s varies with initiation rate and is not equal to
 k_{tr}/k_p . The slope S_s is derived from a least-square fit of
 $1/\bar{X}n_{\text{all}}$ with $[\text{chain-transfer agent}]_{\text{initial}}/[\text{monomer}]_{\text{initial}}$.

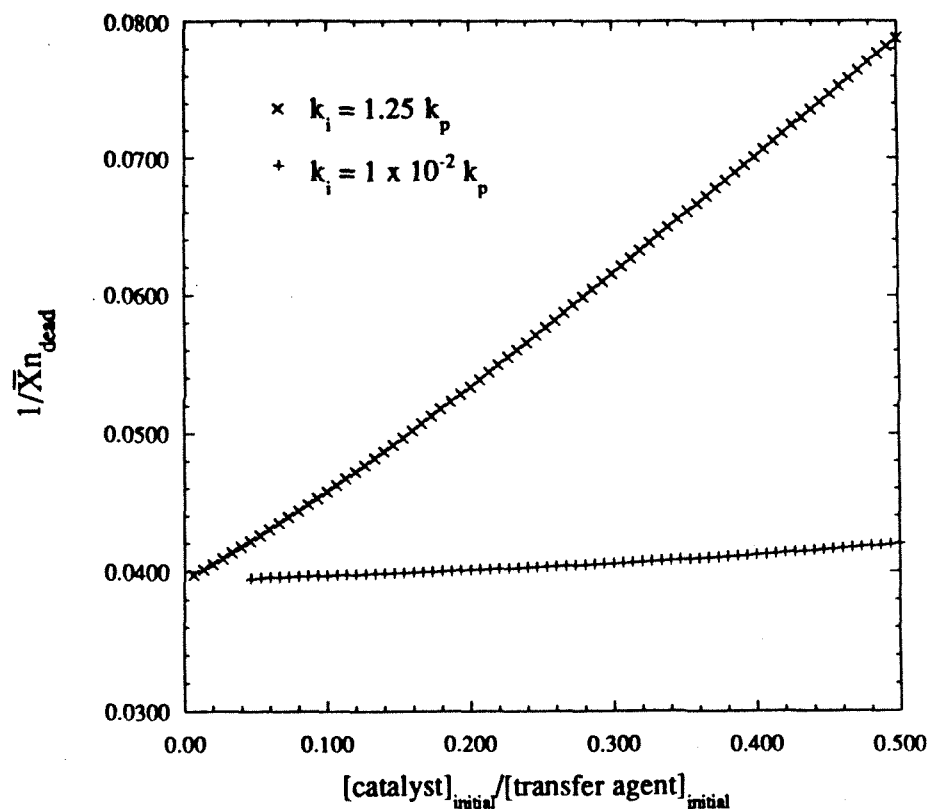


Figure 29. Dependence of number-average degree of polymerization on catalyst concentration. $[\text{chain-transfer agent}]_{\text{initial}}$ is kept constant. $[\text{chain-transfer agent}]/[\text{monomer}] = 0.10$ and $k_{tr}/k_p = 0.10$.

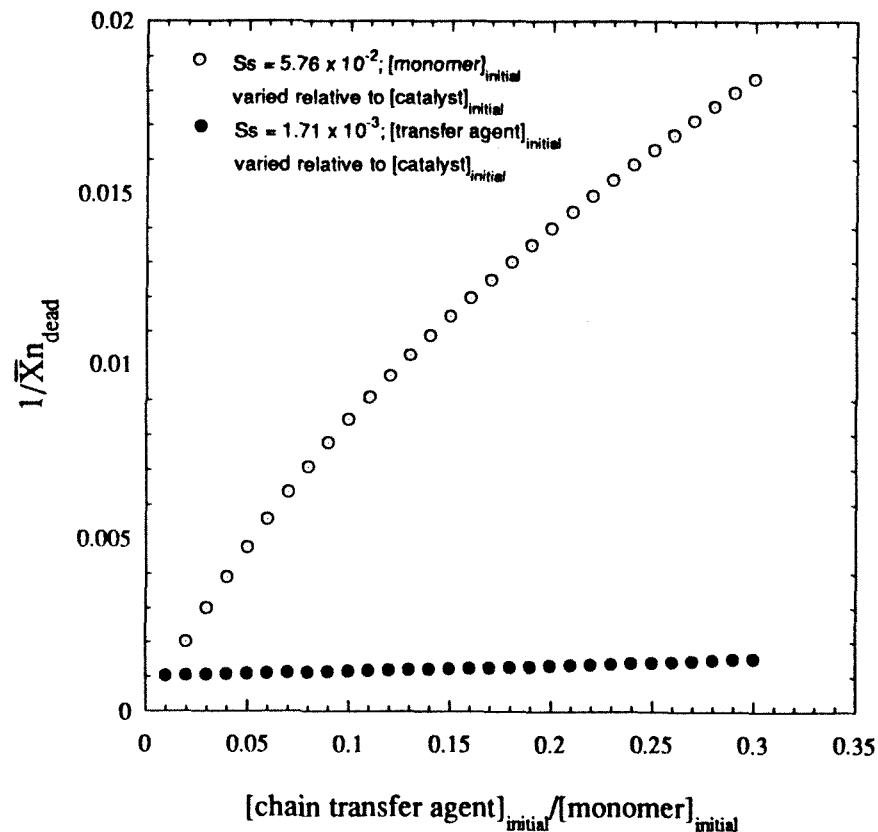


Figure 30. Comparison of the slopes of Mayo plots for two different reaction conditions: (1) $[\text{monomer}]$ varied relative to $[\text{catalyst}]$, and (2) $[\text{transfer agent}]$ varies relative to $[\text{catalyst}]$. $k_i : k_p : k_{tr} = 1 : 100 : 0.01$. The leftmost data point corresponds to catalyst : monomer : chain-transfer agent = 1 : 1000 : 10.

region, the slope S_s converges to 1 (hence $\log S_s = 0$) regardless of the rate of initiation. This behavior is understood by noting that when $k_{tr} \gg k_p$, the expression $\bar{X}_{n,all} = (A + D)/[CAT - W_0] + (CTA - P_0)$ reduces to $\bar{X}_{n,all} \approx MON/CTA$ because $(A + D) = MON$, $P_0 = 0$, and $CAT < CTA$. Hence $1/\bar{X}_{n,all} \approx CTA/MON$, and $S_s = 1$. For the leftmost region, $k_{tr} \ll k_p$, hence \bar{X}_n reduces to the limiting value given by Gold's paper and the slope S_s is independent of the value k_{tr}/k_p .^{16a} Therefore, consistent with the conclusion of the preceding section, k_{tr}/k_p can only take a narrow range of values for the system to exhibit effective molecular weight control.

Similarly, when $[monomer]_{initial}/[catalyst]_{initial}$ is fixed while $[chain-transfer\ agent]_{initial}$ is allowed to vary, the graph also shows three regions of interest (Figure 32). Again, only in the central region where $k_{tr} \sim 0.1 k_p$ or $1.0 k_p$ does the possibility exist for controlling the molecular weight. The rightmost region shows S_s having a value of unity, regardless of how high k_{tr}/k_p gets. This result showing that S_s is not equal to k_{tr}/k_p might explain the observation that apparent rate constants k_{tr}/k_p of reactive acyclic olefins taken from the Mayo plot are usually lower than the results obtained from telomer ratios.^{7c}

Analytical Results and Discussion

Steady-State Approximation and Closed-Form Solution. It is known that in a polymerization scheme consisting only of initiation, propagation, and chain transfer an unsteady-state polymerization results, i.e., the number of active chains is *not* invariant.^{14a} Such cases also exist in our scheme (monomer incapable of acting as chain-transfer agent) (e.g., Figure 9).²⁵

In as much as the steady-state assumption greatly simplifies the analytical expression of \bar{X}_n for a great variety of polymerization schemes (living or non-living), we now impose such an assumption on our system for comparison with the numerical solution obtained above. This assumption is not entirely invalid since certain cases we examined gave steady-state kinetics (e.g., Figures 8, 24, & 25).

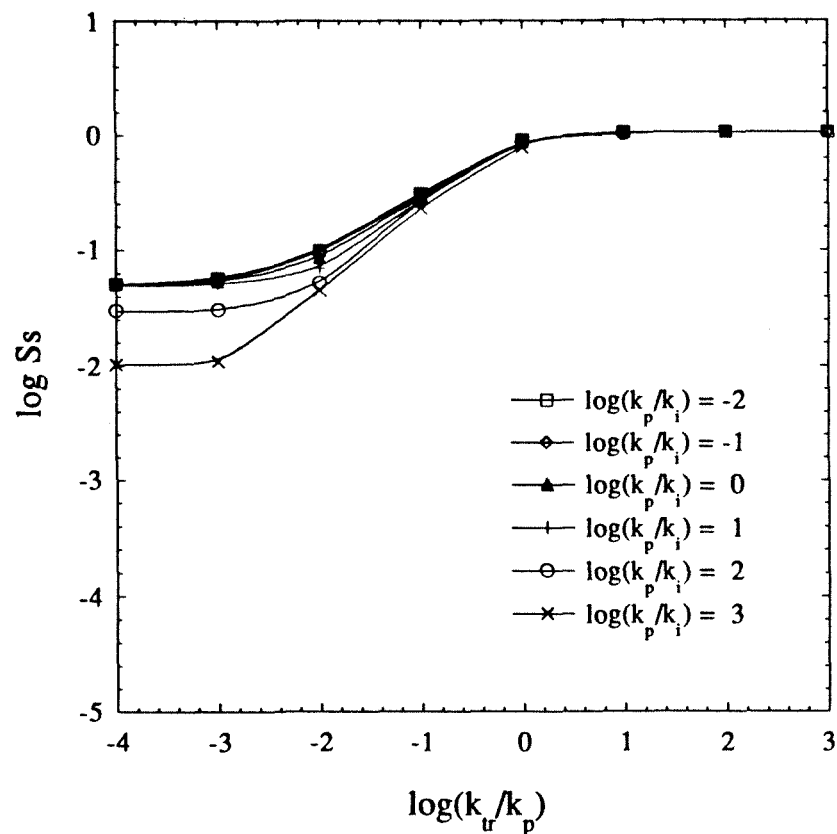


Figure 31. Relationship of the slope S_s of Mayo plot to k_{tr}/k_p for different k_p/k_i . $[\text{chain-transfer agent}]/[\text{catalyst}] = 20$; $[\text{monomer}]$ varies from 2 to 20 times $[\text{chain-transfer agent}]$. The slope S_s is derived from a least-square fit of $1/X_{nall}$ with $[\text{chain-transfer agent}]_{\text{initial}}/[\text{monomer}]_{\text{initial}}$.

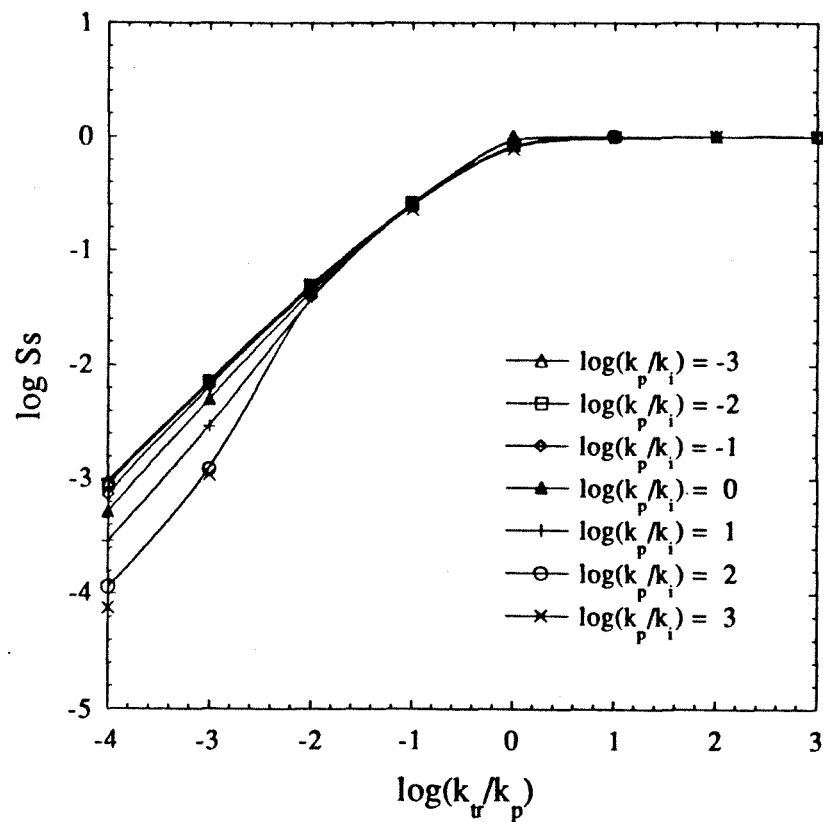


Figure 32. Relationship of the slope S_s of Mayo plot to k_{tr}/k_p for different k_p/k_i . $[\text{monomer}]/[\text{catalyst}] = 100$; $[\text{transfer agent}]$ varies from 2 to 20 times $[\text{monomer}]$. The slope S_s is derived from a least-square fit of $1/X_{nall}$ with $[\text{chain-transfer agent}]_{\text{initial}}/[\text{monomer}]_{\text{initial}}$.

By definition, steady-state is said to occur when the rate of change of the amount of active chains in solution is much less than the rate of active-chain formation or destruction (i.e.,

$$d\left(\sum_{n=1}^{\infty} W_n\right)/dt \ll \text{minimum}(\text{rate of formation, rate of destruction of active species}).^{9e} \quad (37)$$

It is important to observe from this definition that $d\left(\sum_{n=1}^{\infty} W_n\right)/dt \approx 0$ is not a sufficient condition for the existence of steady state.^{9e}

In spite of the above condition, in a non-living polymerization, it is customarily assumed that

$$dW_n/dt = 0 \text{ for } n \geq 0.^{9,15} \quad (38)$$

In a living polymerization, this strong form of the steady-state approximation does not lead to the correct expression for \bar{X}_n .²⁶ However, we have observed (through numerical calculation) that the weaker form of the steady-state approximation

$$dW_0/dt = 0 \quad (39)$$

occurs frequently when $k_{tr} < k_p$ (e.g., Figures 8, 24, & 25). Thus eqn. 19 becomes

$$\sum_{n=1}^{\infty} W_n = (k_i W_0 M) / (k_{tr} P_0). \quad (40)$$

Substituting eqn. 40 into the quotient of eqns. 18 and 22 gives

$$\partial M / \partial P_0 = 1 + (k_p / k_{tr})(M / P_0). \quad (41)$$

Integrating eqn. 41, we have

$$M = \frac{P_0}{1 - \frac{k_p}{k_{tr}}} + \left(\text{MON} - \frac{\text{CTA}}{1 - \frac{k_p}{k_{tr}}} \right) \left(\frac{P_0}{\text{CTA}} \right)^{\frac{k_p}{k_{tr}}}. \quad (42)$$

Consider the case when $k_{tr} < k_p$ and sufficient amount of chain-transfer agents are used in the reaction. At the end of the reaction, $M = 0$. The amount of chain-transfer agent left is

$$P_0 = \text{CTA} \left[1 + \left(\frac{k_p}{k_{tr}} - 1 \right) \left(\frac{\text{MON}}{\text{CTA}} \right) \right]^{-\frac{1}{\frac{k_p}{k_{tr}} - 1}}. \quad (43)$$

Since no active chains are left, the equation $\bar{X}_{n\text{dead}} = \text{MON}/(\text{CTA} - P_0)$ becomes

$$\bar{X}_{n\text{all}} = \bar{X}_{n\text{dead}} = \frac{\text{MON}}{\text{CTA}} \frac{1}{1 - \left[1 + \left(\frac{k_p}{k_{tr}} - 1 \right) \left(\frac{\text{MON}}{\text{CTA}} \right) \right]^{-\frac{1}{\frac{k_p}{k_{tr}} - 1}}} \quad (44)$$

Figure 33 shows an excellent agreement between the analytical solution for $\bar{X}_{n\text{dead}}$ shown above and that obtained by numerical approach discussed in the previous section. The expression for \bar{X}_n in eqn. 44 is independent of the rate of initiation, the catalyst concentration, and the manner by which the experiment is conducted (*cf.* previous section). This results from the requirement that sufficient amount of chain-transfer agent be present in the system, *which implies an initial condition of* $[\text{catalyst}]_{\text{initial}} \ll [\text{chain-transfer agent}]_{\text{initial}}$.^{27a} Eqn. 44 predicts that when the above initial conditions hold, the Mayo plot should be nearly linear with a slope $d(1/\bar{X}_n)/d(\text{CTA}/\text{MON})$ given by^{27b}

$$S_c = \frac{d\left(\frac{1}{\bar{X}_n}\right)}{d\left(\frac{\text{CTA}}{\text{MON}}\right)} = 1 - \left(1 + \frac{1}{\frac{\text{CTA}}{\text{MON}} + \frac{k_p}{k_{tr}} - 1} \right) \left(1 + \frac{\frac{k_p}{k_{tr}} - 1}{\frac{\text{CTA}}{\text{MON}}} \right)^{-\frac{1}{\frac{k_p}{k_{tr}} - 1}} \quad (45)$$

The plot of eqn. 45 is in close agreement with Figure 32, despite the fact that in Figure 32, $[\text{catalyst}]_{\text{initial}}$ is within an order of magnitude of $[\text{chain-transfer agent}]_{\text{initial}}$ (*cf.* Figures 35 & 32). It can be shown that the slope S_c is practically independent of the ratio $[\text{monomer}]/[\text{chain-transfer agent}]$ when the ratio is greater than 10. Thus, the value of k_{tr}/k_p can be determined from a construction of Mayo plot and the use of S_c (Figure 34). It may also be shown analytically that S_c is independent of the quantity CTA/MON when k_{tr}/k_p approaches 0.

Experimental Section

General Methods. All manipulations of air- and/or moisture sensitive compounds were carried out under argon using standard Schlenk and vacuum line techniques. Argon was purified by passing through columns of activated BASF RS-11 (Chemalog™) oxygen

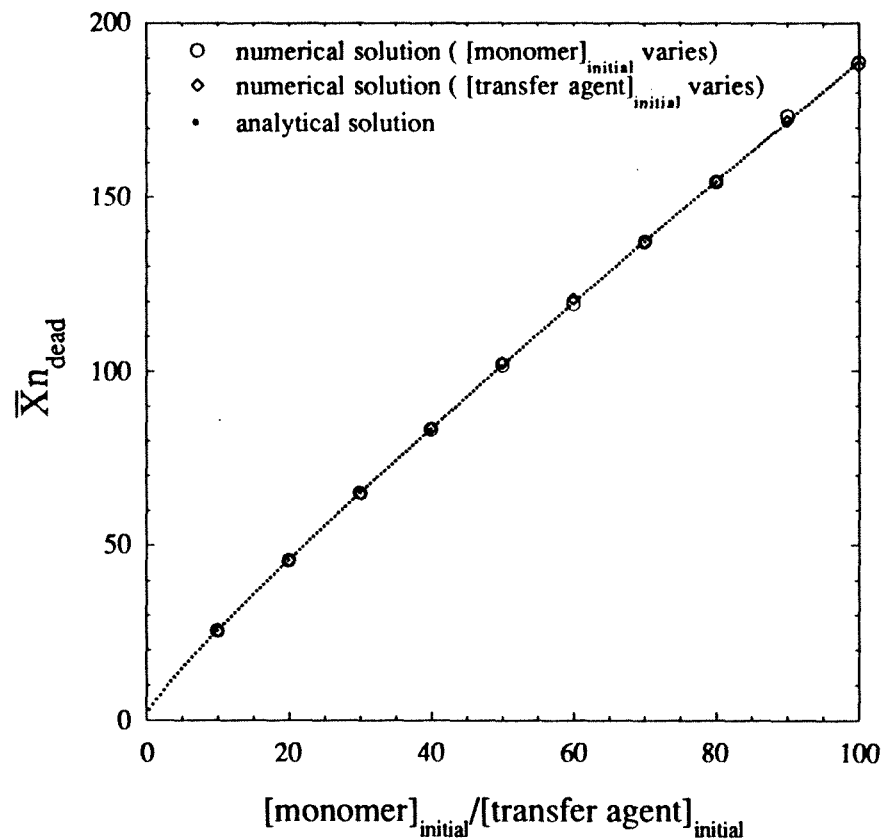


Figure 33 . Comparison of analytical and numerical solutions for \bar{X}_n at different $[\text{monomer}]_{\text{initial}}/[\text{transfer agent}]_{\text{initial}}$ ratios. $k_i : k_p : k_{tr} = 1 : 1 : 0.1$. For the first numerical solution, $[\text{transfer agent}]_{\text{initial}}/[\text{catalyst}]_{\text{initial}} = 2 \times 10^3$ as $[\text{monomer}]_{\text{initial}}$ is varied; for the second numerical solution, $[\text{monomer}]_{\text{initial}}/[\text{catalyst}]_{\text{initial}} = 2 \times 10^4$ as $[\text{transfer agent}]_{\text{initial}}$ is varied.

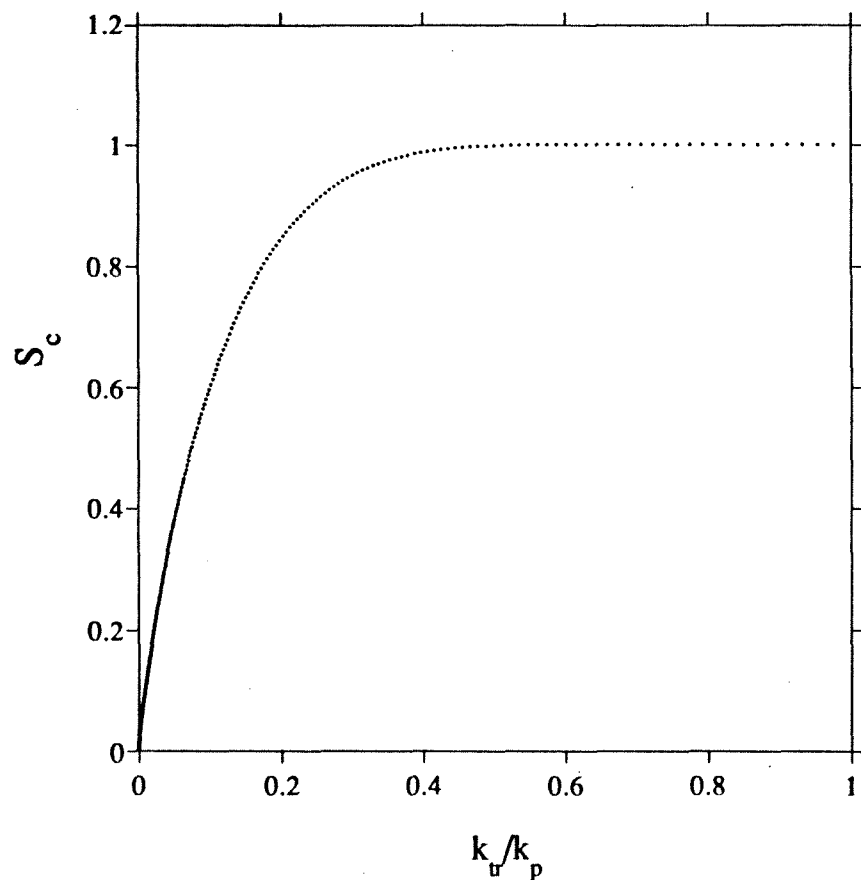


Figure 34. Relationship of S_c (as derived from eqn 45) to k_{tr}/k_p . The plot remains the same whether $[\text{monomer}]/[\text{chain-transfer agent}]$ is 1000, 100, or 10. ²⁷

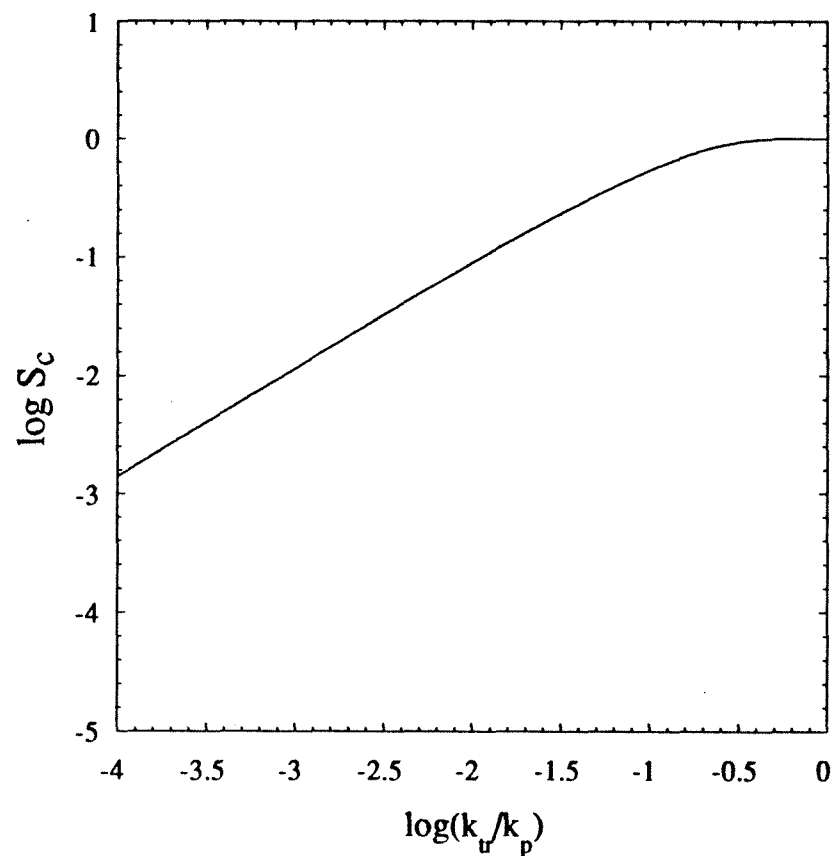


Figure 35. Relationship of $\log S_c$ (as derived from eqn,45) to $\log(k_{tr}/k_p)$. Note the similarity of the graph with that determined numerically (Figure 32).

scavenger and Linde 4A molecular sieves. Solids were weighed in dry box equipped with a MO-40-1 purification train. Toluene and mesitylene were distilled from sodium benzophenone ketyl into solvent flasks equipped with Teflon screw-type valves; norbornene was stirred with sodium at 60°C and distilled into a small Schlenk flask and degassed; neohexene (Aldrich) was distilled from calcium hydride under vacuum into medium Schlenk flask and subsequently freeze-pump-thaw degassed. Prior to use, neohexene was passed through a small column of alumina (activated) inside the dry box. $\text{Mo}(=\text{CH}-\text{CMe}_2\text{Ph})(\text{NAr})(\text{OCMe}_3)_2$ {Ar = 2,6-diisopropylphenyl} (**1**) (Strem Chemicals) was used directly without further purification.

k_i and k_{tr} were measured via ^1H NMR on Jeol GX-400 (399.65 MHz ^1H) while k_p on GE NMR instrument QE-Plus-300 (300.19 MHz ^1H) and on Hewlett Packard 5890 Series II Gas Chromatograph (0.25u Alltech- OV101 column). The molecular weights of the polymers were measured on Waters 150-C ALC/GPC [gel permeation chromatography column (Waters Ultrastayragel 10^5 , 10^4 , 10^3 , 500Å; toluene), relative to polystyrene standard].

Determination of Ratio k_p/k_i . 32.9 mg norbornene was dissolved in 1.6 ml toluene- d_8 mixed with 0.15 ul mesitylene to make a 1.620 ml solution. 400 ul of this solution (0.0864 mmol in norbornene) was placed in an NMR tube at 22°C and the NMR spectrum was taken to ensure that no polymer has been formed. In another vial, 31.9 mg of **1** was dissolved in 950 ul toluene- d_8 . 300 ul of this solution (0.01845 mmol in **1**) was injected into the NMR tube. The tube was shaken vigorously and dropped into the NMR probe at 22°C. After 30 min, when the polymerization was complete, the α -H of the initial carbene **1** and propagating carbene (δ = 11.28 and 11.52, respectively) were integrated relative to the mesitylene standard, respectively. For this trial, ratio of remaining catalyst to total catalyst = 0.574. Hence k_p/k_i = 33.0. From the same stock solution, the same volume of aliquot was withdrawn for a second trial to give k_p/k_i = 28.0. The stock solution was not used again for further k_p/k_i measurements. The two

NMR tubes were saved for subsequent measurement of k_{tr} . New stock solutions were prepared using 17 mg norbornene in 200 μ l toluene, and 5.1 mg, and 6.1 mg of **1** weighed into separate NMR tubes. The results of similar measurements from different preparations gave $k_p/k_i = 35.2, 27.5, 35.6, 29.5, 20.7$. Except for the last value which was obtained through auto-integration from 300MHz NMR spectrometer, all other values were integrated manually via 400MHz NMR spectrometer. Discarding the last value, an average value of 30 was obtained.

Determination of k_{tr} . To each of the two NMR tubes in the preceding section was injected 20 μ l neohexene and shaken vigorously. The disappearance of propagating carbene signal at $\delta = 11.52$ and the appearance of new carbene signal at $\delta = 11.23$ were monitored about every five hours for 1.5 days. From the second-order kinetic plot, the calculated k_{tr} were 0.090, 0.073, 0.170, 0.085. The average $0.105 \pm 0.04 \text{ M}^{-1} \text{ hr}^{-1}$ was obtained (Figure 36).

Determination of k_p .

By NMR. k_p at 22°C was too large to be measured directly by NMR spectroscopy. An Eyring plot was constructed instead. 49.1 mg norbornene with 0.5 μ l mesitylene was dissolved in 2.50 ml toluene- d_8 to make 2550 μ l solution. 500 μ l aliquots were injected into four NMR tubes. NMR spectra were then obtained at several temperatures (-10°C, -19°C, -30.2°C, -46°C).

14.3 mg of **1** was dissolved in 1.00 ml toluene. 20 μ l aliquot of this catalyst solution was injected into the NMR tube dipped in liquid N_2 , and then the tube was immediately transferred into the probe already set at the correct temperature. After about a minute, the tube was ejected, shaken once, and then dropped back down into the probe. Data were collected in two minute intervals for 50 minutes. The disappearance of the signals corresponding to the olefin protons of the monomer in the NMR spectrum was used to determine k_p . The 1H signal of poly(norbornene) was not used due to the chain-

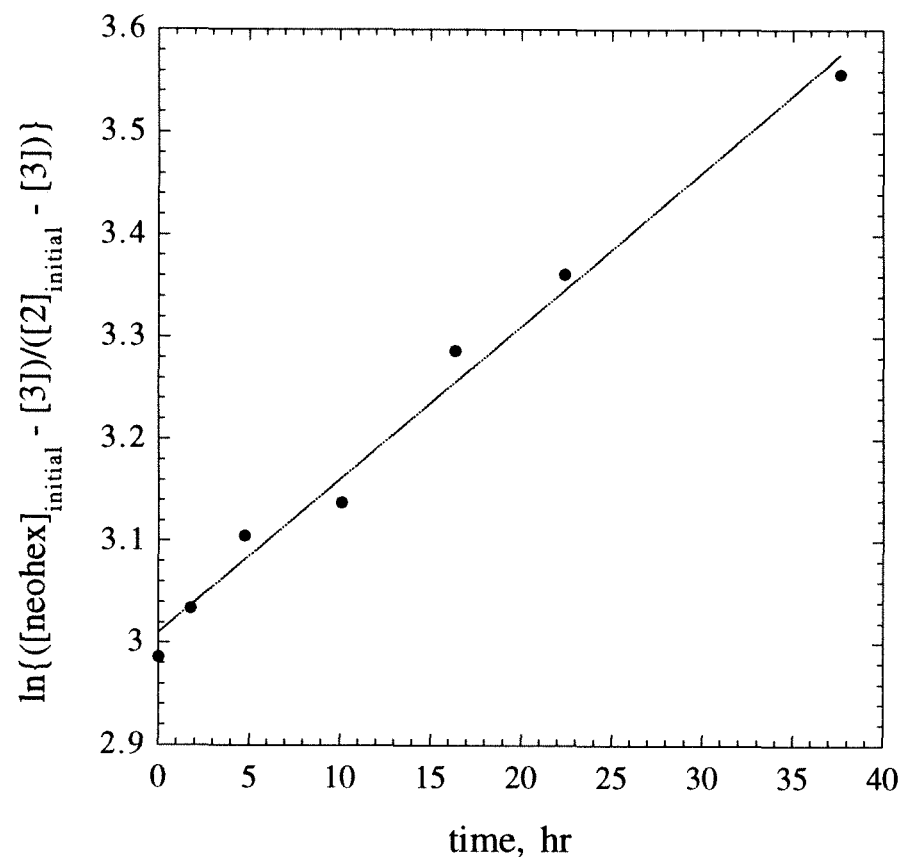


Figure 36. Second-order kinetic plot of formation of 3 from reaction of 2 with neohexene.

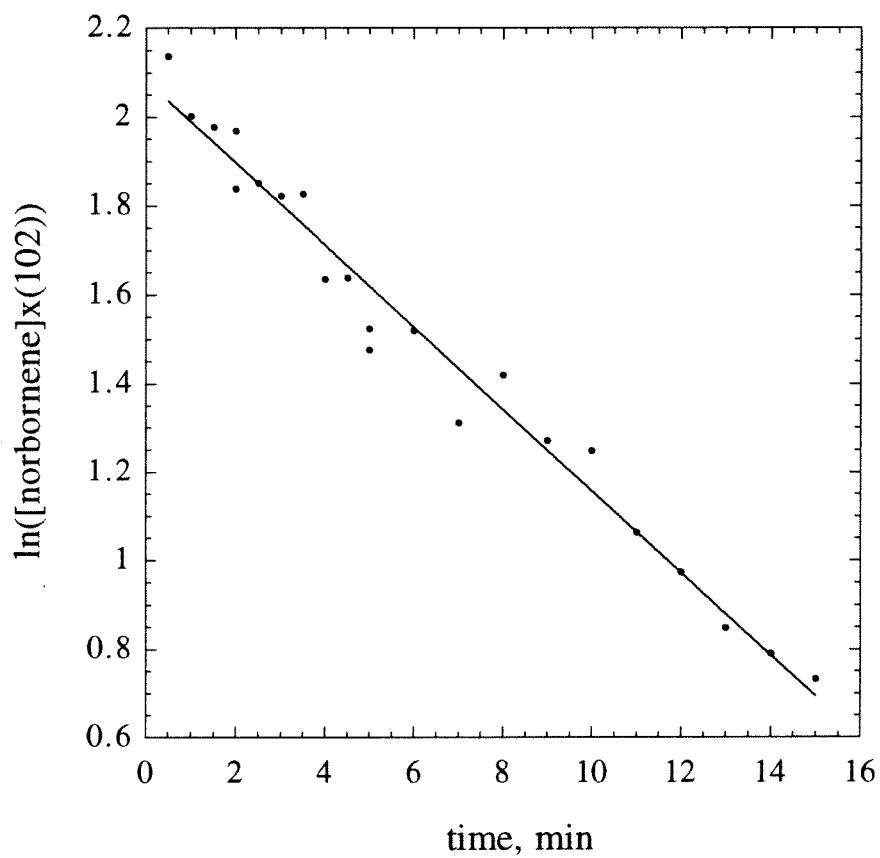


Figure 37. Determination of k_p by GC in the polymerization of norbornene by 1.

length dependence of the relaxation rate of the polymer protons. $k_p = 17 \text{ M}^{-1} \text{ s}^{-1}$ by extrapolation of the Eyring plot (see Table II).

By GC. In the drybox, 38.4 mg (796.6 equivalent) norbornene was dissolved in 5 ml toluene in a vial containing a spinbar. 5 μl mesitylene was added as internal standard. 100 μl aliquot of a solution of 5.6 mg **1** in 2 ml toluene was withdrawn and added to the norbornene solution above. The solution was stirred rapidly. One drop aliquot ($\sim 20 \text{ }\mu\text{l}$) of this solution was withdrawn every 30 seconds for the first five minutes and placed in a series of vials containing 2 drops benzaldehyde (to quench the reaction) and 4 drops toluene. For the next 15 minutes, a drop was collected every minute and mixed with the benzaldehyde/toluene solution. At the end of 20 minutes, the contents of these 25 vials were brought out of the dry box and 4 drops of methanol were added to each vial to precipitate the polymer. The resultant solution was injected into the GC. The integral of norbornene signal relative to mesitylene signal was used in a first-order kinetic plot to obtain the value of k_p of $15 \text{ M}^{-1} \text{ s}^{-1}$. Correlation coefficient = 0.987 (Figure 37).

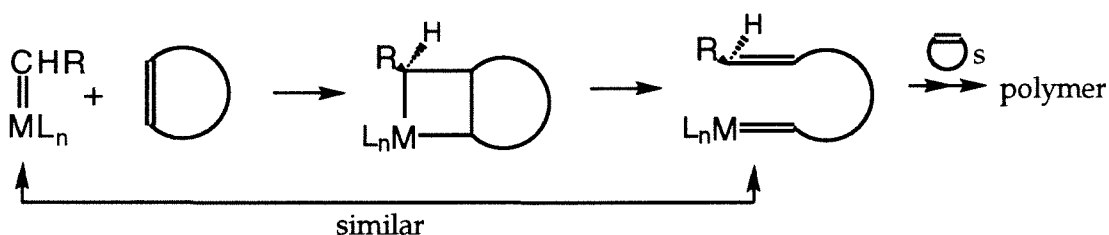
Measurements of Molecular Weights through Size Exclusion Chromatography.

405.2 mg norbornene was dissolved in 2.50 ml toluene to make 2.92 ml solution. To each of 5 vials (with spin bar) was added 500 μl of this solution. The remaining solution was placed into vial 6 (for control). Then 10.0, 7.5, 5.0, 2.5, 2.5, 2.5 ml toluene was added to the six vials, respectively. Then 0, 2.5, 5.0, 7.5, 10.0, 1.0 ml of neohexene was added to the six vials, respectively. To each of the first five vials was injected 150 μl solution of **1** prepared by dissolving 15.7 mg of **1** in 1 ml toluene. The vials were sealed with a Teflon cap and stirred for 1.5 hours at room temperature. All the solutions remained clear during the time period. The volumes of the solution in the first four vials are the same. After two hours, 10 μl benzaldehyde was injected into the six vials. After stirring for another 20 minutes, the vials were exposed to air and heated to 60°C in an oil bath to evaporate off the unreacted neohexene. The solutions were then passed through

alumina to remove the dead catalyst, and subsequently filtered, diluted, and injected into GPC column to obtain the molecular weight.

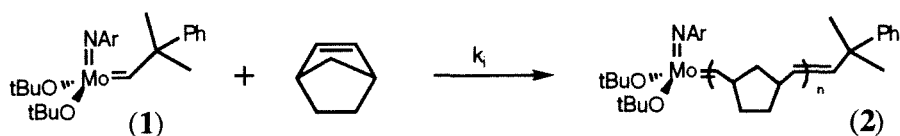
Experimental Results and Discussion

The ring-opening metathesis polymerization (**ROMP**) of norbornene by **1** in the presence of neohexene is chosen as the system to be investigated. ROMP is characterized by [2 + 2] cycloaddition of initial metal-alkylidene species with a strained cyclic olefin to form a metallacyclobutane intermediate which subsequently undergoes ring-opening to regenerate a propagating metal-alkylidene species.

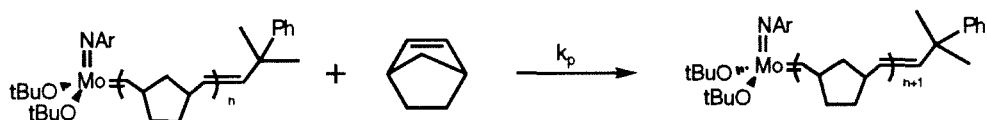


The living polymerizations of norbornene and norbornene-type monomers by **1** are well established by Schrock and co-workers.^{6b;28a,d} The reactions of **1** with several acyclic olefins have also been extensively investigated.^{28b,c} Because the initiating, the propagating, and the chain-transferred metal-alkylidene (**1**, **2**, and **3**, respectively) each exist as one rotamer only (anti, and no syn), the system in Figure 38 thus fits the polymerization scheme outlined above (see Formulation of the Problem).^{6b;28d,f} **1** and **3** also has the same reactivity because the reactivity the catalyst is governed primarily by the alkoxide ligands, the steric influence of the isopropyl ligands on the imido group, and the immediate substituent on carbon making up the metal-alkylidene bond.²⁸ Therefore,

- Initiation Step



- Propagation Step



- Chain-Transfer Step

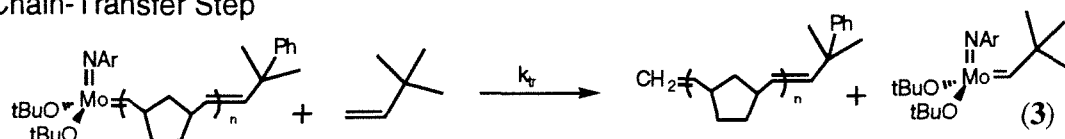


Figure 38. Polymerization of norbornene by molybdenum catalyst in the presence of neohexene.

once the experimental rate constants are known, numerical methods can be used to compute the \bar{X}_n for given concentrations of the reactants. The calculated values can then be compared with the experimental results in order to assess the validity of the *simplified* polymerization scheme outlined in Figure 38.

In the absence of neohexene, the ratio k_p/k_i can be derived experimentally by substituting the values of $[\text{norbornene}]_{\text{initial}}$, $[1]_{\text{initial}}$, and $[1]_{\text{final}}$ from the reaction mixture into the analytical equation^{16a}

$$\frac{k_p}{k_i} = \frac{\frac{M-\text{MON}}{\text{CAT}} - \frac{W_0}{\text{CAT}} + 1}{\ln \frac{W_0}{\text{CAT}} - \frac{W_0}{\text{CAT}} + 1} \quad (46)$$

The value k_p/k_i is very sensitive to the measured value of W_0/CAT when the latter approaches unity (Figure 39). For this system, when $[\text{norbornene}]_{\text{initial}}/[1]_{\text{initial}}$ is about 5, k_p/k_i equals 30 as determined from the amount of unreacted **1**. As calculated from eqn. 25, an error of 6% in the NMR integrals for W_0 and CAT in this case makes k_p/k_i range from 27 to 33.²⁹

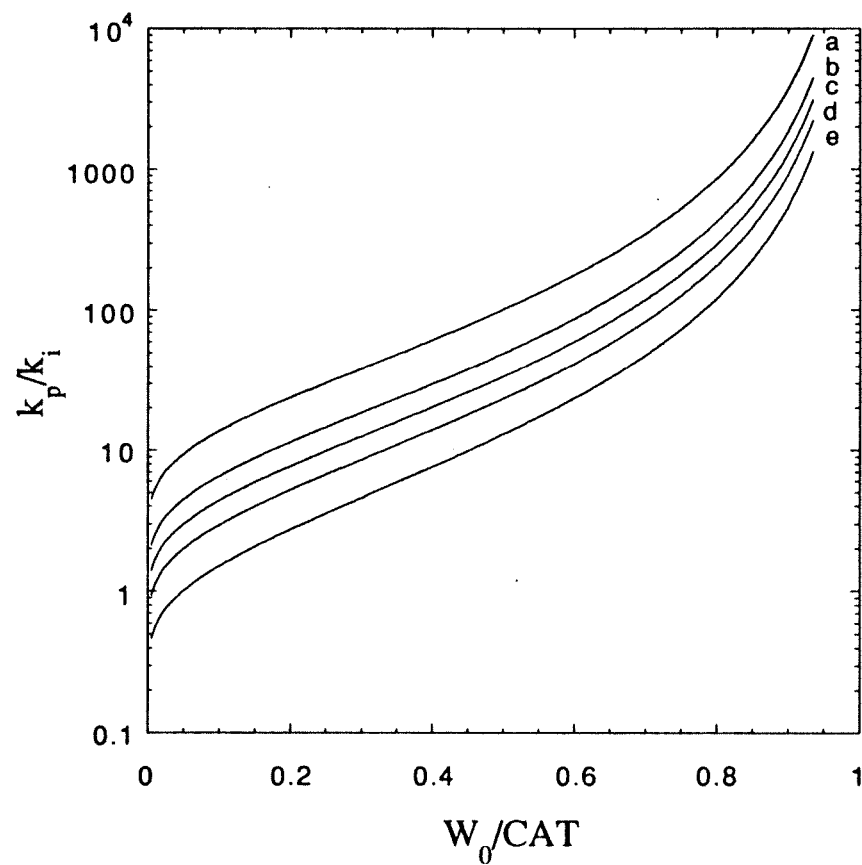


Figure 39. Relationship between k_p/k_i and W_0/CAT when $[monomer]_{initial}/[catalyst]_{initial}$ is (a) 20, (b) 10, (c) 7, (d) 5, (e) 3. W_0 is concentration of unreacted catalyst at the end of reaction. CAT is initial concentration of catalyst.

When k_p is measured, two observations are made. First, from the value $k_p/k_i = 30$, 1000 equiv. of norbornene are needed so that 99% of the catalyst would have been initiated when 11% of the monomer is consumed— as calculated from eqn. 46 (Table I). However, when 1033 equiv. of norbornene are used for polymerization in 0.520 ml toluene, the solution turns into a gel. To minimize viscosity-dependence of the rates measured, 195.5 equiv. of norbornene are used instead. The first 50% of the kinetic data are discarded since theoretically, less than 99% of catalyst would have initiated. (Table I) Otherwise, a smaller-than-actual k_p value would have been measured.

Table I. Theoretical percent catalyst initiated at certain conversion of the monomer for particular starting ratio of monomer to catalyst when $k_p/k_i = 30$

MON/CAT	% conversion monomer	% catalyst initiated
1000	11.0%	99%
547.2	20.0%	99%
214	20.0%	90%
214	51.1%	99%
195.5	56.0%	99%

Secondly, due to the rapid rate of reaction at 22°C, the value of $k_p = 17 \text{ M}^{-1} \text{ s}^{-1}$ at 22°C was obtained by extrapolating the values measured at lower temperatures (Eyring plot) (Table II). Because at low temperatures the formation of the metallacycle intermediate or olefin complex can influence the rate of consumption of norbornene, this might explain the slight non-linearity (upward concavity) of the Eyring plot.³⁰

Table II. Specific rates of propagation for construction of Eyring plot. $\Delta H^\ddagger = 6.6$ kcal/mol. $\Delta S^\ddagger = -15.4$ e.u. Correlation coefficient of Eyring plot is 0.98. k_p at $22^\circ\text{C} = 17 \text{ M}^{-1} \text{ s}^{-1}$ by extrapolation

temperature $^\circ\text{C}$	k_p $\text{M}^{-1} \text{ min}^{-1}$	correlation coeff	$1/T$ $^\circ\text{K}^{-1}$	$\ln(k_p/T)$ $\text{M}^{-1} \text{ s}^{-1} \text{ }^\circ\text{K}^{-1}$
-46	30.1	0.999	0.004405	-6.116
-30.2	64.6	0.994	0.004119	-5.418
-19.0	123	0.998	0.003937	-4.820
-10	276	0.995	0.003802	-4.045

Using GC, much of the difficulties in measuring k_p through NMR are circumvented. Since the solution is diluted (thus slowing the reaction), and faster sampling rate is possible (as compared with the NMR), more data points can be collected allowing the experiment to be conducted at room temperature.³¹ k_p as obtained by GC at 22°C is $15 \text{ M}^{-1} \text{ s}^{-1}$ (correlation coefficient = 0.987), a value comparable to that obtained from NMR. Thus, k_i is $0.57 \text{ M}^{-1} \text{ s}^{-1}$.

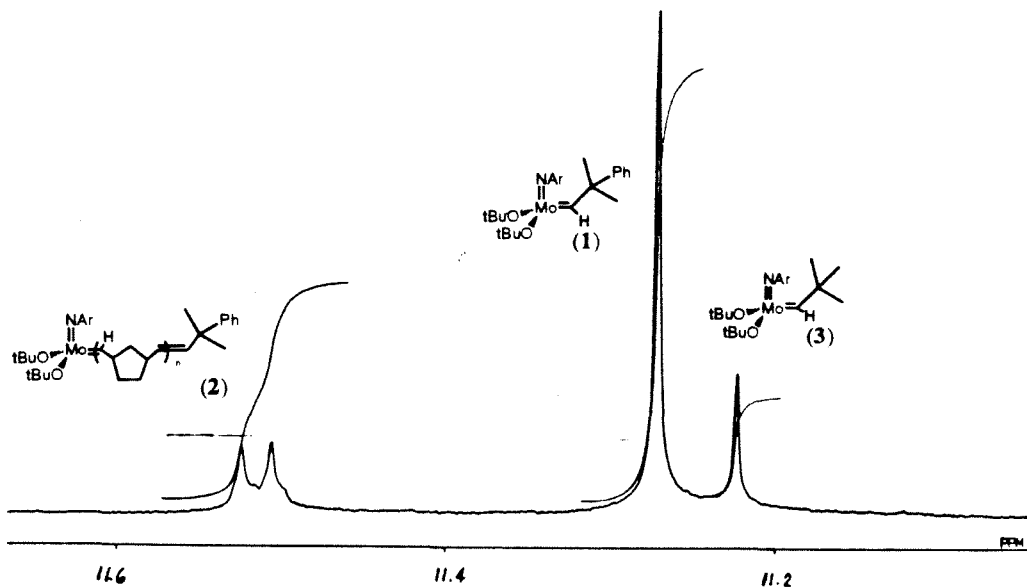


Figure 40. ^1H NMR spectrum of the metal-alkylidene protons of 1, 2, 3.

To measure k_{tr} , the propagating carbene **2** has to be created from initiating carbene **1** (Figure 38). When 4.68 equiv. of norbornene are added to **1**, only 42.6% of **1** reacts to form **2**. No more norbornene is added because the ^1H NMR signals of the alkylidene proton of the catalysts would be too small to be measured with accuracy. Next, 18.6 equiv (relative to **2**) of neohexene are added. The disappearance of **2** and the appearance of **3** through chain transfer by acyclic metathesis with neohexene are then followed by NMR (Figure 40).

To rule out the possibility that **3** is formed directly by the acyclic metathesis of **1** with neohexene, 13.9 equiv. of neohexene are added to **1** in another NMR tube. After a day, no detectable amount of **3** has formed. After a week, about 5% of **1** has been converted to **3**. The fact that neohexene reacts more rapidly with **2** rather than **1** is due to the greater steric crowding at the β -carbon of **1** (quarternary) than that at **2** (tertiary carbon).^{28,32} As expected, **1**, **2**, and **3** are stable for at least the duration of the experiment. From the second-order kinetic plots, k_{tr} at 22°C is $3 \times 10^{-5} \text{ M}^{-1} \text{ s}^{-1}$, suggesting that it is a very poor chain-transfer agent (Figure 36). This small value is not unreasonable because in the reaction of **1** and other acyclic olefins such as *cis*-2-pentene, 1-pentene, and styrene, values as low as 1 to 2 turnovers per day have been reported.^{6b,28c}

Now that all the rate constants are obtained, \bar{X}_n can be calculated for any given reactant concentrations. To illustrate, during the first experiment when the ratios [neohexene]/[norbornene] are 0, 0.218, 0.437, 0.655, 0.874 (with [norbornene]/[**1**] = 223.7), the molecular weights (relative to polystyrene standard) are 57K, 57K, 55K, 57K, 58K, respectively (i.e., unchanged within instrumental error). This experimental result is consistent with the computational result when the above concentrations of the reactants are substituted into eqns. 7 to 13. Using the previously determined rate constants, the predicted change in \bar{X}_n is less than 3 units.

In a second experiment, numerical calculations show that a larger concentration of neohexene has to be used to effect a measurable molecular weight change. Using these values, the experimental \bar{X}_n 's are in good agreement with the computational \bar{X}_n 's within the accuracies of GPC (gel-permeation chromatography) instrument (Table III).³³ Thus, the kinetics of the experimental system can be described by the simplified polymerization scheme in Figure 38.

Table III. Variation of number-average degree of polymerization with [neohexene]/[norbornene] at 22°C when [norbornene]/[1] = 151.7^a

[neohex]/[norb]	\bar{M}_n^b	\bar{X}_n , expt'l ^c	PDI, expt'l	\bar{X}_n , theor ^d	PDI, theor
0	49700	152	1.06	152	1.04
26.51	47500	145	1.05	150	1.05
53.03	45500	139	1.08	147	1.07
79.54	40600	124	1.12	145	1.08
106.05	41900	128 ^e	1.14 ^e	143	1.09

^aThe volume of the solutions is kept constant by addition of appropriate amounts of toluene. The last table entry contains about 14% toluene. ^brelative to polystyrene standard. ^cfactor of 3.5 is used to convert molecular weight referenced to polystyrene to that of polynorbornene.³⁴ ^das calculated from substituting the specific rates into the differential equations. ^eFor this entry, more toluene is added to increase the volume of solution during polymerization to prevent polymer precipitation.

Conclusions

By expressing the kinetic equations governing the molecular weight distribution in terms of moments of distribution, the number-average degree of polymerization and polydispersity index of living polymerization in the presence of chain-transfer agents are computed. The temporal evolution of the concentrations of active and dead chains, monomer, catalyst, and chain-transfer agents is easily followed as well.

The computational results reveal that unsteady-state polymerization exists in certain cases. The Mayo plot is nearly linear; but (as opposed to non-living system) its slope is not equal to k_{tr}/k_p in general, the former differing from the latter by about half to one order of magnitude when $k_{tr}/k_p = 0.01$ to 1.0 . The slope of the Mayo plot is also dependent on whether the experiment is conducted by varying the chain-transfer agent or the monomer. Plots of the slopes of Mayo plot versus k_{tr}/k_p for different values of k_p/k_i reveal that only when k_{tr} is equal or greater than k_p by an order of magnitude can the molecular weight be effectively controlled by addition of chain-transfer agent. Huge k_{tr} ($\gg k_p$) will not control the synthesis of low molecular weight polymers effectively, and a broad bimodal distribution results once all the chain-transfer agent is consumed. Sufficient amount of chain-transfer agent is a necessary but not sufficient condition to ensure monomodal molecular-weight distribution.

In the domain where $k_{tr} < k_p$, a steady-state approximation is applied (as warranted by numerical results) to derive an analytical solution for number-average degree of polymerization $\bar{X}_{n,dead}$ (eqn. 44). The equation holds exactly when $[catalyst]_{initial} \ll [chain-transfer\ agent]_{initial}$. Similarly, an analytical expression relating the slope of the Mayo plot to k_{tr}/k_p has also been obtained. The analytical results are in excellent agreement with the computational results.

An experimental investigation of the kinetics of ring-opening metathesis polymerization (**ROMP**) of norbornene by $Mo(=CH-CMe_2Ph)(NAr)(OCMe_3)_2$ {Ar = 2,6-diisopropylphenyl} (**1**) in the presence of neohexene suggests that this ROMP system

is adequately described by a relatively simple polymerization scheme. As measured from NMR spectroscopy, the specific rate constants of initiation, propagation, and chain transfer at 22°C are 0.57, 17, 0.00003 M⁻¹ s⁻¹, respectively.

References and Notes

- (1) For an introduction to the concepts discussed here, please see (a) Seymour, R.B.; Carraher, C.E. *Structure-Property Relations in Polymers*; Plenum Press: New York, 1984. (b) Odian, G. *Principles of Polymerization*; John Wiley & Sons, Inc.: New York, 1991. (c) Hiemenz, P.C. *Polymer Chemistry*; Marcel Dekker, Inc.: New York, 1984.
- (2) Early selected examples of living systems for anionic, ring-opening metathesis, cationic, and group-transfer polymerization, respectively are as follows: (a) Szwarc, M. *Nature (London)* **1956**, 178, 1168. Szwarc, M.; Levy, M.; Milkovich, R. *J. Am. Chem. Soc.* **1956**, 78, 2656. (b) Gilliom, L.R.; Grubbs, R.H. *J. Am. Chem. Soc.* **1986**, 108, 733. (c) Faust, R.; Kennedy, J.P. *J. Macromol. Sci. Chem.* **1990**, 649. Faust, R.; Kennedy, J.P. *J. Polym. Sci., Polym. Chem. Ed.* **1987**, A25, 1847. (d) Sogah, D.Y.; Webster, O.W. *Macromolecules* **1986**, 19, 1775. Hertler, W.R.; Sogah, D.Y.; Webster, O.W.; Trost, B.M. *Macromolecules* **1984**, 17, 1415. Sogah, D.Y.; Hertler, W.R.; Webster, O.W.; Cohen, G.M. *Macromolecules* **1987**, 20, 1473.
- (3) (a) A restrictive definition of "living polymerization" requires the specific rate constant of initiation to be comparable to that of propagation. (b) Quirk, R.P.; Lee, B. *Polym. Int.* **1992**, 27, 359. (c) Flory, P.J. *J. Am. Chem. Soc.* **1940**, 62, 1561. (d) Brown, W.B.; Szwarc, M. *Trans. Faraday Soc.* **1958**, 54, 416. (e) Schulz, G.V. *Z. physik. Chem.* **1939**, B43, 25.

- (4) (a) Flory, P.J. *Principles of Polymer Chemistry*; Cornell University Press: New York, 1953. (b) Gregg, R.A.; Mayo, F.R. *J. Am. Chem. Soc.* **1948**, *70*, 2373. (c) Mayo, F.R. *J. Am. Chem. Soc.* **1943**, *65*, 2324.
- (5) Cases where a dead chain can react further with an active chain or catalyst are excluded in the treatment here. Cases where there is reactivation of a dead chain and/or the formation of cyclic oligomers will be considered in another paper. Chen, Z.R.; Claverie, J.P.; Grubbs, R.H.; Kornfield, J. Manuscript in preparation.
- (6) For example, catalysts used in ring-opening metathesis polymerization require multi-step synthesis. (a) Schrock, R.R.; Murdzek, J.S.; Bazan, G.C.; Robbins, J.; DiMare, M.; O'Regan, M. *J. Am. Chem. Soc.* **1990**, *112*, 3875. (b) Schrock, R.R.; DePue, R.T.; Feldman, J.; Schaverien, C.J.; Dewan, J.C.; Liu, A.H. *J. Am. Chem. Soc.* **1988**, *110*, 1423.
- (7) For example, (a) Cramail, H.; Fontanille, M.; Soum, A. *J. Mol. Catal.* **1991**, *65*, 193. (b) Hillmyer, M.A.; Grubbs, R.H. *Macromolecules* **1993**, *26*, 872. (c) Goethals, E.J. *Telechelic Polymers: Synthesis and Applications*; CRC Press, Inc.: Boca Raton, Florida, 1989. (d) Chung, T.C.; Chasmawala, M. *Macromolecules* **1992**, *25*, 5137. (e) Ivin, K.J. *Olefin Metathesis*; Academic Press: London, 1983; pp.289-291.
- (8) (a) Bamford, C.H. *Eur. Polym. J.* **1993**, *29*, 313. (b) Bamford, C.H. *Eur. Polym. J.* **1990**, *26*, 1245. (c) Olaj, F.O.; Zifferer, G.; Gleixner, G. *Makromol. Chem., Rapid Commun.* **1985**, *6*, 773. (d) Olaj, O.F.; Zifferer, G.; Gleixner, G. *Macromolecules* **1987**, *20*, 839. (e) Kuchanov, S.I.; Povolotskaya, E.S. *Dokl. Akad. Nauk SSSR* **1976**, *227*, 1147. (f) Andrianov, K.A.; Andronov, Y.I. *Dokl. Akad. Nauk SSSR* **1976**, *231*, 619. (g) Ohnishi, T.; Tabata, Y. *Kobunshi Kagaku* **1968**, *25*, 809.
- (9) (a) Pu, Z. In *Handbook of Polymer Science and Technology*; Cheremisinoff, N.P. Ed.; Marcel Dekker, Inc.: New York, 1989; pp. 1-66. (b) Peebles, L.H., Jr. *Molecular Weight Distribution in Polymers*; Interscience: New York, 1971. (c)

- Rudin, A. In *Comprehensive Polymer Science*; Allen, G.; Bevington, J.C. Ed.; Pergamon Press: Oxford, 1989; pp. 239-244. (d) Billingham, N.C. In *Comprehensive Polymer Science*; Allen, G.; Bevington, J.C. Ed.; Pergamon Press: Oxford, 1989; pp. 43-57. (e) Bamford, C.H. In *Encyclopedia of Polymer Science and Technology*; Mark, H.E.; Bikales, N.M.; Overberger, C.G.; Menges, G.; Kroschwitz, J.I. Ed.; Wiley & Sons: New York, 1988; pp. 708-853.
- (10) Pu, Z.; Yan, D.; Tang, W. *Makromol. Chem.* **1985**, *186*, 159.
- (11) (a) Guyot, A. *J. Polym. Sci., Polym. Lett. Ed.* **1968**, *6*, 123. (b) Litvinenko, G.I.; Arest-Yakubovich, A.A. *Makromol. Chem., Theory Simul.* **1992**, *1*, 321. (c) Olaj, O.F.; Zifferer, G. *Makromol. Chem., Rapid Commun.* **1991**, *12*, 179.
- (12) (a) Tompa, H. In *Comprehensive Chemical Kinetics*; Bamford C.H.; Tipper, C.F.H. Ed.; Elsevier: New York, 1976; Vol.14. Chap.7. (b) Bamford, C.H.; Tompa, H. *Trans. Faraday Soc.* **1954**, *50*, 1097.
- (13) Saito, O.; Nagasubramanian, K.; Graessly, W.W. *J. Polym. Sci. Part A-2*, **1969**, *7*, 1937.
- (14) (a) Kyner, W.T.; Radok, J.R.M.; Wales, M. *J. Chem Phys.* **1959**, *10*, 363. (b) Ginell, R.; Simha, R. *J. Am Chem.Soc.* **1943**, *65*, 706.
- (15) (a) Jain, S.C.; Nanda, V.S. *Eur. Polym. J.* **1977**, *13*, 137. (b) Nanda, V.S.; Jain, S.C. *Eur. Polym. J.* **1970**, *6*, 1605. (c) Yuan, C.; Yan, D. *Eur. Polym. J.* **1988**, *24*, 729 and references therein. (d) Shaginyan, A.A.; Enikolopyan, N.S. *Arm. Khim. Zh.* **1970**, *23*, 581.
- (16) (a) Gold, L. *J. Chem. Phys.* **1958**, *28*, 91. (b) Dostal, H.; Mark, H. *Z. physik. Chem.* **1935**, *B29*, 299. (c) Litt, M. *J. Polym. Sci.* **1962**, *58*, 429.
- (17) Largo-Cabrerizo, J.; Guzman, J. *Macromolecules* **1979**, *12*, 526.
- (18) (a) Sigwalt, P. *Makromol. Chem., Macromol. Symp.* **1991**, *47*, 179. (b) Leleu, J.M.; Tardi, M.; Polton, A.; Sigwalt, P. *Makromol. Chem., Macromol. Symp.* **1991**, *47*, 253. (c) Zsuga, M.; Kennedy, J.P.; Kelen, T. *Polymer Bulletin* **1988**, *19*, 427.

(d) Jain, S.C.; Nanda, V.S. *Indian J. Chem.* **1975**, *13*, 614. (e) Doi, Y.; Ueki, S.; Keii, T. *Polymer* **1980**, *21*, 1352.

- (19) (a) Our notation W_n corresponds to P_n^* in some literature, while our P_0 corresponds to T . We note our notation P_0 is more appropriate because a chain-transfer agent can be viewed as a dead "polymer" chain with 0 units of monomer.
- (b) System where the reactivity of the initiating species produced by the reaction of the transfer agent with the active chain differs from that of the original initiating species is treated in appendix B as are other minor elaborations on the system (e.g., reactivation of a dead polymeric chain by an active chain).
- (20) Figure 3 of Reference 16a has been reproduced.
- (21) Moreover, if one were to isolate the polymers by addition of the reaction mixture into a non-solvent, the oligomers might not precipitate out— which could lead one to isolate only the polymers with long chain lengths and narrow polydispersity, and falsely conclude that chain transfer rarely occurs.
- (22) When the chain-transfer agent is consumed first, eventually all monomer is consumed; but the converse is not necessarily true.
- (23) Mayo plot is a plot of $1/\bar{X}_n$ versus $[\text{chain-transfer agent}]_{\text{initial}}/[\text{monomer}]_{\text{initial}}$. The slope of the Mayo plot for a *non*-living polymerization (whereby the chain-transfer agent is neither a monomer nor initiator) is shown to be equal to the chain-transfer constant C_S – defined to be the ratio k_{tr}/k_p . To avoid confusion, in our plot (for living systems with deliberately addition of chain-transfer agent) we denote the slope by S_s . (see Reference 4) (b) The slope S_s is derived from a least square fit of $1/\bar{X}_{n,\text{all}}$ with $[\text{chain-transfer agent}]_{\text{initial}}/[\text{monomer}]_{\text{initial}}$.
- (24) Figures 26-28 presented here are typical behaviors observed from the wide range of values examined. In these cases, the reaction is followed to completion whereby all active chains have reacted with the chain-transfer agents; therefore, $\bar{X}_{n,\text{all}} = \bar{X}_{n,\text{dead}}$. In the interest of space, Mayo plots where $[\text{catalyst}]/[\text{monomer}]$ ratio is

kept constant while [transfer agent] is varied is not presented. However, the results are summarized in Figure 32.

- (25) For example, when $k_i = k_p = k_{tr} = 1$ and catalyst : monomer : chain-transfer agent = 1:100:100, the concentration of active chains in the reaction varies from 4% to 50% of [catalyst]_{initial} throughout the extent of reaction. Another example is when $k_i : k_p : k_{tr} = 1:10000:5$, and catalyst : monomer : chain-transfer agent = 1:100:10.

- (26) Equating eqns. 19, 20 and 21 to zero gives a difference equation of $W_n = \frac{1}{\left(1 + \frac{k_{tr} P_0}{k_p M}\right)^n} \frac{k_i}{k_p} W_0$, resulting in the active chains having a Flory-Schulz

molecular weight distribution. In the system considered in this paper, the active chains cannot be characterized by such a distribution.

- (27) (a) It is interesting to compare the assumptions used in the third case of Reference 17 and ours (e.g., CTA >> CAT). In particular, their N_1^* is our W_0 if we set our $k_i = k_p$. (b) To avoid confusion, the slope of the Mayo plot derived from the analytical eqn 45 will be denoted by S_C as opposed to S_s .

- (28) (a) Bazan, G.C.; Khosravi, E.; Schrock, R.R.; Feast, W.J.; Gibson, V.C.; Regan, M.B.; Thomas, J.K.; Davis, W.M. *J. Am. Chem. Soc.* **1990**, *112*, 8378. (b) Bazan, G.C.; Oskam, J.H.; Cho, H.N.; Park, L.Y.; Schrock, R.R.; *J. Am. Chem. Soc.* **1991**, *113*, 6899. (c) Crowe, W.E.; Michell, J.P.; Gibson, V.C.; Schrock, R.R. *Macromolecules* **1990**, *23*, 3534. (d) Bazan, G.C.; Schrock, R.R.; Cho, H.N.; Gibson, V.C. *Macromolecules* **1991**, *24*, 4495. (e) Mitchell, J.P.; Gibson, V.C.; Schrock, R.R. *Macromolecules* **1991**, *24*, 1220. (f) Schrock, R.R. *Acc. Chem. Res.* **1990**, *23*, 158. (h) Schrock, R.R.; DePue, R.T.; Feldman, J.; Yap, K.B.; Yang, D.C.; Davis, W.M.; Park, L.Y.; DiMare, M.; Schofield, M.; Anhaus, J.; Walborsky, E.; Evitt, E.; Kruger, C.; Betz, P. *Organometallics* **1990**, *9*, 2262.

- (29) A k_p/k_i value of 15 has been reported. There is less than one order of magnitude difference. Reference 28a.
- (30) (a) Leconte, M.; Bilhou, J.L.; Reimann, W.; Basset, J.M. *J. Chem. Soc. Chem. Commun.* **1978**, 341. (b) Leconte, M.; Basset, J.M. *J. Am. Chem. Soc.* **1979**, 101, 7296. (c) Calderon, N.; Lawrence, J.P.; Ofstead, E.A. *Adv. Organomet. Chem.* **1979**, 17, 449. (d) Casey, C.P.; Albin, L.D.; Burkhardt, T.J. *J. Am. Chem. Soc.* **1977**, 99, 2533. (e) Katz, T.J.; McGinnis, J. *J. Am. Chem. Soc.* **1975**, 97, 1592.
- (31) (a) Diluting an NMR solution to the same concentration as that used in GC experiment would require a large quantity of deuterated solvent. (b) Each pulse sequence (including delay time) in the NMR takes about 5 seconds. Eight scans constitute a spectrum. Therefore, the free induction decay spectrum of the first scan would differ significantly from that of the eighth scan due to the rapid rate of the reaction; thus imparting a degree of uncertainty to the resultant NMR integrals. These difficulties are avoided when GC is used.
- (32) Wu, Z.; Wheeler, D.R.; Grubbs, R.H. *J. Am. Chem. Soc.* **1992**, 114, 146.
- (33) The discrepancy of the last experimental value with the computational result might be due to insufficient amount of toluene solvent used— first, polymers start to precipitate out prior to completion of the reaction; second, the rate constants might be slightly dependent on the polarity of the solution.
- (34) A factor of 2.2 has been suggested. Schrock, R.R.; Feldman, J.; Cannizzo, L.F.; Grubbs, R.H. *Macromolecules* **1987**, 20, 1169.

Appendix A

The following figures illustrate the effect of different initial conditions on the value of \bar{X}_n , PDI, and concentration of propagating chains. These figures may be used to better comprehend Figure 33 (a comparison of analytical and numerical solutions).

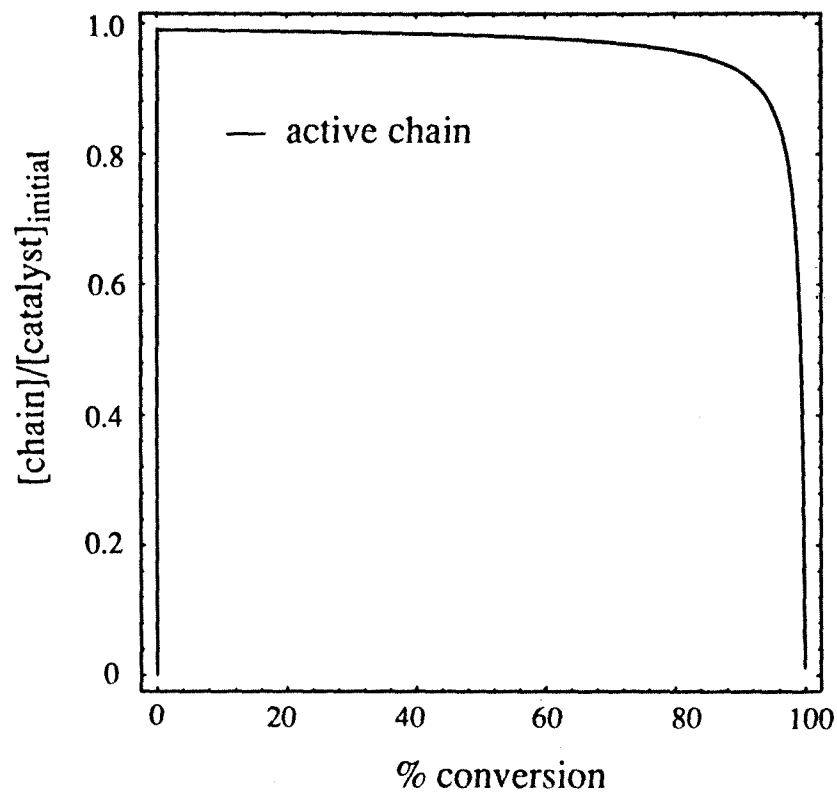


Figure 41. Variation of the number of active chains with conversion. $k_i : k_p : k_{tr} = 1 : 1 : 0.1$. Concentration of catalyst : monomer : chain-transfer agent = 0.005 : 100 : 10.

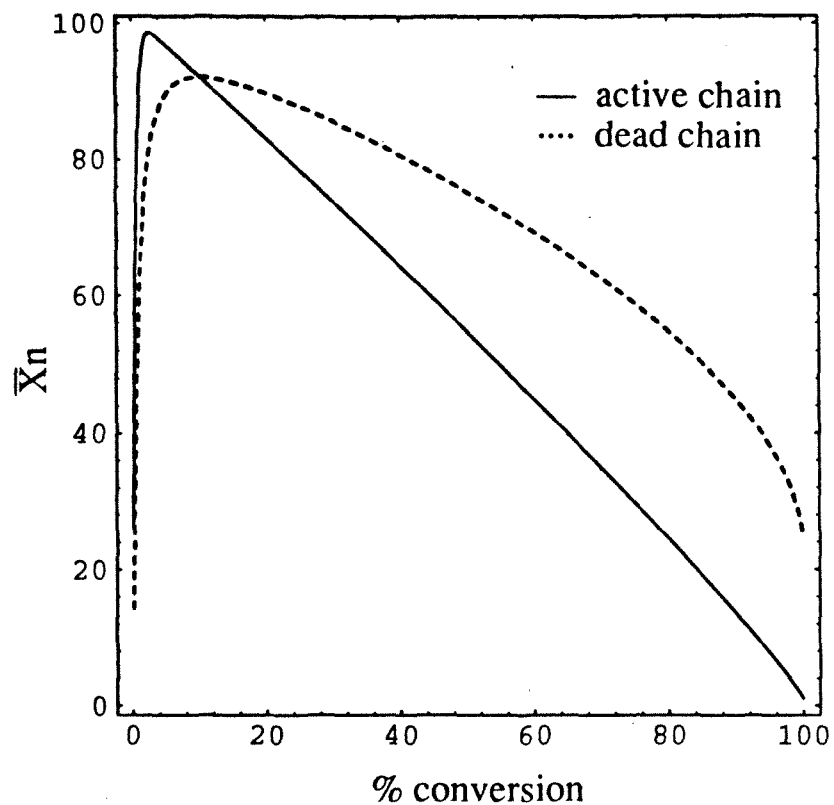


Figure 42. Variation of the number-average degree of polymerization with conversion. $k_i : k_p : k_{tr} = 1 : 1 : 0.1$. Concentration of catalyst : monomer : chain-transfer agent = 0.005 : 100 : 10.

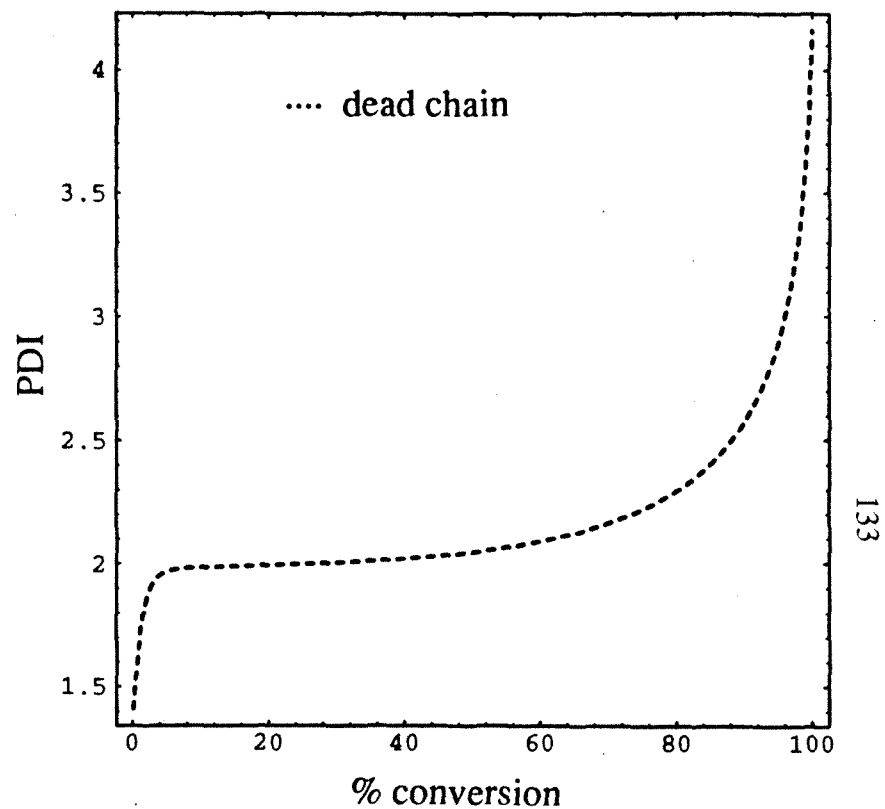


Figure 43. Variation of the polydispersity index with conversion. $k_i : k_p : k_{tr} = 1 : 1 : 0.1$. Concentration of catalyst : monomer : chain-transfer agent = 0.005 : 100 : 10.

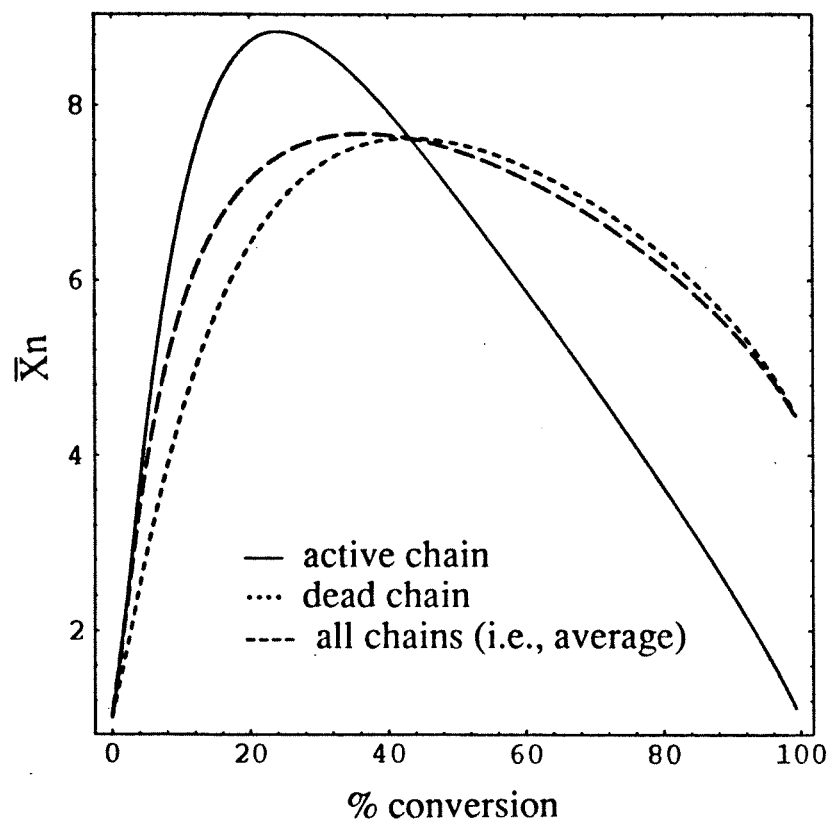


Figure 44. Variation of the number-average degree of polymerization with conversion. $k_i : k_p : k_{tr} = 1 : 1 : 0.1$. Concentration of catalyst : monomer : chain-transfer agent = 1 : 100 : 100.

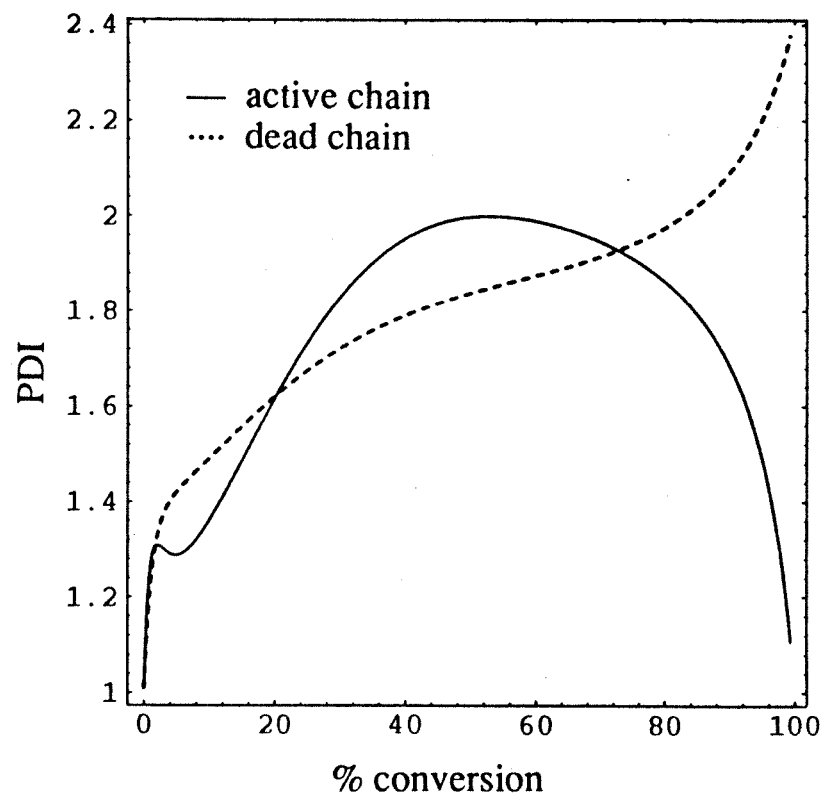


Figure 45. Variation of the polydispersity index with conversion. $k_i : k_p : k_{tr} = 1 : 1 : 0.1$. Concentration of catalyst : monomer : chain-transfer agent = 1 : 100 : 100.

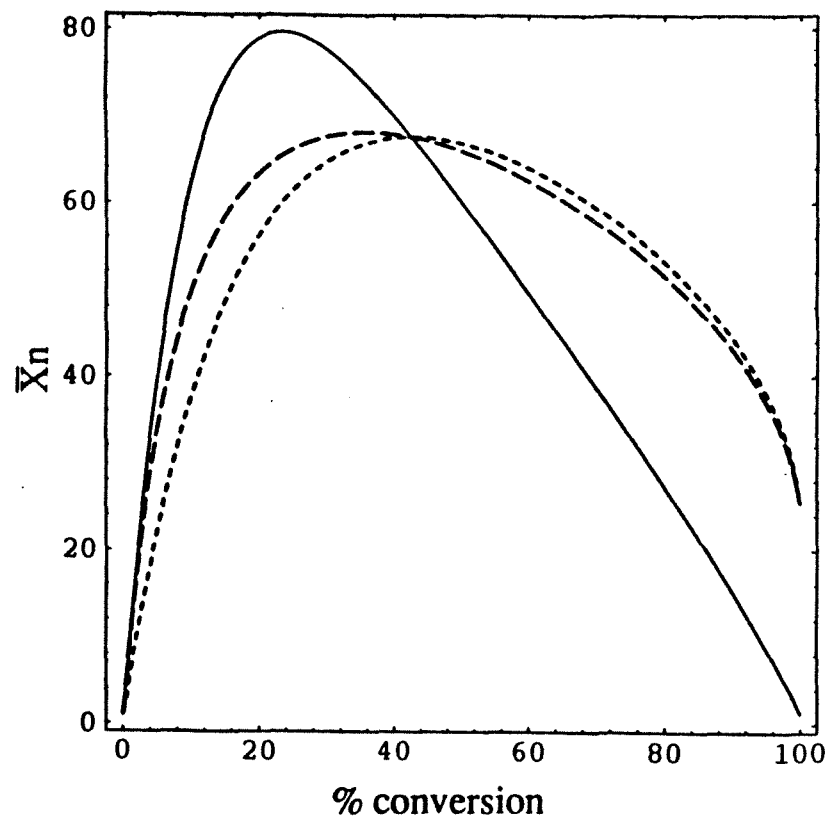


Figure 46. Variation of the number-average degree of polymerization with conversion. $k_i : k_p : k_{tr} = 1 : 1 : 0.1$. Concentration of catalyst : monomer : chain-transfer agent = $0.1 : 100 : 10$ (i.e., $1 : 1000 : 100$).

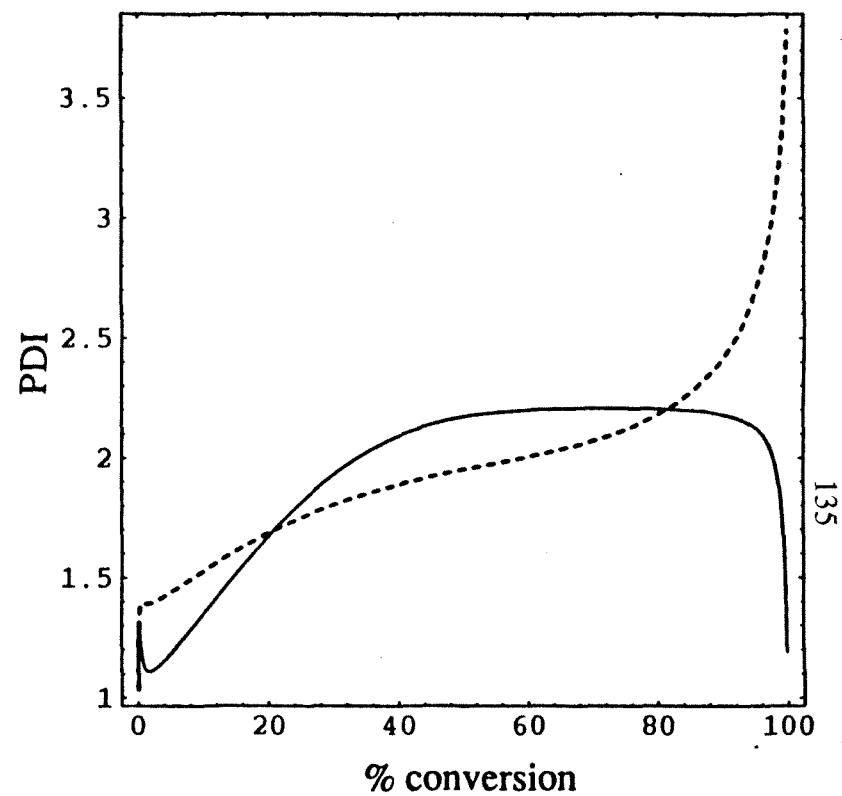


Figure 47. Variation of the polydispersity index with conversion. $k_i : k_p : k_{tr} = 1 : 1 : 0.1$. Concentration of catalyst : monomer : chain-transfer agent = $0.1 : 100 : 10$ (i.e., $1 : 1000 : 100$).

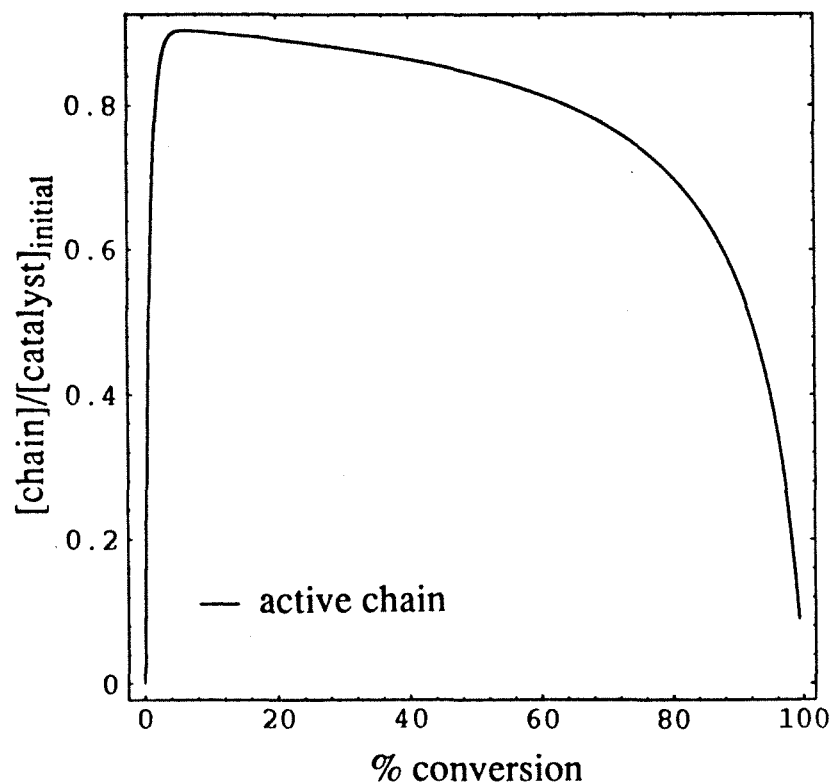


Figure 48. Variation of the number of active chains with conversion. $k_i : k_p : k_{tr} = 1 : 1 : 0.1$. Concentration of catalyst : monomer : chain-transfer agent = 1 : 100 : 100.

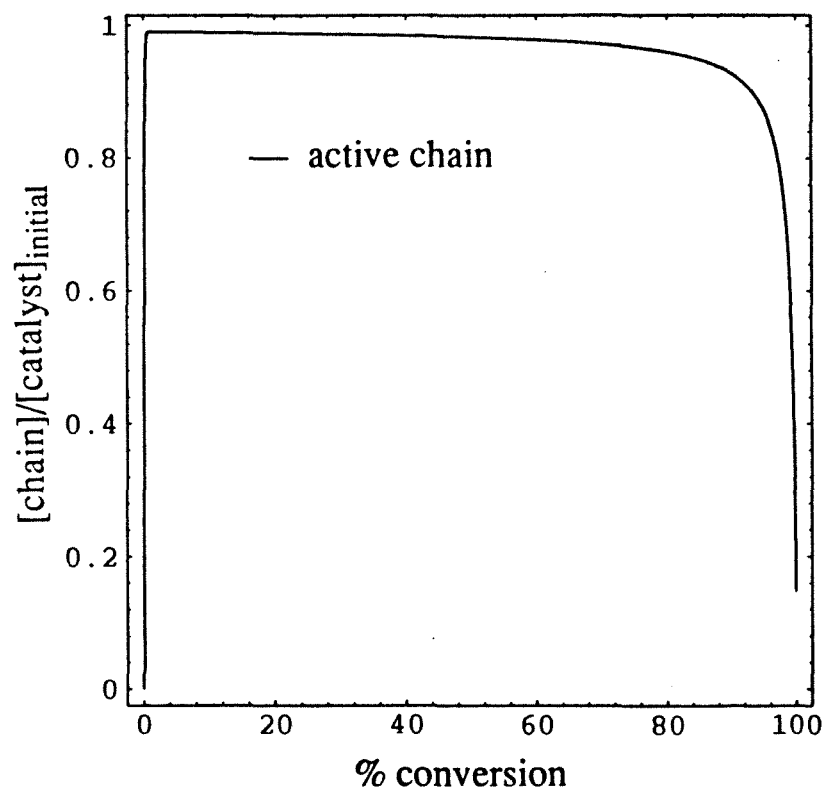


Figure 49. Variation of the number of active chains with conversion. $k_i : k_p : k_{tr} = 1 : 1 : 0.1$. Concentration of catalyst : monomer : chain-transfer agent = 0.1 : 100 : 10 (i.e., 1 : 1000 : 100).

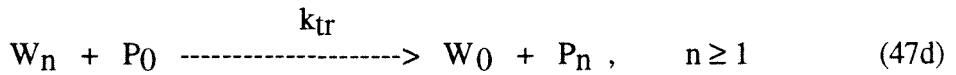
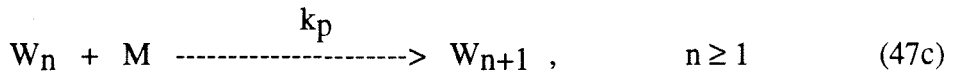
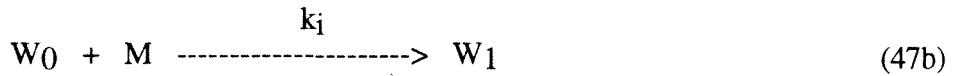
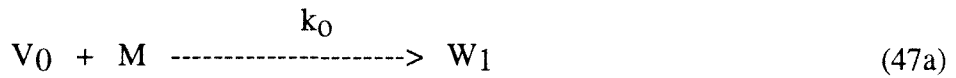
Appendix B

The polymerization scheme (eqns 17a-c) used in the chapter is relative simple since the main objective is to have a fundamental understanding of the behavior of the system. Further elaboration on the polymerization scheme is straightforward. Below are two polymerization schemes, their associated equations, and some experimental systems.

Let CAT, MON, and CTA be the amount of catalyst, monomer, and chain-transfer agent, respectively at time 0; while W_0 (or V_0), M , P_0 are the amount of catalyst, monomer, and chain-transfer agent at time t . W_n and P_n are the amount of active and dead polymer chains containing n units of monomer, respectively, at time t . k_i (or k_0), k_p , and k_{tr} are specific rate constants for initiation, propagation, and chain transfer.

I. First System (Multiple Initiators; Reinitiated Species possesses different reactivity)

A. Polymerization Scheme:



The conservation laws:

$$MON = M + \sum_{n=0}^{\infty} (n W_n) + \sum_{n=0}^{\infty} (n P_n) \quad (48)$$

$$CAT = V_0 + \sum_{n=0}^{\infty} W_n \quad (49)$$

$$CTA = \sum_{n=0}^{\infty} P_n \quad (50)$$

B. Equations governing the above polymerization scheme:

$$dM/dt = (k_p - k_i) M W_0 - (k_p \text{ CAT}) M + (k_p - k_o) M V_0 \quad (51)$$

$$dV_0/dt = -k_i V_0 M \quad (52)$$

$$dW_0/dt = (k_{tr} \text{ CAT}) P_0 - k_i M W_0 - k_{tr} P_0 (W_0 + V_0) \quad (53)$$

$$dP_0/dt = k_{tr} (W_0 + V_0) P_0 - (k_{tr} \text{ CAT}) P_0 \quad (54)$$

$$dA/dt = -k_{tr} P_0 A + (k_p \text{ CAT}) M + (k_i - k_p) M W_0 + (k_o - k_p) M V_0 \quad (55)$$

$$dD/dt = k_{tr} P_0 A \quad (56)$$

$$dB/dt = -k_{tr} P_0 B + k_p M (\text{CAT} + 2A - W_0 - V_0) + (k_i W_0 + k_o V_0) M \quad (57)$$

$$dF/dt = k_{tr} P_0 B \quad (58)$$

$$\text{where } A = \sum_{n=1}^{\infty} (n W_n), \quad B = \sum_{n=1}^{\infty} (n^2 W_n), \quad D = \sum_{n=1}^{\infty} (n P_n), \quad F = \sum_{n=1}^{\infty} (n^2 P_n)$$

The number-average degree of polymerization of the dead and active chains are given by

$$\bar{X}_{n \text{ dead}} = D/(\text{CTA} - P_0) \quad \bar{X}_{n \text{ active}} = A/(\text{CAT} - W_0 - V_0) \quad (59)$$

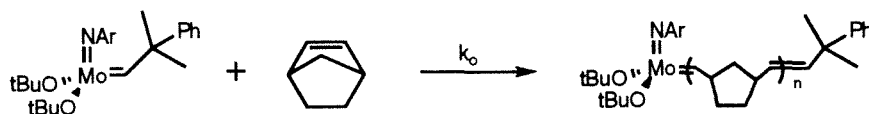
while the polydispersity index of the dead and active chains are

$$\text{PDI}_{\text{dead}} = [F (\text{CTA} - P_0)]/D^2 \quad \text{PDI}_{\text{active}} = [B (\text{CAT} - W_0 - V_0)]/A^2 \quad (60)$$

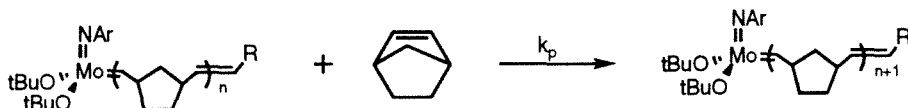
C. Specific examples.

This system examines the effect of two different types of initiating species on the behavior of the system. An example of this is the ring-opening polymerization of norbornene with $\text{Mo}(=\text{CH}-\text{CMe}_2\text{Ph})(\text{NAr})(\text{OCMe}_3)_2$ {Ar = 2,6-diisopropylphenyl} in the presence of styrene. In this case, V_0 represents $\text{Mo}(=\text{CH}-\text{CMe}_2\text{Ph})(\text{NAr})(\text{OCMe}_3)_2$, and W_0 represents $\text{Mo}(=\text{CHPh})(\text{NAr})(\text{OCMe}_3)_2$. Initially, no W_0 would be present. If k_o and k_i are identical, this system reduces to the polymerization scheme 17a-c.

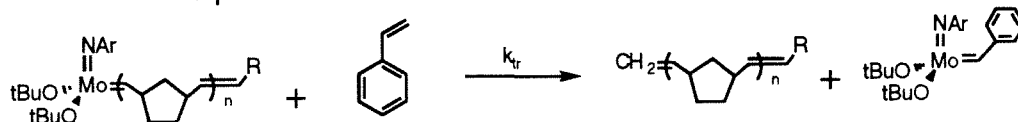
- Initiation Step



- Propagation Step



- Chain-Transfer Step



- Re-initiation Step

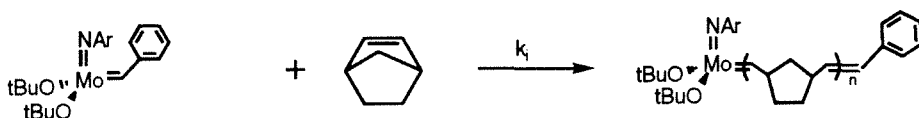
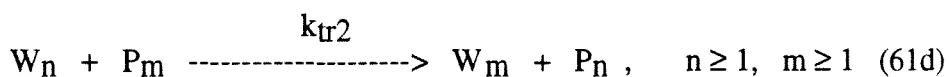
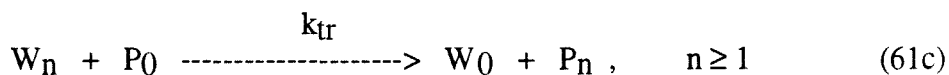
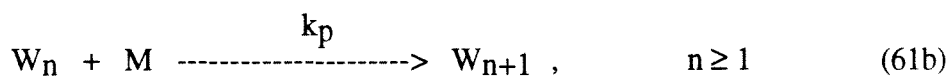
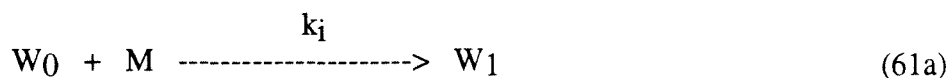


Figure 50. An experimental system.

Another possible example of an experimental system governed by this polymerization scheme is the case where there are two initiating species (major and minor) present. Normally, the minor initiating species is more active than the initiating species present in major amount.

II. Second System (Reactivation of dead chain)

A. Polymerization Scheme:



The conservation laws:

$$\text{MON} = M + \sum_{n=0}^{\infty} (n W_n) + \sum_{n=0}^{\infty} (n P_n) \quad (62)$$

$$\text{CAT} = \sum_{n=0}^{\infty} W_n \quad (63)$$

$$\text{CTA} = \sum_{n=0}^{\infty} P_n \quad (64)$$

B. Equations governing the above polymerization scheme:

$$dM/dt = (k_p - k_i) M W_0 - (k_p \text{CAT}) M \quad (65)$$

$$dW_0/dt = (k_{tr} \text{CAT}) P_0 - k_i M W_0 - k_{tr} P_0 W_0 \quad (66)$$

$$dP_0/dt = k_{tr} W_0 P_0 - (k_{tr} \text{CAT}) P_0 \quad (67)$$

$$dA/dt = -k_{tr} P_0 A + (k_p \text{CAT}) M + (k_i - k_p) M W_0 - k_{tr2} (\text{CTA} - P_0) A + k_{tr2} (\text{CAT} - W_0) D \quad (68)$$

$$dD/dt = k_{tr} P_0 A - k_{tr2} (\text{CTA} - P_0) A + k_{tr2} (\text{CAT} - W_0) D \quad (69)$$

$$dB/dt = -k_{tr} P_0 B + k_p M (\text{CAT} + 2A - W_0) + k_i M W_0 - k_{tr2} (\text{CTA} - P_0) B + k_{tr2} (\text{CAT} - W_0) F \quad (70)$$

$$dF/dt = k_{tr} P_0 B - k_{tr2} (\text{CTA} - P_0) B + k_{tr2} (\text{CAT} - W_0) F \quad (71)$$

$$\text{where } A = \sum_{n=1}^{\infty} (n W_n), \quad B = \sum_{n=1}^{\infty} (n^2 W_n), \quad D = \sum_{n=1}^{\infty} (n P_n), \quad F = \sum_{n=1}^{\infty} (n^2 P_n)$$

The number-average degree of polymerization of the dead and active chains are given by

$$\bar{X}_{n\text{dead}} = D/(\text{CTA} - P_0) \quad \bar{X}_{n\text{active}} = A/(\text{CAT} - W_0) \quad (72)$$

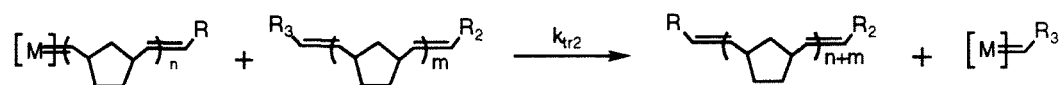
while the polydispersity index of the dead and active chains are

$$\text{PDI}_{\text{dead}} = [F (\text{CTA} - P_0)]/D^2 \quad \text{PDI}_{\text{active}} = [B (\text{CAT} - W_0)]/A^2 \quad (73)$$

C. Example.

A possible example of this type of system is the ring-opening polymerization of norbornene by $(\text{PPh}_3)_2(\text{Cl})_2\text{Ru}(=\text{CH}-\text{CH}=\text{CPh}_2)$. The effect would be a broadening of the distribution accompanied by the presence of bimodal distribution.

- Chain-Transfer Step of Type 2 (i.e., interchain transfer)



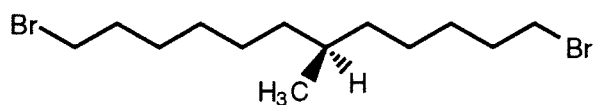
The first three steps of the polymerization scheme are not shown but are similar to the First System (*vide supra*).

Chapter 4

A Chirality Measure for Triangular Polygons (An Algorithm for Evaluating the Chirality Function)

Introduction

Chirality is the property of an object of being nonsuperimposable upon its mirror image. This definition has been expanded to include other mathematical forms and observed phenomena (point structures, fields, displacements), and has been applied to helices, scalene spherical triangle, quaternions, non-symmetric three-dimensional tensors, relaxation processes of chirally deformed structures, etc.¹ Molecules are therefore either chiral or achiral. Chiral molecules exhibit pseudoscalar properties amenable to detection by various spectroscopic techniques. Empirically, the presence of optical activity is deemed a sufficient condition for establishment of chirality.² These pseudoscalar properties (and other observables), however, are not Boolean functions of the variables defining them.³ For example, compounds with a chiral carbon atom in the dibromoalkane series exhibit different specific optical activities as number of carbon atoms attached to the chiral carbon atom is increased.



Therefore, some chemists like to view chiral molecules as possessing degrees of chirality.⁴ Degrees of chirality are quantified by chirality functions, several of which have been introduced.⁵ In chemistry, chirality functions are usually defined based on the atomic coordinates of the molecule, and as such, may serve only a theoretical interest since the magnitudes of the observables measured depends both on the geometric coordinates of the molecule and the nature of the substituents occupying each position.⁶

Mathematically, the concept of central and axial symmetry for ovals (compact, connected, convex sets with nonvoid interior) in E_n (nth dimensional space) is well studied.⁷⁻¹¹ As a consequence, the definition of symmetry for ovals may be readily adapted into chemistry. We say that a real-valued function $f(K)$ where K is the class of all

simplexes (e.g., triangle, tetrahedron, etc.) in E_n is an affine (or similarity) invariant measure of chirality if:⁷

$$\text{i. } 0 \leq f(K) \leq 1 \text{ for every simplex } K \text{ in } E_n \quad (1a)$$

$$\text{ii. } f(K) = 0 \text{ if and only if } K \text{ is achiral} \quad (1b)$$

$$\text{iii. } f(K) = f(T(K)) \text{ for every } K \text{ in } E_n \text{ and every nonsingular affine (or similarity) transformation } T \text{ of } E_n \text{ onto itself.} \quad (1c)$$

$$\text{iv. } f \text{ is a continuous function of } K. \quad (1d)$$

Because of the central role played by carbon atoms (with tetrahedral geometry) in chemistry, the tetrahedron and its various subsymmetries are natural objects of study. An example of a chirality function for the simplex tetrahedron in E_3 satisfying the definition above is:

$$f(K) = 1 - \sup[V(K')/V(K)], \quad (2)$$

where $V(K)$ is the volume of the tetrahedron, $V(K')$ is the common volume of overlap of the tetrahedron with its enantiomer, and "sup" stands for supremum, or maximum value.

$$(\text{Note: In the case of triangles in } E_2, f(K) \text{ is defined as } 1 - \sup[\text{Area}(K')/\text{Area}(K)]) \quad (3)$$

A geometrical interpretation of the function is that the tetrahedron and its mirror image (or enantiomer) are overlapped in such a way that their volume of intersection is a maximum. A chiral molecule is said to be "more chiral" than another if its $f(K)$ is greater than that of the latter. A perfect tetrahedron will have a volume of intersection equal to the tetrahedron's volume, resulting in a value of zero for the chirality function.

The problem of evaluating the maximal volume of overlap in a given distorted tetrahedron necessitated a study of a simpler problem: that of a triangle in a plane. The shape of overlap necessarily possess a line of symmetry.¹² In general, the lower bound for the quantity $(1 - f(K))$ for a centrally symmetric K' is greater than 2^{-n} in n -dimensional space¹³ (better results are known for special types of class¹⁴), while for axially symmetric K' , the lower bound is $5/8$.¹⁵ However, since for centrally symmetric K' , the class K' is

not a compact space, there might not be a K in class K that correspond to the parameters necessary for the greatest lower bound $(1-f(K))$.¹⁴ As applied to the triangles in a plane, this means that most chiral triangle might not exist but may be approximated as closely as desired by a sequence of triangles (*vide infra*).¹⁴ Previous studies have shown that the analytical methods used to derive the expression for $f(K)$ for triangles in a plane cannot be easily extended to that for tetrahedron in E_3 .¹⁶ Therefore, in this study, we approach the evaluation of $f(K)$ for triangle in a plane problem from a numerical perspective in order to evaluate the feasibility of extending the numerical approach to higher dimensions.

Computational Details

From here on, unless specified otherwise, the class K will be taken to be the set of triangles in E_2 , and $f(K)$ will be defined by eqn. 3. Angles will be in degrees rather than in radians. $f(K)$ is defined as in eqn. 3. The numerical approach may be divided into the following sections.^{17,18}

The first section of the program is the "*proper enumeration* of all triangles" (*vide infra*) by specifying the range of values the two interior angles α and β (where α is the smallest interior angle of the triangle, and β is the second smallest) may have. The second section of the program determines the normalized area of overlap and calculates its value (i.e., $\text{Area}(K')/\text{Area}(K)$) for a triangle and its enantiomer for a given configuration (or position). The third section maximizes the normalized area of overlap by the Broyden-Fletcher-Goldfarb-Shanno algorithm, and in essence find $1-f(K)$. Finally, the program prints out the value of α , β , $1-f(K)$, and the relative configuration of the triangle and its enantiomer that is associated with the value $1-f(K)$. Various starting configurations are employed to ensure finding the global maximum overlap for each triangle.

Definition of the Domain. Triangles K in E_2 are defined by its two interior angles α and β , given by

$$0 < \alpha \leq 60 \quad ; \quad \alpha < \beta \leq 90 - (3/2) \alpha \quad (4)$$

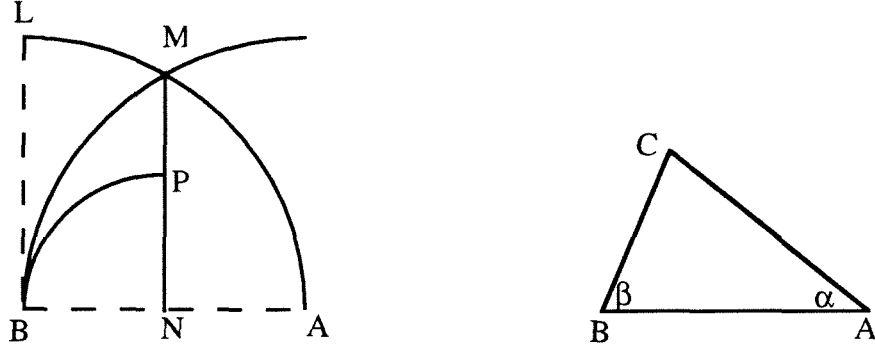


Figure 1. If one were to position the two vertices A and B of the triangle (right figure) to correspond to points A and B in the left figure, then the vertex C of the triangle ABC (right figure) need only lie in the region BMNB (left figure) defined by the interior of BMNB, the arc BM, and the line segment MN, in order to enumerate all possible similar triangles. The value of $f(K)$ will vanish near arc BM and near line segment MN.

All possible configurations of K are readily visualized from Figure 1. α and β are generated by a random number generator. However, since the random variable α may have values outside the closed interval $[0,1]$, and does not take these values with equal likelihood (because as α increases from 0 to 60 degrees, β 's range decreases), the output of the random number generator are transformed to match the desired probability distribution.¹⁹ The probability P of random variable X to lie inside the interval (α_1, α_2) is

$$P(\alpha_1 \leq X \leq \alpha_2) = \int_{\alpha_1}^{\alpha_2} k f(\alpha) d\alpha \quad (5)$$

$$\text{where } f(\alpha) = 90 - (3/2) \alpha, \quad (6)$$

and k is the normalization constant.

Because

$$P(-\infty \leq X \leq \infty) = 1 = k \int_0^{60} f(\alpha) d\alpha, \quad (7)$$

we have $k = 1/2700$, Therefore,

$$P(X \leq \alpha) = \int_0^\alpha \left(\frac{1}{30} - \frac{x}{1800} \right) dx \quad (8)$$

and the inverse of the desired probability distribution is given by

$$\alpha = 60 (1 - \sqrt{1 - P}) . \quad (9)$$

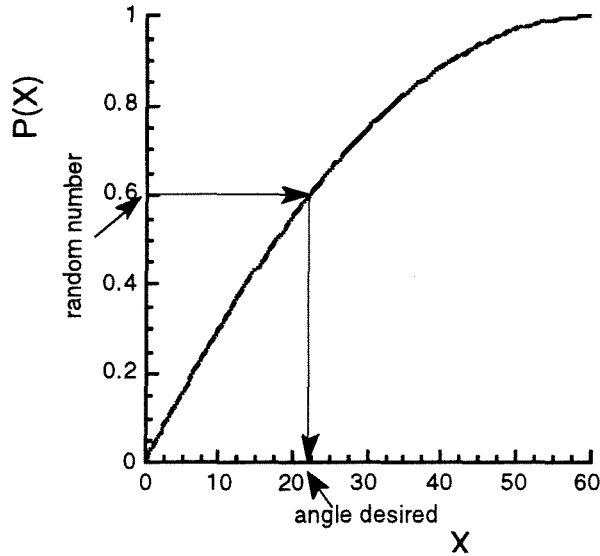


Figure 2. Relation of angle α to the generated random number

Calculation of area of overlap (two methods).

(i) **Exact Area Determination.** The exact area of overlap may be determined from the coordinates of the n -vertices of the convex polygon defining the area of overlap.

Area of polygon = Absolute value of $1/2 (x_1y_2 + x_2y_3 + \dots + x_{n-1}y_n + x_ny_1)$

$$- 1/2(y_1x_2 - y_2x_3 - \dots - y_{n-1}x_n - y_nx_1), \quad (10)$$

where x_i and y_i are the coordinates of the vertices arranged consecutively about the polygon.^{3a}

(ii) **Monte Carlo Approach to Area Determination.** This approach is analogous to throwing darts at a board. Random points (x,y) are generated, and it is determined whether they lie inside the intersection of the triangle and its enantiomer. The

accuracy of the area calculated in this manner increases as the square root of the number of points generated. The algorithm is stopped once the desired precision is reached.

Determination of maximum area of overlap (normalized). The enantiomer is moved relative to the triangle according to the Broyden-Fletcher-Goldfarb-Shanno algorithm (see Appendix). One hundred different starting positions of the enantiomer are generated to explore local extrema. The extremum value is taken as the maximum area of overlap (normalized to the area of the triangle).

Results and Discussion.

The domain of definition of the interior angles of the triangles is easily visualized from Figure 1. If line segment AB were designated to be the longest side of the triangle, point C must lie in the intersection of the sectors BLAB and ABMA. By symmetry, C need only lie in BMNB. Interior angles α and β thus take on values given by eqn. 4. This delimitation of the values of α and β is necessary to avoid redundancy in generating similar triangles.

In the Monte Carlo approach to area determination, the accuracy of the integration affects not only the value of the normalized maximum area of overlap (i.e., $1 - f(K)$ or $\sup[A(K')/A(K)]$), but also the final configuration (or position) of the enantiomer relative to the triangle. This is because different positions of the enantiomer relative to the triangle when the overlap is near maximum would give the same degree of precision in the value of $\sup[A(K')/A(K)]$. Although $\sup[A(K')/A(K)]$ can be determined with precision, the final position of the enantiomer could not be determined with high accuracy and precision. Therefore, the Monte Carlo approach cannot be extended to calculate the overlap of a distorted tetrahedron in E_3 , because the final position of the overlap cannot be determined with high degree of precision.

In the exact area calculation for $A(K')/A(K)$, the problems encountered in the Monte Carlo approach are resolved. The only problem encountered is that as one of the angles of the triangle approaches zero (i.e., triangle becomes "flat"), the increments of motion of the enantiomer relative to the triangle must be made smaller as well in order to allow the algorithm to settle to extremum values. It is therefore feasible to apply this approach to the distorted tetrahedron case. Appendix A graphically illustrates the different relative positions of the triangle and its enantiomer in the course of optimizing their overlap. The program correctly identifies the vertices of the polygon (i.e., triangle, quadrilateral, pentagon, hexagon) common to the triangle and its enantiomer, and then calculates its area.

Figure 4 summarizes the results obtained in the case of the right triangle. We readily observe that only one extremum values is associated with the right triangle. This value corresponds to a right triangle with one of its angles equal to 37.47 degrees. The overlap is 88.5% of the area of the triangle. Because this extremum point is the intersection of two curves, therefore the configurations associated with this value of $1 - f(K)$ are not unique. Indeed, two different configurations (or positions) of the triangle and its enantiomer gives rise to the same value of $(1 - f(K))$, i.e., 0.885 (Figure 3). Figure 4 also allows one to visualize the effect of gradual desymmetrization of the triangle on the values of $(1 - f(K))$.

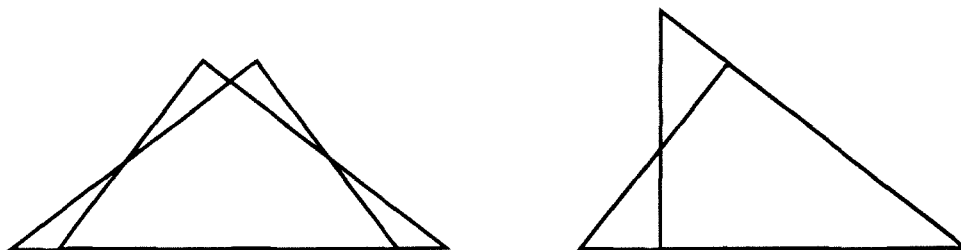


Figure 3. The two configurations of the right triangle with an interior angle 37.47°. Both configurations give rise to $\sup[A(K')/A(K)] = 88.5\%$ of the area of the triangle.

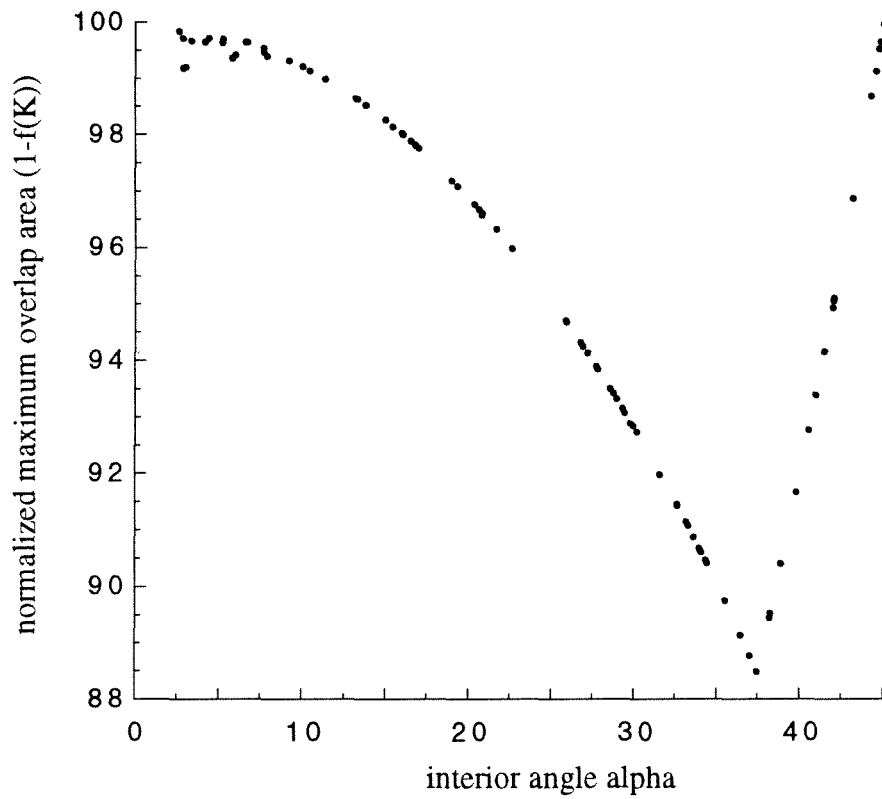


Figure 4. Plot of the normalized maximum overlap area ($(1-f(K))$ or $\sup[A(K')/A(K)]$) vs interior angle α for the case of a right triangle.

By the same method, a 3-D surface plot of $(1 - f(K))$ versus the interior angles α, β may be generated. It is obvious however that the trace formed by the intersection of a plane with the surface $(1 - f(K))$ will have the same form as figure 4.

Conclusion

A numerical solution has been developed to find the values of the chirality function $f(K) = 1 - \sup[A(K')/A(K)]$, where K is any triangle in E_2 , $A(K')$ is the common area of intersection between K and its enantiomer, $A(K)$ is the area of K , \sup is the maximum of such values. This method also gives the configurations of the triangles giving rise to such value, hence allows one to visualize the effect of varying the values of the interior angles on $f(K)$. The results show that Monte Carlo methods are not practical for area calculation. However, by using Exact Area Calculation, the value of the chirality function for triangles can be achieved with relative ease, suggesting that the latter method may be extended to the tetrahedron case.

Acknowledgment

This project was done in collaboration with Prof. Kurt Mislow of Princeton University. I would like to thank Prof. Mislow for the opportunity to work under him. I would also like to thank Dr. Andrzej Buda and Dr. Thomas Auf de Heyde for valuable discussions. Funding was generously provided by the National Science Foundation.

References

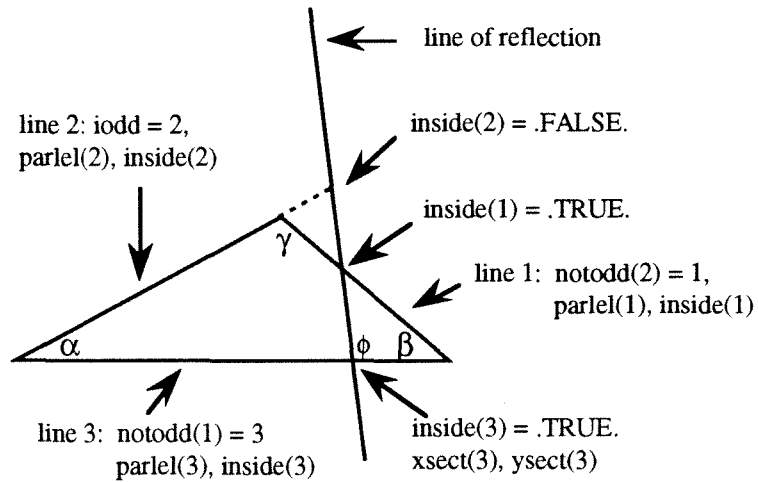
- (1) Whyte, L.L. *Nature* **1958**, 182, 198.
- (2) March, J. *Advanced Organic Chemistry*; John Wiley & Sons: New York, 1985, p.82.

- (3) For an introduction of the mathematical terms used in this chapter, see (a) Bronshtein, I.N.; Semendyayev, K.A. *Handbook of Mathematics*; translated by Hirsch, K.A.; Van Nostrand Reinhold Company: 1985. (b) Buck, R.C. *Advanced Calculus*; McGraw-Hill: New York, 1978. (c) Munkres, J.R. *Topology: A First Course*; Prentice-Hall: Englewood Cliffs, 1975. (d) Coxeter, H.S.M. *Introduction to Geometry*; John Wiley & Sons: New York, 1969.
- (4) Mislow, K.; Bickart, P. *Isr. J. Chem.* **1976/77**, *15*, 1.
- (5) For examples of some chirality functions, see Buda, A.; Auf der Heyde, T.; Mislow, K. *Angew. Chem. Int. Ed. Engl.* **1992**, *31*, 989, and references therein.
- (6) This is not always true. At times, chirality function may just depend on the masses of the ligands attached to the atom. (a) Brown, B.C. *Proc. Royal Soc. Edinburgh* **1890**, *17*, 181. (b) Guye, P. *Compt. Rend.* **1890**, *110*, 714. (c) Richter, W.J.; Richter, B.; Ruch, E. *Angew. Chem. Int. Ed. Engl.* **1973**, *12*, 30.
- (7) Besicovitch, A.S. *J. London Math. Soc.* **1948**, *23*, 237.
- (8) deValcourt, B.A. *Isr. J. Math.* **1966**, *4*, 65.
- (9) Chakerian, G.D.; Stein, S.K. *Can. J. Math.* **1965**, *17*, 497.
- (10) Nohl, W. *Elem. Math.* **1962**, *17*, 59.
- (11) deValcourt, B.A. *Bull. Amer. Math. Soc.* **1966**, *72*, 289.
- (12) Giering, O. *Elem. Math.* **1967**, *22*, 5.
- (13) Stein, S. *Pacific J. Math.* **1967**, *22*, 5.
- (14) Grunbaum, B. *Proceedings of Symposia in Pure Mathematics, Vol VII, Convexity*. Amer. Math. Soc. 1963.
- (15) Krakowski, F. *Elem. Math.* **1963**, *18*, 80.
- (16) Buda, A.; Mislow, K. *J. Mol. Struct. (Theochem)* **1991**, *232*, 1.
- (17) For an introduction to numerical methods, see Press, W.H., et al. *Numerical Recipes in C: The Art of Scientific Computing*, Cambridge University Press: New York, 1988.

- (18) (a) Preparata, F.P.; Shamos, M.I. *Computational Geometry: An Introduction*; Springer-Verlag: New York, 1985, p. 237. (b) Whitesides, S.H. "Computational Geometry and Motion Planning," *Computational Geometry*, G.T. Toussaint ed. Elsevier Science Publishers B.V., North-Holland, 1985
- (19) Kreyszig, E. *Advanced Engineering Mathematics*; John Wiley & Sons: New York, 1979, pp. 863-868.

Appendix A

Nomenclature for Exact Area Calculation:

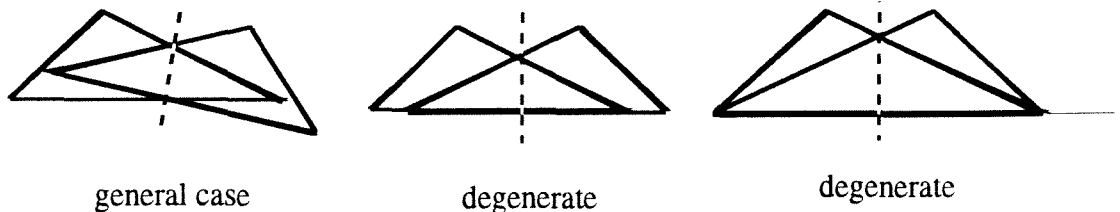


Example. In this case, the ODDSIDE is side 2, since the line of symmetry fails to intersect it directly. The label is stored under IODD. The label of the other two sides are stored under the arrays NOTODD. ϕ is the angle the line of reflection makes with the x-axis.

Some cases (and positions) encountered in the process of optimization.

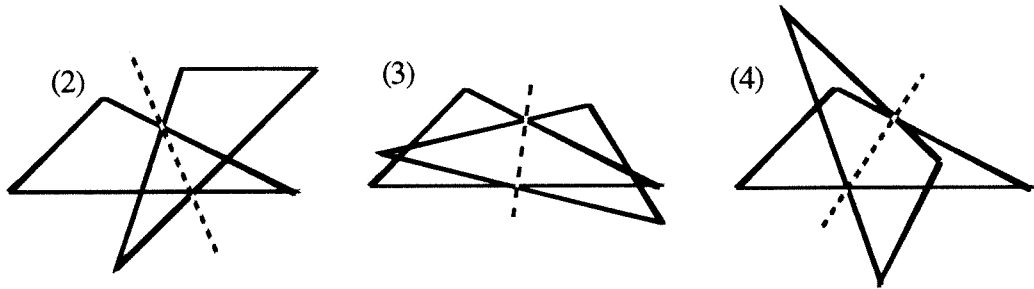
A. Three points "INSIDE"

1. One vertex of triangle is "INSIDE" the triangle



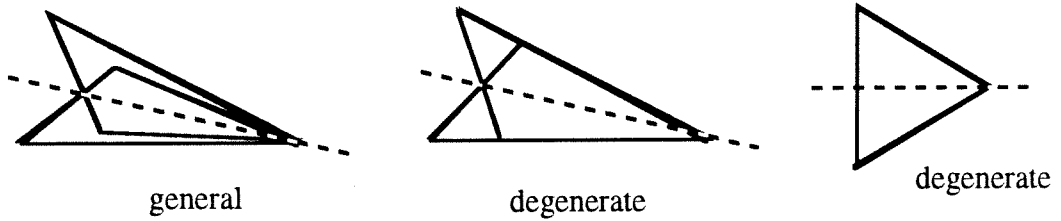
2. two sides that are not ODD intersects (see left figure below)
3. sides that are not ODD intersects with ODDSIDE (see center figure below)

4. only one side (that is not ODD) intersects with ODDSIDE (see right figure below)

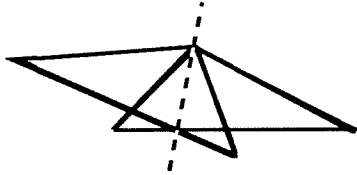


B. Two points "INSIDE"

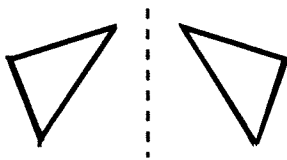
1. one vertex of the triangle is "INSIDE" the triangle



2. side that is not ODD intersects with ODDSIDE



C. No points of intersection



Appendix B: Source Listing of Computer Program "triang"

The following Fortran program is an incomplete listing. To save space, only subroutines written by the author are listed.

Program "triang" calculates the value $1 - f(K)$ where K is a triangle and prints out the results associated with each triangle defined by its two angles α and β (up to similarity). The area by using eqn. 10 (i.e., Exact Area Method). $f(K)$ is defined in the Computational Details. The vertex of angle β is the origin (0,0) of the Cartesian plane while the vertex of angle α is (1,0). The endpoints of the longest side c of the triangle has as its coordinates (0,0) and (1,0). The triangle lies in the first quadrant of the Cartesian plane. The position of the enantiomer may be obtained by knowing the line of reflection (of the triangle with its enantiomer image) which is characterized by ϕ (angle made by the line of reflection with the x-axis, see Appendix A) and coordinate of a point lying on the line of reflection. The generation of α and β is discussed in Computational Details, since angle α does not take on values with equal probability.

Subroutines stran1 and stran2, functions rand1(idum) and rando1(idum) are adapted from Andrzej Buda's program.

The subroutines not written by the author and are therefore omitted from this chapter is:

subroutine flepo: minimizes a real-valued function of n-component real vector according to the procedure of Broyden-Fletcher-Goldfarb-Shanno (see last two pages of Appendix B for description). This subroutine invokes other subroutines which are subroutine compfg and subroutine linmin.

```

program triang
  IMPLICIT DOUBLE PRECISION (A-H,O-Z)

c   calculates the value of the chirality function for all possible
c   triangles.

c   alpha & beta -- store the value of the two angles of a triangle
c   xend & yend  -- store the x- and y-coordinate of the point where
c                   the line of symmetry passes
c   omegae       -- stores the angle (in degrees) that the line of
c                   symmetry makes with the x-axis
c   chifun       -- stores the normalized area of overlap of the
c                   triangle and its enantiomer

  PARAMETER (MAXPAR = 10, MAXHES = 100)
  parameter (maxtri = 20, maxlin = 50)
  COMMON
  ./GRADNT/ GRAD (MAXPAR), GNORM
  ./CTIME / TIME0
  ./OPTIM / IMP, IMP0, LEC, IPRT, HESINV (MAXHES), XVAR (MAXPAR)
  .       , GVAR (MAXPAR), XD (MAXPAR), GD (MAXPAR), GLAST (MAXPAR)
  .       , XLAST (MAXPAR), GG (MAXPAR), PVECT (MAXPAR)
  ./PARAM / XPARAM (50), NVAR
  ./NUMCAL/ NUMCAL
  ./tring / object (2,3), aretri
  ./angtri / angla, anglb
  ./angtr2 / sideb, sidec, cangla, sangla
  ./line / xstart, ystart, omega
  ./TEMA / sidea
  LOGICAL FAIL
  dimension alpha (maxtri), beta (maxtri),
  .       xend (maxtri), yend (maxtri), omegae (maxtri), chifun (maxtri)
  data pi /3.1415926535897932d0 /

  TIME0=SECOND ()
  TIME1=TIME0
  IPRT   = 6
  IINP   = 5
  IFILE1 = 1
  ICNTRL = 0
  NUMCAL = 1

  OPEN (UNIT=IFILE1, FILE='HESSIAN.OPT', FORM='UNFORMATTED',
+ STATUS='UNKNOWN', ACCESS='SEQUENTIAL')
c   OPEN (UNIT=IINP, FILE='OPT.INP', STATUS='OLD', ACCESS='SEQUENTIAL',
c   . BUFFERED='UNBUFFERED', FORM='FORMATTED', BLANK='ZERO')
  OPEN (UNIT=IPRT, FILE='CON', BUFFERED='UNBUFFERED', STATUS='NEW')
c   OPEN (UNIT=IPRT, FILE='D:OPT.LIS', STATUS='UNKNOWN', ACCESS='SEQUENTIAL'
c   . , FORM='FORMATTED')
  OPEN (UNIT=7, FILE='ENUTR7.OUT', FORM='FORMATTED', STATUS='NEW',
  . ACCESS='SEQUENTIAL')

  write (7, (('This generates triangles and find maximum overlap area
  . with its enantiomer')) )
  write (7, (('NOTE: THE GRADIENT CALCN HAS NOT BEEN SCALED YET ')) )
  WRITE (7, (('NOTE: IT MIGHT BE BETTER IF x-coord of line of reflxn
  . COULD VARY >1')) )
  write (7, (('total line of reflxn generated is ', i4)) MAXLIN
  write (7, (('length of side c is always unity ', //)) )
  call stran1
  do 10 jj=1, maxtri

    call trigen
    alpha (jj) = angla

```

```

        beta (jj) = anglb
        iipack = 0
        MISS = 0
        WRITE(7,('Two angles of the triangles are ',2f9.5,21x,i6'))
        .   alpha(jj), beta(jj), jj
        WRITE (7,('length of side b, side a, area are ',3f10.5'))
        .   sideb, sidea, aretri
        call stran2
        chival = 0.
30      call linsym(XPARAM, NVAR)

        FAIL = .FALSE.
        call FLEPO ( XPARAM, NVAR, FUNOPT, FAIL)
        if (FAIL) then
            MISS = MISS + 1
            goto 30
        endif

        if (XPARAM(1) .ge. 0) then
            XTEM = XPARAM(1)
            YTEM = 0.
        else
            XTEM = -XPARAM(1)*cangla
            YTEM = -XPARAM(1)*sangla
        endif
        WTEM = XPARAM(2)*180./pi
c      WRITE (7,('Line of reflxn: (x,y) and phi are ',3f11.5'))
c      .   XTEM, YTEM, WTEM
c      WRITE (7,('percent overlap is ',f8.4)) abs(FUNOPT)

        iipack = iipack + 1
        if (chival .lt. abs(FUNOPT)) then
            omfinl = XPARAM(2)
            chival = abs(FUNOPT)
            if (XPARAM(1) .ge. 0) then
                xfinal = XPARAM(1)
                yfinal = 0.
            else
                xfinal = -XPARAM(1)*cangla
                yfinal = -XPARAM(1)*sangla
            endif
        endif
        if (iipack .lt. maxlin) goto 30
        xend(jj) = xfinal
        yend(jj) = yfinal
        omegae(jj) = omfinl*180./pi
        chifun(jj) = chival

C      write (*,('Angles alpha and beta are ',2f10.4'))
C      .   alpha(jj), beta(jj)
        write(7,('BEST LINE OF REFLECTION:(x,y) and phi are ',3f10.5))
        .   xend(jj), yend(jj), omegae(jj)
        write (7,('BEST PERCENT OVERLAPPED AREA IS ',f10.7))
        .   chifun(jj)
c      write(7,('total line of reflxn generated is ',i9)) MAXLIN+MISS
        WRITE(7,('-----'))
10      continue

C      DETERMINE THE COMPUTATION TIME.
        TIME2=SECOND()
        TIME1=TIME2-TIME1
        IF(MIDDLE.EQ.1) TIME1=SECADD
        WRITE(IPRT,100) TIME1

```



```

100 FORMAT(////5X,'COMPUTATION TIME = ',F8.2,3X,'SECONDS')
      write (7,'(////''total computation time is ''',f8.2,3x,'''seconds''
      .  )') TIME1
      CLOSE (7)
      stop
      end
c -----
c      subroutine trigen
c      generates nonisometric triangles and the area 'aretri' of the
c      triangle. The vertices of the triangles are 'object(p,q)' where
c      p=1 is x-coordinate, p=2 is y-coordinate of vertex.
c      q is vertex number.

      implicit double precision ( a-h, o-z )
      common
      ./tring / object(2,3), aretri
      ./angtri / angla, anglb
      ./angtr2 / sideb, sidec, cangla, sangla
      ./TEMA   / sidea
      data pi / 3.1415926535897932d0 /

      factor = pi/180.d0
c      The length of sidec of triangle is presumed to be unity
      sidec = 1.

10    angla = 60. - sqrt(3600. - 3600.*rand1(1))
      if (angla .le. 0.) goto 10
      anglb = (90. - 3.*angla/2.)*rand1(2) + angla

c      calculates the length of side of triangle, the vertices of the
c      triangle, and the area of the triangle in square units

      anglar = angla*factor
      anglbr = anglb*factor
      anglcr = (pi - anglar - anglbr)

      sangla = sin(anglar)
      sanglb = sin(anglbr)
      sanglc = sin(anglcr)
      cangla = cos(anglar)

      sidea = sidec * sangla/sanglc
      sideb = sidec * sanglb/sanglc

      object(1,1) = 0.
      object(2,1) = 0.
      object(1,2) = sidec
      object(2,2) = 0.
      object(1,3) = sideb * cangla
      object(2,3) = sideb * sangla

      aretri = sidec * object(2,3)/2.

      return
      end
c -----
c      subroutine linsym(XPARAM, NVAR)
c      IMPLICIT DOUBLE PRECISION (A-H,O-Z)

c      generates a line which passes through point ('XPARAM(1)')
c      and makes an angle 'XPARAM(2)' (in radians) with the x-axis
c      assumes that sidec of the triangle is equal to unity. If it isn't,
c      then this subroutine has to be modified.

```

```

      DIMENSION XPARAM(*)
      common
      ./angtr2 / sideb, sidec, cangla, sangla
      ./DERRIV/ DELTA(10)
      data pi /3.1415926535897932d0 /
      NVAR = 2

      XPARAM(1) = (sideb + sidec)*randol(1) - sideb
      XPARAM(2) = randol(2)*pi

      DELTA(1) = 0.01
      DELTA(2) = 0.035
      return
      end
c -----
      subroutine stran1
      implicit double precision ( a-h, o-z )
      external time
      character*8 times
      integer*2 tim(3)
      integer*4 irand

      call time( times )

      j=0
      do 10 i=1,7,3
      j=j+1
      ii=i+1
10 read( times(i:i+1), '(i2)') tim(j)

      irand = ( tim(1)*60 + tim(2) )*60 + tim(3)
      xnull = randl(-irand)
c write(*, '(' xnull = 'f10.9)') xnull
      return
      end
c -----
      function randl(idum)
      implicit double precision ( a-h, o-z )
c return a uniform random deviate between 0.0 and 1.0. Set idum
c to any negative value to initialize or reinitialize the sequence.
c implicit double precision ( a-h, o-z )
      dimension r(97)
      save
      parameter (m1=259200, ia1=7141, ic1=54773, rml=1./m1)
      parameter (m2=134456, ia2=8121, ic2=28411, rm2=1./m2)
      parameter (m3=243000, ia3=4561, ic3=51349 )
      data iff /0/

c as above, initialize on first call even if idumm is not negative.
      if(idum.lt.0 .or. iff.eq.0) then
          iff=1
c seed the first routine
          ix1=mod(ic1-idum,m1)
          ix1=mod(ia1*ix1+ic1,m1)
c and use it to seed the second
          ix2=mod(ix1,m2)
          ix1=mod(ia1*ix1+ic1,m1)
c and third routines
          ix3=mod(ix1,m3)
c fill the table with sequential uniform deviates generated by
c the first two routines.
          do 11 j=1,97
              ix1=mod(ia1*ix1+ic1,m1)
              ix2=mod(ia2*ix2+ic2,m2)

```

```

c          low and high order pieces combined here
          r(j)=(float(ix1)+float(ix2)*rm2)*rml
11  continue
      idum=1
      endif

c  Except when initializing, this is where we start. Generate the
c  next number for each sequence.
      ix1=mod(ial*ix1+icl,m1)
      ix2=mod(ia2*ix2+ic2,m2)
      ix3=mod(ia3*ix3+ic3,m3)
c  use the third sequence to get an integer between 1 and 97.
      j=1+(97*ix3)/m3
      if(j.gt.97 .or. j.lt.1) pause
c  return that table entry, and refill it
      randl=r(j)
      r(j)=(float(ix1)+float(ix2)*rm2)*rml
c  write(*,(' ' randl = ',f20.10)') randl
      return
      end

c  -----
      subroutine stran2
      implicit double precision ( a-h, o-z )
      external time
      character*8 times
      integer*2 tim(3)
      integer*4 irando

      call time( times )

      j=0
      do 10 i=1,7,3
        j=j+1
        ii=i+1
10  read( times(i:i+1), '(i2)') tim(j)

      irando = ( tim(1)*60 + tim(2) )*60 + tim(3)
      xnull = randol(-irando)
c  write(*,(' ' xnull = ',f10.9)') xnull
      return
      end

c  -----
      function randol(idum)
      implicit double precision ( a-h, o-z )
c  return a uniform random deviate between 0.0 and 1.0. Set idum
c  to any negative value to initialize or reinitialize the sequence.
c  implicit double precision ( a-h, o-z )
      dimension r(97)
      save
      parameter (m1=259200, ial=7141, icl=54773, rml=1./m1)
      parameter (m2=134456, ia2=8121, ic2=28411, rm2=1./m2)
      parameter (m3=243000, ia3=4561, ic3=51349 )
      data iff /0/
c  as above, initialize on first call even if idumm is not negative.
      if(idum.lt.0 .or. iff.eq.0) then
        iff=1
c  seed the first routine
        ix1=mod(icl-idum,m1)
        ix1=mod(ial*ix1+icl,m1)
c  and use it to seed the second
        ix2=mod(ix1,m2)
        ix1=mod(ial*ix1+icl,m1)
c  and third routines
        ix3=mod(ix1,m3)

```

```

c      fill the table with sequential uniform deviates generated by
c      the first two routines.
      do 11 j=1,97
        ix1=mod(ia1*ix1+ic1,m1)
        ix2=mod(ia2*ix2+ic2,m2)
c      low and high order pieces combined here
        r(j)=(float(ix1)+float(ix2)*rm2)*rm1
11    continue
      idum=1
    endif

c      Except when initializing, this is where we start. Generate the
c      next number for each sequence.
      ix1=mod(ia1*ix1+ic1,m1)
      ix2=mod(ia2*ix2+ic2,m2)
      ix3=mod(ia3*ix3+ic3,m3)
c      use the third sequence to get an integer between 1 and 97.
      j=1+(97*ix3)/m3
      if(j.gt.97 .or. j.lt.1) pause
c      return that table entry, and refill it
      randol=r(j)
      r(j)=(float(ix1)+float(ix2)*rm2)*rm1
c      write(*, '(' randol = ',f20.10)') randol
      return
    end

c      -----
      function FUNOPT(XPARAM,NVAR)
      implicit double precision (a-h, o-z)

c      calculates the normalized area of intersection 'FUNOPT' of the
c      two triangles described by their vertices 'object' and 'image'

      common
      ./tring / object(2,3), aretri
      ./line / xcoord, ycoord, omega
      ./line2 / reflcA, reflcB, reflcC
      ./angtr2/ sideb, sidec, cangla, sangla
      dimension XPARAM(*)
      real*8 image(2,3)

      if (XPARAM(1) .ge. 0) then
        xcoord = XPARAM(1)
        ycoord = 0.0d0
      else
        xcoord = -XPARAM(1)*cangla
        ycoord = -XPARAM(1)*sangla
      endif
      omega = XPARAM(2)

      call reflec(object, image)
      FUNOPT = OVERLP(image)
      FUNOPT = -(FUNOPT/aretri) * 100.0d0
      return
    end

c      -----
      subroutine reflec(object, image)
      implicit double precision ( a-h, o-z )

c      calculates the equation of line (of reflection) given the angle
c      'omega' of the line and the coordinate ('xcoord','ycoord') of a
c      point on the line. This 'omega' is radian.
c      calculates the image 'image' of the points described by 'object'
c      upon reflection through the line

```

```

common
./line / xcoord, ycoord, omega
./line2 / reflcA, reflcB, reflcC
real*8 object(2,3), image(2,3), project(2,3), dconst(3)
-----
c calculates the equation  $Ax + By + C = 0$  of the line of symmetry.
c 'reflcA' is A, 'reflcB' is B, 'reflcC' is C.

reflcA = sin(omega)
reflcB = -cos(omega)
reflcC = -reflcA*xcoord - reflcB*ycoord

c -----

c calculates the image 'image(p,q)' of object(p,q) upon reflection
c across line  $Ax + By + C = 0$ . p=1 is x-coordinate, and
c p=2 is y-coordinate. q is vertex number.
c First, calculates equation of line normal to line of symmetry
c and passing through each vertices 'object' of the triangle.
c Equation of normal line is  $Bx - Ay + D = 0$ 

do 10 i = 1,3
  dconst(i) = reflcA*object(2,i) - reflcB*object(1,i)
  denomi = reflcA*reflcA + reflcB*reflcB
  project(1,i) = -(reflcB*dconst(i) + reflcA*reflcC)/denomi
  project(2,i) = (reflcA*dconst(i) - reflcB*reflcC)/denomi
  image(1,i) = project(1,i)*2. - object(1,i)
  image(2,i) = project(2,i)*2. - object(2,i)
10 continue
c -----

return
end

c -----
function OVERLP (image)
implicit double precision (a-h, o-z)

c subprogram calculates the area of intersection 'OVERLP'
c of two triangles described by 'object' and 'image'
c 'reflcA' is A; 'reflcB' is B; 'reflcC' is C of the line of
c reflection  $Ax + By + C = 0$ 

common
./tring / object(2,3), aretri
./line2 / reflcA, reflcB, reflcC
logical parrel, inside, interior, oddsid, samesd
dimension objA(3), objB(3), objC(3), parrel(3), inside(3),
. xsect(4), ysect(4), xovrlp(4), yovrlp(4), oddsid(3), notodd(2)
. real*8 image(2,3), imA(3), imB(3), imC(3)
. parameter (tol = 1.0d-60, tol2 = 1.0d-16)

do 10 k = 1,3
  ind1 = 1 + mod(k,3)
  ind2 = 1 + mod(ind1,3)
  call lineqn (object(1,ind1), object(2,ind1),
. object(1,ind2), object(2,ind2), objA(k), objB(k), objC(k))
  call border (reflcA,reflcB,reflcC, objA(k),objB(k),objC(k),
. object(1,ind1), object(2,ind1),
. object(1,ind2), object(2,ind2), -10.,-10.,10.,10.,
. parrel(k), inside(k), xsect(k), ysect(k))
10 continue
c -----

```

```

c      calculates the number of sides of triangle that the line of
c      reflection intersects

      numsec = 0
      do 12 k=1,3
      if ((.not. paralel(k)) .and. (inside(k))) then
          numsec = numsec + 1
      endif
12  continue
c      -----
c      no point of intersection
c      if (numsec .le. 1) then
c          OVERLP = 0.
c          return
c      endif
c      -----
c      three points of intersection
c      if (numsec .eq. 3) then

c      first, calculates three of the vertices of the polygon determined
c      by the overlap of the triangle and its enantiomer
c      Note that of the three vertices, two of them are necessarily
c      identical

          do 14 k =1,3
              xovrlp(k) = xsect(k)
              yovrlp(k) = ysect(k)
14      continue
              iodd = 3
              if (( abs(xovrlp(1)-xovrlp(3)).lt.tol ) .and.
                  ( abs(yovrlp(1)-yovrlp(3)).lt.tol ))
                  then
                  call exchge(xovrlp(2),xovrlp(3))
                  call exchge(yovrlp(2),yovrlp(3))
                  iodd = 2
              endif
              if (( abs(xovrlp(2)-xovrlp(3)).lt.tol ) .and.
                  ( abs(yovrlp(2)-yovrlp(3)).lt.tol ))
                  then
                  call exchge(xovrlp(1),xovrlp(3))
                  call exchge(yovrlp(1),yovrlp(3))
                  iodd = 1
              endif
              if (( abs(xovrlp(1)-xovrlp(2)).gt.tol ) .and.
                  ( abs(yovrlp(1)-yovrlp(2)).gt.tol )) then
c      .      write (*,('Alto's algorithm fail at line 63 of subprogram TR
c      . I22.FOR probably due to computer truncation error'))
c      .      stop
c      .      endif

              notodd(1) = 1 + mod(iodd,3)
              notodd(2) = 1 + mod(notodd(1),3)
c      .      -----
c      calculates the equation of the line which is mirror to the oddsid
c      call lineqn (image(1,notodd(1)), image(2,notodd(1)),
c      .            image(1,notodd(2)), image(2,notodd(2)),
c      .            imA(iodd), imB(iodd), imC(iodd))
c      .      -----
c      calculating the fourth (i.e., last) point that determines the
c      polygon of overlap

c      first calculates whether endpoint of mirror of oddsid is inside
c      the triangle

```

```

if (interior (image(1,notodd(1)),image(2,notodd(1)),
.   objA(1),objB(1),objC(1),object(1,1),object(2,1),
.   objA(2),objB(2),objC(2),object(1,2),object(2,2),
.   objA(3),objB(3),objC(3),object(1,3),object(2,3))) then
  xovrlp(4) = image(1,notodd(1))
  yovrlp(4) = image(2,notodd(1))
else
  if (interior (image(1,notodd(2)),image(2,notodd(2)),
.   objA(1),objB(1),objC(1),object(1,1),object(2,1),
.   objA(2),objB(2),objC(2),object(1,2),object(2,2),
.   objA(3),objB(3),objC(3),object(1,3),object(2,3))) then
    xovrlp(4) = image(1,notodd(2))
    yovrlp(4) = image(2,notodd(2))
  else
c   calculates the point of intersection of sides that are not
c   odd with the mirror of oddsid
    ktem1 = 1+mod(notodd(1),3)
    ktem2 = 1+mod(ktem1,3)
    call border (objA(notodd(1)), objB(notodd(1)),
.               objC(notodd(1)),
.               imA(iodd), imB(iodd), imC(iodd),
.               object(1,ktem1), object(2,ktem1),
.               object(1,ktem2), object(2,ktem2),
.               image(1,notodd(1)), image(2,notodd(1)),
.               image(1,notodd(2)), image(2,notodd(2)),
.               parrel(notodd(1)), inside(notodd(1)),
.               xsect(4), ysect(4))
    if (((.not.(parrel(notodd(1))))).and.(inside(notodd(1)))))
    then
      xovrlp(4) = xsect(4)
      yovrlp(4) = ysect(4)
    else
      ktem1 = 1+mod(notodd(2),3)
      ktem2 = 1+mod(ktem1,3)
      call border (objA(notodd(2)), objB(notodd(2)),
.               objC(notodd(2)),
.               imA(iodd), imB(iodd), imC(iodd),
.               object(1,ktem1), object(2,ktem1),
.               object(1,ktem2), object(2,ktem2),
.               image(1,notodd(1)), image(2,notodd(1)),
.               image(1,notodd(2)), image(2,notodd(2)),
.               parrel(notodd(2)), inside(notodd(2)),
.               xsect(4), ysect(4))
c       if (((parrel(notodd(2))).or.(.not.(inside(notodd(2)))))
c       then
c         write (*,('Algorithm failure at line 217'))
c         stop
c       endif
      xovrlp(4) = xsect(4)
      yovrlp(4) = ysect(4)
    endif
  endif
endif
endif
c   Note that the last 'endif' is for numsec = 3
c   -----
c   two points of intersection
c   if (numsec .eq. 2) then

c   first calculates two of the vertices of the polygon determined by
c   the overlap of the triangle and its enantiomer

  index = 1
  do 20 k=1,3
  if ((.not. parrel(k)) .and. (inside(k))) then

```

```

        xovrlp(index) = xsect(k)
        yovrlp(index) = ysect(k)
        index = index + 3
    else
        iodd = k
    endif
20 continue
c -----
do 25 k=1,3
    if (parlel(k)) then
        tem = reflcA*object(1,1+mod(k,3)) +
            . reflcB*object(2,1+mod(k,3)) + reflcC
        . if (((abs(tem).lt.tol2) .or. ((abs(xovrlp(1)-xovrlp(4)).lt.tol)
        . and.(abs(yovrlp(1)-yovrlp(4)).lt.tol)))) then
c         the line of reflection is either collinear with oddsid,
c         or line of reflection passes through the vertex that
c         is opposite oddsid
            OVERLP = 0.
            return
        endif
    endif
25 continue
c -----
c calculates the other two vertices of the polygon determined by
c the triangle and its enantiomer

c Case #1: vertex opposite the oddsid lies inside the triangle
    if (interior (image(1,iodd),image(2,iodd),
        . objA(1),objB(1),objC(1),object(1,1),object(2,1),
        . objA(2),objB(2),objC(2),object(1,2),object(2,2),
        . objA(3),objB(3),objC(3),object(1,3),object(2,3))) then
c Case 1 scenario satisfied
        xovrlp(2) = image(1,iodd)
        yovrlp(2) = image(2,iodd)
        xovrlp(3) = image(1,iodd)
        yovrlp(3) = image(2,iodd)
        goto 70
    endif
c -----
c calculates the equation of the lines corresponding to mirror of
c sides that are not oddsid

do 30 k = 1,3
    jtem1 = 1 + mod(k,3)
    jtem2 = 1 + mod(jtem1,3)
    call lineqn (image(1,jtem1), image(2,jtem1), image(1,jtem2),
        . image(2,jtem2), imA(k), imB(k), imC(k))
30 continue
c -----
    notodd(1) = 1 + mod(iodd,3)
    notodd(2) = 1 + mod(notodd(1),3)
c -----
c Case #2: sides that are not odd intersects

    call border (objA(notodd(1)), objB(notodd(1)),objC(notodd(1)),
        . imA(notodd(2)), imB(notodd(2)), imC(notodd(2)),
        . object(1,notodd(2)), object(2,notodd(2)),
        . object(1,iodd), object(2,iodd),
        . image(1,notodd(1)), image(2,notodd(1)),
        . image(1,iodd), image(2,iodd),
        . paralel(iodd), inside(iodd),
        . xsect(2), ysect(2))
    if (((.not.(paralel(iodd))).and.(inside(iodd)))) then

```



```

c   Case 2 scenario satisfied
      xovrlp(2) = xsect(2)
      yovrlp(2) = ysect(2)
      xovrlp(3) = xsect(2)
      yovrlp(3) = ysect(2)
      goto 70
    endif
  - - - - -
c   Case #3 and #4: (overlap is pentagon, hexagon)
c   calculates the point of intersection of mirror of oddsid with
c   lines that are not odd

  do 40 k=1,2
    jtem1 = 1 + mod(notodd(k),3)
    jtem2 = 1 + mod(jtem1,3)
    call border (objA(iodd), objB(iodd), objC(iodd),
      .       imA(notodd(k)), imB(notodd(k)), imC(notodd(k)),
      .       object(1,notodd(1)), object(2,notodd(1)),
      .       object(1,notodd(2)), object(2,notodd(2)),
      .       image(1,jtem1), image(2,jtem1),
      .       image(1,jtem2), image(2,jtem2),
      .       parrel(notodd(k)), inside(notodd(k)),
      .       xsect(notodd(k)), ysect(notodd(k)))
    if (((.not.(parrel(notodd(k)))) .and. (inside(notodd(k)))) then
c   Case 3 scenario satisfied
      xovrlp(k+1) = xsect(notodd(k))
      yovrlp(k+1) = ysect(notodd(k))
    else
c   Case 4 scenario possible
      if (interior (object(1,notodd(1)),object(2,notodd(1)),
      .   imA(1),imB(1),imC(1),image(1,1),image(2,1),
      .   imA(2),imB(2),imC(2),image(1,2),image(2,2),
      .   imA(3),imB(3),imC(3),image(1,3),image(2,3))) then
        xovrlp(k+1) = object(1,notodd(1))
        yovrlp(k+1) = object(2,notodd(1))
      else
        if (interior (object(1,notodd(2)),object(2,notodd(2)),
      .   imA(1),imB(1),imC(1),image(1,1),image(2,1),
      .   imA(2),imB(2),imC(2),image(1,2),image(2,2),
      .   imA(3),imB(3),imC(3),image(1,3),image(2,3))) then
          xovrlp(k+1) = object(1,notodd(2))
          yovrlp(k+1) = object(2,notodd(2))
        else
          endif
        endif
      endif
    endif
  40 continue
  - - - - -
c   arrange the vertices in proper order so that the area can be
c   calculated. This procedure is needed only for Case#3 and Case#4
c   of the two-point intersection.

c   first calculates if vertex2 and vertex3 of polygon lie on same
c   side of line determined by vertex1 and vertex4 of polygon

  call lineqn (xovrlp(1),yovrlp(2),xovrlp(4),yovrlp(4),
    .       temA,temB,temC)
  if ((.not. (samesd(xovrlp(2),yovrlp(2),temA,temB,temC,
    .       xovrlp(3),yovrlp(3)))) then
c   calculate the reflection of point (x3,y3) through line Ax+By+C=0
c   where A = 'temA', B = 'temB', C = 'temC'
c   In this way, vertex2 and vertex3 lie on same side
c   write(*,('points 2 and 3 not on same side of line determined by
c   points 1 and 4 '))

```

```

    dtem      = temA*yovrlp(3) - temB*xovrlp(3)
    denomi     = temA*temA + temB*temB
    xproj      = -(temB*dtem + temA*temC)/denomi
    yproj      = (temA*dtem - temB*temC)/denomi
    xovrlp(3) = xproj*2 - xovrlp(3)
    yovrlp(3) = yproj*2 - yovrlp(3)
endif

c    secondly, try to order vertex2 and vertex3 in proper sequence
    if (((abs(xovrlp(1)-xovrlp(3)).lt.tol).and.(abs(yovrlp(1)-
.    yovrlp(3)).lt.tol)) .or. ((abs(xovrlp(2)-xovrlp(4)).lt.tol)
.    .and.(abs(yovrlp(2)-yovrlp(4)).lt.tol))) then
        call exchge (xovrlp(2),xovrlp(3))
        call exchge (yovrlp(2),yovrlp(3))
    endif

    if ((abs(xovrlp(1)-xovrlp(2)).gt.tol) .and.
.    (abs(yovrlp(1)-yovrlp(2)).gt.tol)) then
        call lineqn (xovrlp(1),yovrlp(1),xovrlp(2),yovrlp(2),
.    temA, temB, temC)
        if ((.not. (samesd(xovrlp(3),yovrlp(3),temA,temB,temC,
.    xovrlp(4),yovrlp(4)))) then
            call exchge (xovrlp(2),xovrlp(3))
            call exchge (yovrlp(2),yovrlp(3))
        endif
    endif
endif
endif

c    Note that the last 'endif' above is for numsec = 2
c    -----
c    the area of the polygon is now ready to be calculated

70  OVERLP = area (xovrlp, yovrlp)
    OVERLP = abs(OVERLP)

    return
end

c    -----
subroutine lineqn (x1,y1,x2,y2,A,B,C)
implicit double precision (a-h, o-z)

c    calculates A,B,C of line Ax + By + C = 0 passing through points
c    with coordinates (x1,y1) and (x2,y2)

    A = y2 - y1
    B = x1 - x2
    C = -B*y1 -A*x1

    return
end

c    -----
subroutine border (A1,B1,C1,A2,B2,C2,xllow,ylow,xlhigh,ylhigh,
.    x2low,y2low,x2high,y2high,parlel,inside,xsect,ysect)
implicit double precision (a-h, o-z)

c    calculates the point of intersection (xsect,ysect) of two lines if
c    they are not parallel. Otherwise, 'parlel' is .TRUE. and
c    subprogram returns to calling program.
c    If not parallel, also determines whether the point of intersection
c    lies in the two line segments whose endpoints are (xllow, ylow),
c    (xlhigh, ylhigh); and (x2low, y2low), (x2high, y2high).
c    If so, 'inside' is .TRUE.

    logical parolel, inside
    parameter (tol = 1.0d-16)
    denomi = A1*B2 - A2*B1

```

```

c   if (abs(denomi) .lt. tol) then
the two lines are parallel
      parrel = .TRUE.
      inside = .FALSE.
      return
    else
      parrel = .FALSE.
    endif
    xsect = (B1*C2 - B2*C1)/denomi
    ysect = (A2*C1 - A1*C2)/denomi
c   The next two "if" loops make sure that xhigh and yhigh are largest
    x1lo = x1low
    x1hi = x1high
    x2lo = x2low
    x2hi = x2high
    y1lo = y1low
    y1hi = y1high
    y2lo = y2low
    y2hi = y2high
    if (x1hi .lt. x1lo) then
      call exchge (x1hi, x1lo)
    endif
    if (y1hi .lt. y1lo) then
      call exchge (y1hi, y1lo)
    endif
    if (x2hi .lt. x2lo) then
      call exchge (x2hi, x2lo)
    endif
    if (y2hi .lt. y2lo) then
      call exchge (y2hi, y2lo)
    endif

c   checking if point (xsect,ysect) lies in both line segments
    if ((xsect - x1lo) .ge. 0.0d0) then
      if ((x1hi - xsect) .ge. 0.0d0) then
        if ((ysect - y1lo) .ge. 0.0d0) then
          if ((y1hi - ysect) .ge. 0.0d0) then
            if ((xsect - x2lo) .ge. 0.0d0) then
              if ((x2hi - xsect) .ge. 0.0d0) then
                if ((ysect - y2lo) .ge. 0.0d0) then
                  if ((y2hi - ysect) .ge. 0.0d0) then
                    inside = .TRUE.
                    return
                  endif
                endif
              endif
            endif
          endif
        endif
      endif
    endif
    inside = .FALSE.
    return
  end

c   -----
function area (x, y)
implicit double precision (a-h, o-z)

c   assumes that there is a line of symmetry in the figure of overlap
c   otherwise, this subprogram has to be modified

dimension x(4), y(4)

area = 0.
do 10 i=1,3

```

```

        area = area + x(i)*y(i+1) - y(i)*x(i+1)
10  continue
    area = area + x(4)*y(1) - y(4)*x(1)
    return
end
c -----
    logical function interior (p,q,A1,B1,C1,x1,y1,A2,B2,C2,x2,y2,
                             A3,B3,C3,x3,y3)
    implicit double precision (a-h, o-z)

c    finds out whether point (p,q) is an element of the closure of the
c    triangle whose sides are described by lines  $Ax + By + C = 0$  and
c    whose vertices are (x1,y1), (x2,y2), (x3,y3)

    logical samesd
    if (samesd(p,q,A1,B1,C1,x1,y1)) then
        if (samesd(p,q,A2,B2,C2,x2,y2)) then
            if (samesd(p,q,A3,B3,C3,x3,y3)) then
                interior = .TRUE.
            return
        endif
    endif
    interior = .FALSE.

    return
end
c -----
    logical function samesd (p,q,A,B,C,u,v)
    implicit double precision (a-h, o-z)

c    finds out whether point (p,q) and point (u,v) lie on the same side
c    of the line  $Ax + By + C = 0$ 

    if (abs(B) .gt. abs(A)) then
c    calculates the difference of y-coordinate of "projection" of the
c    point with the y-coordinate of the point
        tem1 = (-C - A*u)/B - v
        tem2 = (-C - A*p)/B - q
    else
c    calculates the difference of x-coordinate of "projection" of the
c    point with the x-coordinate of the point
        tem1 = (-C - B*v)/A - u
        tem2 = (-C - B*q)/A - p
    endif

    if ((tem1*tem2) .lt. 0.0d0) then
        samesd = .FALSE.
    else
        samesd = .TRUE.
    endif

    return
end
c -----
    subroutine exchge (p,q)
    implicit double precision (a-h, o-z)

c    exchanges the value of real numbers p and q

    tem = p
    p = q
    q = tem

    return
end
c -----

```

```

*****
SUBROUTINE FLEPO (XPARAM,NVAR,FUNCT,FAIL)
IMPLICIT DOUBLE PRECISION (A-H,O-Z)
PARAMETER (MAXPAR = 10, MAXHES = 100)
DIMENSION XPARAM(*)
COMMON
./GRADNT/ GRAD (MAXPAR),GNORM
./CTIME / TIMEO
./NUMCAL/ NUMCAL
./OPTIM / IMP,IMP0,LEC,IPRT,HESINV (MAXHES),XVAR (MAXPAR)
.,GVAR (MAXPAR),XD (MAXPAR),GD (MAXPAR),GLAST (MAXPAR)
.,XLAST (MAXPAR),GG (MAXPAR),PVECT (MAXPAR)

*
THIS SUBROUTINE ATTEMPTS TO MINIMIZE A REAL-VALUED FUNCTION OF
THE N-COMPONENT REAL VECTOR XPARAM ACCORDING TO THE
BFGS FORMULA. RELEVANT REFERENCES ARE

BROYDEN, C.G., JOURNAL OF THE INSTITUTE FOR MATHEMATICS AND
APPLICATIONS, VOL. 6 PP 222-231, 1970.
FLETCHER, R., COMPUTER JOURNAL, VOL. 13, PP 317-322, 1970.

GOLDFARB, D. MATHEMATICS OF COMPUTATION, VOL. 24, PP 23-26, 1970.

SHANNO, D.F. MATHEMATICS OF COMPUTATION, VOL. 24, PP 647-656
1970.

SEE ALSO SUMMARY IN

HEAD, J.D.; AND ZERNER, M.C., CHEMICAL PHYSICS LETTERS, VOL. 122,
264 (1985).
SHANNO, D.F., J. OF OPTIMIZATION THEORY AND APPLICATIONS
VOL.46, NO 1 PP 87-94 1985.

*
THE FUNCTION CAN ALSO BE MINIMIZED USING THE
DAVIDON-FLETCHER-POWELL ALGORITHM (COMPUTER JOURNAL, VOL. 6,
P. 163).

THE USER MUST SUPPLY THE SUBROUTINE
COMPPG(XPARAM,NVAR,FUNCT,FAIL,GRAD,LGRAD)
WHICH COMPUTES FUNCTION VALUES FUNCT AT GIVEN VALUES FOR THE NVAR
VARIABLES XPARAM, AND THE GRADIENT GRAD IF LGRAD=.TRUE.
THE .TRUE. VALUE IS RETURNED IN FAIL IF SCF NOT CONVERGED.
THE MINIMIZATION PROCEEDS BY A SEQUENCE OF ONE-DIMENSIONAL
MINIMIZATIONS. THESE ARE CARRIED OUT WITHOUT GRADIENT COMPUTATION
BY THE SUBROUTINE LINMIN, WHICH SOLVES THE SUBPROBLEM OF
MINIMIZING THE FUNCTION FUNCT ALONG THE LINE XPARAM+ALPHA*PVECT,
WHERE XPARAM
IS THE VECTOR OF CURRENT VARIABLE VALUES, ALPHA IS A SCALAR
VARIABLE, AND PVECT IS A SEARCH-DIRECTION VECTOR PROVIDED BY THE
BFGS OR DAVIDON-FLETCHER-POWELL ALGORITHM. EACH ITERATION STEP CARRIED
OUT BY FLEPO PROCEEDS BY LETTING LINMIN FIND A VALUE FOR ALPHA
WHICH MINIMIZES FUNCT ALONG XPARAM+ALPHA*PVECT, BY
UPDATING THE VECTOR XPARAM BY THE AMOUNT ALPHA*PVECT, AND
FINALLY BY GENERATING A NEW VECTOR PVECT. UNDER
CERTAIN RESTRICTIONS (POWELL, J.INST.MATHS.APPLICS.(1971),
V.7,21-36) A SEQUENCE OF FUNCT VALUES CONVERGING TO SOME
LOCAL MINIMUM VALUE AND A SEQUENCE OF
XPARAM VECTORS CONVERGING TO THE CORRESPONDING MINIMUM POINT
ARE PRODUCED.

```

CONVERGENCE TESTS.

HERBERTS TEST: THE ESTIMATED DISTANCE FROM THE CURRENT POINT
POINT TO THE MINIMUM IS LESS THAN TOLERA.

"HERBERTS TEST SATISFIED - GEOMETRY OPTIMISED"

GRADIENT TEST: THE GRADIENT NORM HAS BECOME LESS THAN TOLERG
TIMES THE SQUARE ROOT OF THE NUMBER OF VARIABLES.

"TEST ON GRADIENT SATISFIED".

XPARAM TEST: THE RELATIVE CHANGE IN XPARAM, MEASURED BY ITS NORM,
OVER ANY TWO SUCCESSIVE ITERATION STEPS DROPS BELOW
TOLERX.

"TEST ON XPARAM SATISFIED".

FUNCTION TEST: THE CALCULATED VALUE OF THE HEAT OF FORMATION
BETWEEN ANY TWO CYCLES IS WITHIN TOLERF OF
EACH OTHER.

"HEAT OF FORMATION TEST SATISFIED"

FOR THE GRADIENT, FUNCTION, AND XPARAM TESTS A FURTHER CONDITION,
THAT NO INDIVIDUAL COMPONENT OF THE GRADIENT IS GREATER
THAN TOLERG, MUST BE SATISFIED, IN WHICH CASE THE
CALCULATION EXITS WITH THE MESSAGE

"PETERS TEST SATISFIED"

AN UNSUCCESSFUL TERMINATION WILL TAKE PLACE AFTER
COMPPG HAS BEEN CALLED MORE TIMES THAN THE USER-SUPPLIED VALUE
OF MAXEND. IN THIS CASE THE COMMENT

"*** TERMINATION FROM TOO MANY COUNTS ***"

WILL BE PRINTED, AND FUNCT AND XPARAM WILL CONTAIN THE LAST
FUNCTION VALUE CUM VARIABLE VALUES REACHED.

SIMILAR UNSUCCESSFUL TERMINATIONS WILL TAKE PLACE IF THE COSINE OF
THE SEARCH DIRECTION TO GRADIENT VECTOR IS LESS THAN RST ON TWO
CONSECUTIVE ITERATIONS.

THE BROYDEN-FLETCHER-GOLDFARB-SHANNO AND DAVIDON-FLETCHER-POWELL
ALGORITHMS CHOOSE SEARCH DIRECTIONS
ON THE BASIS OF LOCAL PROPERTIES OF THE FUNCTION. A MATRIX H,
WHICH IN FLEPO IS PRESET WITH THE IDENTITY, IS MAINTAINED AND
UPDATED AT EACH ITERATION STEP. THE MATRIX DESCRIBES A LOCAL
METRIC ON THE SURFACE OF FUNCTION VALUES ABOVE THE POINT XPARAM.
THE SEARCH-DIRECTION VECTOR PVECT IS SIMPLY A TRANSFORMATION
OF THE GRADIENT GRAD BY THE MATRIX H. THE USER MAY THROW OUT H
AND BEGIN AGAIN WITH THE IDENTITY MATRIX
WHENEVER THE COSINE OF THE ANGLE BETWEEN GRAD AND PVECT BECOMES
LESS THAN RST. IN DFP, H IS ALSO RESET AFTER NRST ITERATION STEPS.
THIS CAN BE SUPPRESSED ENTIRELY IF NRST .GT. MAXEND
AND RST .LT. 0.0. RESTARTING IS DISCUSSED marginally IN THE
PAPER BY FLETCHER AND POWELL, BUT THERE ARE NO GOOD RULES ABOUT
WHEN OR WHETHER THIS SHOULD BE DONE FOR ANY GIVEN FUNCTION.

Appendix C

If one desires to calculate the area of overlap not by the Exact Area Method of Appendix B but by Monte Carlo Method (listed here), then some of the subroutines in Appendix B has to be replaced by the following subroutines.

```

c -----
c function FUNOPT(XPARAM,NVAR)
c IMPLICIT DOUBLE PRECISION ( A-H, O-Z )

c calculates the normalized area of intersection 'FUNOPT' of the
c two triangles described 'object' and 'image'
c area is calculated by Monte Carlo integration
c calculates box parameters and integrate the overlap area

      common
      ./tring / object(2,3), aretri
      ./line / xcoord, ycoord, omega
      ./angtr2/ sideb, sidec, cangla, sangla
      dimension XPARAM(*)
      real*8 image(2,3), boxorg(2), boxsiz(2)

      if (XPARAM(1) .ge. 0) then
        xcoord = XPARAM(1)
        ycoord = 0.
      else
        xcoord = -XPARAM(1)*cangla
        ycoord = -XPARAM(1)*sangla
      endif
      omega = XPARAM(2)

      call reflec( object, image)
      call boxdim( object, image, boxorg, boxsiz)
      FUNOPT = -area(object, image, boxorg, boxsiz(1), boxsiz(2),aretri)
      FUNOPT = FUNOPT * 100.
      return
      end
c -----
c subroutine boxdim( object, image, boxorg, boxsiz )
c implicit double precision ( a-h, o-z )
c dimension object(2,3), image(2,3), boxorg(2), boxsiz(2),
c          sortit(6)
c real*8 image

c calculates the box length 'boxsiz(1)', box width 'boxsiz(2)
c and the origin (boxorg(1), boxorg(2)) of the box

      do 10 i=1,2
        do 20 j=1,3
          sortit(j) = object(i,j)
          sortit(j+3) = image(i,j)
20        continue
        call sort(6, sortit)
        boxsiz(i) = sortit(6) - sortit(1)
        boxorg(i) = sortit(1)
10      continue

      return
      end
c -----

```

```

subroutine sort(items, sorted)
implicit double precision ( a-h, o-z )

c  sorts an array called 'sorted' of length 'items' into ascending
c  numerical order, by straight insertion.  'items' is input;
c  array 'sorted' is replaced on output by its sorted arrangement.

dimension sorted(items)
do 12 j=2,items
  a = sorted(j)
  do 11 i= j-1, 1, -1
    if (sorted(i) .le. a) goto 10
    sorted(i+1) = sorted(i)
11  continue
    i=i-1
10  sorted(i+1) = a
12  continue

return
end

-----
c  function area (object, image, boxorg, boxlen, boxwid, aretri)
implicit double precision ( a-h, o-z )

c  calculates the normalized area of intersection (area) of
c  a triangle (object) and its mirror image (image).  Variables
c  'object' and 'image' keeps the coordinates of the vertices of
c  the triangle.

dimension object(2,3), image(2,3), boxorg(2)
real*8 image
logical samesd, pass1

call side( object(1,1), object(1,2), object(1,3), slpob3, cepob3,
.          xyob3, patob3)
call side( object(1,3), object(1,1), object(1,2), slpob2, cepob2,
.          xyob2, patob2)
call side( object(1,2), object(1,3), object(1,1), slpob1, cepob1,
.          xyob1, patob1)

call side(image(1,1), image(1,2), image(1,3), slpim3, cepim3,
.          xyim3, patim3)
call side(image(1,3), image(1,1), image(1,2), slpim2, cepim2,
.          xyim2, patim2)
call side(image(1,2), image(1,3), image(1,1), slpim1, cepim1,
.          xyim1, patim1)

draw = 0.
hit  = 0.
ipack = 10000
pass1 = .TRUE.
tol   = 0.001

20 call setran
do 10 i = 1, ipack
  xran = ran1(1)*boxlen + boxorg(1)
  yran = ran1(2)*boxwid + boxorg(2)
  draw = draw + 1.

  if (samesd(xran,yran,slpob3,cepob3,xyob3,patob3)) then
    if (samesd(xran,yran,slpob2,cepob2,xyob2,patob2)) then
      if (samesd(xran,yran,slpob1,cepob1,xyob1,patob1)) then
        if (samesd(xran,yran,slpim3,cepim3,xyim3,patim3)) then
          if (samesd(xran,yran,slpim2,cepim2,xyim2,patim2)) then

```



```

        if (samesd(xran,yran,slpim1,cepim1,xyim1,patim1)) then
            hit = hit + 1.
        endif
    endif
endif
endif
endif
10 continue

area = hit/draw * boxlen*boxwid/aretri

if (pass1) then
    areal = area
    pass1 = .FALSE.
    goto 20
C elseif (abs(area - areal) .gt. tol) then
C     improve the accuracy of the integration !
C     areal = area
C     goto 20
endif

return
end

C -----
subroutine side(vertex1, vertex2, vertex3, slp, xycept, xyside,
               pathxy)
implicit double precision ( a-h, o-z )

C calculates the slope and intercept (xycept) of the line
C passing through vertex1 and vertex2 and the position of vertex3
C against that line (xyside). Intercept may be x or y-intercept
C depending on whether slope is greater than 1 or not, respectively.
C If slope is greater than 1, slope 'slp' is with respect to y-axis.
C Otherwise, slope 'slp' is with respect to x-axis.

dimension vertex1(2), vertex2(2), vertex3(2)
xdiff = vertex2(1) - vertex1(1)
ydiff = vertex2(2) - vertex1(2)
if (abs(ydiff) .gt. abs(xdiff)) then

C slope is greater than 1. Hence, equation is  $x = my + b$ , where b
C is x-intercept, and slope m (denoted by 'slp') is with respect to
C y-axis
    slp = xdiff/ydiff
    xycept = vertex2(1) - slp*vertex2(2)
    xyside = slp * vertex3(2) + xycept
    xyside = sign(1.d0, (vertex3(1)-xyside))
    pathxy = 1

else
C slope is less than 1. Hence equation is  $y = mx + b$ 
    slp = ydiff/xdiff
    xycept = vertex2(2) - slp*vertex2(1)
    xyside = slp * vertex3(1) + xycept
    xyside = sign(1.d0, (vertex3(2)-xyside))
    pathxy = 2
endif
return
end
C -----

```

```

logical function samesd( xran, yran, slp, xycept, xyside, pathxy)
implicit double precision ( a-h, o-z )

c  samesd finds whether the ran point (xran,yran) is on the same
c  side of the line (determined by two vertices, with slope slp)
c  and third vertex characterized by variable 'xyside'.

  if (pathxy .eq. 1) then
    xory = slp * yran + xycept
    samesd = sign(1.d0, (xran - xory)) .eq. xyside
  else
    xory = slp * xran + xycept
    samesd = sign(1.d0, (yran - xory)) .eq. xyside
  endif
  return
end

c  -----
subroutine setran
implicit double precision ( a-h, o-z )
external time
character*8 times
integer*2 tim(3)
integer*4 iran

  call time( times )

  j=0
  do 10 i=1,7,3
    j=j+1
    ii=i+1
10  read( times(i:i+1), '(i2)') tim(j)

  iran = ( tim(1)*60 + tim(2) )*60 + tim(3)
  xnull = ran1(-iran)
c  write(*, '(' xnull = 'f10.9)') xnull
  return
end
c  -----

```